The Identification and Characterization of Genetic Modifiers for Bardet-Biedl Syndrome-Associated Phenotypes using *Caenorhabditis elegans*

by

Calvin Ka Fay Mok

A thesis submitted in conformity with the requirements
for the degree of Doctor of Philosophy

Institute of Medical Science
University of Toronto

© Copyright by Calvin Ka Fay Mok 2012

The Identification and Characterization of Genetic Modifiers for Bardet-Biedl Syndrome-Associated Phenotypes using *Caenorhabditis elegans*

Calvin Ka Fay Mok

Doctor of Philosophy

Institute of Medical Science

University of Toronto

2012

Abstract

Primary cilia are evolutionarily conserved organelles required in a number of signalling pathways influencing the development and behaviour of a diverse range of organisms. More recently, studies into a new class of human diseases known as ciliopathies have helped to shed light on the critical role of this once-ignored signalling centre. Bardet-Biedl syndrome (BBS) proteins localize to the primary cilium and participate in cilium biogenesis and function. BBS is a pleiotropic human disorder with variable severity that is suitable as a disease model for investigating the pathogenesis of a number of common ciliopathy features such as photoreceptor degeneration, renal cysts, and obesity.

The *C. elegans* genome encodes a number of BBS proteins which undergo intraflagellar transport (IFT) at the primary cilium. Given the conservation between *C. elegans* and human BBS proteins, I hypothesize the existence of unidentified conserved genetic pathways related to the functions of these proteins. Using *C. elegans*, I characterize novel features of *bbs* mutants

while identifying sources of genomic variation that may elucidate the variability of human BBS features. I show that *C. elegans bbs* mutants exhibit smaller body size, delayed development, and decreased exploration behaviour. Moreover, I identify a role for the soluble guanylate cyclases GCY-35/GCY-36 in modifying these *bbs* phenotypes. I conclude that BBS proteins non-cell autonomously influence a set of body cavity neurons in which GCY-35/GCY-36 function genetically upstream of a cGMP-dependent protein kinase (PKG), EGL-4, to control body size. Furthermore, the role of GCY-35/GCY-36 is unique amongst a large number of guanylate cyclases and BBS proteins may influence body size via an IFT-independent function.

I explore the biological functions of EGL-4 and conclude that it may regulate body size through multiple cellular mechanisms. I also examine potential candidate genes related to cGMP production and turnover, confirming that additional cGMP-related factors can influence body size although not necessarily in body cavity neurons. In conclusion, I propose a model where BBS-expressing sensory neurons influence body size and development through cGMP-PKG signalling in body cavity neurons while functioning in parallel with additional sensory neurons (possibly BBS-independent) that use similar cGMP-PKG signalling dynamics.

Acknowledgments

Over the past years, many individuals have helped to make this work possible.

I would like to begin by thanking my supervisors Dr. Elise Héon and Dr. Mei Zhen for taking on this risky project and helping to guide it, over many years, to fruition. As well, I thank them both for the mentorship, support, and opportunities they have given to me throughout my growth as a scientist and for their collective wisdom and experience without which this thesis would not be possible.

I would like to thank my thesis committee members Dr. Brent Derry and Dr. John Parkinson for their comments, suggestions, support and guidance throughout the course of this doctoral thesis.

I thank Gail Partridge and Dr. Wesley Hung, both of whom I am indebted to for teaching me a number of molecular techniques, answering my many questions and for occasionally offering their wisdom as a sounding board to my many and sometimes bizarre experimental ideas.

For their technical support, I thank Ying Wang, Dr. Hang Li and Dr. Madhavan Jagadeesan, who also offered advice and help to me in my many endeavours.

I thank Dr. Cornelia Bargmann, Dr. Mario De bono, and Dr. Michel Leroux for sharing reagents used in this thesis.

I thank a number of former undergraduate students who contributed to enhancing the work in this thesis, especially Tanvi Shekhar, Rebecca Mok, and Olesya Solomonova.

I thank both the Héon and Zhen labs for their support both technical and moral throughout the many years of graduate school. I have come to consider these labs as part of my second family and although many members have come and gone over the course of my work, their advice and friendship have been invaluable to me. I especially thank Diana “Mama” Quon who has helped keep my life organized all these many years.

The Sick Kids Program in Genetics and Genome Biology has been the other half of my second family, exposing me to new fields of research, and ample opportunities to expand my horizons and friendships. Both students and PIs alike have been a source of support and advice. I especially thank Rosa Freire whom I have relied upon constantly for her help and wisdom.

Special thanks to all my friends and family, especially Jing Jin, Sanjeev Pullenayegum, Derek Leung, Michael DiBernardo, and my sisters Sue-Ann and Sharon Mok; all of whom have fueled my work with their interest and support.

Finally I would like to thank my parents for encouraging me to find the passion of my life. To them I dedicate this work.

Table of Contents

Table of Contents

Acknowledgments iv
Table of Contents v
List of Tables xi
List of Figures xii
List of Appendices xiv
Nomenclature and List of Abbreviations xv
Chapter 1 Introduction 1
1.1 Primary Cilia are Important, Evolutionarily Conserved Organelles 1
1.2 Ciliopathies are a Growing Class of Disorders Related to Ciliary Dysfunction 4
1.3 Bardet-Biedl Syndrome, a Pleiotropic, Heterogeneous, Ciliopathy Model 5
1.4 Animal Models of Bardet-Biedl Syndrome 11
1.4.1 Mouse BBS Models Recapitulate Human Phenotypes 11
1.4.2 Zebrafish BBS Models Identify Signalling Pathways 12
1.4.3 *Caenorhabditis elegans* BBS Models Dissect Molecular Functions 14
1.4.4 Additional Models of BBS 18
1.5 Deciphering the Function of Bardet-Biedl Syndrome Proteins 18
1.5.1 BBS Proteins Co-ordinate Antagonistic IFT Motor Movement 21
1.5.2 Evolutionarily Conserved BBS Proteins Form a Complex Required for Vesicular Trafficking 21
1.5.3 BBS3 May Act as a Molecular Switch Between BBSome Vesicular Trafficking and IFT Functions 24
1.5.4 BBS Chaperonin-like and CCT Chaperonin Proteins Form a Complex Required for BBSome Formation 26
1.5.5 BBS4 and BBS8 are Required for Proper Microtubule Organization 27
1.5.6 A BBS3 Retina-Specific Isoform is Required for Proper Inner Segment Organization and Photoreceptor Function 28
1.5.7 BBIP10 is a BBSome Subunit Required for Ciliogenesis and formation of the BBSome 29

1.6 Additional BBS Interactions 29
1.7 Cilia-specific signalling pathways 30
1.7.1 Cilia and basal body proteins play roles regulating canonical and non-canonical Wnt signalling 30
1.7.2 Sonic Hedgehog Signalling is Perturbed in BBS and Ciliary Mutants 32
1.7.3 Planar Cell Polarity 33
1.8 The study of genetic modifying influences of the Bardet-Biedl Syndrome phenotypes 34
1.8.1 *CCDC28B* as a Modifier of BBS Severity 35
1.8.2 *RPGRIP1L* as a Modifier of Ciliopathy Eye Phenotype 37
1.8.3 Identifying Remaining Genetics Modifiers? 38
1.9 Summary of the Ciliopathy Field 40
1.10 Objectives of This Thesis 41
1.10.1 Mutations in a Guanylate Cyclase GCY-35/GCY-36 Modify Bardet-Biedl Syndrome-Associated Phenotypes in *Caenorhabditis elegans* 42
1.10.2 Analysis of Signalling Pathways Affecting the Body size of *Caenorhabditis elegans* 43
1.11 References 43
Chapter 2 Methods and Materials 57
2 57
2.1 Strain Culture Conditions 57
2.2 Phenotyping Protocols 57
2.2.1 DiI uptake 57
2.2.2 Body size assessment 57
2.2.3 Developmental timing 58
2.2.4 Roaming assay 58
2.2.5 Fluorescence Microscopy 59
2.3 Mapping and cloning of *hp433* 59
2.4 Molecular Biology 59
2.5 References 60
Chapter 3 Mutations in a Guanylate Cyclase GCY-35/GCY-36 Modify Bardet-Biedl Syndrome-Associated Phenotypes in *Caenorhabditis elegans* 61

3 61
3.1 Abstract 61
3.2 Author Summary 61
3.3 Introduction 62
3.4 Results 64
3.4.1 *C. elegans bbs* mutants share ciliary defects, reduced body size, delayed developmental timing and reduced roaming 64
3.4.2 The Loss of Function of a Guanylate Cyclase GCY-35 Rescues a Subset of Phenotypes in *bbs* Mutants 69
3.4.3 The GCY-35/GCY-36 sGC Complex Influences the Body Size of *bbs* Mutants Through a Subset of Oxygen Sensing Body Cavity Neurons 71
3.4.4 The Expression and Localization of GFP::GCY-35 and GFP::GCY-36 are Grossly Normal in *bbs* Mutants 73
3.4.5 The cGMP-Dependent Protein Kinase (PKG) EGL-4 is an sGC Effector in Body Size Regulation 75
3.4.6 BBS Proteins are Required in Multiple Sensory Neurons to Regulate Body Size 79
3.4.7 GCY-35/GCY-36 Acts as a Dominant Effector in BBS-Mediated Body Size Regulation 79
3.5 Discussion 82
3.5.1 *C. elegans bbs* Mutants Exhibit Non-Cell Autonomous Phenotypes 82
3.5.2 The GCY-35/GCY-36 sGC Regulates Body Size Through a Mechanism Divergent from Oxygen Sensing 83
3.5.3 BBS Proteins Affect Body Size Indirectly Through Body Cavity Neurons 84
3.5.4 A Potential Involvement of Aberrant cGMP Signalling in Ciliopathies 86
3.6 References 86
Chapter 4 Analysis of Signalling Pathways that Affect the Body size of *Caenorhabditis elegans* 92
4 92
4.1 Introduction 92
4.2 Putative cGMP Signalling Components 93
4.2.1 cGMP-Dependent Protein Kinases 95

4.2.2 Phosphodiesterases 96
4.2.3 DAF-21 Regulates Receptor Guanylate Cyclase Functions 98
4.3 Results 101
4.3.1 EGL-4 Overexpression Does Not Phenocopy *bbs* Body Size Defects 101
4.3.2 EGL-4 May Regulate Body Size Through Multiple Modalities 101
4.3.3 C09G4.2 is not a Modifier of *bbs* Body Length 103
4.3.4 PDE-5 Regulates Body Size in Parallel to BBS Proteins 106
4.3.5 GPA-3 Overexpression Does Not Suppress BBS Body Size Defects 108
4.3.6 The Loss of Non-Redundant rGCs Does Not Rescue Body Size Defects of *bbs* Mutants 111
4.3.7 DAF-21, the Mammalian HSP90 Orthologue, Rescues *bbs* Body Size Defects 111
4.3.8 *mobs-2*: an Additional Suppressor of *bbs-7* Body Size Defects through a Forward Genetics Approach 113
4.4 Discussion 114
4.4.1 A change in cGMP/EGL-4 Signalling in *bbs* Mutants May be Transient or Does not involve Nuclear Translocation 114
4.4.2 Phophodiesterases Do Not Directly Influence *bbs* Body Size in Body Cavity Neurons 115
4.4.3 Receptor Guanylate Cyclases May Regulate *bbs* Body Size 116
4.5 References 116
Chapter 5 Discussion and Future Directions 120
5 120
5.1 Discussion 120
5.1.1 BBS Proteins Have Novel Roles in *C. elegans* Development 120
5.1.2 Body Cavity Neurons Influence Body Size in a Context-Specific Manner 121
5.1.3 GCY-35/GCY-36 Play Specific Roles in Body Size Regulation 122
5.1.4 EGL-4 Signalling Influences Body Size Via Separate Neurons in Multiple Cellular Pathways 123
5.2 Future Directions 124
5.2.1 Further Dissecting the Role of BBSome Proteins in IFT 124

5.2.2 The Role of cGMP Production in *C. elegans* Body Cavity Neurons.....125
5.2.3 Determining the Temporal Requirements of cGMP in BBS-Associated Phenotypes 126
5.2.4 Determining if Nuclear Localization of PKEG EGL-4 is Required for Body Size Regulation 126
5.2.5 How do BBS Proteins Regulate Body Size Non-Cell Autonomously From Sensory Neurons to Body Cavity Neurons.....128
5.2.6 Investigating BBS-Associated Phenotypes in Relation to the mTOR Signalling Pathway 129
5.2.7 Does cGMP Signalling Influence or Contribute to Ciliopathy Phenotypes in Other Model Organisms.....129
5.3 Conclusion and Model.....132
5.3.1 *bbs* Mutants Have Hyperactive Neuroendocrine Secretion defects.....132
5.3.2 Hyperactive Neuroendocrine Secretion May Modulate cGMP-PKG Regulation of Body Size in Body Cavity Neurons. 132
5.4 References.....135
Appendices 139
6 Appendix 1*: mobs-1(hp433)* Mapping 139
6.1 *mobs-1(hp433)* Rough Maps to LGI.....139
6.2 *mobs-1(hp433)* Snip-SNP Mapping Identifies 93kb Interval.....140
6.3 *mobs-1(hp433)* Fosmids Containing *gcy-35* Rescue *bbs-7* Body Size Suppression 142
6.4 Genomic Sequencing Analysis Identified 2bp Deletion in *gcy-35(hp433)* 144
6.5 References.....145
7 Appendix 2: *GUCY1B2* Tissue Expression Pattern.....146
8 Appendix 3: Strains Used in this Study 147
8.1 *bbs* Strains 147
8.2 *dyf* Strains 147
8.3 sGC Strains.....147
8.4 rGC Strains 147
8.5 cGMP-related Strains.....147
8.6 *pde* Strains.....147

8.7 TGF-β Strains....148
8.8 sGC Combination Strains....148
8.9 rGC Combination Strains....148
8.10 *dyf* Combination Strains....149
8.11 *pde* Combination Strains....149
8.12 TGF-β Combination Strains....150
8.13 Additional Candidate *bbs* Suppressor Strains....150
8.14 Strains used for mapping *gcy-35(hp433)*....150
8.15 Transgenic strains used in this study....150
8.15.1 Rescuing Lines for *bbs* Animals....150
8.15.2 Rescuing Lines for *gcy-35(hp433)I; bbs-7(ok1351)III* Animals....151
8.15.3 Cell-specific Rescue Lines for *gcy-35(hp433)I;bbs-7(ok1351)III* Animals....151
8.15.4 Transgenic Lines to Examine the Subcellular Localisation of GCY-35 and GCY-36....151
8.15.5 EGL-4 Gain of Function Expression Lines....151
8.15.6 EGL-4 Rescue and Expression Lines....151
9 Appendix 4: Additional *Pegl-4a*::GFP::EGL-4 localization images....153

List of Tables

Chapter 1. Introduction

Table 1. Overlapping clinical features in ciliary dysfunction syndromes 5

Table 2. Bardet-Biedl Syndrome diagnostic criteria..... 6

Table 3. Human BBS genes with *Caenorhabditis elegans* orthologues and alleles..... 8

Table 4. Features observed in BBS models of *Mus musculus* 12

Table 5. Features observed in BBS models of *Danio rerio* 13

Table 6. Ciliated neurons, grouping, and functions 15

Table 7. Features observed in BBS models of *Caenorhabditis elegans*..... 18

Table 8. BBS functional domains and homology 19, 20

Table 9. Additional BBS protein interactors..... 30

Chapter 3. Mutations in a Guanylate Cyclase GCY-35/GCY-36 Modify Bardet-Biedl Syndrome-Associated Phenotypes in Caenorhabditis elegans

Table 10. *C. elegans bbs* alleles used in this study 65

Chapter 4. Analysis of Signalling Pathways that Affect the Body size of Caenorhabditis elegans

Table 11. List of *C. elegans* phosphodiesterases 97

Table 12. Guanylate cyclases and their expression patterns in *C. elegans*..... 99, 100

Appendix 1. *mobs-1(hp433)* Mapping

Table 13. Summary of SNP mapping results using *dpy-5* and *unc-54* markers 142

Table 14. Summarized results of *mobs-1* fosmid rescue injections..... 144

Table 15. Summary of *gcy-35* sequencing results 144

List of Figures

Chapter 1. Introduction

Figure 1. Basic diagram of the primary cilium 2

Figure 2. Distribution of the observed BBS mutational load..... 9

Figure 3. Diagram of observed interactions between BBS proteins and BBS-related components 10

Figure 4. Diagram of *C. elegans* ciliated neuron anatomical distribution, structure, and BBS function 16

Figure 5. The BBSome targets/traffics vesicles to the ciliary membrane..... 23

Chapter 3. Mutations in a Guanylate Cyclase GCY-35/GCY-36 Modify Bardet-Biedl Syndrome-Associated Phenotypes in Caenorhabditis elegans

Figure 6. Multiple phenotypes exhibited by *bbs* mutants 66

Figure 7. *bbs* mutants exhibit a smaller body size in late larvae and adulthood stages 67

Figure 8. *dyf* (dye-filling) mutants show variable body size and genetic interaction with *gcy-35(lf)*..... 68

Figure 9. *gcy-35(lf)* suppresses a subset of *bbs* phenotypes 70

Figure 10. GCY-35 and GCY-36 are required in body cavity neurons to influence body size.... 72

Figure 11. *bbs* mutants show no visible defects in GCY-35 or GCY-36 localisation 74

Figure 12. EGL-4 is an effector of GCY-35/GCY-36 in influencing body length and developmental timing..... 76

Figure 13. The cGMP-gated ion channel TAX-2/4 does not suppress the body size defects of *bbs* mutants..... 78

Figure 14. Multiple sensory neurons influence the body size of *bbs* mutants..... 80

Figure 15. Mutations in other guanylate cyclases do not suppress *bbs-7* body size defects 81

Chapter 4. Analysis of Signalling Pathways that Affect the Body size of Caenorhabditis elegans

Figure 16. Candidate components of the *C. elegans* cGMP signalling pathway 94

Figure 17. EGL-4 does not regulate body size through body cavity neurons alone 102

Figure 18. *bbs* mutants show no visible defects to EGL-4 localisation in body cavity neurons 104

Figure 19. *bbs* mutants show no visible defects to EGL-4 localisation in endogenously expressing neurons 105

Figure 20. Hypothesized model of PDE interaction in *bbs* mutant animals 107

Figure 21. Phosphodiesterases do not play a direct role in body cavity neurons to regulate *bbs* body size 108

Figure 22. *pde-5* regulates body size in parallel to *bbs* defects 110

Figure 23. Additional receptor-type guanylate cyclases and related components can play a synergistic role to body size 112

Figure 24. Model of receptor-type guanylate cyclises in *bbs* body size control 113

Figure 25. *mobs-2* is a suppressing locus similar to *gcy-35* 114

Chapter 5. Discussion and Future Directions

Figure 26. Model of cGMP-PKG body size regulation 134

Appendix 1. *mobs-1(hp433)* Mapping

Figure 27. Generic rough mapping scheme for *mobs-1* 139

Figure 28. Snip SNP mapping scheme using mutational markers on LGI 141

Figure 29. Snip-SNP mapping interval encompasses a number of fosmids 143

Figure 30. Sequencing results of *gcy-35* in *mobs-1(hp433);bbs-7* mutants 145

Appendix 2. GUCY1B2 Tissue Expression Pattern

Figure 31. Expression of *GUCY1B2* across multiple tissue panels 146

Appendix 4. Additional *Pegl-4a*::GFP::EGL-4 localization images

Figure 32. Additional representative images of EGL-4 localisation in endogenously expressing neurons 153-155

List of Appendices

Appendix 1. *mobs-1(hp433)* Mapping 139

Appendix 2. *GUCY1B2* Tissue Expression Pattern 146

Appendix 3. Strains used in this study 147

Appendix 4. Additional *Pegl-4a*::GFP::EGL-4 localization images 153

Nomenclature and List of Abbreviations

Species	**Gene Example**	**Protein Example**
Homo sapiens	*BBS1*	BBS1
Mus musculus	*Bbs1*	BBS1
Danio rerio	*bbs1*	Bbs1
Caenorhabditis elegans	*bbs-1*	BBS-1

ADP – Adenosine diphosphate

AHI1 – Abelson helper integration site 1

AKT – v-akt murine thymoma viral oncogene homolog

ALDOB – Aldolase B

APC – Adenomatous polyposis coli

ARL – ADP-ribosylation factor-like

ATP – Adenosine triphosphate

BBIP10 – BBSome interacting protein 1

BBS – Bardet-Biedl syndrome

BBSome – Octameric complex of evolutionarily conserved BBS proteins (BBS1, BBS2, BBS4, BBS5, BBS7, BBS8, BBS9) and one novel protein (BBIP10)

CaM – Calmodulin

CCT – Chaperonin containing TCP1

cDNA – Complementary DNA

CEP290 – Centrosomal protein 290kDA

CHE-2 – Abnormal chemotaxis

cGMP – Cyclic guanosine monophosphate

CNG – Cyclic nucleotide-gated ion channel

COPI/COPII – Coat protein complex

CYP11A1 - Cytochrome P450, family 11, subfamily A, polypeptide 1

CSN – ciliated sensory neuron

DAF-21 – Abnormal dauer formation

DAPI - 4',6-diamidino-2-phenylindole

DCTN1 – Dynactin 1

DiI – 1,1' - Dioctadecyl - 3,3,3',3' - tetramethylindocarbocyanine iodide

DNA – Deoxyribonucleic acid

Dnttip1 – Deoxynucleotidyltransferase interacting protein 1

Ds – Dachsous

Dsh – Dishevelled

dyf – abnormal dye filling

EEF1A1 – Eukaryotic translation elongation factor 1 alpha 1

EGL – Egg laying defective

Fmi – Flamingo

Fj – Four-jointed

flp-8 – FMRF-like peptide

FOXO – Forkhead box O1

FRET – Fluorescent resonance electron transfer

Ft – Fat

Fz – Frizzled

IFT – Intraflagellar transport

GAE – Gamma-adaptin ear domain

GC – guanylyl cyclase

GCaMP – GFP, Calmodulin, M13

GCY – Guanylate cyclase

GEF – Guanosyl exchange factor

gf – gain of function

GFP – Green fluorescent protein

GMP-PNP – 5′-Guanylyl-imidodiphosphate trisodium salt hydrate

GPA-3 – G-protein alpha subunit

GPCR – G protein-coupled receptor

GSK3β – Glycogen synthase kinase 3β

GTP – Guanosine triphosphate

GUCY1A1 – Guanylate cyclase 1, soluble alpha 1

GUCY1B1 – Guanylate cyclase 1, soluble beta 1

GUCY1B2 – Guanylate cyclase 1, soluble beta 2

HEK – Human embryonic kidney

HNOB – heme/NO-binding

HNOBA – heme/NO-binding associated

HSP90 – Heat shock protein 90kDA

IFT – Intraflagellar transport

IMCD3 – Inner medullary collecting duct

JATD – Jeune asphyxiating thoracic dystrophy

JBTS – Joubert syndrome

KAP-11 – Kinesin-associated protein

KIF3A – Kinesin family member 3A

KLP-1/KLP-20 – Kinesin-like protein

KV – Kuppfer's vesicle

LCA – Lebers congenital amaurosis

lf – Loss of function

lpo-6 – lipophilic dye abnormal

Ltap – Looptail

MCHR1 – Malanin-concentrating hormone receptor 1

MEF – Mouse embryonic fibroblast

MKKS – McKusick-Kaufman syndrome

MKS – Meckel-Gruber syndrome

MO – Morpholino

MT – Microtubule

MTOC – Microtubule organizing centre

mTOR – Mammalian target of rapamycin

NLS – Nuclear localization signal

NPHP – Nephronophthisis

NPY – neuropeptide Y

ODR-1 – Odorant response abnormal

OFD1 – Oral-facial-digital syndrome 1

OMIM – Online Mendelian Inheritance in Man

ONL – Outer nuclear layer

ORPK – Oak Ridge polycystic kidney

OSM-3 – Osmotic avoidance abnormal

PAS – Period, Arnt, Sim

PCM1 – Pericentriolar material 1

PCP – Planar cell polarity

PDE – phosphodiesterase

pdl-1 – Phosphodiesterase Delta like

Pk – Prickle-spiny-legs

PKD1 – Polycystic kidney disease 1

PKG – cGMP-dependent protein kinase

Ras – Rat Sarcoma

rGC – receptor-type guanylyl cyclase

RNA – Ribonucleic acid

RP – Retinitis pigmentosa

RPE – Retinal pigment epithelium

RPGR – Retinitis pigmentosa GTPase regulator

RPGRIP1L – Retinitis pigmentosa GTPase regulator interacting protein 1-like

saeg-1 – Suppressors of activated EGL-4

SDCCAG8 – Serologically defined colon cancer antigen 8

sGC – soluble guanylyl cyclase

Shh – Sonic hedgehog

siRNA – Small interfering RNA

SSTR3 – Somatostatin receptor type 3

STR-2 – Seven transmembrane receptor

tax-2 – Abnormal chemotaxis

TeTx – Tetanus toxin

TGF-β – Transforming growth factor β

TORC1/2 – Target of rapamycin complex

TPR – Tetratricopeptide repeat

TRERF1 – Transcriptional regulating factor 1

UCR1 – Upstream conserved region

Vang – Van gogh

WDPCP – WD repeat containing planar cell polarity effector

WT – wild-type

ZNF541 – Zinc-finger protein

ZPA – Zone of polarizing activity

Chapter 1
Introduction

1.1 Primary Cilia are Important, Evolutionarily Conserved Organelles

Cilia, as well as flagella, are ancient, evolutionarily conserved organelles that project from the plasma membrane of eukaryotic cell bodies. These cellular projections participate in a number of roles ranging from mechanistic forms of movement (whole-cell locomotion, fluid movement, and sexual reproduction) to signalling (chemo-, thermo-, mechano-, and photosensation) (Evans *et al.* 2006). Primary cilia, unlike eukaryotic flagella, are thought to be ubiquitously present in all mammalian cell types (Satir *et al.* 2008) and play important sensory functions in receiving stimuli such as light, odour, sound, and fluid flow. In invertebrates such as *Caenorhabditis elegans*, these sensory organs are responsible for behavioural reactions to simple chemo-, thermo- and mechanostimuli (Inglis *et al.* 2007).

Structurally, the cilium begins at the basal body, which is located internally near the plasma membrane (**Figure 1**). The basal body originates from a mother centriole and acts as a microtubule (MT) organizing centre. From here, a circular set of nine MT doublets extends past the cell surface, surrounded by a specialized ciliary membrane distinct from that of the plasma membrane (Gilula *et al.* 1972) (reviewed in (Rohatgi *et al.* 2010)). Generally, the non-motile primary cilium has no additional MT structures (9+0) while motile cilia and flagella include a pair of single MTs surrounded by the nine MT doublets (9+2) (Fawcett 1954; Perkins *et al.* 1986). There are, however, instances of (9+0) motile cilia and vice versa (Sobkowicz *et al.* 1995; Nonaka *et al.* 1998). In both organelles, the lipid and protein composition of the ciliary membrane is tightly regulated to display a wide array of specialized receptors that participate in a number of specific roles (Haimo *et al.* 1981; Pazour *et al.* 2002; Davenport *et al.* 2005; Schneider *et al.* 2005; Rohatgi *et al.* 2007; Baker *et al.* 2009).

The biogenesis, function, and maintenance of primary cilia require the bidirectional movement of specialized motors and rafts that help to transport additional proteins to and from the cilium surface (reviewed in (Bisgrove *et al.* 2006)). First described in *Chlamydomonas reinhardtii* (Kozminski *et al.* 1993), this process of organized movement is known as intraflagellar transport

(IFT). IFT proteins involved in anterograde loading and movement include a heterotrimeric kinesin-II complex, an OSM-3/KIF17 and IFT raft B cargoes whereas dynein and raft A proteins comprise the machinery for retrograde turnover and movement (Johnson *et al.* 1992; Cole *et al.* 1993; Cole *et al.* 1998; Pazour *et al.* 1998; Pazour *et al.* 1999; Signor *et al.* 1999).

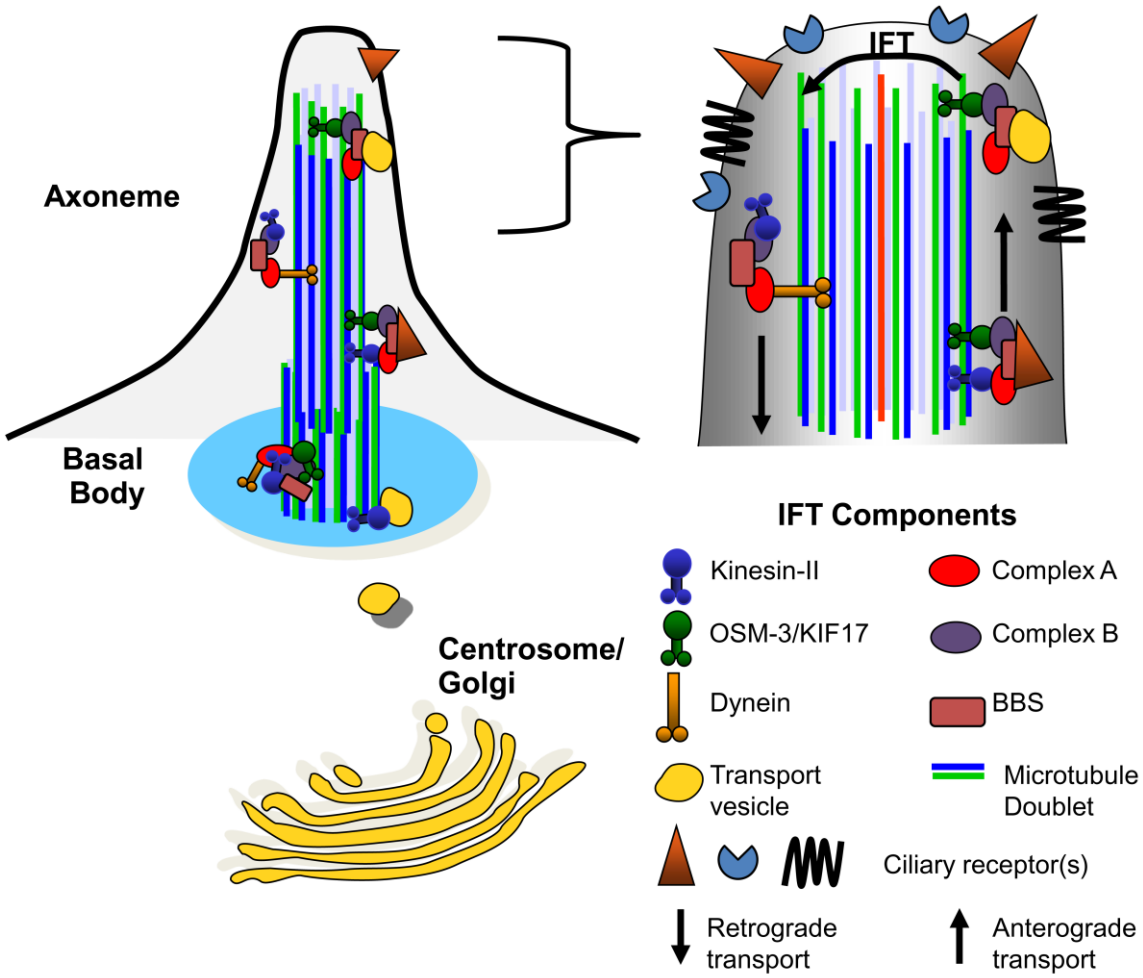

Figure 1. Basic diagram of the primary cilium. The primary cilium forms an organelle extending from the plasma membrane. Beginning with a basal body composed of a mother centriole, this extends to form the basis of the ciliary axoneme which is composed of nine microtubule doublets arrayed in a circular fashion. The ciliary membrane's lipid and protein composition vary from that of the plasma membrane through the specialized movement of cargoes including ciliary receptors via intraflagellar transport (IFT). Modified from (Mok *et al.* 2010).

The entrance of ciliary components to the axoneme is tightly controlled at the basal body and transition zone, which acts as a gate for the primary cilium (Craige *et al.* 2010; Williams *et al.* 2011). Some proteins which localize only at the basal body may participate in the initial formation of the primary cilium through selective loading and/or the sorting of IFT cargoes as they arrive from the centrosome.

Primary cilia are evolutionarily conserved throughout the eukaryotes as far back as early protists (Carvalho-Santos *et al.* 2011). It is hypothesized that these organelles were present prior to the divergence from the last eukaryotic common ancestor (Satir *et al.* 2008). They may be present as sensory structures, and/or act in modes of movement such as in *C. reinhardtii*. This simple alga consists of a single cell with two motile ciliary projections that also participate in phototactic signal transduction responses. More recently, the study of diseases through animal models has expanded the role of the primary cilia to include complex developmental signalling pathways such as Sonic Hedgehog, Wnt, and planar cell polarity pathways (see section 1.7).

The primary cilium is therefore a specialized signalling center at which a number of molecules specifically localize such as polycystin-1 (PKD1) and polycystin-2 (PKD2) (Yoder *et al.* 2002); the vertebrate Sonic hedgehog proteins Patched1 (Rohatgi *et al.* 2007) and Smoothened (Corbit *et al.* 2005); G-protein coupled receptors such as somatostatin receptor type 3 (SSTR3) and melanin-concentrating hormone receptor 1 (MCHR1) (Berbari *et al.* 2008b); and Jouberin (AHI1), which facilitates the nuclear translocation of β-catenin in Wnt signalling (Lancaster *et al.* 2011). Dependent upon the cell-type, these organelles can accumulate specific signalling molecules with a diverse range of purposes. *C. elegans*, for example, expresses an array of guanylate cylcases across different subsets of ciliated neurons, augmenting or contributing to the specialization of these sensory neurons (Yu *et al.* 1997; Birnby *et al.* 2000; Cheung *et al.* 2004; Inada *et al.* 2006). Even specialized ciliary targeting peptide motifs are required for the transport of some signalling molecules to the cilium (Berbari *et al.* 2008a). In some cases, specific signalling events can shift the localization pattern of proteins to the axoneme of the primary cilium (Corbit *et al.* 2005; Lancaster *et al.* 2011)(**Figure 1**). The activation of ciliary receptors, which include the G-protein-coupled-receptors (GPCRs) can activate downstream signalling cascades, resulting in the transduction of external signals along the membrane or even to the nucleus (Liu *et al.* 2010; Hao *et al.* 2011). The transport to, accumulation in, and movement of cargo along the primary cilium requires a number of proteins that are also involved in the structure of this specialized signalling apparatus (reviewed in (Carvalho-Santos *et al.* 2011)). This seemingly simple organelle participates in a plethora of signalling pathways and its dysfunction is associated with a growing class of complex human disorders known as the ciliopathies.

1.2 Ciliopathies are a Growing Class of Disorders Related to Ciliary Dysfunction

In recent years, a number of human disorders have been recognized as part of an emerging disease class: ciliopathies, based on a common relationship with the primary cilium. Some diseases such as Bardet-Biedl Syndrome (BBS; OMIM 209900), Meckel-Gruber syndrome (MKS; OMIM 249000), Nephronophthisis (NPHP, OMIM 256100) and Joubert Syndrome (JBTS; OMIM 213300) are pleiotropic, while others such as Lebers Congenital Amaurosis (LCA; 204000) and Jeune asphyxiating thoracic dystrophy (JATD; 208500) have fewer cardinal features (**Table 1**).

Until recently, these conditions were considered isolated clinical entities, associated with the primary cilium either through localization patterns, shared molecular pathways, or known associations with the ciliary proteome (reviewed in (Dryja *et al.* 2001; Mollet *et al.* 2002; Roepman *et al.* 2005; Delous *et al.* 2007; Zaghloul *et al.* 2009)). Extensive phenotyping of ciliopathy animal models also revealed phenotypes that expanded the human clinical features of BBS (Kulaga *et al.* 2004; Ross *et al.* 2005; Tan *et al.* 2007). For example, defects to cochlear stereocilia formation in *Bbs4*$^{-/-}$ and *Bbs6*$^{-/-}$ mice, led to the identification of subclinical hearing loss in human BBS patients (Ross *et al.* 2005) (see section 1.4.1). Despite the underlying genetic heterogeneity of these disorders, their relationship with the primary cilium suggests common molecular pathways. Moreover, there is growing evidence to support that the allelic variants of some ciliopathy genes can be linked to specific clinical diagnoses. In the case of *MKS1*, hypomorphic alleles have been identified in patients diagnosed for BBS while null alleles have only been verified in MKS patients (Kyttala *et al.* 2006; Khaddour *et al.* 2007; Leitch *et al.* 2008). These findings confirm a shared genetic basis for the pathophysiology of overlapping features (Leitch *et al.* 2008; Otto *et al.* 2009).

Alone, the occurrence of each specific clinically defined ciliopathy is relatively low. The overall incidence of the ciliopathies as a group, however, exceeds 1 in 1,000, making the impact of this group much higher (Zaghloul *et al.* 2009). Given the combined occurrence for this class of diseases, it is advantageous to study a disease model that will best elucidate a wide range of ciliopathy features.

Table 1. Overlapping Clinical Features in Ciliary Dysfunction Syndromes

Disease	BBS	OFD1	SLS	MKS	JBTS	JATD	MKKS	NPHP	LCA
Retinitis pigmentosa	✓		✓	✓	✓			✓	✓
Renal cystic disease	✓	✓	✓	✓	✓	✓		✓	
Polydactyly	✓	✓		✓	✓		✓		
Obesity	✓				✓				
Situs inversus/isomerism	✓		✓	✓	✓				
Mental retardation/ developmental delay	✓	✓		✓	✓			✓	✓
Hypoplasia of corpus callosum	✓	✓		✓	✓			✓	
Dandy-Walker malformation	✓		✓	✓	✓				
Posterior encephalocele	✓†			✓	✓				
Hepatic disease	✓	✓†	✓	✓	✓			✓	
Hydrometrocolpos	✓						✓		
Total number of consistently observed phenotypes in each disorder	11	5	5	9	10	1	2	5	2

Modified from (Baker *et al.* 2009; Zaghloul *et al.* 2009) † in mice

1.3 Bardet-Biedl Syndrome, a Pleiotropic, Heterogeneous, Ciliopathy Model

Bardet-Biedl Syndrome is an autosomal recessive, genetically heterogeneous, pleiotropic disorder. BBS was defined in the early 1900's by the association of digit anomalies, retinal degeneration, obesity and mental retardation (Laurence 1866; Bardet 1920; Biedl 1922). The estimated prevalence is 1 in 160,000 individuals in North American and European populations with nearly a ten-fold higher rate found in some isolated populations (Klein *et al.* 1969; Farag *et al.* 1988; Farag *et al.* 1989).

Since being first described, the diagnosis of BBS has been refined to include primary features such as photoreceptor degeneration, obesity, hypogonadism, digit anomalies and renal anomalies, as well as developmental delay (as opposed to mental retardation). Secondary features include but are not limited to hearing loss, diabetes mellitus, cardiovascular abnormalities, and liver anomalies (**Table 2**). The current suggested clinical diagnosis of BBS requires the presence of either four primary features or three primary and two secondary features (Beales *et al.* 1999). These patients have a shortened life expectancy, largely due to cystic renal disease or the complications associated with obesity (Riise 1996).

Table 2. Bardet-Biedl Syndrome Diagnostic criteria

Primary Features		Secondary Features	
Photoreceptor degeneration	93%	Speech/Developmental delay	47/50%
Digit anomaly	69%	Strabismus/cataracts/astigmatism	-
Overweight/Obese	72/52%	Polyuria/polydipsia (nephrogenic diabetes insipidus)	33%
Learning disabilities	62%	Ataxia/poor coordination/imbalance	40%
Hypogonadism (males)/genital abnormalities (females)	96%	Mild spasticity	-
Renal abnormalities	46%	Diabetes mellitus	6%
		Dental crowding/hypodontia/small roots/high arched palate	27%-88%
		Left ventricular hypertrophy/congenital heart disease	-
		Hepatic fibrosis	
		Hyposmia/anosmia, Hearing deficits	
		Nociception/thermosensation	

Modified from (Beales *et al.* 1999; Kulaga *et al.* 2004; Ross *et al.* 2005; Tan *et al.* 2007). Percentages modified from (Beales *et al.* 1999)

To date, sixteen genes have been identified as causal to BBS (**Table 3**) (Katsanis *et al.* 2000; Mykytyn *et al.* 2001; Nishimura *et al.* 2001; Mykytyn *et al.* 2002; Ansley *et al.* 2003; Badano *et al.* 2003a; Koenekoop 2003; Chiang *et al.* 2004; Fan *et al.* 2004; Li *et al.* 2004; Nishimura *et al.* 2005; Chiang *et al.* 2006; Stoetzel *et al.* 2006; Stoetzel *et al.* 2007; Leitch *et al.* 2008; Kim *et al.* 2010; Otto *et al.* 2010). The mutational analysis of a number of BBS patient cohorts shows that a large percentage of BBS mutation load (60%) is attributed to *BBS1*, *BBS2*, *BBS10* and *BBS12* (**Figure 2**) (Zaghloul *et al.* 2009; Deveault *et al.* 2011). The remaining genes each share 5% or less of the known mutation load while 21-24% of cases have no mutation identified (Zaghloul *et*

al. 2009; Deveault *et al.* 2011; Mockel *et al.* 2011). A recent calculation based on the reported mutational load in BBS cohorts, estimated the number of BBS carriers within the general population as 1 in 50 in Northern European populations (Laurier *et al.* 2006). Clinical assessment of BBS patients also identified a range of phenotype variability (**Table 2**) both within and between families suggesting the involvement of environmental or genetic modifiers. Although there has been no formal assessment of environmental influence on BBS phenotype severity, there has been evidence to suggest that second-site genetic modifiers could explain some cases of phenotypic variability (see section 1.8) (Katsanis *et al.* 2001; Badano *et al.* 2006; Khanna *et al.* 2009; Zaghloul *et al.* 2010).

In other species, a subgroup of BBS proteins are conserved across a diverse evolutionary background that includes *Caenorhabditis elegans* (38-64% similarity) and *Chlamydomonas reinhardtii* (33-52%) (Lechtreck *et al.* 2009) while the remainder appear to be vertebrate-specific. As a whole, these proteins lack a high degree of domain similarity; loss of function, however, leads to similar disease features. A majority of the BBS proteins are classified into two functional groups; the BBSome and the chaperonin-like complex. The BBSome is a heptameric complex consisting of BBS1, 2, 4, 5, 7, 8, 9 which transiently associates with an activated (GTP-bound) form of BBS3 (Nachury *et al.* 2007; Jin *et al.* 2010). The BBS chaperonin-like proteins of BBS6, 10, and 12 form the other known functional complex from these diverse proteins and are responsible for the formation of the BBSome (Seo *et al.* 2010) (see section 1.5.4). Of these two known subcomplexes, the BBSome localizes to the evolutionarily conserved and ubiquitous primary cilium (Ansley *et al.* 2003). Of the remaining BBS proteins, BBS13/MKS1 and BBS14/CEP290 are thought to participate in a transition zone complex to regulate the formation of the primary cilium (Williams *et al.* 2011), while BBS11, BBS15, and BBS16 have yet to be assigned to specific protein complexes (**Figure 3**).

Below I describe the study of different model organisms of BBS, which has been essential to clarifying some of the pathobiological mysteries of this disease.

Table 3. Human BBS genes with *C. elegans* orthologues and alleles

Human Gene	Locus	Putative function	*C. elegans* gene	Locus	Mutants/Alleles available
BBS1	11q3	BBSome, Vesicular Trafficking	*Y105E8A.5, bbs-1*	I:24.52	**ok1111**
BBS2	16q21	BBSome, Vesicular Trafficking	*F20D12.3, bbs-2*	IV:3.50	**gk544**, tm321, tm3044, ok2053
BBS3, ARL6	3p11.2	Vesicular Trafficking	*C38D4.8, bbs-3*	III:-2.45	ok3472
BBS4	15q22.3	BBSome, Vesicular Trafficking, Centriolar Satellite Organization	*F58A4.14, bbs-4*	III:0.75	tm3038
BBS5	2q31	BBSome, Vesicular Trafficking	*R01H10.6, bbs-5*	III:2.10	gk507, gk537
BBS6, MKKS	20p12	Chaperonin-like/CCT complex, BBSome assembly	--	--	--
BBS7	4q27	BBSome, Vesicular Trafficking	*Y75B8A.12, bbs-7, osm-12*	III:16.13	**n1606**, **ok1351**
BBS8, TTC8	14q32.11	BBSome, Vesicular Trafficking	*T25F10.5, bbs-8*	V:0.13	**nx77**, ut306
BBS9, PTHB1	7p14	BBSome, Vesicular Trafficking	*C48B6.8, bbs-9*	I:1.50	**gk471**, ok5011
BBS10	12q	Chaperonin-like/CCT complex, BBSome assembly	--	--	--
BBS11, TRIM32	9q33.1		--	--	--
BBS12	4q27	Chaperonin-like/CCT complex, BBSome assembly	--	--	--
BBS13, MKS1	17q23	Ciliary gate	*R148.1, xbx-7*	III:-7.81	tm2705
BBS14, CEP290	12q21.3	Ciliary gate	--	--	--
BBS15, Fritz, C2orf86, WDPCP	2p15	Unknown	--	--	--
BBS16, SDCCAG8	1q43	Unknown	--	--	--

***Bold** = alleles used in this study

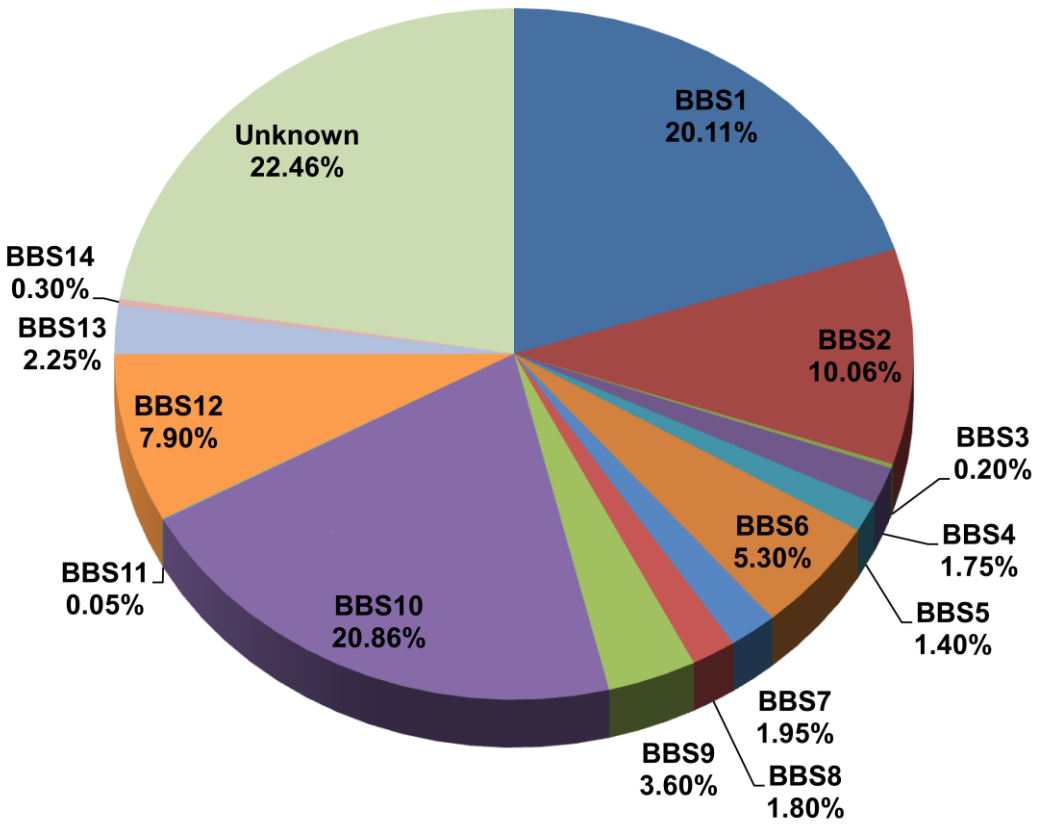

Figure 2. Distribution of the observed BBS mutational load. The distribution of mutational load for BBS patients after molecular analysis of BBS genes reported for BBS1 through BBS14. BBS15 and BBS16 are reported to have a minor (1%) contribution in some cohorts. Data combined from (Zaghloul *et al.* 2009; Deveault *et al.* 2011)

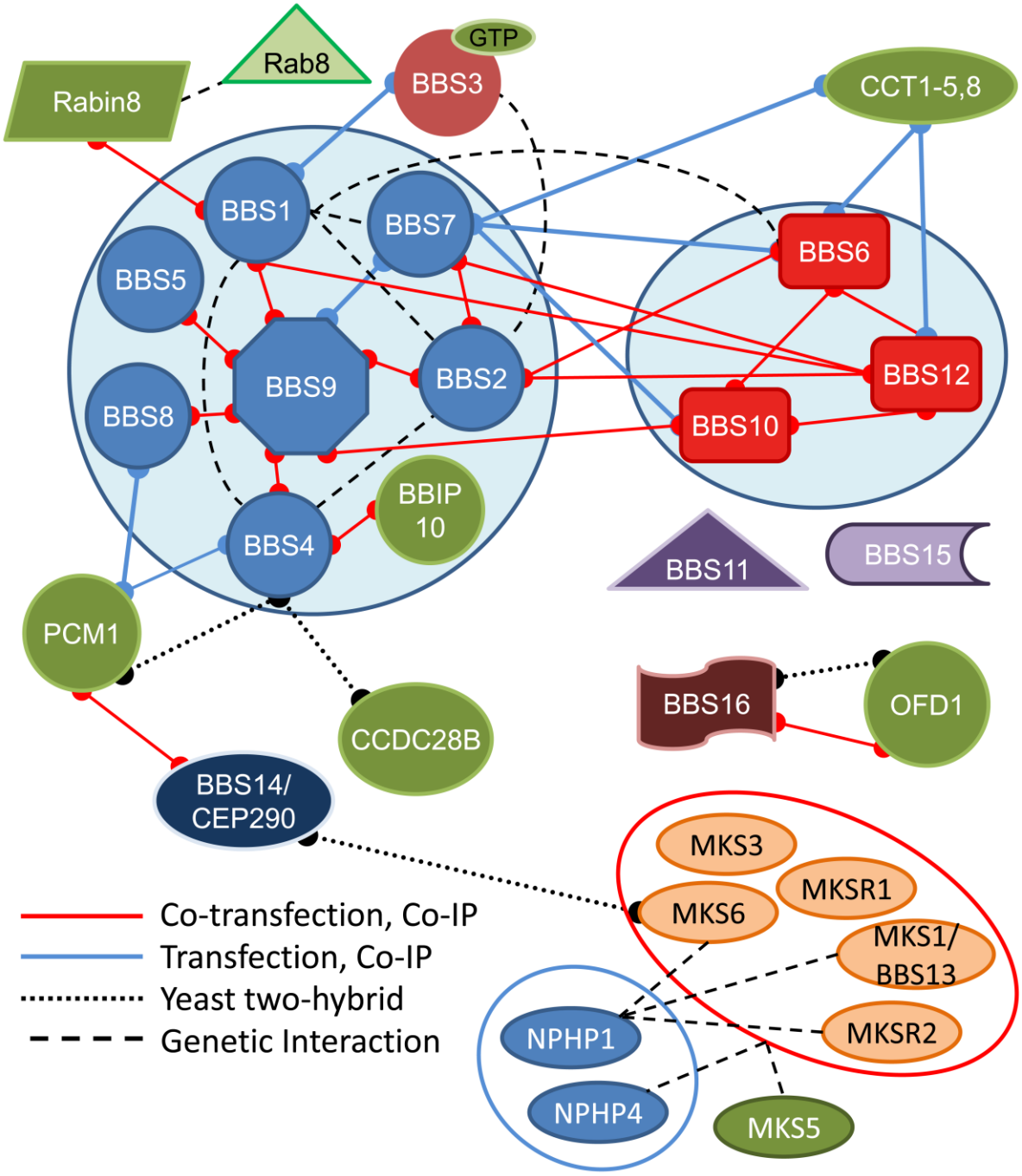

Figure 3. Diagram of observed interactions between BBS and BBS-related components. Most BBS proteins can be classified into 3 main groups: BBSome (BBS1, 2, 4, 5, 7, 8, 9), type II chaperonin-like (BBS6, 10, 12), and transition zone (BBS13/MKS1, BBS14/MKS4/CEP290) components. The GTP-bound (activated form) of BBS3 associates transiently with the BBSome. BBS11, BBS14, BBS15 and BBS16 have no reported interactions with other BBS components. The transition zone proteins appear to function in 3 distinct groups where both NPHP4 and MKS5 appear to interact with all other MKS proteins while NPHP1 only has genetic interactions with some. Solid lines represent protein interactions, dotted lines represent yeast two-hybrid data and dashed lines represent genetic interactions. Where applicable, genetic interactions are replaced by protein interactions. Data combined from (Gorden *et al.* 2008; Nachury 2008; Tayeh *et al.* 2008; Jin *et al.* 2010; Seo *et al.* 2010; Williams *et al.* 2011)

1.4 Animal Models of Bardet-Biedl Syndrome

1.4.1 Mouse BBS Models Recapitulate Human Phenotypes

Murine models of BBS have been extraordinary in not only recapitulating but expanding the spectrum of human clinical features as well, (**Table 4**) while helping to dissect certain aspects of pathophysiology in this disease. Murine BBS knockout mice (*Bbs2*$^{-/-}$, *Bbs 4*$^{-/-}$, and *Bbs 6*$^{-/-}$) are first born slightly underweight in comparison to wild-type littermates. By 12-16 weeks these animals along with *Bbs3*$^{-/-}$ and the knock-in model *Bbs1*$^{M390R/M390R}$ are larger and have significantly higher stores of fat, when fed ad libitum (Mykytyn *et al.* 2004; Nishimura *et al.* 2004; Fath *et al.* 2005; Davis *et al.* 2007; Zhang *et al.* 2011). These models have been helpful in highlighting BBS-related obesity as due to defects in both adipogenesis and satiety (Seo *et al.* 2009)(reviewed in (Mok *et al.* 2010)). Photoreceptor degeneration is documented across all *Bbs* models but is observed as early as six weeks (*Bbs2*$^{-/-}$, *Bbs6*$^{-/-}$) by electroretinography and leads to complete absence of photoreceptor cells as early as 7-8 months (*Bbs4*$^{-/-}$, *Bbs6*$^{-/-}$) (Mykytyn *et al.* 2004; Nishimura *et al.* 2004; Fath *et al.* 2005; Davis *et al.* 2007; Zhang *et al.* 2011). Cystic renal phenotypes are reported to develop by 5 months of age in *Bbs2*$^{-/-}$ animals while there is an absence of this phenotype in the *Bbs1*$^{M390R/M390R}$ knock-in animals. Olfaction defects are also a common trait amongst some *Bbs*$^{-/-}$ animals. The primary feature of polydactyly has not been recapitulated in any models of BBS (Mykytyn *et al.* 2004; Nishimura *et al.* 2004; Fath *et al.* 2005; Davis *et al.* 2007; Zhang *et al.* 2011). This is especially interesting given that digit anomalies have been observed in a genetrap model of the ciliary gene, *Ift80*, which is associated with Jeune asphyxiating thoracic dystrophy (Rix *et al.* 2011), thus suggesting that BBS protein function has diverged between humans and mice.

Through these studies, the murine model has also been key to identifying a number of previously uncharacterized human features including anosmia, encephalocele, hydrocephalus, abnormal cochlear stereociliary organization, as well as thermo- and mechanosensory deficits among others (Kulaga *et al.* 2004; Ross *et al.* 2005; Tan *et al.* 2007).

Table 4. Features observed in BBS models of *Mus musculus*

Phenotype	*Bbs1*$^{M390R/M390R}$	*Bbs2*$^{-/-}$	*Bbs3*$^{-/-}$	*Bbs4*$^{-/-}$	*Bbs6*$^{-/-}$
Photoreceptor Degeneration	Functional differences at 11 weeks ONL significantly degenerated at 6 months	ONL loss observed at 6-8 weeks ONL absent at 10 months	ONL loss observed by 4 months	ONL loss observed at 6 weeks ONL absent at 7 months	ONL loss observed at 2-3 months ONL absent at 8 months
Stunted at birth	Not identified	Until 3 months	Not measured	Until at least 3 weeks	Until at least 3 weeks
Obese	3.5-6 months	4 months	Increased fat mass but not obese	3 months	7 months
Renal anomalies	None	Cysts	Not measured	Not measured	Not measured
Sperm flagellar defects	Yes	Yes	Yes	Yes	Yes
Decreased acoustic response	Not measured	Yes	Not measured	Not significant	Not significant
Diminished olfaction	Not measured	Yes	Not measured	Yes	Yes
Polydactyly	No	No	No	No	No
Neuroanatomical defects	Enlarged ventricles	Not measured	Hydrocephalus	Not measured	Not measured
Cardiovascular	Increased heart rate	Not measured	Elevated heart rate	Not measured	Not measured

Data combined from (Mykytyn *et al.* 2004; Nishimura *et al.* 2004; Eichers *et al.* 2006; Davis *et al.* 2007; Zhang *et al.* 2011)

1.4.2 Zebrafish BBS Models Identify Signalling Pathways

Danio rerio, in recent years, has been a helpful model for studying BBS function and genetic interactions using a morpholino knockdown technology. This technique has facilitated the assessment of *bbs* loss of function and variant phenotypes (**Table 5**). Morpholino technology has also allowed the validation of a number of *bbs* loss-of-function, *bbs*-interacting or *bbs*-modifying genes (Ross *et al.* 2005; Badano *et al.* 2006; Tayeh *et al.* 2008; Zaghloul *et al.* 2010; Pretorius *et al.* 2011).

The cardinal *bbs* morpholino zebrafish phenotypes include dorsal thinning and defective somite morphology, as well as defects to the formation of the transiently ciliated organelle called the Kuppfer's vesicle (KV) (Ross *et al.* 2005; Yen *et al.* 2006). At the cellular level, *bbs* morphants possess significant defects to retrograde melanosome transport, and renal malformation. These

morphants also exhibit an expansion of Sonic Hedgehog expression although this does not result in any discernible defective limb bud formation (Yen *et al.* 2006; Tayeh *et al.* 2008; Tobin *et al.* 2008). Furthermore, in the "startle/reaction" test, *bbs* morphants show severe delays in reacting to light, indicating defective phototransduction (Pretorius *et al.* 2010; Pretorius *et al.* 2011).

Landmark studies in zebrafish include bringing to light the relationships between BBS and planar cell polarity (PCP) signalling, as well as the importance of tissue-specific BBS isoforms in phototransduction (Ross *et al.* 2005; Tayeh *et al.* 2008; Pretorius *et al.* 2010; Pretorius *et al.* 2011). Additionally, morpholino studies in zebrafish have also shown genetic interactions between *bbs1* and five other *bbs* genes (*bbs2*, *bbs3*, *bbs4*, *bbs6*, and *bbs7*) as well as between *bbs2* and three *bbs* genes (*bbs3*, *bbs4*, and *bbs6*) helping to identify some possible structural relationships within the BBSome (Tayeh *et al.* 2008).

Table 5. Features observed in BBS models of *Danio rerio*

Phenotype	*bbs1*	*bbs2*	*bbs3*	*bbs4*	*bbs5*	*bbs6*	*bbs7*	*bbs8*	*bbs9*	*bbs10*	*bbs11*	*bbs12*	*bbs13*	*bbs14*	*bbs15*	*bbs16*
Kupffer's Vesicle abrogation	✓	✓	✓	✓	✓	✓	✓	✓			✓					
Retrograde melanosome transport defects	✓	✓	✓	✓	✓	✓	✓	✓			✓					
Increased organ laterality defects	✓	✓	✓	✓	✓	✓	✓	✓			✓					
Developmental defects (convergent extension, gastrulation)	✓	✓	✓	✓	✓	✓	✓	✓	✓	✓		✓	✓	✓		✓
Expanded Shh signalling	✓						✓									
Renal cyst				✓		✓		✓								
Startle response defect			✓													
Rescued by human mRNA	✓	✓	✓	✓	✓	✓	✓	✓		✓	✓	✓	✓	✓		

Data combined from (Ross *et al.* 2005; Badano *et al.* 2006; Chiang *et al.* 2006; Yen *et al.* 2006; Stoetzel *et al.* 2007; Leitch *et al.* 2008; Tobin *et al.* 2008; Otto *et al.* 2010; Pretorius *et al.* 2010; Zaghloul *et al.* 2010) No data available on *bbs9* and *bbs15*

1.4.3 *Caenorhabditis elegans* BBS Models Dissect Molecular Functions

The nematode *Caenorhabditis elegans* is a simple, diploid invertebrate organism with a short reproductive life cycle, a well studied cellular lineage, and a compact genome of ~100 Mb that encodes approximately 20,000 genes (Brenner 1974; Sulston *et al.* 1977; Sulston *et al.* 1983). Its small and translucent body is particularly suitable for live imaging studies using GFP or other fluorescent molecular tags (Chalfie *et al.* 1994; Ou *et al.* 2005).

Of the 959 somatic cells in the mature adult hermaphrodite worm, 302 are specified as neurons. Approximately 60 of those neurons are ciliated and are the only ciliated cells within *C. elegans* (Ward *et al.* 1975). Many of these ciliated neurons are exposed to the worm's environment, providing sensory input for the nematode to interpret its surroundings (Evans *et al.* 2006).

Of the 60 ciliated neurons, twenty-four are distributed into two anatomically symmetric bundles (twelve pairs) collectively identified as the amphids (**Figure 4A**, **Table 6**) and two symmetric pairs are bundled in the posterior region identified as the phasmids. The remaining groups of neurons include the inner and outer labial neurons, the ciliated deirid neurons, neurons that terminate at the lateral lips of the worm (BAG, FLP) and the pseudocoelomic neurons (AQR, PQR), whose cell bodies and cilia are exposed to the pseudocoelomic cavity.

The basic components of *C. elegans* cilia are similar to most primary cilia and encompass a number of important features including the anterograde and retrograde transport of protein cargoes (IFT) and the presence of a small basal body, which is just proximal to what is historically known as the transition zone (Inglis *et al.* 2007; Williams *et al.* 2011) (**Figure 4B**). The axoneme of the *C. elegans* cilium, similar to that of the vertebrate axoneme in many human cell types, is divided into a middle and distal segment although the composition can vary between some ciliated neurons (for review see (Silverman *et al.* 2009)). The middle segment is composed of a 9 MT doublet structure encompassing a variable number of MT singlets, while the distal segment is composed of 9+0 MT singlets. The middle segment of MT doublets is traversed by two motor anterograde motors: heterotrimeric Kinesin-II (KAP-1, KLP-11, KLP-20) and the homodimeric OSM-3/KIF17. At the distal segment, only OSM-3 actively undergoes IFT as identified in motor-dynamics studies (Snow *et al.* 2004; Ou *et al.* 2005; Pan *et al.* 2006).

Table 6. *C. elegans* ciliated neurons, grouping, and functions

Ciliated Neuron	Cilium Structure	Sensory Group	DiI/FITC	General Function
ASE (L/R)	Single rod	Amphid		Asymmetrical Chemoattraction
ADF (L/R)	Pair of rods	Amphid	DiI, FITC	Dauer entry, Chemoattraction
ASG (L/R)	Single rod	Amphid		Chemoattraction, dauer entry, lifespan
ASH (L/R)	Single rod	Amphid	DiI, FITC	Mechano (nose touch) and osmotic sensation, chemorepulsion
ASI (L/R)	Single rod	Amphid	DiI, FITC	Chemoattraction, dauer entry
ASJ (L/R)	Single rod	Amphid	DiI, FITC	Dauer exit, Chemotaxis, lifespan
ASK (L/R)	Single rod	Amphid	DiI, FITC	Chemoattraction, lifespan
ADL (L/R)	Pair of rods	Amphid	DiI, FITC	Chemorepulsion, social feeding behaviour
AWA (L/R)	Winged	Amphid		Chemoattraction, lifespan
AWB (L/R)	Winged	Amphid		Chemorepulsion
AWC (L/R)	Winged	Amphid		Chemo- and thermosensation, lifespan
AFD (L/R)	Small, enclosed by dendritic villi	Amphid		Thermosensation, CO_2
IL1(L/R), (DL/DR), (VL/VR)		Inner Labial		Mechanosensation (nose touch)
IL2 (L/R), (DL/DR), (VL/VR)		Inner Labial	DiI	Nictation
CEP (DL/DR), (VL/VR)		Cephalic	FITC *	Mechanosensation (Basal slowing response)
OLQ (DL/DR), (VL/VR)		Outer Labial		Mechanosensation (Nose touch and basal slowing response)
OLL (L/R)		Outer Labial		Mechanosensation (putative)
BAG (L/R)		Bag-like		O_2 and CO_2 sensation
FLP (L/R)		Flap-like		Mechanosensation (nose touch)
ADE (L/R)	Single rod	Ciliated Deirid	FITC *	Mechanosensation (Basal slowing response)
PDE (L/R)	Single rod	Ciliated Deirid	FITC *	Mechanosensation (Basal slowing response)
PHA (L/R)	Single rod	Phasmid	DiI, FITC	Chemorepulsion
PHB (L/R)	Single rod	Phasmid	DiI, FITC	Chemorepulsion
AQR		Pseudocoelomic		Oxygen-sensation, social feeding
PQR		Pseudocoelomic		Oxygen-sensation, social feeding

L (left), R (right), D (dorsal), V (ventral), * (occasional). Modified from (Inglis *et al.* 2007)

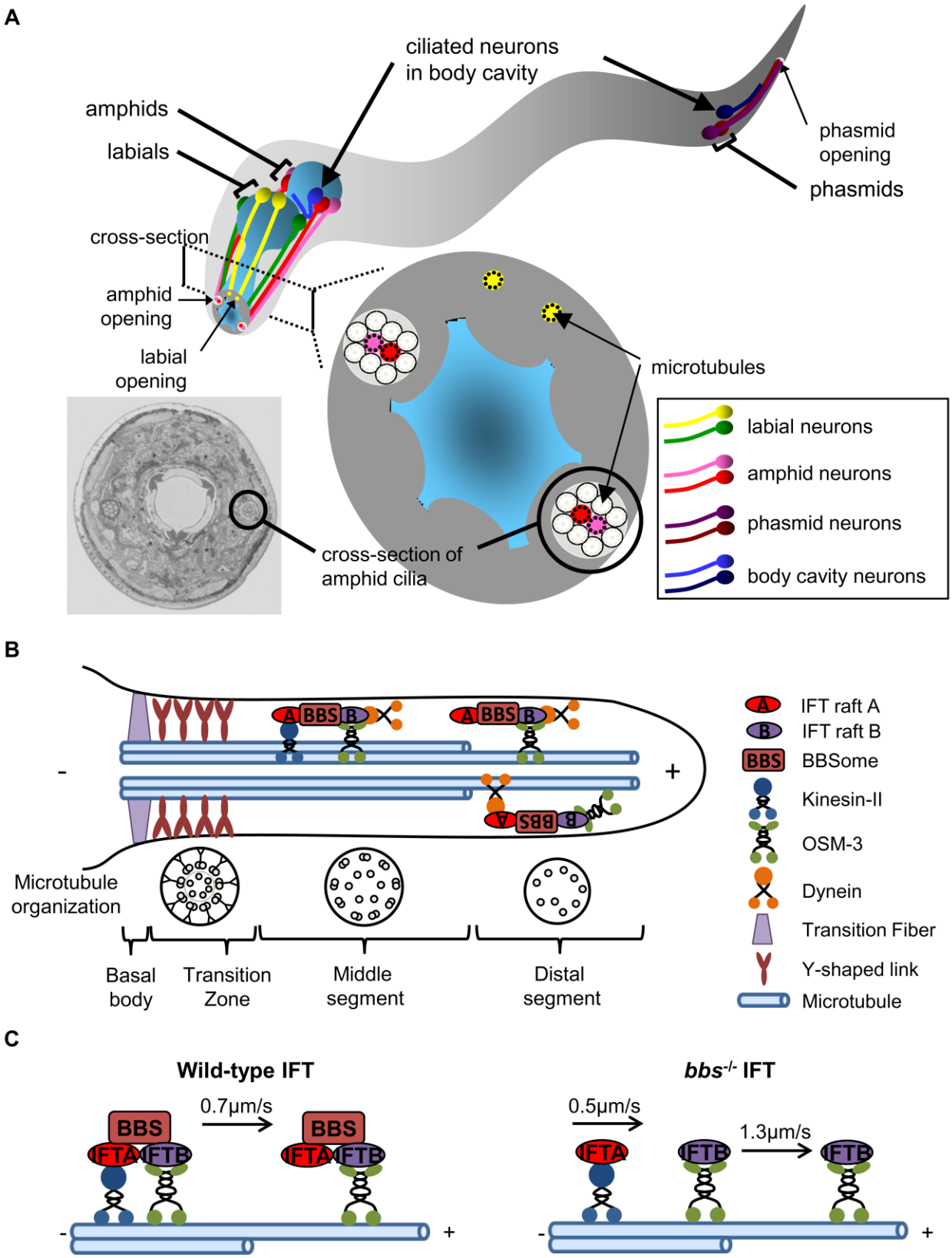
A
ciliated neurons
in body cavity
amphids
labials
phasmid
opening
phasmids
cross-section
amphid
opening
labial
opening
microtubules
cross-section of
amphid cilia
labial neurons
amphid neurons
phasmid neurons
body cavity neurons
B
BBS
A
B
-
+
Microtubule
organization
Basal
body
Transition
Zone
Middle
segment
Distal
segment
IFT raft A
IFT raft B
BBSome
Kinesin-II
OSM-3
Dynein
Transition Fiber
Y-shaped link
Microtubule
C
Wild-type IFT
0.7μm/s
BBS
IFTA
IFTB
bbs-/- IFT
0.5μm/s
1.3μm/s

Figure 4. Diagram of *C. elegans* ciliated neuron anatomical distribution, structure, and BBS function. (A) The 60 ciliated neurons of *C. elegans* are distributed mostly in the head as a sensory group known as the amphids and in a tail group known as the phasmids. The remaining groups of neurons include the labial, deirid, cephalic, and pseudocoelomic (body cavity) neurons. Also depicted is a cross-section of the amphid cilia positioning at the *C. elegans* nose. (B) Cartoon of *C. elegans* cilia depicting known structural elements. A series of transition fibers make up the basal body which has distinct protein composition in comparison to the transition zone which also has unique Y-shaped links identified through electron micrographs. Together the basal body and transition zone form the "ciliary gate". Modified from (Williams *et al.* 2011). The middle segment is composed of an organized structure of 9 microtubule doublets surrounding a variable number of visible microtubule singlets while the distal segment is composed of microtubule singlets. (C) Experiments using *C. elegans bbs* mutants and GFP-tagged IFT components identified a role for BBS proteins in bridging IFT anterograde motors (heterotrimeric Kinesin-II and homodimeric OSM-3) along the middle microtubule segment of the cilium (wild-type IFT). Loss of BBS proteins (bbs$^{-/-}$ IFT) results in a destabilization of motors and the dissociation of IFTA cargo from IFTB as the anterograde motors move at disparate speeds. Modified from (Ou *et al.* 2005; Pan *et al.* 2006)

Of 16 BBS genes, 9 have putative orthologues in *C. elegans* (**Table 2**) all of which have deletion mutants available for phenotypic analysis. The initial indication that BBS proteins were associated with primary cilia came from the seminal observation that several *C. elegans bbs* GFP transcriptional reporters were expressed solely in ciliated neurons (*bbs-1*, *bbs-2*, *bbs-7*, *bbs-8*) (Ansley *et al.* 2003) while GFP-tagged fusions of the same BBS proteins localized at the transition zone and axonemes of *C. elegans* cilia (Blacque *et al.* 2004). Soon after the cloning of *BBS8*, studies using comparative genomics analyses of ciliated organisms (including *C. elegans*), were key to the cloning of *BBS3* and *BBS5*, both of which also localized to the transition zone and axonemes of *C. elegans* ciliated neurons (Fan *et al.* 2004; Li *et al.* 2004). These findings suggest a relatively high degree of BBS protein functional conservation in this invertebrate model

Previously reported phenotypes of *bbs-7* and *bbs-8* mutant animals include chemo- and thermosensory defects, general ciliary disruption observed as the failure of lipophilic DiI uptake, and the mislocalization of GPF-tagged IFT cargo proteins CHE-2 (IFTB), CHE-11 (IFTA), and OSM-5 (IFTB) (Blacque *et al.* 2004; Tan *et al.* 2007). *bbs-1* mutants were characterized as having increased lipid accumulation (Mak *et al.* 2006) (**Table 7**).

This model has also proven very useful in deciphering the molecular functions of BBS proteins through mutant analysis and *in vivo* imaging techniques (see section 1.5.1) (Ou *et al.* 2005; Pan *et al.* 2006). Furthermore, shown in later chapters of my thesis, *C. elegans* makes an excellent genetic model capable of identifying additional *bbs* modifying loci.

Table 7. Features observed in BBS models of *Caenorhabditis elegans*

Phenotype	*bbs-1*	*bbs-7*	*bbs-8*
DiI filling defects (dyf)	✓	✓	✓
Chemosensory defects	✓	✓	✓
Thermosensory defects		✓	✓
IFT raft mislocalization		✓	✓
Shortened/broken cilia		✓	✓
Lipid accumulation	✓		
IFT motor decoupling	✓	✓	✓

Data combined from (Blacque *et al.* 2004; Ou *et al.* 2005; Mak *et al.* 2006; Ou *et al.* 2007; Tan *et al.* 2007)

1.4.4 Additional Models of BBS

An additional model of BBS is the ancient alga *Chlamydomonas reinhardtii* in which recent work has shown that BBS proteins prevent the aberrant accumulation of sensory receptors within its flagellum (Lechtreck *et al.* 2009). These experiments suggest that BBS proteins could be important to the regulation of protein turnover within the cilium.

Ex vivo retinal pigment epithelial (RPE) models of BBS have been useful in dissecting the complex associations between BBS proteins, indentifying their role in vesicular trafficking (see section 1.5.2) (Nachury *et al.* 2007; Nachury 2008; Jin *et al.* 2010).

1.5 Deciphering the Function of Bardet-Biedl Syndrome Proteins

Many BBS proteins, are novel proteins whose functional domains remained poorly characterized until recently (Kim *et al.* 2004; Jin *et al.* 2010; Seo *et al.* 2010). There is shared domain homology among a subset of these novel BBS proteins (**Table 8**). BBS1, BBS2, BBS7, and BBS9, for example share domains of high homology (Mykytyn *et al.* 2002; Badano *et al.* 2003a; Jin *et al.* 2010) as do BBS4 and BBS8 by sharing a tetratricopeptide repeat motif. On the other hand, BBS3 is an ADP-ribosylation factor-like (ARL6) gene and BBS5 is a member of the Ras superfamily of small GTP-binding proteins, both of which exhibit no apparent sequence similarity to other BBS proteins. Thus far, BBS6, BBS10, and BBS12 are the best characterized proteins; they form a new vertebrate-specific class of proteins known as the type-II chaperonin-like complex. This chaperonin complex appears to be ATP-independent and to be structurally distinct from the known type-II chaperonins. BBS11 (TRIM32) has homology to an E3 ubiquitin ligase. Meanwhile BBS13 (MKS1) has a B9 domain which is shared with some transition zone

proteins and BBS14 (CEP290) is known to interact with some ciliary and transition zone-associated proteins (reviewed in (Coppieters *et al.* 2010)). Both of these may act as gatekeepers to the axoneme (Williams *et al.* 2011). BBS15 (WDPCP/Fritz), the vertebrate orthologue of the *Drosophila* PCP signalling protein Fritz, most notably is involved with convergent extension although the confirmed number of BBS cases is currently limited to a single family (Kim *et al.* 2010), and BBS16 (SDCCAG8) localizes tightly to centrosomes and may have a more general role in centrosomal function (Otto *et al.* 2010). Despite an overall lack of sequence homology in BBS proteins, there are a number of model organisms that have been useful in deciphering the functions of these molecules.

Table 8. BBS functional domains and homology

Protein	Structure/Domains	Complex or Component	Putative Function
BBS1	β-propeller fold, amphipathic helical linker, γ-adaptin ear [a]	BBSome [j]	IFT motor coordination [k], vesicular trafficking/transport [a]
BBS2	β-propeller fold, amphipathic helical linker, γ-adaptin ear, α/β platform, α helix [a]	BBSome [j]	Vesicular trafficking/transport [a]
BBS3/ARL6	ADP-ribosylation factor-like	BBSome-interactor, GTPase [a]	Vesicular trafficking/transport [a]
BBS4	13 Tetratricopeptide repeats (α-solenoid) [a]	BBSome, PCM1-interactor	Centriolar satellite organization, vesicular trafficking/transport [a]
BBS5	2 Pleckstrin Homology (PH) domains [a]	BBSome [j]	Vesicular trafficking/transport [a]
BBS6/MKKS	Type II Chaperonin subgroup: Equatorial, intermediate, and apical domains [b]	BBS/CCT complex [i]	BBSome assembly [i]
BBS7	β-propeller fold, amphipathic helical linker, γ-adaptin ear, α/β platform, α helix [a]	BBSome [j]	IFT motor coordination, vesicular trafficking/transport [a]
BBS8/TTC8	12.5 Tetratricopeptide repeats (α-solenoid) [a]	BBSome [j]	IFT motor coordination [k], vesicular trafficking/transport [a]
BBS9/ Parathyroid	β-propeller fold, amphipathic helical linker, γ-adaptin ear,	BBSome, central component [j]	Vesicular trafficking/transport [a]

hormone-responsive B1	α/β platform, α helix [a]		
BBS10	Type II Chaperonin subgroup: Equatorial, intermediate, and apical domains [b]	BBS/CCT complex [i]	BBSome assembly [i]
BBS11/TRIM32	N-terminal tripartite motif (zinc RING finger, zinc B-box, coiled-coil domains), C-terminal NHL repeats [c]	E3 Ubiquitin ligase [c]	
BBS12	Type II Chaperonin subgroup: Equatorial, intermediate, and apical domains [b]	BBS/CCT complex [i]	BBSome assembly [i]
BBS13/MKS1	B9 domain [d]	Transition zone, MKS complex, interaction with MKS5/RPGRIP1L [h]	Ciliary protein gating/sorting [h]
BBS14/CEP290 /NPHP6	13 Coiled-coil domains, 6 KID motifs, 3 tropomyosin homology domains, ATP/GTP binding site motif A [e]	Transition zone, NPHP complex interaction with MKS5/RPGRIP1L [h]	Ciliary protein gating/sorting [h]
BBS15/ Fritz	Coiled-coil, 2 WD40 repeats [f]	Functional interaction with septins [f]	Convergent extension, governs ciliogenesis [f]
BBS16/SDCCA G8/SLSN7/ NPHP10	N-terminal globular domain, nuclear localization signal, 8 coiled-coil domains, glutamine-rich region [g]	Complexes related to centrosomes and/or cell-cell junctions [g]	Epithelial lumen formation, OFD1 interaction [g]
BBIP10	2 α helices[a]	BBSome [j]	Vesicular trafficking/transport
	[a] (Jin *et al.* 2010) [b] (Stoetzel *et al.* 2007) [c] (Chiang *et al.* 2006) [d] (Kyttala *et al.* 2006) [e] (Sayer *et al.* 2006) [f] (Collier *et al.* 2005) [g] (Otto *et al.* 2010)	[a] (Jin *et al.* 2010) [g] (Otto *et al.* 2010) [h] (Williams *et al.* 2011) [i] (Seo *et al.* 2010) [j] (Nachury *et al.* 2007)	[a] (Jin *et al.* 2010) [g] (Otto *et al.* 2010) [h] (Williams *et al.* 2011) [i] (Seo *et al.* 2010) [k] (Ou *et al.* 2005)

1.5.1 BBS Proteins Co-ordinate Antagonistic IFT Motor Movement

Using GFP-tagged IFT proteins (OSM-6::GFP), IFT was observed *in vivo* along *C. elegans* amphid and phasmid neurons (Snow *et al.* 2004). *C. elegans* IFT consists of two anterograde motors – kinesin-II and OSM-3 which coordinate the transport of IFT A and B particles along the axoneme before being returned by dynein motors. In wild-type animals, OSM-6::GFP is observed to move at a rate of $0.7\mu m \cdot s^{-1}$; an intermediary transport speed that suggests the coordinated movement of these two motors. In Kinesin-II (*kap-1*) mutants, the OSM-6::GFP/OSM-3 complex travelled at $1.3\mu m \cdot s^{-1}$. Conversely, in *osm-3* mutant animals, the OSM-6::GFP/kinesin-II complex is observed at $0.5\mu m \cdot s^{-1}$ (Snow *et al.* 2004). Therefore, these motors move in a coordinated fashion along the axonemal middle segment of the primary cilium. These IFT dynamics were key to deciphering the function of BBS-1, BBS-7, and BBS-8 proteins in *C. elegans*. In the loss of function *bbs-1*, *bbs-7*, and *bbs-8* mutants, KAP-1::GFP particles moved at $0.5\mu m \cdot s^{-1}$, while OSM-3::GFP particles were observed to move at $1.3\ \mu m \cdot s^{-1}$ (Ou *et al.* 2005; Ou *et al.* 2007). Further investigation of both raft A (CHE-11::GFP) and B complexes (CHE-2::GFP, OSM-5::GFP) in *bbs* mutant backgrounds identified that raft A cargos moved at kinesin-II rates while raft B cargos moved at the same rate as OSM-3, thereby identifying the specific rafts that associate with each motor. From these experiments, it was also concluded that BBS proteins keep raft A-kinesin-II and raft B-OSM-3 motor-cargo complexes associated during IFT. These experiments were the first to hint that the BBS proteins functioned within a common complex (**Figure 4C**).

1.5.2 Evolutionarily Conserved BBS Proteins Form a Complex Required for Vesicular Trafficking

Using immortalized cell lines for retinal pigment epithelium (RPE), Nachury *et al*. hypothesized that the use of tandem-affinity purification with GFP-tagged BBS4 could identify associated protein complexes, which could then be characterized with mass spectrometry analysis (Nachury *et al.* 2007). Interestingly, the most highly evolutionarily conserved BBS proteins (BBS1, BBS2, [BBS 4], BBS 5, BBS 7, BBS 8, and BBS 9) were co-precipitated with BBS4 in stoichiometric amounts along with PCM1 - a known BBS4 interactor – and α/β-tubulin. A number of hydrodynamic analyses showed that the association of these BBS proteins and an additional novel protein, BBIP10, formed a stable octameric complex of approximately 483kDa. This complex was named the BBSome and through additional co-transfection and co-

immunoprecipitation experiments, two “near-quantitative” (BBS2/BBS7 and BBS9/BBS8) and four moderate (BBS9/BBS4, BBS9/BBS1, BBS9/BBS2, and BBS9/BBS5) interactions were identified. The abundance of BBS9 cross-interactions led Nachury *et al*. to theorize that BBS9 may act as a central point of cohesion in the organization of the BBSome (**Figure 3**). Furthermore, Nachury *et al*. observed that the single BBSome complex associates with membrane structures, likely in the ciliary or periciliary membranes. This was further supported by bioinformatic and experimental analysis of BBS5 that indicated possible interactions with phosphoinositides, which also appeared critical to ciliogenesis. Nachury *et al*. further investigated the potential relationship between the BBSome and PCM1. BBSome components are evolutionarily conserved across ciliated organisms while PCM1 is absent amongst invertebrates and protozoa. siRNA-mediated BBS depletion showed that while the BBSome (BBS1 and BBS5) is required for ciliation, its absence did not perturb BBS4/PCM1 interaction nor did it affect centriolar satellite or centrosome organization. These results implied the existence of two potential pools of BBS proteins – PCM1-associated versus ciliogenesis-associated BBSomes (**Figure 3**).

Nachury *et al*. also identified Rab8 and Rabin8 as interacting proteins with the BBSome (**Figure 3**). Specifically, they showed that the C-terminus of Rabin8 interacts with BBS1. Rabin8 is a guanosyl exchange factor (GEF) for Rab8 and it co-localizes with the BBSome at the centrosome/basal body. Moreover, Rab8 is localized along the primary cilium but requires Rabin8 for GTP loading and correct localization. Both Rabin8 and Rab8 are required for proper ciliogenesis in RPE cells. *rab8* zebrafish morpholino experiments further validated the manifestation of BBS-like phenotypes.

Nachury *et al*. concluded that the BBSome was an octameric complex that may be sequestered initially by PCM1 before reaching the periciliary membrane. The BBSome was then hypothesized to interact with the ciliary membrane and aid in IFT by potentiating interactions such as those between Rabin8 and Rab8 **(Figure 3)**.

Jin *et al*. extended these observations and further investigated the potential vesicular transport properties of the BBSome (Jin *et al.* 2010). Jin *et al*. first identified that the remaining evolutionarily conserved BBS protein, Arf-like GTPase ARL6 (BBS3) associated with the BBSome in its GTP-bound form. Since this association implied that the BBSome possibly

functioned as a coat complex, they performed bioinformatic analysis on BBSome components for coat-like structural elements (**Figure 5**). Jin *et al*. predicted that BBS1, BBS2, BBS7, and

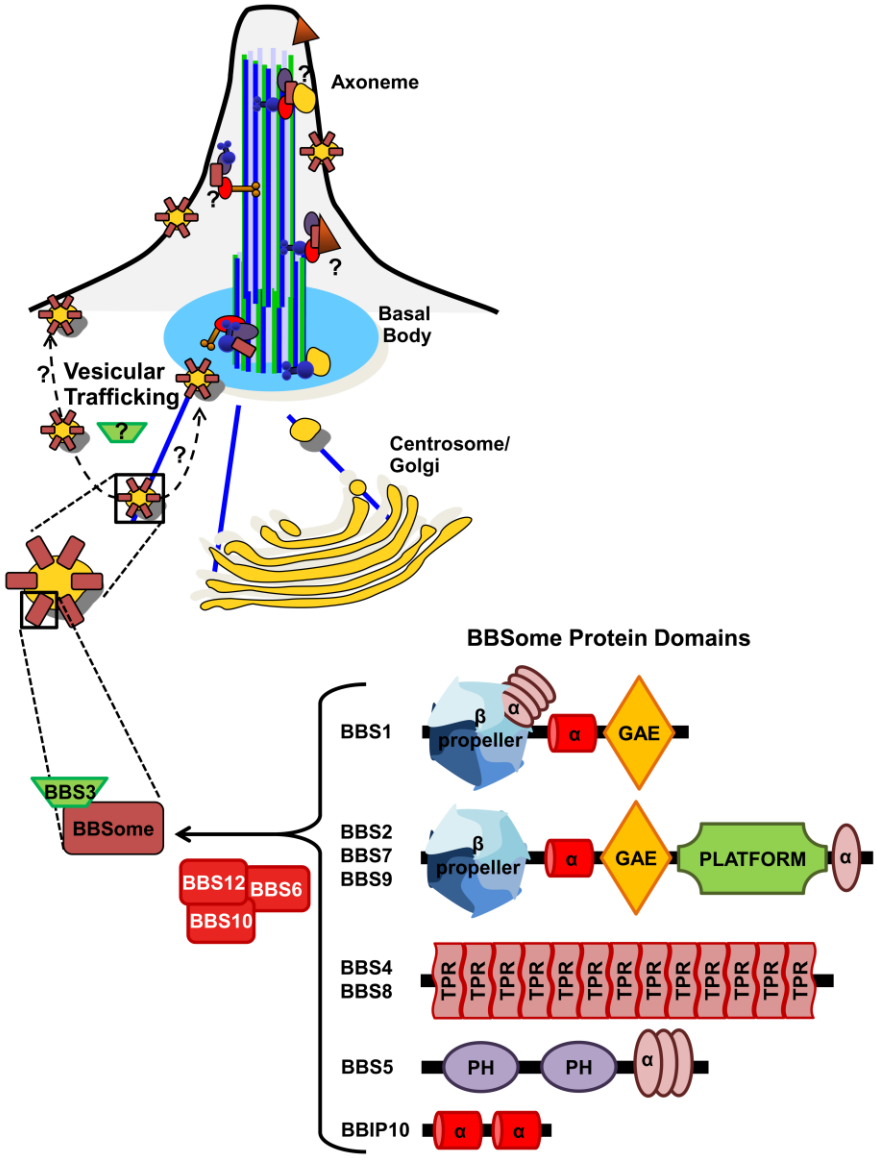

Figure 5. The BBSome targets/traffics vesicles to the ciliary membrane. The BBSome components are similar to other known coat complexes (Jin *et al.* 2010). BBS1/2/7/9 all share a β propeller domain, an amphipathic helical linker, and a γ-adaptin ear (GAE) domain. BBS2/7/9 also share an α/β platform followed by an α helix. BBS1 additionally has a four-helix section located between the second and third blades of its β propeller. BBS4 and BBS8 have 13 and 12.5 tetratricopeptide repeats (TRP) respectively that form into an α-solenoid shape. BBS5 contains two pleckstrin homology (PH) domains which function normally in protein recruitment to different membranes as well as a three-helix domain. BBIP10 (for which no diseases have been associated) is predicted to have two α helices. With the assistance of BBS6/10/12, the BBSome is formed and transiently associated with the activated form of BBS3 although the exact spatio-temporal interaction is currently unknown. The BBSome is capable of recruiting proteins and forming vesicles similar to those of COPI/COPII proteins. Furthermore, certain cilia targeting signals such the one found on SSTR3 are required by the BBSome to transport these proteins to their final destination. Modified from (Jin *et al.* 2010).

BBS9 all have a predicted β propeller fold (Chaudhuri *et al.* 2008) and a domain distantly related to the γ-adaptin ear (GAE). BBS2, BBS7, and BBS9 also have an α/β platform domain that in combination with the GAE domain could form an "appendage" combination found in several clathrin adaptors and other coat proteins such as COPI (McMahon *et al.* 2004). Jin *et al*. also predicted that the BBS4 and BBS8 TPR domains would form α solenoid rods (Jinek *et al.* 2004). This combination of α solenoids and β propellers is reminiscent of the structures found in COPII or clathrin cages (Stagg *et al.* 2007). In conjunction with appendage domains, this bioinformatic analysis implies a distant evolutionary relationship to the canonical coat complexes.

To validate these findings, Jin *et al*. next showed that the BBSome, only in conjunction with BBS3 and the GTP analog GMP-PNP, bound directly to liposome mixes of neutral and acidic phospholipids *in vitro*. Furthermore the ultrastructure of liposomes incubated with BBSome, BBS3 and GMP-PNP, showed ordered structures reminiscent of budding 50nm coated vesicles seen in earlier COPI and COPII experiments (Matsuoka *et al.* 1998; Bremser *et al.* 1999; Wang *et al.* 2006). Lastly, Jin *et al*. showed that SSTR3, which is normally present in hippocampal neurons but lost in *bbs2*$^{-/-}$ and *bbs4*$^{-/-}$ mutants (Berbari *et al.* 2008a), has a specific ciliary targeting signal (Berbari *et al.* 2008a) required for its recognition by the entire BBSome/BBS3 complex to properly localize to cilia. Thus the highly conserved components of BBSome/BBS3 act as a coat complex to target specific molecules to the primary cilium (**Figure 5**).

1.5.3 BBS3 May Act as a Molecular Switch Between BBSome Vesicular Trafficking and IFT Functions

BBS3 is an Arf-like (ARL) GTPase and Wiens *et al*. recently solved the crystal structure of the N-terminus (residues 16-186) of this ciliary protein (Wiens *et al.* 2010). Furthermore, they identified that although this small GTPase shows a typical GTPase fold, it is distinct from most small GTPases. This analayis of BBS3 was also useful in characterizing the nature of some bona fide BBS patient alleles. In particular, Wiens *et al*. identified using dot-blot assay that a T31R mutation that caused BBS3 to bind exclusively to GDP nucleotide in contrast to wild-type controls.

Using a polyclonal antibody, Wiens et al. confirmed that BBS3 colocalized with the basal body in multiple ciliated cell lines including IMCD3, hTERT-RPE and other ciliated mammalian tissues. This localization appeared independent of both microtubules and dynein retrograde

motors as treamtment with both nocodazole (MT depolymerizing) and p50-dynamitin overexpression (motor disruption) had no effect in IMCD3 cells (Wiens *et al.* 2010). Interestingly, BBS3 was observed to concentrate at the distal end of only a single centriole (likely the mother centriole) during interphase in an hTERT-RPE cell. During this phase, the cell does not have a visible cilium. The ring-like localization is unique to BBS3 in comparison to the known localization pattern of other BBSome components, suggesting that it acts at or near the ciliary gate. This is in line with its known transient association with the BBSome (Jin *et al.* 2010).

To probe the functions of BBS3, Wiens *et al*. overexpressed wild-type, GDP-locked (T31R), and GTP-locked (Q73L) variants of this protein in hTERT-RPE cell lines. Wiens *et al*. observed an overall increase in ciliated cells for the RPE populations expressing the GDP- and GTP-locked variants. On the other hand, overexpression of wild-type BBS3 resulted in a significant decrease to ciliation in transfected RPE cells. Furthermore, the overexpression of BBS3 locked variants resulted in longer cilia whereas cilia length was normal in wild-type overexpression in comparison to untransfected controls (Wiens *et al.* 2010). These combined data suggested that BBS3 mediates the possible disassembly of cilia. In contrast, Rabin8, which is required to activate the small GTPase, Rab8, interacts with the BBSome, and is required for the assembly of primary cilia (Nachury *et al.* 2007). The localization of Rabin8 is predominantly centrosomal and not concentrated within the primary cilium (Nachury *et al.* 2007).

Wiens *et al*. concluded that given its ring-like localization and close association with the distal end of basal body or beginning of the transition zone (as opposed to ciliary axoneme) BBS3 may play a specialized role in the transition between the vesicular trafficking properties (Jin *et al.* 2010) and that of its known IFT properties (Ou *et al.* 2005). Functionally, BBS3 may play an important role in cilium resorption based on their overexpression experiments. The trafficking of proteins, back from the primary cilium to the centrosome may require a molecular switch and BBS3 is a likely candidate in that role (Wiens *et al.* 2010).

Thus, although no single model organism has unified the two observed functions of the BBSome in IFT and vesicular trafficking, there is now more evidence to support that both of these functions may co-ordinately manage ciliary biogenesis, maintenance, and resorption through BBS3.

1.5.4 BBS Chaperonin-like and CCT Chaperonin Proteins Form a Complex Required for BBSome Formation

BBS6, BBS10 and BBS12 share a high degree of homology. Seo *et al*. investigated whether these chaperonin-like proteins interacted as a complex *in vivo*. They identified that BBS6 and BBS12 precipitated in low amounts with BBS10 while precipitating strongly with six CCT chaperonin proteins (CCT1-5, and CCT8) as well as the BBSome subunit BBS7 in transient transfection of HEK293T cells (**Figure 3**). Further analysis showed these proteins were present as a 770-1,000 kDa BBS/CCT complex although a smaller 260-340kDa complex of BBS6/BBS10/BBS12/BBS7 was also observed. Co-transfection and co-immunoprecipitation with single BBSome units and BBS chaperonins identified additional physical interactions (**Figure 3**), indicating that the chaperonin-like BBS proteins can interact with a subset of BBSome subunits *ex vivo*.

Seo *et al*. next examined the requirement of chaperonin-like BBS proteins in the assembly of the BBSome using mouse eye and testis extracts. In wild-type tissues, Bbs1, Bbs2, Bbs4, Bbs7, and Bbs8 eluted within the same fractionations. In *Bbs6* null tissues, Bbs1, Bbs4, and Bbs8 eluted in non-overlapping fractionations, while Bbs2, and Bbs7 profiles showed strongly reduced protein levels. Notably, different tissues eluted different sizes of BBSome complexes, regardless of wild-type or *Bbs6* null genotype, indicating the presence of tissue-dependent forms of the BBSome sub-complexes.

Furthermore, in HEK293T cells the depletion of BBS6, BBS10, or BBS12 interfered with BBSome formation by greatly reducing BBS2 and BBS7 interaction with BBS9, along with a moderate reduction in BBS1/BBS9 interaction. Similar results were obtained for siRNA-mediated depletion of CCT1, CCT2, and CCT3 in HEK293 cells while confirming that chaperonin-like BBS proteins are required for BBS7/CCT-specific association. Morpholino knockdown of a subset of these *cct* genes in zebrafish recapitulated *bbs*-MO phenotypes although additional *cct*-specific phenotypes also manifested. Overall, these results implicated a role for the chaperonin-like BBS/CCT complex in regulating BBSome assembly, likely through BBS7 and BBS2 (**Figure 3**).

1.5.5 BBS4 and BBS8 are Required for Proper Microtubule Organization

Centrosomes are the primary cytoplasmic microtubule organizing centres (MTOC) composed of a centriole pair surrounded by an electron-dense mass of pericentriolar material that includes the pericentriolar protein PCM1. From the centrosome, a number of cytoplasmic microtubules extend to anchor other organelles, provide cytoskeletal support, polarize, and stabilize the cell. The centrosome is proposed to coordinate with the Golgi to transport cargo to the basal body/primary cilium (reviewed in (Bettencourt-Dias *et al.* 2007; Sutterlin *et al.* 2010; Carvalho-Santos *et al.* 2011)).

Utilizing yeast two-hybrid screens, Kim *et al*. showed that the C-terminal region of PCM1 interacted with BBS4 (Kim *et al.* 2004). BBS4 co-localized with PCM1 in pericentriolar regions *in vivo* in a number of mammalian cell types. Similar results were noted by Ansley *et al*. showing that BBS8 also binds to the C-terminus of PCM1 and colocalizes with it *in vivo* (Ansley *et al.* 2003) (**Figure 3**). In ciliated cells, BBS4 co-localizes at the basal body with both the mother and daughter centriole. Its proximity to the pericentriolar region was constant throughout the cell cycle, and is independent of PCM1, which became dispersed during metaphase and anaphase. Conversely, PCM1 localization could be perturbed with the expression of specific N-terminal deletion constructs of BBS4, which Kim *et al*. hypothesized as a dominant negative effect related to the overexpression of these specific BBS4 constructs.

Similar to PCM1, BBS4 localization was dependent upon dynein-dynactin retrograde transport along microtubules. These results were verified with a yeast two-hybrid assay that confirmed more specifically that the C-terminus of the $p150^{glued}$ subunit of dynactin (DCTN1) interacted with BBS4 to transport it to the pericentriolar region. Based on the association with this motor complex, Kim *et al*. hypothesized that PCM1 localization may be dependent upon BBS4. BBS4 siRNA transfection in HeLa cells resulted in the complete dispersion of PCM1 in the cytosol. Concomitantly, the knockdown of BBS4 also resulted in a destabilization of microtubule anchoring. Furthermore, transfected HeLa cells failed to divide and in instances were observed to be multinucleated while containing replicated centrioles, and in some cases cells were apoptotic. Interestingly the co-expression of BBS4 with PCM1 was found mainly in tissues specific to BBS features, indicating that this relationship may help elucidate the pleiotropic nature of BBS.

1.5.6 A BBS3 Retina-Specific Isoform is Required for Proper Inner Segment Organization and Photoreceptor Function

More recent work identified that tissue-specific *BBS* isoforms can play different roles within model systems. Pretorius *et al*. first identified a BBS3 isoform, BBS3L, which was predominantly expressed in eye tissues (Pretorius *et al.* 2010). BBS3L contains an additional 13bp exon, which results in a frameshift and inclusion of seven additional amino acids altering the C-terminal transcript of BBS3. This alternative transcript is moderately conserved between human, mouse, and zebrafish and based on these observations, Pretorius *et al.* concluded that this isoform may have some significance within the retina.

Using zebrafish morpholinos that knocked down either the *bbs3L* (*bbs3L*-MO) isoform or both *bbs3* (*bbs3*-MO) isoforms simultaneously, Pretorius *et al.* observed KV phenotypes during development reminiscent of other *bbs* MOs for only *bbs3*-MO animals. The same contrasting phenotypes were seen in examining retrograde melanosome transport in *bbs3L*-MO versus *bbs3*-MO animals. Furthermore, in human isoform-specific RNA co-injection rescue experiments, *bbs3*-MO phenotypes were rescued by human *BBS3* RNA but not by human *BBS3L* RNA. Both *bbs3*-MO and *bbs3L*-MO animals exhibited statistically significant delays to startle response. Co-injection of human *BBS3* RNA was unable to rescue startle responses in either *bbs3*-MO or *bbs3L*-MO backgrounds while *BBS3L* RNA rescued in both MO experiments. Similar results were observed in examining the localization of the retina-specific protein green opsin. Normally found in the outer segment of the green cone photoreceptor, green opsin was observed ectopically in outer nuclear layer cell bodies and throughout the entire retina in both sets of MO-injected animals.

Pretorius *et al*. validated their findings in mouse models. They confirmed BBS3 localization in mouse and human retinal sections. Creating a *BBS3L*-specific KO mouse, they also observed perturbations to inner segment organization. Finally, in a follow-up study, Pretorius *et al*. identified a BBS3 variant (A89V) that results in retinopathy without the manifestation of other BBS features. *bbs3*-MO studies showed that the co-injection of human *BBS3(A89V)* RNA transcript was capable of rescuing canonical *bbs3* defects to melanosome transport but co-injection of *BBS3L(A89V)* did not rescue the startle response defect in comparison to wild-type *BBS3L* transcripts. Taken together these studies demonstrate that BBS3L has tissue-specific function in photoreceptor health in vertebrates.

1.5.7 BBIP10 is a BBSome Subunit Required for Ciliogenesis and formation of the BBSome

Soon after the identification of the BBSome, Loktev *et al*. investigated an additional protein that was identified in association with this complex (**Figure 3**). Although BBIP10 strongly associated with BBS4, it was also found to elute at low-molecular weight fractions with other unidentified proteins. Interestingly, while BBIP10 localizes at the primary cilium, it is not at centriolar satellites where the BBSome/PCM1 complex is also observed to localize(Loktev *et al.* 2008).

Loktev *et al*. confirmed that *BBIP10* knockdown results in the abrogation of cilia formation. The transfection of RPE cells with *BBIP10* siRNA resulted in a significant decrease in ciliation while *bbip10*-MO experiments in zebrafish resulted in KV and retrograde melanosome transport defects similar to those seen in *bbs*-MO control animals. Furthermore, Loktev *et al*. were unable to isolate any BBSome subunits in association with BBS4 after the depletion of BBIP10 in RPE cells, implying a role for BBIP10 in BBSome formation.

Loktev *et al*. also identified a number of BBSome-independent roles for BBIP10 including microtubule acetylation and stabilization. Therefore, while BBIP10 remains a core subunit critical for BBSome assembly, its proposed additional functions require further investigation.

1.6 Additional BBS Interactions

Other possible interactors of BBS1, BBS2, BBS4, and BBS7 have been identified using yeast two-hybrid strategies (**Table 9**) (Oeffner *et al.* 2008). Using BBS1 and BBS4 as bait, Oeffner *et al*. identified 39 and 102 interactive clones from a human fetal kidney cell line cDNA library. Subsequent screening of these positive clones was completed using BBS2 and -BBS7 as bait. Several candidates, such as ALDOB, EEF1A1, and PCM1 (a known BBS4 interactor) were verified by co-immunoprecipitation experiments. Lastly GFP-tagged constructs of some candidate interactors also yielded positive colocalization with RFP-tagged BBS1, BBS2, BBS4, and BBS7 as well as anti-γ-tubulin staining that labels centrosome-associated microtubules in HeLa cells. These results provide a list of potential BBS-interacting proteins requiring functional validation.

Table 9. Additional BBS protein interactors

Prey	OMIM	BBS1	BBS2	BBS4	BBS7
ACTB[a]	102630			✓	
ACY[b]	609924	✓	✓	✓	✓
ALDOB[c]	229600	✓	✓	✓	✓
BHMT[b]	602888	✓	✓	✓	
CALCA[b]	114130	✓		✓	
DCTN1[a]	601143	✓		✓	
DJ1[b]	602533	✓			
EEF1a1[c]	130590	✓	✓	✓	
eIF3[c]	602039	✓		✓	
EPAS1[c]	603349	✓	✓	✓	
EXOC7[a]	608163	✓	✓	✓	
FHOD1[b]	606881	✓	✓	✓	✓
FLOT[c]	606998	✓	✓	✓	✓
HSC20[c]	608142	✓	✓	✓	
KRT18	148070	✓	✓	✓	✓
PAX2[b]	167409	✓	✓	✓	✓
PCM1[c]	600299			✓	
TM4SF2[c]	300096	✓			

Data modified from (Oeffner *et al.* 2008) [a]Clones detected repeatedly. [b]Interaction is plausible based on expression pattern and biological function. [c]Interaction is plausible based on subcellular localization.

1.7 Cilia-specific signalling pathways

1.7.1 Cilia and basal body proteins play roles regulating canonical and non-canonical Wnt signalling

The Wnt signalling pathway plays important roles in influencing development, for example, the specification of cell fate and or function in both embryonic and adult tissues (Logan *et al.* 2004). Wnt signalling can be divided into canonical and non-canonical pathways in which the response to Wnt proteins differs (Veeman *et al.* 2003). In canonical signalling, Wnt binds to the Frizzled (Fz) family of receptors, which transmit this signal to the primarily cytoplasmic protein, Dishevelled (Dsh). β-catenin is responsive to Wnt signalling and its translocation to the nucleus facilitates the activation of target genes. Normally, a complex of axin, adenomatous polyposis coli (APC), and glycogen synthase kinase 3β (GSK3β) recruits and phosphorylates β-catenin, targeting it for proteolytic degradation (Aberle *et al.* 1997). In the canonical Wnt pathway, this complex is disrupted by the activation of cytoplasmic Dsh. This leads to the stabilization of β-catenin, its subsequent accumulation in the cytoplasm, and the translocation of β-catenin and Dsh to the nucleus (reviewed in (van Amerongen *et al.* 2009)). The non-canonical Wnt pathway is

classically differentiated by specific Wnt ligands (Wnt5 for example) and receptors that interact outside the Wnt/Fz pathway (van Amerongen *et al.* 2009).

Primary cilia were first found to play a role in Wnt signalling in *Kif3a* and *Ift88*^{orpk} knockout mice, where expanded or mislocalized β-catenin signals were observed in kidney and pancreas respectively (Lin *et al.* 2003; Cano *et al.* 2004). Mouse embryonic fibroblasts (MEFs) provided a more direct demonstration for the role of primary cilia in Wnt signalling (Corbit *et al.* 2008). MEFs derived from *Kif3a*$^{-/-}$ mice that were stimulated by Wnt3a, displayed a higher level of β-catenin in the cytoplasm as well as nucleus compared to heterozygote controls.

Based on previous reports of the involvement of BBS in zebrafish planar cell polarity (PCP) convergent extension phenotypes (see section 1.7.3), Gerdes *et al*. proposed a role for the BBS proteins in regulating Wnt signalling (Gerdes *et al.* 2007). Gerdes *et al*. showed that sub-phenotypic dosages of *bbs1*, *bbs4*, and *bbs6* MOs resulted in the exacerbation of the non-canonical convergent extension phenotypes of zebrafish *wnt11* and *wnt5b* heterozygous alleles. Furthermore, the canonical Wnt signalling transcriptional target *axin2* had a substantially expanded expression domain in the tail region of *bbs* morphants versus control samples.

Gerdes *et al*. further identified increased transcriptional activation of canonical Wnt3a targets in BBS4-depleted HEK293T cells. This effect was cilia-specific as the pharmaceutical disruption of cytoplasmic microtubule networks (normally regulated by BBS4) did not perturb Wnt signalling. Gerdes *et al*. confirmed this cilia-specific role by the disruption of cytoplasmic MT and suppression of the Kinesin-II motor KIF3A, which resulted in *bbs*-MO-like phenotypes. From these studies, Gerdes *et al*. concluded that *bbs*-MO phenotypes were attributed to increased accumulation of phosphorylated and unphosphorylated forms of β-catenin in the cytoplasm, which implied potential defects in both degradation and phosphorylation pathways. These findings are supported by observations in the *Kif3a*$^{-/-}$ mouse models and indicate a role for the primary cilium in restricting the signal response to Wnt (Corbit *et al.* 2008).

Additional evidence of ciliary roles in Wnt signalling includes studies examining the effects of BBS proteins on adipogenesis (Marion *et al.* 2009). These results, however, showed an opposite role for cilia, wherein the loss of the primary cilium in white adipocyte tissues resulted in decreased GSK3β phosphorylation. This, in turn, increased β-catenin phosphorylation and degradation, which resulted in an upregulation of the pro-adipogenic peroxisome proliferator-

activated receptor-γ. Meanwhile, *BBS10* and *BBS12*-deficient adipocytes derived from human patient fibroblasts exhibited higher triglyceride levels and increased secretion of leptin implicating lipid storage defects in conjunction with increased adipogenesis. Together, these studies suggest that BBS and primary cilia may play tissue-specific roles in Wnt signalling.

1.7.2 Sonic Hedgehog Signalling is Perturbed in BBS and Ciliary Mutants

Sonic Hedgehog (Shh) is a well studied morphogen involved in the patterning of limbs, brain, and spinal cord during development (Louvi *et al.* 2011). The past decade has seen the emergence of the primary cilium as a primary signal co-ordination centre for Shh. For example, IFT-dependent localization of the Shh receptors to the primary cilium is required for Shh signalling in mouse and zebrafish embryos (Corbit *et al.* 2005; May *et al.* 2005; Rohatgi *et al.* 2007). Furthermore, disrupting the function of raft components IFT172, TG737/IFT88 and the motor KIF3A resulted in mouse mutants exhibiting phenotypes characteristic of Shh mutants (Huangfu *et al.* 2003).

Similarly the BBS proteins have been shown to play roles in Shh signalling. Recently, Tayeh *et al*. used zebrafish to examine whether Shh signalling is regulated by BBS. Yen *et al*. previously identified the presence of *bbs7* in the developing fin bud at 36 hours post-fertilization (Yen *et al.* 2006). In *bbs*-MO models, however, Tayeh *et al.* did not observe apparent defects in fin growth or viability. The zone of polarizing activity (ZPA) is important for the specification of digits in chick limb bud where additional or expanded Shh activity results in additional digit formation (Tickle *et al.* 1975). Given the importance of the ZPA in digit formation and the apparent expression of *bbs7* in the developing fin bud Tayeh *et al*. postulated that Shh signalling may be perturbed in *bbs* morphants. Tayeh *et al*. examined *bbs* morphants for increased Shh activity in the ZPA and found that pectoral fin Shh expression was expanded. Despite a lack of visible fin defects, pectoral fin structure was perturbed in 6-7 day-old morphant larvae, which included an enlarged scapulacoracoid that presented with disorganized and/or extra cell layers. Tayeh *et al*. posited that these particular changes may be representative of the digit anomalies seen in BBS patients.

Currently, the primary cilium appears to be the only organelle responsible for Sonic Hedgehog signalling although there is evidence to show that cilia are not absolutely required for correct Shh signalling (Jia *et al.* 2009).

1.7.3 Planar Cell Polarity

In both vertebrates and *Drosophila*, the orientation of epithelial cells along an axis that is orthogonal to the apical-basal membrane is known as planar cell polarity (PCP). The signalling pathway that governs PCP plays an integral role in cochlear stereociliary symmetry in vertebrates (Curtin *et al.* 2003; Montcouquiol *et al.* 2003; Lu *et al.* 2004), the convergent extension pathways of *Danio rerio* during development (Keller 2002; Torban *et al.* 2004), and the orientation of hair cells on *Drosophila* wing (Wong *et al.* 1993).

Planar cell polarity (PCP) signalling is best characterized as part of the non-canonical Wnt pathway. A number of genes have been identified as playing a role in PCP based on their characteristic phenotypes – mostly from *Drosophila* (reviewed in (Axelrod *et al.* 2011)). A core PCP module consisting of Frizzled (Fz), Flamingo (Fmi), Van gogh (Vang), Prickle-spiny-legs (Pk), and Dishevelled (Dsh), coordinate polarity between neighbouring cells in a molecular pathway beginning with the Fz receptor (Vinson *et al.* 1989; Adler *et al.* 1990; Adler 1992; Klingensmith *et al.* 1994; Theisen *et al.* 1994; Shulman *et al.* 1998; Taylor *et al.* 1998; Wolff *et al.* 1998; Chae *et al.* 1999; Gubb *et al.* 1999; Usui *et al.* 1999; Feiguin *et al.* 2001; Das *et al.* 2004).

Mutations of these core PCP genes result in mouse phenotypes that include cochlear stereociliary bundle orientation defects and disruptions to neural tube closure (Curtin *et al.* 2003; Montcouquiol *et al.* 2003; Lu *et al.* 2004). *Drosophila* mutants have disruptions to both wing hair patterns and ommatidia orientation in the eye (Gho *et al.* 1998; Bellaiche *et al.* 2001a; Bellaiche *et al.* 2001b). A number of tissue-specific effector components are thought to help transduce cell-specific responses to the core pathway while also influencing neighboring cells (Adler *et al.* 1990; Adler 1992; Klingensmith *et al.* 1994; Theisen *et al.* 1994; Shulman *et al.* 1998; Taylor *et al.* 1998; Wolff *et al.* 1998; Chae *et al.* 1999; Gubb *et al.* 1999; Usui *et al.* 1999; Feiguin *et al.* 2001; Das *et al.* 2004). Globally, Four-jointed (Fj) and the atypical cadherins Dachsous (Ds) and Fat (Ft) are thought to influence PCP in all tissues upstream of the core pathway (Mahoney *et al.* 1991; Clark *et al.* 1995; Villano *et al.* 1995; Brodsky *et al.* 1996; Adler

et al. 1998; Zeidler *et al.* 1999; Zeidler *et al.* 2000; Casal *et al.* 2002; Yang *et al.* 2002; Ma *et al.* 2003).

Ross *et al*. identified a number of PCP-like phenotypes in both BBS mouse models and zebrafish (Ross *et al.* 2005). *Bbs1*$^{-/-}$, *Bbs4*$^{-/-}$, and *Mkks*$^{-/-}$ mouse embryos exhibited midbrain exencephaly, which was always associated with open eyelids, as well as rotated cochlear stereociliary bundles. Further investigation with PCP mouse mutants of Looptail (Ltap/Vangl2) showed that *Mkks*$^{+/-}$ *Ltap*$^{+/-}$ and *Bbs1*$^{+/-}$*Ltap*$^{+/-}$ animals had a significant amount of embryonic lethality (7-10%) in comparison to *Mkks*$^{-/-}$, *Bbs1*$^{-/-}$, or *Ltap*$^{-/-}$ single mutants, indicating their genetic interactions. *Bbs1*$^{+/-}$*Ltap*$^{+/-}$ animals also exhibited cochlear defects as observed in *Mkks*$^{-/-}$ mutants which concurred with an interaction between the *Bbs* and PCP genes.

Ross *et al*. also examined the convergent extension phenotypes of zebrafish mutants for *vangl2* which share phenotypes with additional PCP mutants *wnt11* and *wnt5*. These mutants exhibited and array of shortened and widened body axis morphologies, defective gastrulation movements, and the posterior migration of hindbrain neurons. Morpholino knockdown of *bbs4* in *vangl2* mutants resulted in dramatic synergistic effects with more severe body axis compression and morphological defects apparent in early stages of embryogenesis in comparison to *vangl2* mutant controls. Immunostaining of VANGL2 localization in mouse IMCD3 kidney epithelial cells showed strong expression at the base of the cilium. Human respiratory epithelial cells also had strong VANGL2 staining at the base and axonemes of cilia. Moreover, the ciliary component *Ift88* interacts with *Vangl2* to regulate stereociliary bundle orientation, although core PCP proteins appeared to localize normally in these mutants further implicating ciliary involvement in PCP signalling (Jones *et al.* 2008).

The genetic interaction between BBS and IFT components with PCP core components are therefore consistent with cilia playing a modulatory role in transducing PCP signalling.

1.8 The study of genetic modifying influences of the Bardet-Biedl Syndrome phenotypes

Variability in BBS features have been observed within and between families suggesting the influence of genetic modifiers. There have been a small set of cases with proposed oligogenic inheritance in which three mutations across two BBS loci are associated with the manifestation

of BBS features (Katsanis *et al.* 2001; Katsanis *et al.* 2002; Beales *et al.* 2003; Fauser *et al.* 2003). These additional alleles could either increase phenotype severity or suppress gene expression (Badano *et al.* 2003b). The recent identification of hypomorphic alleles for other ciliopathies such MKS, NPHP, and JBTS revealed genetic overlap between ciliopathies (Leitch *et al.* 2008; Otto *et al.* 2009). Together, this evidence argues strongly in favour for the presence of underlying genetic factors that can influence the manifestation of BBS defects. Challenges for identifying such modifying genetic loci include the multiple pathways that may cause the pleiotropic aspects of the disease, genetic heterogeneity, and the low rate of occurrence for this disease in the diverse human genomic background. Animal models, with reduced genomic complexity can prove beneficial in the search for modifying loci using different approaches.

1.8.1 *CCDC28B* as a Modifier of BBS Severity

Using a reverse genetics approach in yeast and zebrafish to search for potential BBS modifiers, Badano *et al*. identified a candidate modifier, Coiled-coil domain containing 28B (CCDC28B/MGC1203) (Badano *et al.* 2006). Their strategy involved a combination of multiple rounds of BBS4 yeast two-hybrid screens that led to the identification of >60 putative interactors followed by a cross-comparison to the comparative genomics ciliary proteome used previously to identify *BBS5* (Li *et al.* 2004). A polyclonal antibody raised against CCDC28B identified a localization pattern concomitant with basal bodies and centrosomes, much like many BBS proteins. Examining tissues relevant to BBS features, Badano *et al*. also identified overlapping localization patterns between BBS proteins and CCDC28B, suggesting a potential genetic interaction.

Sequencing *CCDC28B* in unrelated BBS patients, Badano *et al*. identified a higher frequency of BBS patients (3/64) carrying a heterozygous (C430T) mutation versus ethnically matched controls (4/274). The C430T mutation was located in the penultimate position of exon 3. Further analysis of 162 additional unrelated BBS patients identified 11 additional carriers making the frequency of C430T in BBS patients 6.2% versis 1.4% in controls (Fisher's exact tests, $p<0.006$). Of the screened BBS patients, Badano *et al*. further screened *CCDC28B* in available parents and identified 27 trios in which one parent was heterozygous for C430T. Performing a transmission disequilibrium test in these trios, Badano *et al*. identified the transmission of the C430T allele in 20/27 trios, which is greater than the expected transmission rate of 50% if by chance alone

($p<0.007$). No homozygous *CCDC28B*(*C430T*) BBS patients were identified, while a homozygous C430T, unaffected parent was also identified, suggesting *CCDC28B* is not likely a cause of BBS.

Badano *et al*. further identified three BBS families in which only one of two affected siblings was a carrier of the C430T allele. In all three families, a masked assessment of the affected siblings identified more severe RP and ocular phenotypes in the C430T carrier versus the matched affected sibling. Lastly, molecular sequencing identified a complex case of inheritance in which two affected siblings were homozygous for the bona fide *BBS1(M390R)* mutation as well as carriers for the *CCDC28B(C430T)* allele while the unaffected father was homozygous for *BBS1(M390R)* and wildtype for *CCDC28B*. These analyses led Badano *et al*. to the hypothesis that the perturbation of this putative interactor could exacerbate or catalyse BBS feature manifestation.

A molecular analysis of *CCDC28B* transcripts in C430T heterozygotes using emetine (to suppress nonsense-mediated decay) identified that carriers of this silent mutation also generated a transcript with a 5 base pair deletion in the 5' end of exon 3 causing a frameshift leading to a premature termination codon. This aberrantly spliced transcript resulted from the utilization of a cryptic splice acceptor site that was enhanced by the C430T variant. The same heterozygote patient samples not treated with emetine had an overall decrease by 20% in *CCDC28B* mRNA levels. The decreased levels of *CCDC28B* transcript were surmised to be epistatic in influencing BBS severity.

To validate this hypothesis, Badano *et al*. conducted morpholino experiments on zebrafish, to compare the phenotypes of *bbs1*, *bbs4*, *bbs6* and *ccdc28b*-MOs. *ccdc28b* morphants shared overlapping phenotypes with *bbs1*, *bbs4* and *bbs6* morphants, which could be rescued when co-injected with wild-type *ccdc28b* RNA. Furthermore, the co-injection of sub-phenotypic dosages of *bbs*-MO or *ccdc28b*-MO resulted in >70% normal embryos while the subphenotypic co-injection of both a single *bbs*-MO with an *ccdc28b*-MO resulted in a synergistic increase to >68% of embryos having moderate to severe *bbs*-MO phenotypes (dorsal thinning and shortened body axis). In *bbs6*-MO/*ccdc28b*-MO double injections Badano *et al*. observed a much more severe phenotype than in high dose *bbs6*-MO controls. Meanwhile, *bbs1*-MO/*ccdc28b*-MO animals had more severe disruption of somatic definition in comparison to the other *bbs*-

MO/*ccdc28b*-MO animals. These data thus argue in favour of CCDC28B as a BBS interacting protein, whose disruption is observed to exacerbate BBS phenotypes in both zebrafish models and a small group of human patients.

1.8.2 *RPGRIP1L* as a Modifier of Ciliopathy Eye Phenotype

More recently, Khanna *et al*. explored the phenotypic variability between ciliopathies also through a reverse genetics approach. Mutations in the gene *CEP290* (*NPHP6/BBS14*) are observed in a number of ciliopathies including MKS, NPHP, BBS, and JBTS (Sayer *et al.* 2006; Valente *et al.* 2006; Baala *et al.* 2007; Leitch *et al.* 2008). Based on this and additional overlapping genetic components between ciliopathies (Arts *et al.* 2007; Delous *et al.* 2007), Khanna *et al*. hypothesized that common genetic components in some of these diseases may also have a genetic contribution to phenotypic variability in other ciliopathies. In one case, for example, *CEP290* (*NPHP6/BBS14*) mutations are associated with MKS, NPHP, BBS, and JBTS (Sayer *et al.* 2006; Valente *et al.* 2006; Baala *et al.* 2007; Leitch *et al.* 2008).

Khanna *et al*. chose *RPGRIP1L* as a possible candidate for other ciliopathies given its prior associations with MKS and JBTs (Arts *et al.* 2007; Delous *et al.* 2007). Khanna *et al*. screened 166 unrelated northern European individuals diagnosed with MKS (17), NPHP (15), BBS (34), or LCA (100). They identified ten novel and two common *RPGRIP1L* non-synonymous variants present across 24 individuals. Of the variants identified, an Alanine229Threonine (685G>A; rs61747071) variant was present slightly more frequently (11/332 chromosomes) in the ciliopathy cohort than in Northern European control populations (84/3016 chromosomes).

Further investigation using transmission disequilibrium testing of BBS trios in which one parent was an A229T carrier, identified an over-transmission of the A229T allele (15/18 trios) to BBS probands, suggesting that the change was associated with the manifestation of BBS features. Of the original 166 ciliopathy patients screened, Khanna *et al*. noted that the A229T allele was present in only ciliopathy patients in which retinal degeneration (RP ciliopathies) is a primary feature. Medical resequencing of Northern European RP ciliopathy patients (LCA, SLS, JBTS, BBS) identified an enrichment of the A229T allele in ciliopathy RP patients (4.5%, n=974 chromosomes) versus unaffected Northern Europeans (2.8%, n=3016 chromosomes). On the other hand, a combined NPHP and MKS ciliopathy cohort in which RP is not a clinical feature, did not have any A229T carriers (n=230 chromosomes). Together these data suggested that the

presence of the A229T variant may predispose ciliopathy patients to photoreceptor degeneration. Zebrafish *rpgrip1l* morphants displayed dose-dependent gastrulation defects similar to those of *bbs*-MO models, which could be rescued by co-injection with human *RPGRIP1L* mRNA. Furthermore, Threonine229 human mRNA transcript co-injection, unlike Alanine229, was ineffective at rescuing *rpgrip1l*-MO phenotypes and was comparable to co-injection defects of previously described human *RPGRIP1L* pathogenic variants. Similar observations were also made for abnormal tail phenotypes in *rpgrip1l* morphants that also failed to be rescued by Threonine229.

RPGRIP1L may be interacting biochemically with the ciliary protein RPGR. Yeast two-hybrid screens showed interaction between full-length RPGR and the C-terminal domain of RPGRIP1L. A reciprocal result was found in co-IP experiments while the RPGRIP1L (A229T) variant had poor interaction with RPGR in comparison to wild-type controls. Lastly, RPGRIP1L was found to localize to the basal body and primary cilium in mouse IMCD3 cells and to the inner segment and connecting cilium of mouse photoreceptors. Further supporting the role of RPGR in RP, mutations in *NPHP5*, in contrast to other NPHP genes, have been associated with an increased incidence of SLS (with retinal degeneration) and NPHP5 has been shown to interact with RPGR (Otto *et al.* 2005). Furthermore RPGR has been implicated in a high frequency of cases of X-linked RP, suggesting a core of RP-associated proteins in ciliopathies.

Taken together this candidate gene study suggests a role for the RPGRIP1L A229T variant as an indicator of photoreceptor degeneration within ciliopathy patients. Khanna *et al*. hypothesize that additional interacting candidates (genetic or biochemical) with the RPGR/RPGRIP1L complex could share a similar influence on the manifestation of RP features in ciliopathy patients. The full impact of this variant on the features of ciliopathy patients as well as the portion of variability that it may account for, remains to be fully elucidated.

1.8.3 Identifying Remaining Genetics Modifiers?

The above studies identify possible genetic modifiers of BBS through a combination of physical interaction, bioinformatic, human molecular, and animal model studies. In the case of *CCDC28B*, Badano *et al*. proposed that within a compromised background, such as BBS, a decrease in *CCDC28B* transcripts could adversely affect the progression of this disease (Badano *et al.* 2006). Khanna *et al*. identified that a specific variant of the ciliary protein RPGRIP1L may

be associated with the manifestation of RP phenotypes in a range of ciliopathies (Khanna *et al.* 2009).

Recent guidelines created by the National Cancer Institute and National Human Genome Research Institute on the replication of genotype-phenotype associations list a number of criteria in regards to genome-wide and candidate gene studies . These standards may therefore be applied to identifying genotype-phenotype correlations for modifying loci in BBS cohorts. For example, Chanock *et al*. suggest the use of robust methods such as transmission disequilibrium testing in family based studies (Chanock *et al.* 2007). Both Badano *et al*. and Khanna *et al*. take care to apply this method to their own studies. Molecular analyses using a zebra fish morpholino system supported the conclusions in both of these studies.

The analysis of *CCDC28B*, however, remains to be positively replicated as only a small number of families (three) shared a structure amenable to genotype-phenotype analysis. Additional analyses in other research groups and cohorts have failed to identify *CCDC28B* mutations as a contributing factor in phenotypic variation, suggesting the existence of other causes (Azari *et al.* 2006; Bin *et al.* 2009). In one case, Azari *et al*. examined 10 patients (8 homozygous and 2 heterozygous BBS1(M390R) patients) for differences in ocular phenotypes. Despite identifying variability in the severity of retinal disease, direct sequencing of *CCDC28B* confirmed wild-type alleles (430C), and did not detect additional changes at this locus to explain phenotype variability in this cohort (Azari *et al.* 2006).

The association of *RPGRIP1L* with RP-related ciliopathies also requires additional verification. Khanna *et al*. combine a number of Northern European cohorts to increase the power of their study but do not include phenotype data in their assessment of these populations as suggested by published guidelines (Chanock *et al.* 2007). A phenotype comparison of both *RPGRIP1L*(G685A) carriers and wild-type (G685) patients from the RP-ciliopathy cohort would aid in supporting these findings.

Do these two genes account for all of the phenotype variability observed amongst BBS patients? New evidence makes a case for dominant negative BBS alleles as second-site modifiers, which may influence disease manifestation (Zaghloul *et al.* 2010). Given the heterogeneity and complex pathophysiology of BBS, however, it is possible that additional uncharacterized loci could be associated with the intragenic and intrafamilial variability of BBS features. The

identification of novel modifying loci may require alternative strategies beyond cataloging direct protein interactions and known ciliary components. As an example, the relationship between cilia and specific signalling pathways required a careful assessment of phenotypes and examination of genetic interactions in model organisms in combination with forward genetics screens (Huangfu *et al.* 2003; Ross *et al.* 2005). Utilizing similar methods will not only expand the pool of human candidate modifier genes but aid in the eventual deciphering of BBS pathophysiology as well.

1.9 Summary of the Ciliopathy Field

BBS and other ciliopathies comprise a relatively small but growing group of pleiotropic disorders that also share relevant features with diseases of much higher incidence (Zaghloul *et al.* 2009). Despite recent findings from animal models that have revealed new phenotypes and molecular insights into BBS, the causes of pleiotropy and the pathophysiology of ciliopathy features remains relatively unclear. The pathogenesis of important features such as photoreceptor degeneration and renal cysts are not well explored despite the effect these can have on quality of life or survival in general. Research groups in the field have begun to decipher some of the genetic and molecular aspects of these features but exact mechanisms remains to be elucidated (Tobin *et al.* 2008; Jin *et al.* 2010; Seo *et al.* 2010; Pretorius *et al.* 2011; Williams *et al.* 2011).

The proposed oligogenic nature of BBS implies that additional heterozygous mutant BBS loci may contribute to the severity of some BBS cases. Given the variability of the human genome, it is likely that other modifying loci can account for the phenotypic variability observed at the intergenic and intragenic level as well as the interfamilial and intrafamilial level (Badano *et al.* 2006; Leitch *et al.* 2008; Khanna *et al.* 2009).

Furthermore, this evolutionarily conserved organelle plays an important role as a signalling centre for developmental pathways such as Wnt, Shh and PCP as well as metabolic homeostasis as in leptin signalling. It is unknown if other well-conserved signalling events are also mediated through the primary cilium, and what their relationship with BBS or other ciliopathies may be. The BBSome is a protein complex reported to participate in vesicular trafficking to the cilium, the coordination of anterograde transport during IFT, and the negative regulation of axonemal contents (Lechtreck *et al.* 2009; Jin *et al.* 2010; Seo *et al.* 2010; Williams *et al.* 2011). It remains to be determined if these functions are evolutionarily conserved across all ciliated species.

Each of the three major BBS model organisms - mouse, zebrafish, and nematode – offers advantages and disadvantages. Mice share the most phenotypes while being less tractable to genetically compare in cases of complex inheritance. Zebrafish offer a simplified knock down system to observe developmental phenotypes but the morpholino system is only transient, making long-term functional studies less feasible. Nematodes are very amenable to genetic manipulation and analysis, with various systems for gene deletion, knock down, and expression but lack higher order phenotypes and the vertebrate-specific BBS proteins. Finally, the search for genetic modifiers of BBS phenotype has yielded only two candidates thus far. The first, *CCDC28B*, used a reverse genetics approach in which the candidate gene was selected by comparing groups of potential interactors (Badano *et al.* 2006). The phenotype and molecular data supported an exacerbating effect for a specific allele in a small group of patients, although there have been no following studies that positively replicate these findings. The second, *RPGRIP1L*, has strong biochemical evidence to support a conserved role for the A229T allele as an indicator of retinopathy but requires clarification of human genotype-phenotype data to further support these results (Khanna *et al.* 2009).

BBS, a multisystemic disease of significant morbidity, is an excellent model ciliopathy which may also help elucidate more common human disorders that include obesity and photoreceptor degeneration. A careful molecular study to reveal the basis of BBS pathogenesis through cilia-related pathways may also aid in the diagnosis, prognosis, and treatment of this disorder.

1.10 Objectives of This Thesis

The work of my thesis focuses on an approach to elucidate the genetic influences of the phenotype variability of BBS, which may have an impact on other ciliopathy-related phenotypes. The importance of studying a disease such as BBS is several-fold. First, given the significant morbidity of this disorder, an understanding of disease pathophysiology and its relationship with genetic factors will serve to improve both the diagnosis and management of patients. Second, the shared features of BBS with other ciliopathies, makes it a prime candidate for elucidating this particular class of disease. Third, the pleiotropic features of the ciliopathies include retinal degeneration, obesity, and cystic renal disease, making BBS a possible alternative model for studying common human disorders.

Given the evolutionary conservation of the primary cilium, I hypothesize that the function of this organelle will also encompass interactions with well-conserved signalling pathways. In elucidating the genetic and biochemical mechanisms of BBS, the use of a forward genetics approach in combination with a well-phenotyped cohort is multi-purposed by identifying 1) genetic loci that exacerbate or ameliorate BBS features, 2) downstream molecular components (without predisposing for only those identified as cilia-associated) that may alter some or all BBS features, 3) factors that positively correlate with altering BBS phenotypes in an unbiased fashion.

In a forward genetics approach, *C. elegans* is an excellent model to screen for genetic BBS modifiers given 1) its fast reproductive life cycle and simple genetic manipulation, 2) its strong conservation of core BBSome proteins, 3) its well-studied developmental programming and simple phenotypes and 4) its transparent body, which is excellent for live imaging experiments involving cellular localization.

Thus an elucidation of BBS mechanisms using the model organism *C. elegans* will contribute to the cumulative knowledge regarding this and related diseases. My work in the following chapters shows that *C. elegans* is a suitable a model organism for the study of BBS and genetic modifiers and that it has the potential to yield additional insights into the functions of these evolutionarily conserved proteins.

1.10.1 Mutations in a Guanylate Cyclase GCY-35/GCY-36 Modify Bardet-Biedl Syndrome-Associated Phenotypes in *Caenorhabditis elegans*

I began with a phenotypic investigation of available *bbs* mutants in order to help identify a set of features that was suitable to use in a forward genetics screen. During the course of my investigation, I identified the guanylate cyclase GCY-35/GCY-36 as a modifier of the small body size found in *bbs* mutants. My work demonstrated that a PKG, EGL-4, acts downstream of the GCY-35/GCY-36 cGMP pathway to regulate body size. This finding is unique in comparison to multiple other guanylate cyclase mutants that were tested. Localization experiments failed to identify significant changes to the expression or localization of GCY-35 and GCY-36, while cell-specific rescue experiments established a non-cell autonomous role for BBS proteins that may be

extra-ciliary as well as identifying cGMP signalling as a factor that may contribute to human BBS features.

1.10.2 Analysis of Signalling Pathways Affecting the Body size of *Caenorhabditis elegans*

With the identification of the cGMP-EGL-4 pathway as important to *bbs* mutant body size regulation, I investigated the role of known EGL-4 signalling properties and observed that EGL-4 may be signalling in a cytoplasmic or transiently nuclear fashion to regulate body size. I also intiated a candidate gene approach to identify additional upstream and downstream components that influence the molecular mechanisms involved in *bbs* mutant body size. My candidate approach included an additional PKG (*C09G4.2*), phosphodiesterases (PDEs), and *daf-21* the *C. elegans* orthologue of HSP90. My results identify that *C09G4.2* does not influence *bbs* body size while *daf-21* (possibly via rGC activation) and *pde-5* play a role in body size regulation but in a parallel manner to *bbs* mutants. I also identify an additional modifier of body size, *mobs-2*. I conclude that *bbs* mutant body size may be regulated through unidentified synaptic communication in parallel to additional neuronal groups that regulate the effect of EGL-4 signalling in *C. elegans* neurons.

1.11 References

Aberle, H., A. Bauer, *et al.* (1997). "beta-catenin is a target for the ubiquitin-proteasome pathway." EMBO J **16**(13): 3797-3804.

Adler, P. N. (1992). "The genetic control of tissue polarity in Drosophila." Bioessays **14**(11): 735-741.

Adler, P. N., J. Charlton, *et al.* (1998). "Mutations in the cadherin superfamily member gene dachsous cause a tissue polarity phenotype by altering frizzled signaling." Development **125**(5): 959-968.

Adler, P. N., C. Vinson, *et al.* (1990). "Molecular structure of frizzled, a Drosophila tissue polarity gene." Genetics **126**(2): 401-416.

Ansley, S. J., J. L. Badano, *et al.* (2003). "Basal body dysfunction is a likely cause of pleiotropic Bardet-Biedl syndrome." Nature **425**(6958): 628-633.

Arts, H. H., D. Doherty, *et al.* (2007). "Mutations in the gene encoding the basal body protein RPGRIP1L, a nephrocystin-4 interactor, cause Joubert syndrome." Nat Genet **39**(7): 882-888.

Axelrod, J. D. and C. J. Tomlin (2011). "Modeling the control of planar cell polarity." Wiley Interdiscip Rev Syst Biol Med **3**(5): 588-605.

Azari, A. A., T. S. Aleman, *et al.* (2006). "Retinal disease expression in Bardet-Biedl syndrome-1 (BBS1) is a spectrum from maculopathy to retina-wide degeneration." Invest Ophthalmol Vis Sci **47**(11): 5004-5010.

Baala, L., S. Audollent, *et al.* (2007). "Pleiotropic effects of CEP290 (NPHP6) mutations extend to Meckel syndrome." Am J Hum Genet **81**(1): 170-179.

Badano, J. L., S. J. Ansley, *et al.* (2003a). "Identification of a novel Bardet-Biedl syndrome protein, BBS7, that shares structural features with BBS1 and BBS2." Am J Hum Genet **72**(3): 650-658.

Badano, J. L., J. C. Kim, *et al.* (2003b). "Heterozygous mutations in BBS1, BBS2 and BBS6 have a potential epistatic effect on Bardet-Biedl patients with two mutations at a second BBS locus." Hum Mol Genet **12**(14): 1651-1659.

Badano, J. L., C. C. Leitch, *et al.* (2006). "Dissection of epistasis in oligogenic Bardet-Biedl syndrome." Nature **439**(7074): 326-330.

Baker, K. and P. L. Beales (2009). "Making sense of cilia in disease: the human ciliopathies." Am J Med Genet C Semin Med Genet **151C**(4): 281-295.

Bardet, G. (1920). "Sur un syndrome d'obesite congenitale avec polydactylie et retinite pigmentaire (contribution a l'etude desformes cliniques de l'obesite hypophysaire)." University de Paris **Thesis no. 470. Amedee LeGrand. Paris, France.**

Beales, P. L., J. L. Badano, *et al.* (2003). "Genetic interaction of BBS1 mutations with alleles at other BBS loci can result in non-Mendelian Bardet-Biedl syndrome." Am J Hum Genet **72**(5): 1187-1199.

Beales, P. L., N. Elcioglu, *et al.* (1999). "New criteria for improved diagnosis of Bardet-Biedl syndrome: results of a population survey." J Med Genet **36**(6): 437-446.

Bellaiche, Y., M. Gho, *et al.* (2001a). "Frizzled regulates localization of cell-fate determinants and mitotic spindle rotation during asymmetric cell division." Nat Cell Biol **3**(1): 50-57.

Bellaiche, Y., A. Radovic, *et al.* (2001b). "The Partner of Inscuteable/Discs-large complex is required to establish planar polarity during asymmetric cell division in Drosophila." Cell **106**(3): 355-366.

Berbari, N. F., A. D. Johnson, *et al.* (2008a). "Identification of ciliary localization sequences within the third intracellular loop of G protein-coupled receptors." Mol Biol Cell **19**(4): 1540-1547.

Berbari, N. F., J. S. Lewis, *et al.* (2008b). "Bardet-Biedl syndrome proteins are required for the localization of G protein-coupled receptors to primary cilia." Proc Natl Acad Sci U S A **105**(11): 4242-4246.

Bettencourt-Dias, M. and D. M. Glover (2007). "Centrosome biogenesis and function: centrosomics brings new understanding." Nat Rev Mol Cell Biol **8**(6): 451-463.

Biedl, A. (1922). "Ein Geschwisterpaar mit adiposo-genitaler Dystrophie." Dtsch. Med. Wochenschr.(48).

Bin, J., J. Madhavan, *et al.* (2009). "BBS7 and TTC8 (BBS8) mutations play a minor role in the mutational load of Bardet-Biedl syndrome in a multiethnic population." Hum Mutat **30**(7): E737-746.

Birnby, D. A., E. M. Link, *et al.* (2000). "A transmembrane guanylyl cyclase (DAF-11) and Hsp90 (DAF-21) regulate a common set of chemosensory behaviors in caenorhabditis elegans." Genetics **155**(1): 85-104.

Bisgrove, B. W. and H. J. Yost (2006). "The roles of cilia in developmental disorders and disease." Development **133**(21): 4131-4143.

Blacque, O. E., M. J. Reardon, *et al.* (2004). "Loss of C. elegans BBS-7 and BBS-8 protein function results in cilia defects and compromised intraflagellar transport." Genes Dev **18**(13): 1630-1642.

Bremser, M., W. Nickel, *et al.* (1999). "Coupling of coat assembly and vesicle budding to packaging of putative cargo receptors." Cell **96**(4): 495-506.

Brenner, S. (1974). "The genetics of Caenorhabditis elegans." Genetics **77**(1): 71-94.

Brodsky, M. H. and H. Steller (1996). "Positional information along the dorsal-ventral axis of the Drosophila eye: graded expression of the four-jointed gene." Dev Biol **173**(2): 428-446.

Cano, D. A., N. S. Murcia, *et al.* (2004). "Orpk mouse model of polycystic kidney disease reveals essential role of primary cilia in pancreatic tissue organization." Development **131**(14): 3457-3467.

Carvalho-Santos, Z., J. Azimzadeh, *et al.* (2011). "Evolution: Tracing the origins of centrioles, cilia, and flagella." J Cell Biol **194**(2): 165-175.

Casal, J., G. Struhl, *et al.* (2002). "Developmental compartments and planar polarity in Drosophila." Curr Biol **12**(14): 1189-1198.

Chae, J., M. J. Kim, *et al.* (1999). "The Drosophila tissue polarity gene starry night encodes a member of the protocadherin family." Development **126**(23): 5421-5429.

Chalfie, M., Y. Tu, *et al.* (1994). "Green fluorescent protein as a marker for gene expression." Science **263**(5148): 802-805.

Chanock, S. J., T. Manolio, *et al.* (2007). "Replicating genotype-phenotype associations." Nature **447**(7145): 655-660.

Chaudhuri, I., J. Soding, *et al.* (2008). "Evolution of the beta-propeller fold." Proteins **71**(2): 795-803.

Cheung, B. H., F. Arellano-Carbajal, *et al.* (2004). "Soluble guanylate cyclases act in neurons exposed to the body fluid to promote C. elegans aggregation behavior." Curr Biol **14**(12): 1105-1111.

Chiang, A. P., J. S. Beck, *et al.* (2006). "Homozygosity mapping with SNP arrays identifies TRIM32, an E3 ubiquitin ligase, as a Bardet-Biedl syndrome gene (BBS11)." Proc Natl Acad Sci U S A **103**(16): 6287-6292.

Chiang, A. P., D. Nishimura, *et al.* (2004). "Comparative genomic analysis identifies an ADP-ribosylation factor-like gene as the cause of Bardet-Biedl syndrome (BBS3)." Am J Hum Genet **75**(3): 475-484.

Clark, H. F., D. Brentrup, *et al.* (1995). "Dachsous encodes a member of the cadherin superfamily that controls imaginal disc morphogenesis in Drosophila." Genes Dev **9**(12): 1530-1542.

Cole, D. G., S. W. Chinn, *et al.* (1993). "Novel heterotrimeric kinesin-related protein purified from sea urchin eggs." Nature **366**(6452): 268-270.

Cole, D. G., D. R. Diener, *et al.* (1998). "Chlamydomonas kinesin-II-dependent intraflagellar transport (IFT): IFT particles contain proteins required for ciliary assembly in Caenorhabditis elegans sensory neurons." J Cell Biol **141**(4): 993-1008.

Collier, S., H. Lee, *et al.* (2005). "The WD40 repeat protein fritz links cytoskeletal planar polarity to frizzled subcellular localization in the Drosophila epidermis." Genetics **169**(4): 2035-2045.

Coppieters, F., S. Lefever, *et al.* (2010). "CEP290, a gene with many faces: mutation overview and presentation of CEP290base." Hum Mutat **31**(10): 1097-1108.

Corbit, K. C., P. Aanstad, *et al.* (2005). "Vertebrate Smoothened functions at the primary cilium." Nature **437**(7061): 1018-1021.

Corbit, K. C., A. E. Shyer, *et al.* (2008). "Kif3a constrains beta-catenin-dependent Wnt signalling through dual ciliary and non-ciliary mechanisms." Nat Cell Biol **10**(1): 70-76.

Craige, B., C. C. Tsao, *et al.* (2010). "CEP290 tethers flagellar transition zone microtubules to the membrane and regulates flagellar protein content." J Cell Biol **190**(5): 927-940.

Curtin, J. A., E. Quint, *et al.* (2003). "Mutation of Celsr1 disrupts planar polarity of inner ear hair cells and causes severe neural tube defects in the mouse." Curr Biol **13**(13): 1129-1133.

Das, G., A. Jenny, *et al.* (2004). "Diego interacts with Prickle and Strabismus/Van Gogh to localize planar cell polarity complexes." Development **131**(18): 4467-4476.

Davenport, J. R. and B. K. Yoder (2005). "An incredible decade for the primary cilium: a look at a once-forgotten organelle." Am J Physiol Renal Physiol **289**(6): F1159-1169.

Davis, R. E., R. E. Swiderski, *et al.* (2007). "A knockin mouse model of the Bardet-Biedl syndrome 1 M390R mutation has cilia defects, ventriculomegaly, retinopathy, and obesity." Proc Natl Acad Sci U S A **104**(49): 19422-19427.

Delous, M., L. Baala, *et al.* (2007). "The ciliary gene RPGRIP1L is mutated in cerebello-oculo-renal syndrome (Joubert syndrome type B) and Meckel syndrome." Nat Genet **39**(7): 875-881.

Deveault, C., G. Billingsley, *et al.* (2011). "BBS genotype-phenotype assessment of a multiethnic patient cohort calls for a revision of the disease definition." Hum Mutat.

Dryja, T. P., S. M. Adams, *et al.* (2001). "Null RPGRIP1 alleles in patients with Leber congenital amaurosis." Am J Hum Genet **68**(5): 1295-1298.

Eichers, E. R., M. M. Abd-El-Barr, *et al.* (2006). "Phenotypic characterization of Bbs4 null mice reveals age-dependent penetrance and variable expressivity." Hum Genet **120**(2): 211-226.

Evans, J. E., J. J. Snow, *et al.* (2006). "Functional modulation of IFT kinesins extends the sensory repertoire of ciliated neurons in Caenorhabditis elegans." J Cell Biol **172**(5): 663-669.

Fan, Y., M. A. Esmail, *et al.* (2004). "Mutations in a member of the Ras superfamily of small GTP-binding proteins causes Bardet-Biedl syndrome." Nat Genet **36**(9): 989-993.

Farag, T. I. and A. S. Teebi (1988). "Bardet-Biedl and Laurence-Moon syndromes in a mixed Arab population." Clin Genet **33**(2): 78-82.

Farag, T. I. and A. S. Teebi (1989). "High incidence of Bardet Biedl syndrome among the Bedouin." Clin Genet **36**(6): 463-464.

Fath, M. A., R. F. Mullins, *et al.* (2005). "Mkks-null mice have a phenotype resembling Bardet-Biedl syndrome." Hum Mol Genet **14**(9): 1109-1118.

Fauser, S., M. Munz, *et al.* (2003). "Further support for digenic inheritance in Bardet-Biedl syndrome." J Med Genet **40**(8): e104.

Fawcett, D. W. a. P. K. R. (1954). "A Study of the Fine Strucutre of Ciliated Epithelia." Journal of Morphology **94**(2).

Feiguin, F., M. Hannus, *et al.* (2001). "The ankyrin repeat protein Diego mediates Frizzled-dependent planar polarization." Dev Cell **1**(1): 93-101.

Gerdes, J. M., Y. Liu, *et al.* (2007). "Disruption of the basal body compromises proteasomal function and perturbs intracellular Wnt response." Nat Genet **39**(11): 1350-1360.

Gho, M. and F. Schweisguth (1998). "Frizzled signalling controls orientation of asymmetric sense organ precursor cell divisions in Drosophila." Nature **393**(6681): 178-181.

Gilula, N. B. and P. Satir (1972). "The ciliary necklace. A ciliary membrane specialization." J Cell Biol **53**(2): 494-509.

Gorden, N. T., H. H. Arts, *et al.* (2008). "CC2D2A is mutated in Joubert syndrome and interacts with the ciliopathy-associated basal body protein CEP290." Am J Hum Genet **83**(5): 559-571.

Gubb, D., C. Green, *et al.* (1999). "The balance between isoforms of the prickle LIM domain protein is critical for planar polarity in Drosophila imaginal discs." Genes Dev **13**(17): 2315-2327.

Haimo, L. T. and J. L. Rosenbaum (1981). "Cilia, flagella, and microtubules." J Cell Biol **91**(3 Pt 2): 125s-130s.

Hao, Y., N. Xu, *et al.* (2011). "Nuclear cGMP-Dependent Kinase Regulates Gene Expression via Activity-Dependent Recruitment of a Conserved Histone Deacetylase Complex." PLoS Genet **7**(5): e1002065.

Huangfu, D., A. Liu, *et al.* (2003). "Hedgehog signalling in the mouse requires intraflagellar transport proteins." Nature **426**(6962): 83-87.

Inada, H., H. Ito, *et al.* (2006). "Identification of guanylyl cyclases that function in thermosensory neurons of Caenorhabditis elegans." Genetics **172**(4): 2239-2252.

Inglis, P. N., G. Ou, *et al.* (2007). "The sensory cilia of Caenorhabditis elegans." WormBook: 1-22.

Jia, J., A. Kolterud, *et al.* (2009). "Suppressor of Fused inhibits mammalian Hedgehog signaling in the absence of cilia." Dev Biol **330**(2): 452-460.

Jin, H., S. R. White, *et al.* (2010). "The conserved Bardet-Biedl syndrome proteins assemble a coat that traffics membrane proteins to cilia." Cell **141**(7): 1208-1219.

Jinek, M., J. Rehwinkel, *et al.* (2004). "The superhelical TPR-repeat domain of O-linked GlcNAc transferase exhibits structural similarities to importin alpha." Nat Struct Mol Biol **11**(10): 1001-1007.

Johnson, K. A. and J. L. Rosenbaum (1992). "Polarity of flagellar assembly in Chlamydomonas." J Cell Biol **119**(6): 1605-1611.

Jones, C., V. C. Roper, *et al.* (2008). "Ciliary proteins link basal body polarization to planar cell polarity regulation." Nat Genet **40**(1): 69-77.

Katsanis, N., S. J. Ansley, *et al.* (2001). "Triallelic inheritance in Bardet-Biedl syndrome, a Mendelian recessive disorder." Science **293**(5538): 2256-2259.

Katsanis, N., P. L. Beales, *et al.* (2000). "Mutations in MKKS cause obesity, retinal dystrophy and renal malformations associated with Bardet-Biedl syndrome." Nat Genet **26**(1): 67-70.

Katsanis, N., E. R. Eichers, *et al.* (2002). "BBS4 is a minor contributor to Bardet-Biedl syndrome and may also participate in triallelic inheritance." Am J Hum Genet **71**(1): 22-29.

Keller, R. (2002). "Shaping the vertebrate body plan by polarized embryonic cell movements." Science **298**(5600): 1950-1954.

Khaddour, R., U. Smith, *et al.* (2007). "Spectrum of MKS1 and MKS3 mutations in Meckel syndrome: a genotype-phenotype correlation. Mutation in brief #960. Online." Hum Mutat **28**(5): 523-524.

Khanna, H., E. E. Davis, *et al.* (2009). "A common allele in RPGRIP1L is a modifier of retinal degeneration in ciliopathies." Nat Genet **41**(6): 739-745.

Kim, J. C., J. L. Badano, *et al.* (2004). "The Bardet-Biedl protein BBS4 targets cargo to the pericentriolar region and is required for microtubule anchoring and cell cycle progression." Nat Genet **36**(5): 462-470.

Kim, S. K., A. Shindo, *et al.* (2010). "Planar cell polarity acts through septins to control collective cell movement and ciliogenesis." Science **329**(5997): 1337-1340.

Klein, D. and F. Ammann (1969). "The syndrome of Laurence-Moon-Bardet-Biedl and allied diseases in Switzerland. Clinical, genetic and epidemiological studies." J Neurol Sci **9**(3): 479-513.

Klingensmith, J., R. Nusse, *et al.* (1994). "The Drosophila segment polarity gene dishevelled encodes a novel protein required for response to the wingless signal." Genes Dev **8**(1): 118-130.

Koenekoop, R. (2003). "The major gene for Bardet-Biedl syndrome is BBS1." Ophthalmic Genet **24**(2): 127.

Kozminski, K. G., K. A. Johnson, *et al.* (1993). "A motility in the eukaryotic flagellum unrelated to flagellar beating." Proc Natl Acad Sci U S A **90**(12): 5519-5523.

Kulaga, H. M., C. C. Leitch, *et al.* (2004). "Loss of BBS proteins causes anosmia in humans and defects in olfactory cilia structure and function in the mouse." Nat Genet **36**(9): 994-998.

Kyttala, M., J. Tallila, *et al.* (2006). "MKS1, encoding a component of the flagellar apparatus basal body proteome, is mutated in Meckel syndrome." Nat Genet **38**(2): 155-157.

Lancaster, M. A., J. Schroth, *et al.* (2011). "Subcellular spatial regulation of canonical Wnt signalling at the primary cilium." Nat Cell Biol **13**(6): 700-707.

Laurence, J., and Moon, R.C. (1866). "Four cases of retinitis pigmentosa occuring in the same family accompanied by general imperfection of development." Ophthalmic Rev. **2**: 10.

Laurier, V., C. Stoetzel, *et al.* (2006). "Pitfalls of homozygosity mapping: an extended consanguineous Bardet-Biedl syndrome family with two mutant genes (BBS2, BBS10), three mutations, but no triallelism." Eur J Hum Genet **14**(11): 1195-1203.

Lechtreck, K. F., E. C. Johnson, *et al.* (2009). "The Chlamydomonas reinhardtii BBSome is an IFT cargo required for export of specific signaling proteins from flagella." J Cell Biol **187**(7): 1117-1132.

Leitch, C. C., N. A. Zaghloul, *et al.* (2008). "Hypomorphic mutations in syndromic encephalocele genes are associated with Bardet-Biedl syndrome." Nat Genet **40**(4): 443-448.

Li, J. B., J. M. Gerdes, *et al.* (2004). "Comparative genomics identifies a flagellar and basal body proteome that includes the BBS5 human disease gene." Cell **117**(4): 541-552.

Lin, F., T. Hiesberger, *et al.* (2003). "Kidney-specific inactivation of the KIF3A subunit of kinesin-II inhibits renal ciliogenesis and produces polycystic kidney disease." Proc Natl Acad Sci U S A **100**(9): 5286-5291.

Liu, J., A. Ward, *et al.* (2010). "C. elegans phototransduction requires a G protein-dependent cGMP pathway and a taste receptor homolog." Nat Neurosci **13**(6): 715-722.

Logan, C. Y. and R. Nusse (2004). "The Wnt signaling pathway in development and disease." Annu Rev Cell Dev Biol **20**: 781-810.

Loktev, A. V., Q. Zhang, *et al.* (2008). "A BBSome subunit links ciliogenesis, microtubule stability, and acetylation." Dev Cell **15**(6): 854-865.

Louvi, A. and E. A. Grove (2011). "Cilia in the CNS: The Quiet Organelle Claims Center Stage." Neuron **69**(6): 1046-1060.

Lu, X., A. G. Borchers, *et al.* (2004). "PTK7/CCK-4 is a novel regulator of planar cell polarity in vertebrates." Nature **430**(6995): 93-98.

Ma, D., C. H. Yang, *et al.* (2003). "Fidelity in planar cell polarity signalling." Nature **421**(6922): 543-547.

Mahoney, P. A., U. Weber, *et al.* (1991). "The fat tumor suppressor gene in Drosophila encodes a novel member of the cadherin gene superfamily." Cell **67**(5): 853-868.

Mak, H. Y., L. S. Nelson, *et al.* (2006). "Polygenic control of Caenorhabditis elegans fat storage." Nat Genet **38**(3): 363-368.

Marion, V., C. Stoetzel, *et al.* (2009). "Transient ciliogenesis involving Bardet-Biedl syndrome proteins is a fundamental characteristic of adipogenic differentiation." Proc Natl Acad Sci U S A **106**(6): 1820-1825.

Matsuoka, K., L. Orci, *et al.* (1998). "COPII-coated vesicle formation reconstituted with purified coat proteins and chemically defined liposomes." Cell **93**(2): 263-275.

May, S. R., A. M. Ashique, *et al.* (2005). "Loss of the retrograde motor for IFT disrupts localization of Smo to cilia and prevents the expression of both activator and repressor functions of Gli." Dev Biol **287**(2): 378-389.

McMahon, H. T. and I. G. Mills (2004). "COP and clathrin-coated vesicle budding: different pathways, common approaches." Curr Opin Cell Biol **16**(4): 379-391.

Mockel, A., Y. Perdomo, *et al.* (2011). "Retinal dystrophy in Bardet-Biedl syndrome and related syndromic ciliopathies." Prog Retin Eye Res **30**(4): 258-274.

Mok, C. A., E. Heon, *et al.* (2010). "Ciliary dysfunction and obesity." Clin Genet **77**(1): 18-27.

Mollet, G., R. Salomon, *et al.* (2002). "The gene mutated in juvenile nephronophthisis type 4 encodes a novel protein that interacts with nephrocystin." Nat Genet **32**(2): 300-305.

Montcouquiol, M., R. A. Rachel, *et al.* (2003). "Identification of Vangl2 and Scrb1 as planar polarity genes in mammals." Nature **423**(6936): 173-177.

Mykytyn, K., T. Braun, *et al.* (2001). "Identification of the gene that, when mutated, causes the human obesity syndrome BBS4." Nat Genet **28**(2): 188-191.

Mykytyn, K., R. F. Mullins, *et al.* (2004). "Bardet-Biedl syndrome type 4 (BBS4)-null mice implicate Bbs4 in flagella formation but not global cilia assembly." Proc Natl Acad Sci U S A **101**(23): 8664-8669.

Mykytyn, K., D. Y. Nishimura, *et al.* (2002). "Identification of the gene (BBS1) most commonly involved in Bardet-Biedl syndrome, a complex human obesity syndrome." Nat Genet **31**(4): 435-438.

Nachury, M. V. (2008). "Tandem affinity purification of the BBSome, a critical regulator of Rab8 in ciliogenesis." Methods Enzymol **439**: 501-513.

Nachury, M. V., A. V. Loktev, *et al.* (2007). "A core complex of BBS proteins cooperates with the GTPase Rab8 to promote ciliary membrane biogenesis." Cell **129**(6): 1201-1213.

Nishimura, D. Y., M. Fath, *et al.* (2004). "Bbs2-null mice have neurosensory deficits, a defect in social dominance, and retinopathy associated with mislocalization of rhodopsin." Proc Natl Acad Sci U S A **101**(47): 16588-16593.

Nishimura, D. Y., C. C. Searby, *et al.* (2001). "Positional cloning of a novel gene on chromosome 16q causing Bardet-Biedl syndrome (BBS2)." Hum Mol Genet **10**(8): 865-874.

Nishimura, D. Y., R. E. Swiderski, *et al.* (2005). "Comparative genomics and gene expression analysis identifies BBS9, a new Bardet-Biedl syndrome gene." Am J Hum Genet **77**(6): 1021-1033.

Nonaka, S., Y. Tanaka, *et al.* (1998). "Randomization of left-right asymmetry due to loss of nodal cilia generating leftward flow of extraembryonic fluid in mice lacking KIF3B motor protein." Cell **95**(6): 829-837.

Oeffner, F., C. Moch, *et al.* (2008). "Novel interaction partners of Bardet-Biedl syndrome proteins." Cell Motil Cytoskeleton **65**(2): 143-155.

Otto, E. A., T. W. Hurd, *et al.* (2010). "Candidate exome capture identifies mutation of SDCCAG8 as the cause of a retinal-renal ciliopathy." Nat Genet **42**(10): 840-850.

Otto, E. A., B. Loeys, *et al.* (2005). "Nephrocystin-5, a ciliary IQ domain protein, is mutated in Senior-Loken syndrome and interacts with RPGR and calmodulin." Nat Genet **37**(3): 282-288.

Otto, E. A., K. Tory, *et al.* (2009). "Hypomorphic mutations in meckelin (MKS3/TMEM67) cause nephronophthisis with liver fibrosis (NPHP11)." J Med Genet **46**(10): 663-670.

Ou, G., O. E. Blacque, *et al.* (2005). "Functional coordination of intraflagellar transport motors." Nature **436**(7050): 583-587.

Ou, G., M. Koga, *et al.* (2007). "Sensory ciliogenesis in Caenorhabditis elegans: assignment of IFT components into distinct modules based on transport and phenotypic profiles." Mol Biol Cell **18**(5): 1554-1569.

Pan, X., G. Ou, *et al.* (2006). "Mechanism of transport of IFT particles in C. elegans cilia by the concerted action of kinesin-II and OSM-3 motors." J Cell Biol **174**(7): 1035-1045.

Pazour, G. J., B. L. Dickert, *et al.* (1999). "The DHC1b (DHC2) isoform of cytoplasmic dynein is required for flagellar assembly." J Cell Biol **144**(3): 473-481.

Pazour, G. J., J. T. San Agustin, *et al.* (2002). "Polycystin-2 localizes to kidney cilia and the ciliary level is elevated in orpk mice with polycystic kidney disease." Curr Biol **12**(11): R378-380.

Pazour, G. J., C. G. Wilkerson, *et al.* (1998). "A dynein light chain is essential for the retrograde particle movement of intraflagellar transport (IFT)." J Cell Biol **141**(4): 979-992.

Perkins, L. A., E. M. Hedgecock, *et al.* (1986). "Mutant sensory cilia in the nematode Caenorhabditis elegans." Dev Biol **117**(2): 456-487.

Pretorius, P. R., M. A. Aldahmesh, *et al.* (2011). "Functional analysis of BBS3 A89V that results in non-syndromic retinal degeneration." Hum Mol Genet.

Pretorius, P. R., L. M. Baye, *et al.* (2010). "Identification and functional analysis of the vision-specific BBS3 (ARL6) long isoform." PLoS Genet **6**(3): e1000884.

Riise, R. (1996). "The cause of death in Laurence-Moon-Bardet-Biedl syndrome." Acta Ophthalmol Scand Suppl(219): 45-47.

Rix, S., A. Calmont, *et al.* (2011). "An Ift80 mouse model of short rib polydactyly syndromes shows defects in hedgehog signalling without loss or malformation of cilia." Hum Mol Genet **20**(7): 1306-1314.

Roepman, R., S. J. Letteboer, *et al.* (2005). "Interaction of nephrocystin-4 and RPGRIP1 is disrupted by nephronophthisis or Leber congenital amaurosis-associated mutations." Proc Natl Acad Sci U S A **102**(51): 18520-18525.

Rohatgi, R., L. Milenkovic, *et al.* (2007). "Patched1 regulates hedgehog signaling at the primary cilium." Science **317**(5836): 372-376.

Rohatgi, R. and W. J. Snell (2010). "The ciliary membrane." Curr Opin Cell Biol **22**(4): 541-546.

Ross, A. J., H. May-Simera, *et al.* (2005). "Disruption of Bardet-Biedl syndrome ciliary proteins perturbs planar cell polarity in vertebrates." Nat Genet **37**(10): 1135-1140.

Satir, P., D. R. Mitchell, *et al.* (2008). "How did the cilium evolve?" Curr Top Dev Biol **85**: 63-82.

Sayer, J. A., E. A. Otto, *et al.* (2006). "The centrosomal protein nephrocystin-6 is mutated in Joubert syndrome and activates transcription factor ATF4." Nat Genet **38**(6): 674-681.

Schneider, L., C. A. Clement, *et al.* (2005). "PDGFRalphaalpha signaling is regulated through the primary cilium in fibroblasts." Curr Biol **15**(20): 1861-1866.

Seo, S., L. M. Baye, *et al.* (2010). "BBS6, BBS10, and BBS12 form a complex with CCT/TRiC family chaperonins and mediate BBSome assembly." Proc Natl Acad Sci U S A **107**(4): 1488-1493.

Seo, S., D. F. Guo, *et al.* (2009). "Requirement of Bardet-Biedl syndrome proteins for leptin receptor signaling." Hum Mol Genet **18**(7): 1323-1331.

Shulman, J. M., N. Perrimon, *et al.* (1998). "Frizzled signaling and the developmental control of cell polarity." Trends Genet **14**(11): 452-458.

Signor, D., K. P. Wedaman, *et al.* (1999). "Role of a class DHC1b dynein in retrograde transport of IFT motors and IFT raft particles along cilia, but not dendrites, in chemosensory neurons of living Caenorhabditis elegans." J Cell Biol **147**(3): 519-530.

Silverman, M. A. and M. R. Leroux (2009). "Intraflagellar transport and the generation of dynamic, structurally and functionally diverse cilia." Trends Cell Biol **19**(7): 306-316.

Snow, J. J., G. Ou, *et al.* (2004). "Two anterograde intraflagellar transport motors cooperate to build sensory cilia on C. elegans neurons." Nat Cell Biol **6**(11): 1109-1113.

Sobkowicz, H. M., S. M. Slapnick, *et al.* (1995). "The kinocilium of auditory hair cells and evidence for its morphogenetic role during the regeneration of stereocilia and cuticular plates." J Neurocytol **24**(9): 633-653.

Stagg, S. M., P. LaPointe, *et al.* (2007). "Structural design of cage and coat scaffolds that direct membrane traffic." Curr Opin Struct Biol **17**(2): 221-228.

Stoetzel, C., V. Laurier, *et al.* (2006). "BBS10 encodes a vertebrate-specific chaperonin-like protein and is a major BBS locus." Nat Genet **38**(5): 521-524.

Stoetzel, C., J. Muller, *et al.* (2007). "Identification of a novel BBS gene (BBS12) highlights the major role of a vertebrate-specific branch of chaperonin-related proteins in Bardet-Biedl syndrome." Am J Hum Genet **80**(1): 1-11.

Sulston, J. E. and H. R. Horvitz (1977). "Post-embryonic cell lineages of the nematode, Caenorhabditis elegans." Dev Biol **56**(1): 110-156.

Sulston, J. E., E. Schierenberg, *et al.* (1983). "The embryonic cell lineage of the nematode Caenorhabditis elegans." Dev Biol **100**(1): 64-119.

Sutterlin, C. and A. Colanzi (2010). "The Golgi and the centrosome: building a functional partnership." J Cell Biol **188**(5): 621-628.

Tan, P. L., T. Barr, *et al.* (2007). "Loss of Bardet Biedl syndrome proteins causes defects in peripheral sensory innervation and function." Proc Natl Acad Sci U S A **104**(44): 17524-17529.

Tayeh, M. K., H. J. Yen, *et al.* (2008). "Genetic interaction between Bardet-Biedl syndrome genes and implications for limb patterning." Hum Mol Genet **17**(13): 1956-1967.

Taylor, J., N. Abramova, *et al.* (1998). "Van Gogh: a new Drosophila tissue polarity gene." Genetics **150**(1): 199-210.

Theisen, H., J. Purcell, *et al.* (1994). "dishevelled is required during wingless signaling to establish both cell polarity and cell identity." Development **120**(2): 347-360.

Tickle, C., D. Summerbell, *et al.* (1975). "Positional signalling and specification of digits in chick limb morphogenesis." Nature **254**(5497): 199-202.

Tobin, J. L. and P. L. Beales (2008). "Restoration of renal function in zebrafish models of ciliopathies." Pediatr Nephrol **23**(11): 2095-2099.

Torban, E., C. Kor, *et al.* (2004). "Van Gogh-like2 (Strabismus) and its role in planar cell polarity and convergent extension in vertebrates." Trends Genet **20**(11): 570-577.

Usui, T., Y. Shima, *et al.* (1999). "Flamingo, a seven-pass transmembrane cadherin, regulates planar cell polarity under the control of Frizzled." Cell **98**(5): 585-595.

Valente, E. M., J. L. Silhavy, *et al.* (2006). "Mutations in CEP290, which encodes a centrosomal protein, cause pleiotropic forms of Joubert syndrome." Nat Genet **38**(6): 623-625.

van Amerongen, R. and R. Nusse (2009). "Towards an integrated view of Wnt signaling in development." Development **136**(19): 3205-3214.

Veeman, M. T., J. D. Axelrod, *et al.* (2003). "A second canon. Functions and mechanisms of beta-catenin-independent Wnt signaling." Dev Cell **5**(3): 367-377.

Villano, J. L. and F. N. Katz (1995). "four-jointed is required for intermediate growth in the proximal-distal axis in Drosophila." Development **121**(9): 2767-2777.

Vinson, C. R., S. Conover, *et al.* (1989). "A Drosophila tissue polarity locus encodes a protein containing seven potential transmembrane domains." Nature **338**(6212): 263-264.

Wang, C. W., S. Hamamoto, *et al.* (2006). "Exomer: A coat complex for transport of select membrane proteins from the trans-Golgi network to the plasma membrane in yeast." J Cell Biol **174**(7): 973-983.

Ward, S., N. Thomson, *et al.* (1975). "Electron microscopical reconstruction of the anterior sensory anatomy of the nematode Caenorhabditis elegans.?2UU." J Comp Neurol **160**(3): 313-337.

Wiens, C. J., Y. Tong, *et al.* (2010). "Bardet-Biedl syndrome-associated small GTPase ARL6 (BBS3) functions at or near the ciliary gate and modulates Wnt signaling." J Biol Chem **285**(21): 16218-16230.

Williams, C. L., C. Li, *et al.* (2011). "MKS and NPHP modules cooperate to establish basal body/transition zone membrane associations and ciliary gate function during ciliogenesis." J Cell Biol **192**(6): 1023-1041.

Wolff, T. and G. M. Rubin (1998). "Strabismus, a novel gene that regulates tissue polarity and cell fate decisions in Drosophila." Development **125**(6): 1149-1159.

Wong, L. L. and P. N. Adler (1993). "Tissue polarity genes of Drosophila regulate the subcellular location for prehair initiation in pupal wing cells." J Cell Biol **123**(1): 209-221.

Yang, C. H., J. D. Axelrod, *et al.* (2002). "Regulation of Frizzled by fat-like cadherins during planar polarity signaling in the Drosophila compound eye." Cell **108**(5): 675-688.

Yen, H. J., M. K. Tayeh, *et al.* (2006). "Bardet-Biedl syndrome genes are important in retrograde intracellular trafficking and Kupffer's vesicle cilia function." Hum Mol Genet **15**(5): 667-677.

Yoder, B. K., X. Hou, *et al.* (2002). "The polycystic kidney disease proteins, polycystin-1, polycystin-2, polaris, and cystin, are co-localized in renal cilia." J Am Soc Nephrol **13**(10): 2508-2516.

Yu, S., L. Avery, *et al.* (1997). "Guanylyl cyclase expression in specific sensory neurons: a new family of chemosensory receptors." Proc Natl Acad Sci U S A **94**(7): 3384-3387.

Zaghloul, N. A. and N. Katsanis (2009). "Mechanistic insights into Bardet-Biedl syndrome, a model ciliopathy." J Clin Invest **119**(3): 428-437.

Zaghloul, N. A., Y. Liu, *et al.* (2010). "Functional analyses of variants reveal a significant role for dominant negative and common alleles in oligogenic Bardet-Biedl syndrome." Proc Natl Acad Sci U S A **107**(23): 10602-10607.

Zeidler, M. P., N. Perrimon, *et al.* (1999). "The four-jointed gene is required in the Drosophila eye for ommatidial polarity specification." Curr Biol **9**(23): 1363-1372.

Zeidler, M. P., N. Perrimon, *et al.* (2000). "Multiple roles for four-jointed in planar polarity and limb patterning." Dev Biol **228**(2): 181-196.

Zhang, Q., D. Nishimura, *et al.* (2011). "Bardet-Biedl syndrome 3 (Bbs3) knockout mouse model reveals common BBS-associated phenotypes and Bbs3 unique phenotypes." Proc Natl Acad Sci U S A.

Chapter 2
Methods and Materials

2

2.1 Strain Culture Conditions

All strains were maintained on NGM plates at 20°C. *C. elegans bbs*, *gcy* and *egl-4* strains were obtained from the *CGC*. CX7102 was obtained from the Bargmann lab. Genotypes for all strains are listed in the Appendix (**A3**). All strains used in the phenotyping studies were back-crossed to N2 (wild-type) backgrounds between four and eight times before assessing for phenotype analysis.

2.2 Phenotyping Protocols

2.2.1 DiI uptake

DiI assays were performed on mixed populations of strains as previously described (Uchida *et al.* 2003). *C. elegans* were washed twice in M9 buffer and resuspended in 400ul M9 with 2ng of DiI. Samples were incubated 2-3 hours before washing three times with M9 buffer. Worms were allowed to recover overnight before scoring for uptake phenotypes. Uptake was scored as positive in an animal if DiI staining was observed in amphid, phasmid or both sets of neurons on a minimum of 20 animals per strain.

2.2.2 Body size assessment

Three gravid adult animals per strain were allowed to lay eggs for 24-30 hours before being removed from each plate. F1 animals were allowed to grow for an additional 48 hours. Approximately 20-40 L4 animals were measured for each strain. L4 animals were allowed to grow 16-18 hours before measurement for adult data. Some populations were measured again 48 hours later to complete growth curve analysis.

All the strains could not be measured in a single sitting, therefore each measurement session included at least one wild-type population as a point of reference to normalize against other measurement sessions. External variables such as temperature, growth conditions, and developmental age were kept as constant as possible by incubating animals in the same

environment, growing them on the same batch of NGM plates, and measuring them in a small time frame.

For body size measurement, images were captured on a Zeiss Stemi SVII dissecting microscope at 50X magnification using a Zeiss Axiocam digital camera at a 1388x1040 resolution. These images were then analysed using Axiovision software to measure length (cubic splines) and/or width of individual animals.

Statistical analyses were completed using ANOVA with the Tukey post-hoc test to compare between multiple groups; *** $p<0.001$ ** $p<0.01$, * $p<0.05$, and ns $p\geq0.05$. In comparing the growth curve in multiple measurement sessions, it was found that the mean body size of wild-type animals could vary by ~3.5% from the beginning of a session to the end. Thus statistical significance is only noted for a body size difference of >3.5% of wild-type length. Data on all graphs represent mean ± standard deviation relative to wild-type body length.

2.2.3 Developmental timing

The developmental timing assay was modified from (Sulston *et al.* 1988). Briefly, eggs were collected from gravid adults and hatched in 7.5mL M9 for 20-22 hours. Synchronized L1 larvae were centrifuged again and animals were deposited onto multiple OP50 seeded NGM plates (from the same batch) at about 50-80 animals per plate. Animals were grown at 20ºC for ~42 hours before being assessed for developmental staging based on described anatomical landmarks for L4 larvae at 30-minute intervals. Each plate was analysed as a single population, with at least 10 replicate plates per strain. The ANOVA with Tukey post-hoc test was used for statistical analyses; *** $p<0.001$ ** $p<0.01$, * $p<0.05$, and ns $p\geq0.05$ in comparing between strains.

2.2.4 Roaming assay

Animals at the L4 stage were transferred individually to the centre of 35mm seeded plates. Individual animals were removed 18 hours later and their tracking pattern was analysed using a 5mm x 5mm grid. Inclusion criteria for grids were any bacterial squares that the animals had traversed in the given time. For each strain a minimum of 25 animals was examined. Statistical analyses were completed using the Kruskal-Wallis non-parametric test with Dunn's post-hoc to compare between multiple groups; *** $p<0.001$ ** $p<0.01$, * $p<0.05$, and ns $p\geq0.05$. Data on all graphs represent mean ± standard error of mean (SEM) for squares traversed.

2.2.5 Fluorescence Microscopy

Animals were bleach synchronized and examined at various stages including at L3, L4 and 12-20 hours later. Animals were immobilised on 2-5% dry agarose imaging pads, with approximately 12ul of M9 solution. All images were acquired on a Zeiss Axioskop 2 fluorescent microscope equipped with a CCD camera. Images were taken at 63x unless otherwise indicated

2.3 Mapping and cloning of *hp433*

bbs-7(n1606);hp433 mutants were outcrossed twice against N2 by selecting animals that were genotyped for *n1606* mutation, but exhibited normal body size. The *hp433* mutation was crossed into *bbs-7(ok1351)* mutants and mapped based on the suppression of small body size and roaming defects using the SNP markers in the CB4856 strain, which placed it at a 93.5kb interval between the SNPs *pkp1133* and *uCE1-1426*. We conclude that *hp433* encodes *gcy-35* by: 1) Injection of three overlapping fosmids covering *gcy-35*, T04D3.5, and T04D3.t2, reverted the body size suppression in *hp433; bbs-7* animals. A fragment of WRM641cB09 that encompassed a truncated *gcy-35*, but complete T04D3.5 and T04D3.t2 failed to revert the *hp433* suppression; a genomic fragment containing only *gcy-35* fully reverted the suppression. 2) *gcy-35(ok769)* animals shared the same synthetic phenotypes and genetic interactions with *bbs-7* as *hp433*, while *hp433;bbs-7(ok1351)* animals also failed to complement *gcy-35(ok769);bbs-7(ok1351)*. 3) Sequencing of *gcy-35* identified a 2bp deletion in exon 8. For more details see Appendix (**A1**).

2.4 Molecular Biology

Genomic rescues of *bbs-1*, *bbs-7*, and *bbs-8* used PCR products of each respective genomic sequence, including 2080, 1262, and 531bp of 5' upstream sequence respectively. Rescue of *bbs-2* animals used *bbs-2* cDNA (F20D12.3 ordered from OpenBiosystems, catalog # OCE1182-7243861) driven by an F25B3.3 (*rgef-1*) promoter sequence of 3444bp. *gcy-35* rescues were carried out with clones *Pgcy-36::GCY-35* (*non-isoprenylated)* (Gray *et al.* 2004) and *Plad-2::GCY-35* (*isoprenylated)* (Chang *et al.* 2006) courtesy of Dr. Cornelia Bargmann. Promoters for these two plasmids were 1095bp and 4013bp respectively and exchanged using FseI and AscI sites to generate *pJH1374 (Pgcy-36::GCY-35 isoprenylated)* and *pJH1390 (Plad-2::GCY-35 non-isoprenylated)*. *pJH1493 (Pflp-8::GCY-35 isoprenylated)* was created by insertion of a FseI/AscI tagged, 2.3kb sequence 5' of the *flp-8* start site PCR'd from N2 genomic DNA (p3548:

ATTggccggccTCAGAAACCCCGATTCAAAC, p3549: gtcGGCGCGCCTTTCTACTTG AAAAGTGTGGAC).

Subcellular localisation of GCY-36 was analysed using a vector of *Pgcy-36::GFP::GCY-36* (Cheung *et al.* 2004) courtesy of Dr. Mario de Bono that included 2021bp of upstream promoter sequence. *pJH1867 (Pgcy-36::GFP::GCY-35)* was constructed by replacing GCY-36 in the above construct with a subcloned GCY-35 from *pJH1374* using p3639 SfoI-tagged (ATTGGCGCCacaATGTTCGGCT GGATTCACG) and p3640 HpaI-tagged (GTCgttaacttaAGAAATTGTGCAAGTCG) primers.

2.5 References

Chang, A. J., N. Chronis, *et al.* (2006). "A distributed chemosensory circuit for oxygen preference in C. elegans." PLoS Biol **4**(9): e274.

Cheung, B. H., F. Arellano-Carbajal, *et al.* (2004). "Soluble guanylate cyclases act in neurons exposed to the body fluid to promote C. elegans aggregation behavior." Curr Biol **14**(12): 1105-1111.

Gray, J. M., D. S. Karow, *et al.* (2004). "Oxygen sensation and social feeding mediated by a C. elegans guanylate cyclase homologue." Nature **430**(6997): 317-322.

Sulston, J. E. and H. J. A. (1988). Methods. The Nematode Caenorhabditis elegans. New York, Cold Spring Harbor Laboratory Press**:** 587-606.

Uchida, O., H. Nakano, *et al.* (2003). "The C. elegans che-1 gene encodes a zinc finger transcription factor required for specification of the ASE chemosensory neurons." Development **130**(7): 1215-1224.

Chapter 3
Mutations in a Guanylate Cyclase GCY-35/GCY-36 Modify Bardet-Biedl Syndrome-Associated Phenotypes in *Caenorhabditis elegans*

Calvin A. Mok, Michael P. Healey, Tanvi Shekhar, Michel R. Leroux, Elise Héon & Mei Zhen

3

This chapter is reprinted using the Creative Commons Attribution License (CCAL) as applied by the Public Library of Science (PLoS) from PLoS Genetics 2011 Oct; 7(10):e1002335. I performed all experiments and analyzed data reported in this chapter except the following: Mr. Healey generated the *bbs-7* cell-specific rescue lines and their body size measurements. Ms. Shekhar performed the *bbs*, *gcy-35;bbs*, and *bbs-7;tax* mutant developmental timing assays. Dr. Zhen and I drafted the manuscript. Drs. Héon and Leroux edited the manuscript.

3.1 Abstract

Ciliopathies are pleiotropic and genetically heterogeneous disorders caused by defective development and function of the primary cilium. Bardet-Biedl syndrome (BBS) proteins localize to the base of cilia and undergo intraflagellar transport and the loss of their functions leads to a multisystemic ciliopathy. Here I report the identification of mutations in guanylate cyclases (GCYs) as modifiers of *Caenorhabditis elegans bbs* phenotypes. The loss of GCY-35 or GCY-36 suppresses the small body size, developmental delay, and exploration defects exhibited by multiple *bbs* mutants. Moreover, an effector of cGMP signalling, a cGMP-dependent protein kinase, EGL-4, also modifies *bbs* mutant defects. I propose that a misregulation of cGMP signalling, which underlies developmental and some behavioural defects of *C. elegans bbs* mutants, may also contribute to some BBS features in other organisms.

3.2 Author Summary

Bardet-Biedl syndrome (BBS) is a genetically heterogeneous, multisystemic disorder. Defects to the cilium, an evolutionarily conserved organelle cause ciliopathies, a growing class of diseases that includes BBS. The BBS proteins are involved in the vesicular transport of proteins to the cilium, and the process of intraflagellar transport. Here I show that in addition to sensory defects,

Caenorhabditis elegans bbs mutants exhibit reduced body size and delayed developmental timing. The reduced body size phenotype is not fully recapitulated by IFT mutants, suggesting that BBS proteins may have additional functions beyond bridging IFT motors. I further identify that loss of function mutations in the soluble guanylate cyclase complex, GCY-35/GCY-36, results in a suppression of these defects. Interestingly, GCY-35/GCY-36 influences the body size of *C. elegans* through a cGMP-dependent protein kinase EGL-4 in a group of body cavity neurons. BBS proteins, on the other hand, function through a non-overlapping set of ciliated sensory neurons, in an IFT-independent manner, to influence cGMP signalling in the body cavity neurons. In conclusion, this study reveals a non-cell autonomous role for the BBS proteins in ciliated sensory neurons in regulating cGMP signalling during development. I propose that aberrant cGMP signalling, essential for a number of cellular processes, may also contribute to some ciliopathy features in other systems.

3.3 Introduction

The cilium plays diverse cellular functions in metazoans which include imparting motility, enabling sensory processes and regulating the activity of cell signalling pathways during development (Berbari *et al.* 2009). The biogenesis and maintenance of this evolutionarily conserved organelle relies on intraflagellar transport (IFT) – the bidirectional transportation of diverse cargo proteins along the microtubule-based axoneme. Defective IFT or ciliary dysfunction result in ciliopathies, a growing class of pleiotropic human diseases with overlapping clinical features, some being of significant morbidity (Tobin *et al.* 2009). Bardet-Biedl syndrome (BBS, OMIM 209900) is an autosomal recessive and genetically heterogeneous ciliopathy with hallmark clinical features that include photoreceptor degeneration, renal abnormalities, obesity, cognitive impairment, and digit and genital anomalies (Baker *et al.* 2009). To date, sixteen genes are associated with BBS (Baker *et al.* 2009; Kim *et al.* 2010; Otto *et al.* 2010); of these, seven function mostly as a conserved protein complex (BBSome) (Nachury *et al.* 2007) to regulate vesicular sorting and packaging (Jin *et al.* 2010), IFT (Ou *et al.* 2005; Pan *et al.* 2006), as well as cilium maintenance and function (reviewed in (Zaghloul *et al.* 2009)).

Animal models have been instrumental in deciphering the physiological functions of BBS proteins (Tobin *et al.* 2009; Zaghloul *et al.* 2009). Initial characterization of *Caenorhabditis elegans* BBS orthologues led to the discovery of BBS proteins as ciliary components, associating

ciliary defects with the loss of BBS protein function (Ansley *et al.* 2003; Blacque *et al.* 2004; Inglis *et al.* 2007). The loss of BBS-7 and BBS-8 led to shortened cilia, reduced uptake of a lipophilic dye (DiI) by the cilium, and defective chemo- and thermotaxis (Blacque *et al.* 2004; Tan *et al.* 2007).

Murine *Bbs* mutants recapitulate several human BBS features including photoreceptor degeneration, renal anomalies and obesity (Nishimura *et al.* 2004; Eichers *et al.* 2006). Additionally, these models led to the identification of new features such as neural tube closure defects (Ross *et al.* 2005), anosmia (Kulaga *et al.* 2004), and behavioural, mechano- and thermosensory deficits (Tan *et al.* 2007) that expanded the diagnostic features of human ciliopathies. Morpholino-mediated knockdown of *bbs* in zebrafish led to developmental phenotypes such as dorsal thinning, poor somitic definition and Kupffer's Vesicle malformation (Badano *et al.* 2006; Yen *et al.* 2006; Tayeh *et al.* 2008), while defects characteristic of ciliopathy such as delayed retrograde melanosome transport (Yen *et al.* 2006) and vision impairment (Pretorius *et al.* 2010) also manifested.

In addition to a role in sensory transduction, the primary cilium functions as a signalling 'apparatus' to regulate development (Berbari *et al.* 2009). For example, IFT-dependent localization of Sonic Hedgehog (Shh) receptors to primary cilia is required for Shh signalling (Corbit *et al.* 2005; Rohatgi *et al.* 2007). Disrupting IFT components IFT172, TG737/Polaris and the motor KIF3A in mouse models resulted in phenotypes typical of Shh mutants (Huangfu *et al.* 2003). Similarly, defective planar cell polarity (PCP) signalling (Ross *et al.* 2005; Jones *et al.* 2008) and/or aberrant Wnt signalling (Lin *et al.* 2003; Corbit *et al.* 2008) were associated with the inactivation of BBS, Polaris or KIF3A components. These, and others studies (Schneider *et al.* 2005; Berbari *et al.* 2008a) suggest that the cilium may modulate multiple signalling pathways in a tissue-specific manner. Aberrant PCP, Shh and Wnt signalling have been implicated in underlying a number of ciliopathy features, such as neural tube closure, polydactyly and obesity (Ross *et al.* 2005; Marion *et al.* 2009; Seo *et al.* 2009; Pretorius *et al.* 2010). The pathophysiology of other features such as photoreceptor degeneration remains largely unexplained, indicating the presence of unidentified cellular processes that are regulated by the cilium.

C. elegans BBS orthologues are exclusively expressed in the 60 ciliated neurons of the adult hermaphrodite. Localizing at the base of cilia, they undergo active IFT, and their absence results in the destabilization of IFT and sensory defects (Ou *et al.* 2005). *C. elegans* sensory neurons play key roles in multiple developmental processes (Fujiwara *et al.* 2002; Inglis *et al.* 2007). Some chemosensory mutants exhibit a reduced body size (Fujiwara *et al.* 2002), indicating that sensory function may influence this developmental process. Another key regulator for body size is the cGMP-dependent protein kinase (PKG) EGL-4 (Fujiwara *et al.* 2002; L'Etoile *et al.* 2002; Hirose *et al.* 2003; Raizen *et al.* 2006); a loss of EGL-4 function leads to increased body size that is genetically epistatic to that of chemosensory mutants (Fujiwara *et al.* 2002). The mechanisms for sensory neuron-mediated body size regulation, however, remain to be fully elucidated. In the present study, in order to identify additional cilium-regulated signalling events in *C. elegans*, I carried out the phenotypic characterization of *bbs* mutant animals, and identified genetic modifiers that associate aberrant cGMP signalling with a subset of *bbs* features.

3.4 Results

3.4.1 *C. elegans bbs* mutants share ciliary defects, reduced body size, delayed developmental timing and reduced roaming

I performed an array of phenotypic and behavioural assessments of severe or complete loss-of-function (*lf*) mutants for the *C. elegans bbs-1*, *bbs-2*, *bbs-7*, *bbs-8* and *bbs-9* genes (**Table 10**). Consistent with previous reports on *bbs-7* and *bbs-8* (Blacque *et al.* 2004), all examined *bbs* mutants exhibited a failure in the uptake of a lipophilic dye DiI by sensory neurons (**Figure 6A**), confirming a common structural and functional deficit in the sensory cilia. In addition to sensory defects, I identified three novel *bbs*-associated phenotypes: decreased body size, altered dwelling/exploration behaviour and delayed developmental timing.

Despite grossly normal body morphology, *bbs* mutants shared a reduced body length by ~11-28% when compared to wild-type animals. Defects were visible during early larval stages and persisted throughout adulthood (**Figure 6B and 7**). In these analyses, I defined a 3.5% or greater difference as biologically relevant in body size change, as this was the upper range for the coefficient of variance in young adult wild-type populations (**Methods**). The reduced body length is caused by the loss of BBS function, as it was significantly rescued by introducing a wild-type genomic or cDNA array of *bbs* into the respective mutants (**Figure 6C**). A decrease in

body width was also characteristic of *bbs* mutants **(Figure 6D)**. By DAPI staining of nuclei I did not observe differences in tissue and cell numbers between wild-type and *bbs-7* animals (**data not shown**). The overall decrease in body size is thus best attributed to a smaller, averaged cell size in *bbs* mutants.

Table 10. *C. elegans bbs* alleles used in this study

Gene	Allele	Strain	Chromosome	Exons Deleted	Domains Deleted or Deletion Result
bbs-1	*ok1111*	VC837	I	7,8,9 (partial)	C-terminal truncation. No known domain information
bbs-2	*gk544*	VC1168	IV	1 (partial), 2, 3 (partial)	Ochre stop (aa34)
bbs-7	*n1606*	MT3645	III	4 (Single base-pair mutation)	Opal stop (aa223)
bbs-7	*ok1351*	RB1268	III	6,7	Likely loss of γ-adaptin ear domain
bbs-8	*nx77*	MX52	V	3 (partial), 4, 5, 6(partial)	Likely truncation of protein and loss of TPR, Coatomer_E, Pilf, TadD, NrfG domains
bbs-9	*gk471*	VC1062	I	1,2,3	Truncation of N-terminal β propeller

bbs double and triple mutants exhibited smaller body sizes that were no more severe than the smallest *bbs* single mutant (*bbs-9*). Although small differences between the body length of *bbs* single, double and triple mutant strains were observed as animals aged, the effects were not additive (**Figure 6B**); consistent with BBS proteins functioning in the same biological processes to regulate ciliary development and function (Nachury *et al.* 2007; Ou *et al.* 2007; Jin *et al.* 2010).

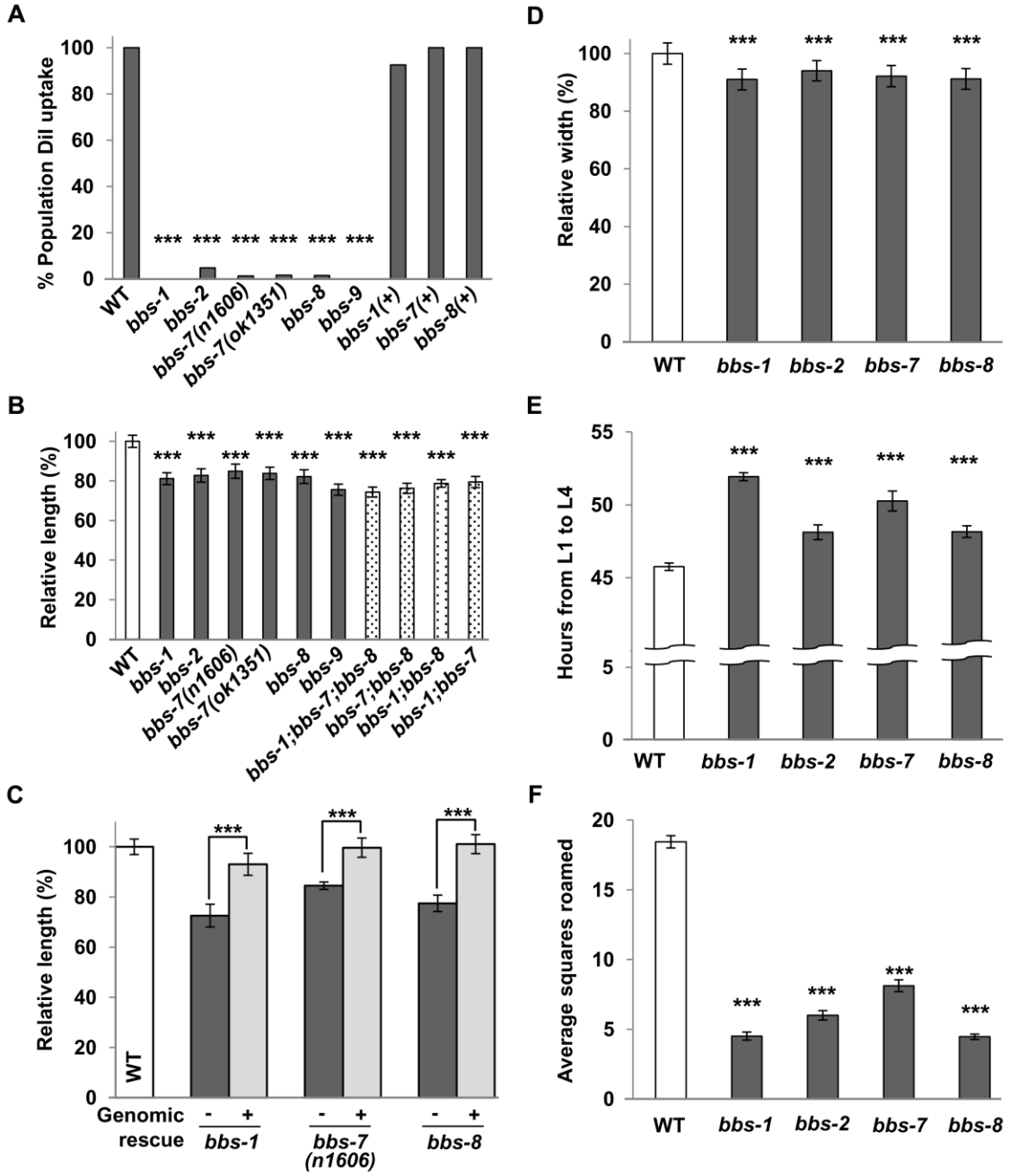

Figure 6. Multiple phenotypes exhibited by *bbs* mutants (A) DiI uptake of *bbs* mutants was reduced compared to wild-type and transgenic *bbs* mutants carrying genomic DNA fragments for respective *bbs* genes. Fisher's Exact test, *** p<0.001. (B) The body length of young adult *bbs* single, double and triple mutants was smaller in comparison to wild-type animals. ANOVA with Tukey, *** p<0.001, n≥20. Data represent mean ± SD normalized against wild-type body length. (C) The body length defects of *bbs* mutants were rescued by the expression of wild-type *bbs* genes (+) compared to their non-transgenic siblings (-). ANOVA with Tukey, *** p<0.001, n≥15. (D) The body width of *bbs* mutants was also decreased in comparison to wild-type animals. ANOVA with Tukey, *** p<0.001, n≥20. (E) Developmental timing (from L1 to L4 stage) was increased for *bbs* mutants in comparison to wild-type animals. ANOVA with Tukey, *** p<0.001, n≥50, N≥10 replicates. Data represent mean (hours) ± SD. (F) *bbs* mutants roamed less compared to wild-type animals. Kruskal-Wallis with Dunn's, *** p<0.001, n≥25, N≥2 replicates. Data represent mean squares roamed ± SEM. For *bbs-7* dataset, the *ok1351* deletion allele was used unless otherwise noted.

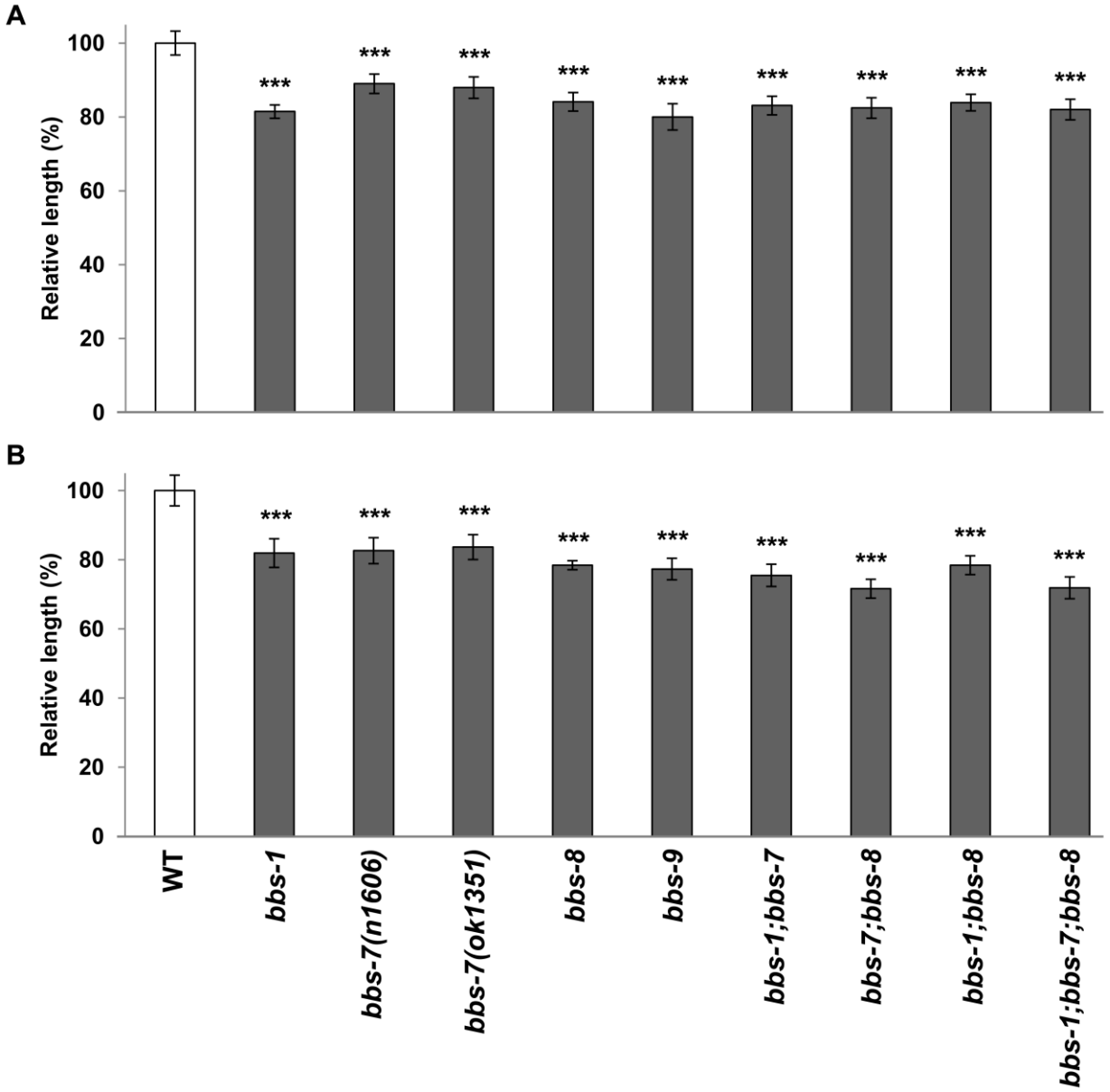

Figure 7. *bbs* mutants exhibit a smaller body size in late larvae and adulthood stages The body length measurements of *bbs* mutants at L4 (A) and 66-hours post-L4(B) showed consistent size defects when compared to similarly staged wild-type animals. ANOVA with Tukey, *** $p<0.001$ in comparison to wild-type animals, $n\geq20$. Data represent mean ± SD normalized against wild-type body length.

I next examined the body size of a number of IFT mutants, including *che-2*, *che-3*, and *che-11*, as well as *osm-3*, *osm-5*, *osm-6* and *klp-11*, nearly all of which display defects to cilia structure and abnormal dye filling (*dyf)*. Only some exhibited decreases in body size; among them, *che-11* mutants exhibited the most significant decrease (by 11% in young adulthood), but not as severely as in age-matched *bbs-7* mutants (**Figure 8A**). Notably, a loss of the IFT motors, KLP-11 kinesin-II subunit, OSM-3 kinesin, and CHE-3 dynein had little or no effect on body size.

Therefore while sensory neurons affect body size, the *dyf* phenotype, caused by ciliary dysfunction (ie. defective IFT transport), is not indicative of severe body size defects. The BBSome, exclusively expressed in ciliated sensory neurons, has a greater influence in the regulation of body size, indicating a role beyond bridging IFT motors for BBS proteins in these neurons.

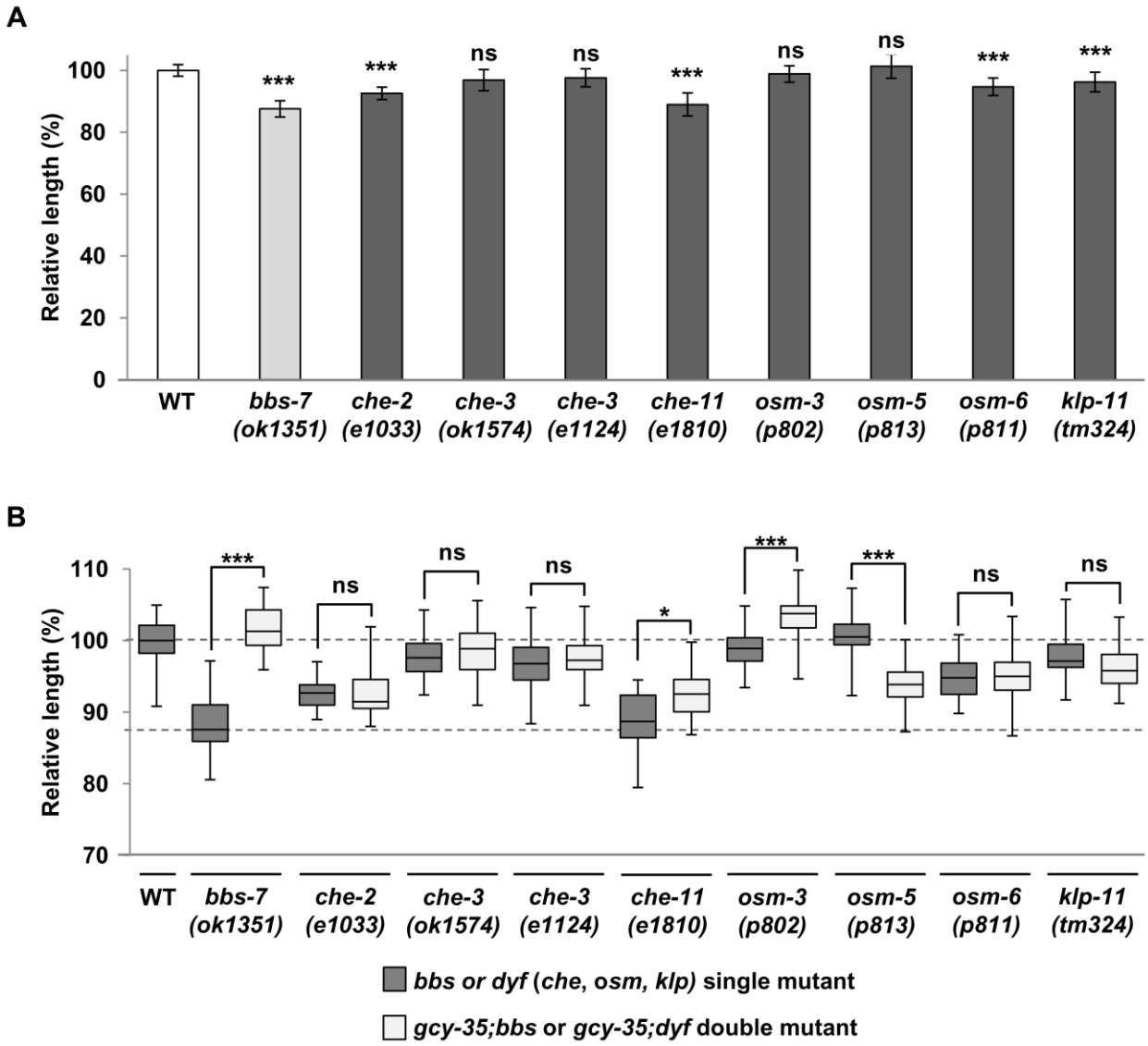

Figure 8. *dyf* (dye-filling) mutants show variable body size and genetic interaction with *gcy-35(lf)* (A) The relative length of *dyf* mutants in comparison to wild-type animals. Some *dyf* mutants had variable degrees of body length defects, while others showed little to no change in body length. ANOVA with Tukey, *** $p<0.001$; ns – $p\geq0.05$ or length difference <3.5% relative to wild-type animals, $n\geq30$. Data represent mean ± SD normalized against wild-type body length. (B) The body size of only a subset of *dyf* mutants (dark boxes) was mildly altered by the loss of *gcy-35* (light boxes). Boxes represent 25th-75th percentile of populations with maximum and minimum values as whiskers. ANOVA with Tukey, *** $p<0.001$; * $p<0.05$; ns – $p\geq0.05$ or length difference <3.5%, $n\geq30$. Data represent mean ± SD normalized against wild-type body length.

C. elegans exhibits a defined developmental time course (Brenner 1973). Multiple *bbs* mutant strains exhibited slower larval development (**Figure 6E**), resulting in a 2.3 - 6.2 hour delay between the first (L1) and last (L4) larval stage. During foraging, *C. elegans* exhibits a combination of dwelling and exploration/roaming behaviours that are altered in some chemosensory defective mutants (Fujiwara *et al.* 2002). Multiple *bbs* mutants showed a 56% to 76% decrease in overall movement, or roaming (**Figure 6F**) when compared to wild-type animals. This behavioural change does not reflect a general loss of locomotor activity, as *bbs* mutant animals exhibit normal (co-ordinated) locomotion during roaming. These additional phenotypes support a notion that the *C. elegans* cilia regulate cellular processes in addition to taxis behaviours.

3.4.2 The Loss of Function of a Guanylate Cyclase GCY-35 Rescues a Subset of Phenotypes in *bbs* Mutants

Unlike all other *bbs* strains examined, MT3645 *bbs-7(n1606)* (received from the *Caenorhabditis Genetics Center),* displayed body size, roaming behaviour, and developmental timing characteristics similar to wild-type animals. Upon genetic outcrossing, I re-isolated a homozygous *bbs-7(n1606)* strain that exhibited phenotypes characteristic of other *bbs* mutants. These defects were fully rescued by the expression of the wild-type genomic copy of *bbs-7* (**Figure 6C**). I concluded through genetic analyses that a single modifying locus from the original *MT3645* strain rescued a subset of the *bbs-7* mutant phenotypes (**Figure 9**).

I mapped this modifier allele, *hp433*, to *gcy-35* (**Methods, Appendix A1**), a gene encoding the α subunit of a soluble guanylate cyclase (sGC). sGC proteins are composed of a heme/NO binding (HNOB), a heme/NO binding associated (HNOBA), and a GC catalytic domain (reviewed in (Koesling *et al.* 1999)). They are heterodimeric complexes consisting of α and β subunits to catalyze the conversion of GTP to cGMP. *hp433* results in a frame-shift in the coding sequence and a premature termination codon in the HNOBA domain, causing a truncation of the GC catalytic domain (**Figure 9A**). I also observed that a deletion allele in the GC domain of *gcy-35*, *ok769*, functions as a recessive suppressor of *bbs-7* mutants (**Figure 9A and 9B**).

While both *gcy-35*(*lf*) alleles exhibit similar body length to that of wild-type animals, they suppressed the significant body length defects of multiple *bbs* mutants (**Figure 9B**). In contrast,

gcy-35(lf);dyf mutants showed little or no improvement to body length (**Figure 8B**). The consistent suppression observed in *bbs* mutant animals advocated strongly for the further

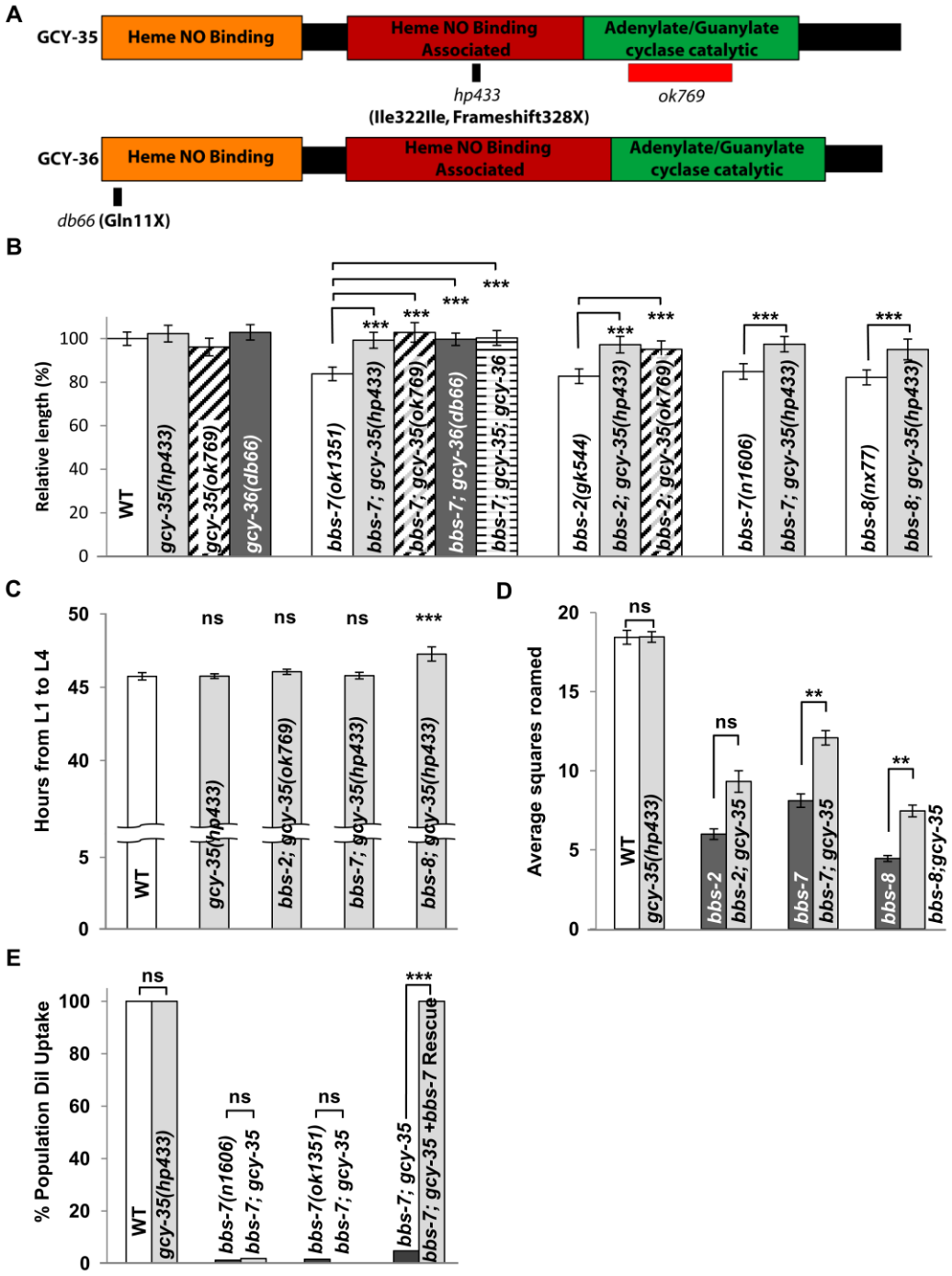

Figure 9. *gcy-35(lf)* suppresses a subset of *bbs* phenotypes (A) A schematic of the functional domains of GCY-35 and GCY-36 including allelic information of the respective mutants. (B) *gcy-35(lf)* and *gcy-36(lf)* alleles suppressed body length defects in multiple *bbs* mutant alleles. ANOVA with Tukey, *** p<0.001, n≥20. Data represent mean ± SD normalized against wild-type body length. (C) *gcy-35(lf)* fully or partially suppressed *bbs* mutant developmental defects. ANOVA with Tukey, *** p<0.001 with respect to wild-type controls; ns – p≥0.05, n≥50, N≥10 replicates. Data represent mean (hours) ± SD. (D)

Exploration patterns of *gcy-35;bbs-7* and *gcy-35;bbs-8* animals (light bars) were partially rescued compared to respective *bbs* genotypes (dark bars). Kruskal-Wallis with Dunn's, ** $p<0.01$; ns – $p\geq0.05$, $n\geq25$, $N\geq2$. Data represent mean squares roamed ± SEM. (E) *gcy-35* did not rescue the DiI uptake of *bbs-7* mutants, while *gcy-35(lf)* alone did not result in any DiI defects. Fisher's Exact test, *** $p<0.001$; ns – $p>0.05$. For *bbs-7* data depicted, the *ok1351* deletion allele was used unless otherwise noted.

investigation of *gcy-35(lf)* as an epistatic suppressor of *bbs*-mediated phenotypes. *gcy-35* also modified the *bbs* phenotypes in developmental timing and roaming. Both the developmental timing from the first (L1) to the last (L4) stages, and roaming scores of *gcy-35* mutants were comparable to that of wild-type (**Figure 9C and 9D**). The developmental timing of *gcy-35;bbs-7* and *gcy-35;bbs-2* mutants was identical to that of wild-type animals, whereas *gcy-35;bbs-8* animals exhibited a partial improvement over that of *bbs-8* animals (**Figure 9C**). Roaming defects of *bbs-2*, *bbs-7*, and *bbs-8* mutants were partially suppressed by *gcy-35* (**Figure 9D**).

Other *bbs* phenotypes, such as shortened cilia and defective DiI uptake (**Figure 9E and data not shown**), were not rescued by *gcy-35(lf)* mutants. These results suggest that the ciliary structures remain impaired in *gcy-35;bbs* mutants, and that the cellular pathways regulating body size, developmental timing and roaming behaviours either function genetically downstream of, or differ from those involved in sensory perception.

3.4.3 The GCY-35/GCY-36 sGC Complex Influences the Body Size of *bbs* Mutants Through a Subset of Oxygen Sensing Body Cavity Neurons

GCY-35 and its partner GCY-36 form a heterodimeric sGC that modulates *C. elegans* behaviour in response to ambient oxygen concentrations (Cheung *et al.* 2004; Gray *et al.* 2004). *gcy-36(db66)* (*lf*) mutants (Cheung *et al.* 2004) rescued the body size defect of *bbs-7* mutants (**Figure 9B**). Moreover, *gcy-35;gcy-36;bbs-7* animals exhibited a body size no different from either *gcy-35;bbs-7* or *gcy-36;bbs-7* (**Figure 9B**), consistent with GCY-35 and GCY-36 also functioning as a heterodimeric sGC to regulate body size.

I examined in which neurons this sGC influences body size using *bbs* mutants. Both GCY-35 and GCY-36 are expressed in the ciliated body cavity sensory neurons AQR and PQR, and a non-ciliated body cavity neuron URX; GCY-35 is additionally expressed in the non-ciliated ALN, PLN, and SDQ neurons (Gray *et al.* 2004). AQR, PQR and URX expression of wild-type GCY-35 in *gcy-35;bbs-7* animals reverted body size similarly to that of *bbs-7* mutants, whereas GCY-35 expression in ALN, PLN, and SDQ had no effect (**Figure 10A**). Similarly, the

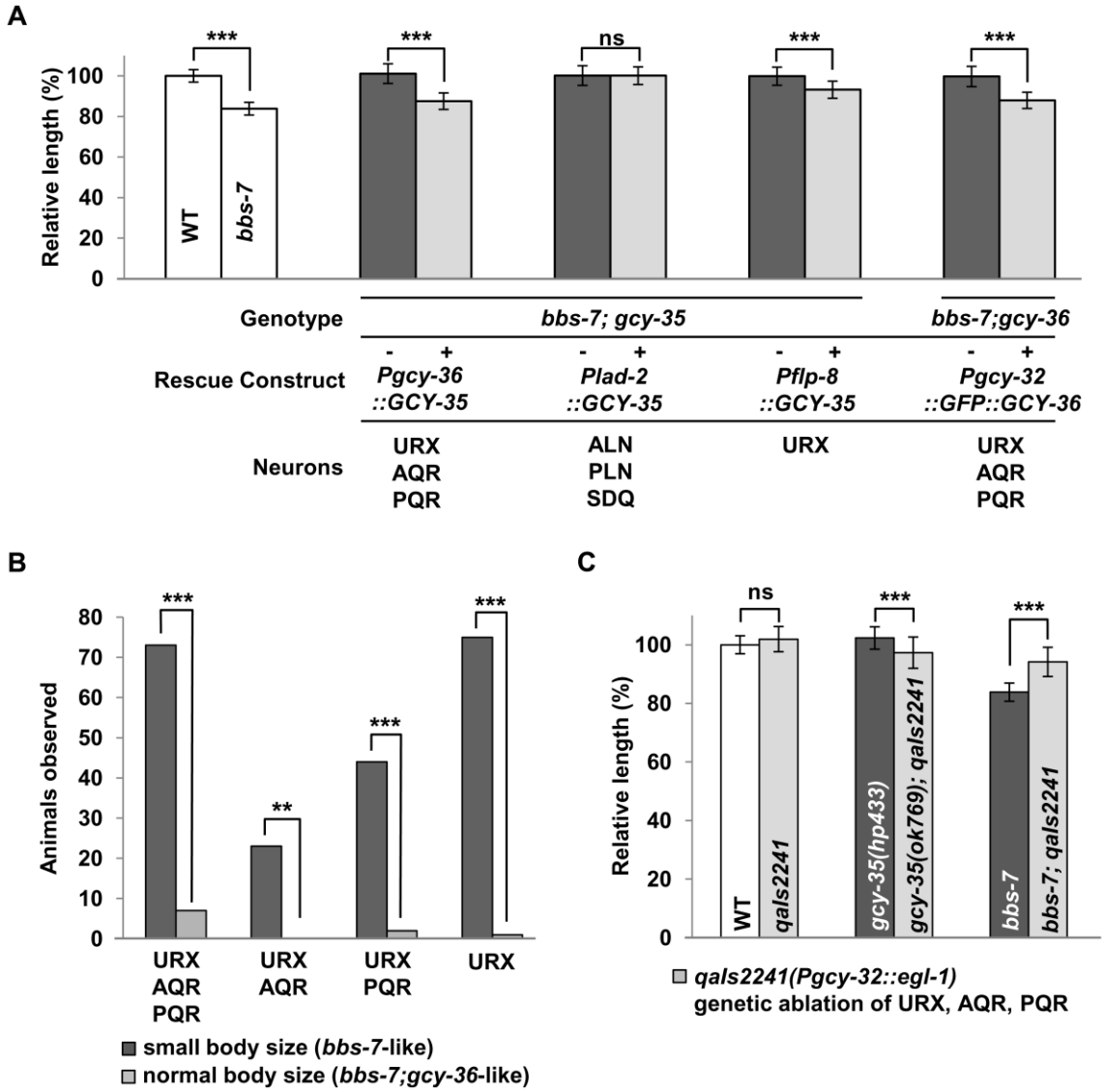

Figure 10. GCY-35 and GCY-36 are required in body cavity neurons to influence body size (A) The body length of transgenic (+, light bars) *gcy-35;bbs-7* animals expressing GCY-35 or GFP::GCY-36 constructs versus non-transgenic siblings (-, dark bars). Endogenous GCY-35 expressed in the body cavity neurons (*Pgcy-32, Pgcy-36*: URX, AQR, PQR), reverted *gcy-35(lf)*-mediated body size suppression, while expression in other endogenous GCY-35-expressing neurons (*Plad-2*: ALN, PLN, SDQ) did not. Expression of GCY-35 in URX and non-overlapping neurons (*Pflp-8*: URX, ASE, PVM) partially reverted the suppression in transgenic *gcy-35;bbs-7* animals. ANOVA with Tukey, *** $p<0.001$, ns – $p\geq0.05$, $n\geq20$. Data represent mean ± SD normalized against wild-type body length. (B) Mosaic analysis of *bbs-7;gcy-36* transgenic animals expressing GFP::GCY-36 showed a requirement for URX expression in rescuing suppression effects. Animals were first separated by body size into two groups: small body size (*bbs-7-like*, dark bars) or normal body size (*bbs-7;gcy-36*-like, light bars); they were then examined for the presence or absence of GFP::GCY-36 expression in the AQR, PQR and URX neurons. Fisher's Exact test, *** $p<0.001$; ** $p<0.01$, $n\geq20$. Y-axis indicates the pooled number of animals of respective neuronal expression patterns. (C) The genetic ablation of AQR, PQR, and URX neurons using the *qaIs2241 (pgcy-32::egl-1)* transgene rescued the body size defects of *bbs-7* mutants. The body length of wild-type, *gcy-35* and *bbs-7* animals (dark bars) was compared to those in combination with *qals2241* (light bars). ANOVA with Tukey, *** $p<0.001$; ns – $p\geq0.05$, $n\geq20$. Data represent mean ± SD normalized against wild-type body length. For *bbs-7* dataset, the *ok1351* deletion allele was used.

expression of a GFP-tagged GCY-36 in AQR, PQR and URX neurons in *bbs-7;gcy-36* animals was also sufficient to revert body size close to that of *bbs-7* mutants (**Figure 10A**). This suggests a specific requirement of GCY-35 and GCY-36 in body cavity neurons to regulate body size. An analysis of developmental timing and roaming behaviours was not completed.

Among them, URX appears to be the most essential neuron, as restoring GCY-35 in URX (and other neurons not normally expressing *gcy-35/gcy-36*) by an exogenous promoter caused a partial, but significant reversion of the body size in *gcy-35;bbs-7* animals **(Figure 10A)**. Similarly, GCY-36 is most essential in URX: I conducted a mosaic analysis of *bbs-7;gcy-36* animals carrying a functional GFP::GCY-36 transgene, and observed expression of GFP::GCY-36 in URX of all the rescued animals (**Figure 10B**). URX expression of the GCY-35/GCY-36 sGC is therefore essential, although not fully sufficient, to regulate the body size of *bbs* mutants.

Finally, if the body cavity neurons contribute to the small size phenotype of *bbs* mutants, their ablation by the transgene *qaIs2241*(*Pgcy-36::EGL-1*) (Chang *et al.* 2006) in a *bbs* background should also have a rescuing effect. While both *qaIs2241* and *gcy-35;qaIs2241* animals exhibited normal body sizes, *bbs-7;qaIs2241* mutants showed a significantly increased body size when compared to *bbs-7* animals (**Figure 10C**), further supporting that these neurons modulate the body size of *bbs* mutants.

3.4.4 The Expression and Localization of GFP::GCY-35 and GFP::GCY-36 are Grossly Normal in *bbs* Mutants

My genetic analyses indicate that BBS proteins negatively regulate sGC-mediated signalling activity. I examined if *bbs* mutants exhibit an elevated expression and/or expanded localization of sGC in these neurons. As reported (Cheung *et al.* 2004), a functional GFP::GCY-36 localized largely to the soma and along the dendrites of AQR, PQR and URX. I did not observe significant changes in its expression or localization in *bbs* mutants (**Figure 11**), nor did I observe a loss of ciliary localization as reported for the loss of a putative isoprenylation signal at the C-terminus (Cheung *et al.* 2004). *bbs* mutations did not perturb, at a gross level, the expression and localization of GFP::GCY-35 either (**Figure 11**). I did observe a high degree of morphological variability in the dendritic endings of URX, AQR, and PQR neurons as previously reported (Swoboda *et al.* 2000) in both wild-type and *bbs* mutants. However, given the morphological variability, I cannot exclude the possibility of subtle alterations in the cilium length of *bbs*

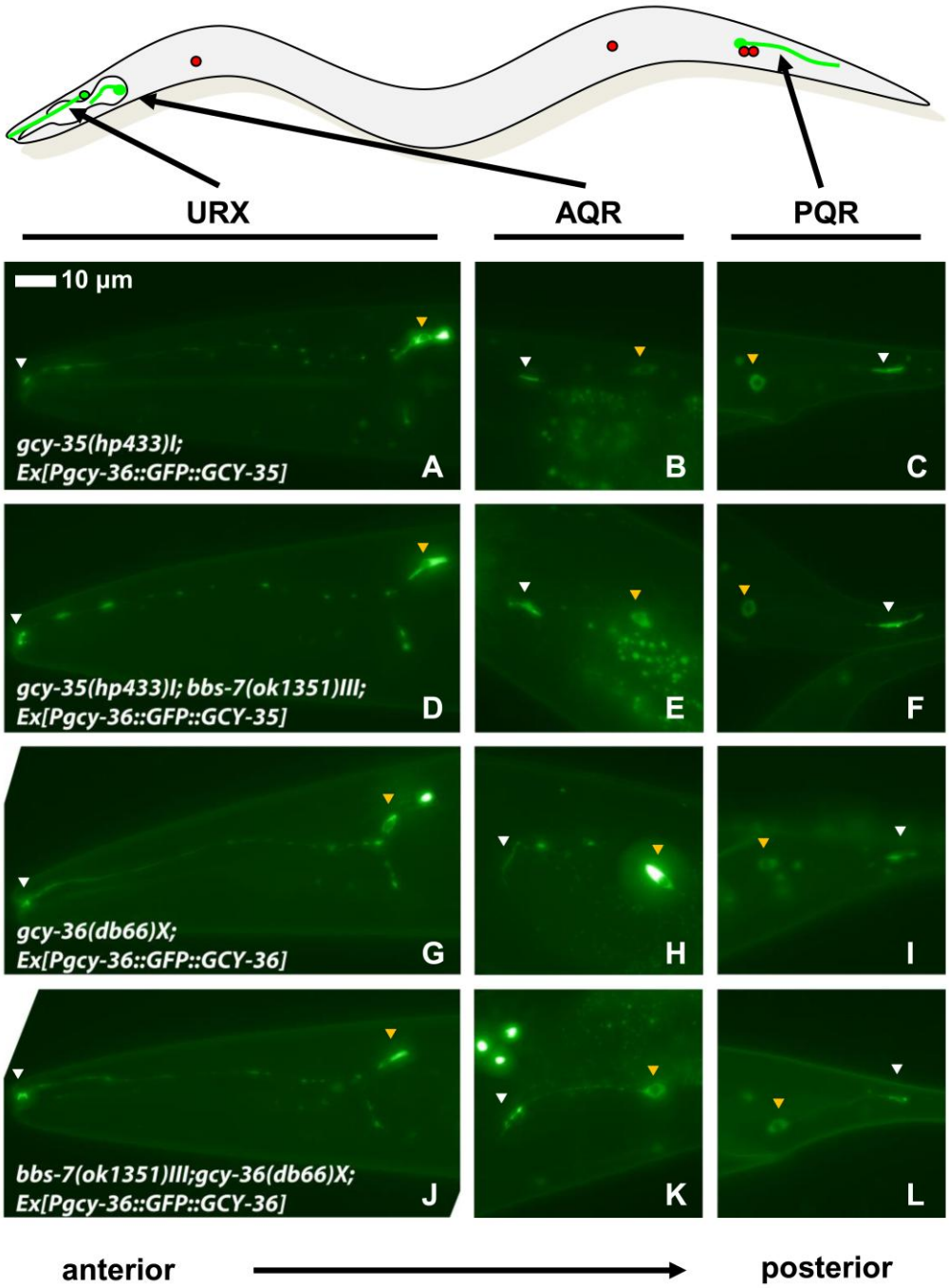

Figure 11. *bbs* mutants show no visible defects in GCY-35 or GCY-36 localisation GFP signals by *Pgcy-36::GFP::GCY-35* or *Pgcy-32::GFP::GCY-36* expressed in *gcy-35(hp433)* (A-C) or *gcy-36(db66)* (G-I) mutants. Strong signals were observed in the soma (orange arrowheads) and tips of the dendrites (white arrowheads) in AQR, PQR, and in the soma and dendrites of URX neurons. Expression of the same constructs in a *gcy-35;bbs-7* (D-F) or *bbs-7;gcy-36* (J-L) backgrounds exhibited no gross changes to localization in comparison to wild-type animals. Shown here are representative images of young adult animals.

mutants. Likewise, I cannot exclude the possibility of subtle differences to GCY-35/GCY-36 expression or localization due to the overexpression of these translational reporters as a quantitative analysis of *gcy-35* or *gcy-36* transcript levels was not completed. Therefore, while AQR, PQR and URX neurons regulate the body size through a process that involves sGC activity, it does not appear to result directly from altered sGC protein level or subcellular localization.

3.4.5 The cGMP-Dependent Protein Kinase (PKG) EGL-4 is an sGC Effector in Body Size Regulation

cGMP is a key secondary messenger (reviewed in (Lucas *et al.* 2000)). In *C. elegans*, cGMP activates a heteromeric cGMP-gated ion channel TAX-2/TAX-4 for oxygen sensation and other sensory processes (Zimmer *et al.* 2009). cGMP also activates a PKG, EGL-4, to regulate olfactory adaptation, life span, behavioural states and body size (Fujiwara *et al.* 2002; Hirose *et al.* 2003; Nagamatsu *et al.* 2004; You *et al.* 2008). Specifically, *egl-4(lf)* mutants exhibit a large body size, and are epistatic to the reduced body size and roaming behaviour of some sensory mutants; whereas a gain-of-function (*gf*) *egl-4* mutation, causes a small body size (Raizen *et al.* 2006). The shared effects of *bbs* and *egl-4* suggested that EGL-4 could be a downstream effector of sGCs in body size regulation.

I examined the *egl-4* mutants (**Figure 12A**) for their genetic interactions with *bbs-7* and *gcy-35* mutants. *egl-4(lf)* alleles were epistatic to *bbs-7*, *gcy-35* and *bbs-7;gcy-35* for body size and developmental timing (**Figure 12B and 12C**). *egl-4(gf)* also exhibited an epistatic effect to *bbs-7* and *bbs-7;gcy-35* mutants, although *egl-4(gf);bbs-7* and *egl-4(gf);bbs-7;gcy-35* mutants may exhibit a slightly more severe phenotype than *egl-4(gf)* that was only distinguished by statistical analyses (**Figure 12B**). Roaming behaviours in *egl-4(lf)* mutant combinations appeared improved in comparison to *bbs* populations while *egl-4(gf)* mutant displayed decreased roaming defects much like *bbs* animals (**data not shown**). By contrast, *lf* mutants for another cGMP effector, the cGMP-gated cation channel subunit TAX-2 and TAX-4, did not exert body size suppression for *bbs-7* (**Figure 13**). Moreover, some TGF-β signalling mutants exhibited altered body size (Patterson *et al.* 2000; Morita *et al.* 2002; Gumienny *et al.* 2007). While EGL-4 was proposed to function genetically downstream of TGF-β signalling (Fujiwara *et al.* 2002), body size defects of several TGF-β mutants exhibited additive effects in *bbs-7* or *bbs-7;gcy-35* backgrounds (**Figure 12D**), suggesting that TGF-β signalling and BBS-mediated body size

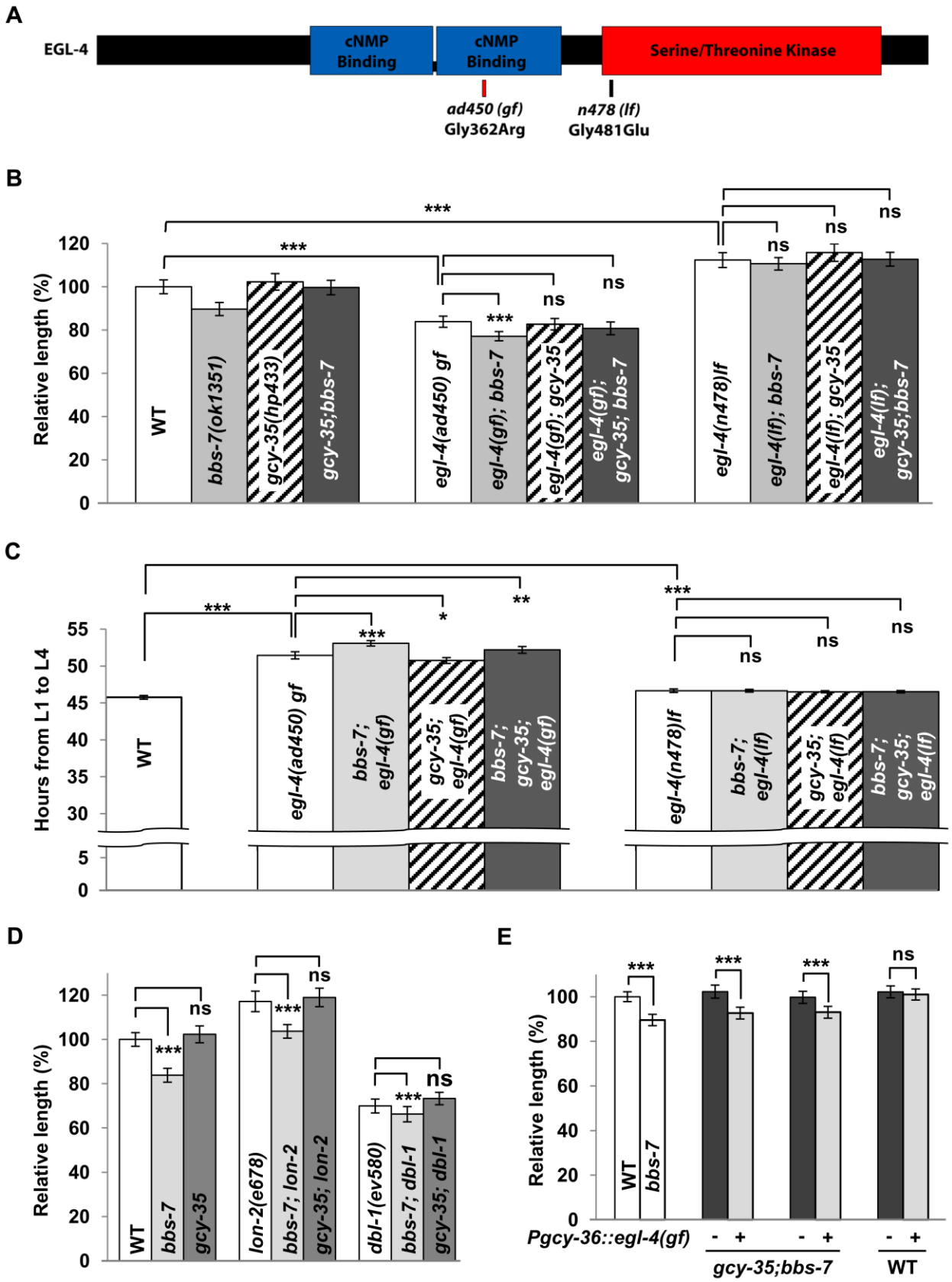
A
EGL-4
cNMP Binding
cNMP Binding
Serine/Threonine Kinase
ad450 (gf)
Gly362Arg
n478 (lf)
Gly481Glu
B
Relative length (%)
WT
bbs-7(ok1351)
gcy-35(hp433)
gcy-35;bbs-7
egl-4(ad450) gf
egl-4(gf); bbs-7
egl-4(gf); gcy-35
egl-4(gf); gcy-35; bbs-7
egl-4(n478)lf
egl-4(lf); bbs-7
egl-4(lf); gcy-35
egl-4(lf); gcy-35;bbs-7
C
Hours from L1 to L4
WT
egl-4(ad450) gf
bbs-7; egl-4(gf)
gcy-35; egl-4(gf)
bbs-7; gcy-35; egl-4(gf)
egl-4(n478)lf
bbs-7; egl-4(lf)
gcy-35; egl-4(lf)
bbs-7; gcy-35; egl-4(lf)
D
Relative length (%)
WT
bbs-7
gcy-35
lon-2(e678)
bbs-7; lon-2
gcy-35; lon-2
dbl-1(ev580)
bbs-7; dbl-1
gcy-35; dbl-1
E
Relative length (%)
WT
bbs-7
Pgcy-36::egl-4(gf)
gcy-35;bbs-7
WT

Figure 12. EGL-4 is an effector of GCY-35/GCY-36 in influencing body length and developmental timing (A) A schematic of EGL-4 showing allelic information on the *ad450sd* (gain-of-function) and *n478* (loss-of-function). *egl-4(gf)* and *egl-4(lf)* are epistatic to *bbs-7(ok1351)* (gray bars), *gcy-35(hp443)* (diagonal striped bars) and *gcy-35;bbs-7* (dark bars) for both body size (B) and developmental timing (C). ANOVA with Tukey, *** $p<0.001$; ns – $p\geq0.05$ or body length difference <3.5%. For body length, data represent mean ± SD normalized against wild-type body length, n≥20. For developmental timing, data represent mean (hours) ± SD, n≥50, N≥10 replicates. (D) Loss of function mutations in the TGF-β pathway (*BMP-5*/*dbl-1* and *lon-2,* white bars) had an additive effect on regulating body size in conjunction with *bbs* mutants (light bars), while being unaffected by the loss of *gcy-35(ok769)* (dark bars). ANOVA with Tukey, *** $p<0.001$; ns – $p\geq0.05$, n≥20. Data represent mean ± SD normalized against wild-type body length. (E) The transgenic expression (+, light bars) of *egl-4(gf)* in body cavity neurons reverted the body size suppression in *gcy-35;bbs-7* in comparison to non-transgenic siblings (-, dark bars). EGL-4(gf) expression within body cavity neurons did not affect the body size of wild-type transgenic controls. ANOVA with Tukey, *** $p<0.001$; ns – $p\geq0.05$, n≥20. Data represent mean ± SD normalized against wild-type body length.

regulation likely operates in an additive or parallel manner. Taken together, these results confirm a specific genetic relationship between *bbs-7*, *gcy-35* and *egl-4* for cilia-mediated body size regulation and developmental timing.

To further test if the body size influence of GCY-35/GCY-36 sGC functions through EGL-4, I expressed *egl-4* cDNA harbouring the *ad450(gf)* mutation in AQR, PQR and URX neurons of *gcy-35;bbs-7* animals. The *egl-4(ad450)* allele is a gain of function allele that appears to have increased kinase activity (Raizen *et al.* 2006). This mutation, present in the cGMP-binding domain, may result in faster association kinetics with cGMP, or a loss of autoinhibitory interactions with N-terminal residues. I postulated that if this *gf* allele is either cGMP-independent or highly active in decreased cGMP concentrations, then its expression in body cavity neurons may abrogate the body size suppression of *bbs* mutants by the loss of *gcy-35*. Indeed, this transgene reverted *gcy-35;bbs-7* animals to a *bbs-7*-like body size (**Figure 12E**). Wild- type animals expressing the same transgene did not exhibit changes in body size (**Figure 12E**). Not only is this result indicative of elevated cGMP signalling contributing to the reduced body size in *bbs* mutants, it also suggests that GCY-35/GCY-36 regulates body size through EGL-4 in the body cavity neurons.

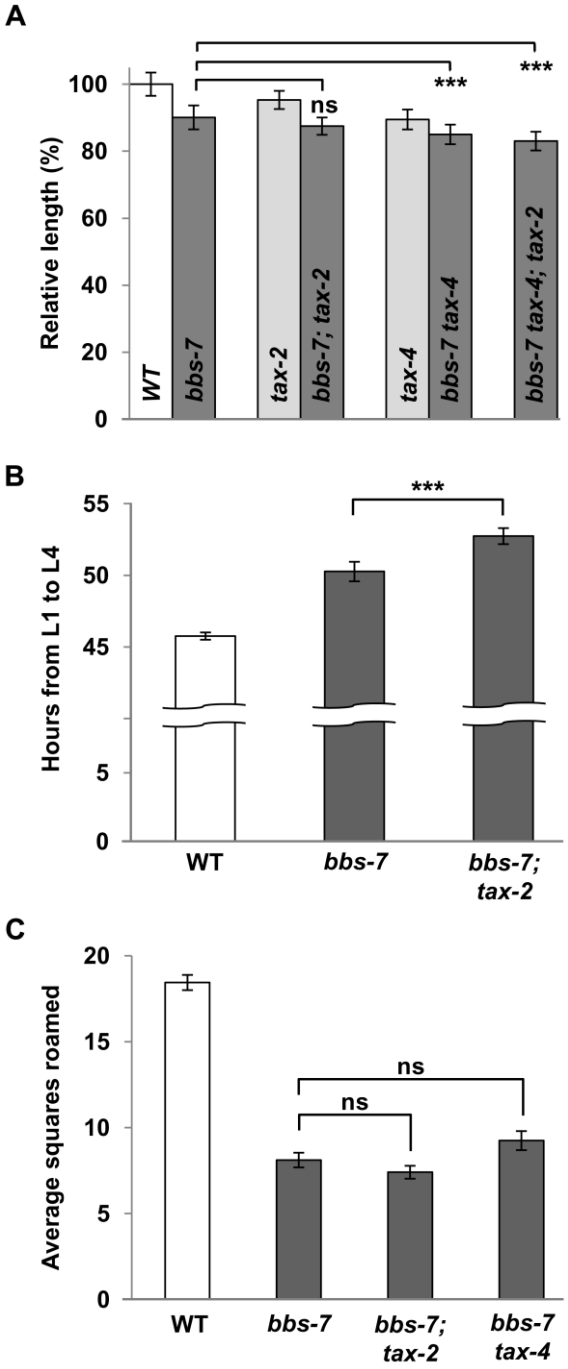

Figure 13. The cGMP-gated ion channel TAX-2/4 does not suppress the body size defects of *bbs* mutants (A) *tax-2* and *tax-4* failed to rescue *bbs-7* mutant body size defects. ANOVA with Tukey, *** $p<0.001$; ns – $p\geq0.05$ or length difference <3.5%, $n\geq20$. Data represent mean ± SD normalized against wild-type body length. (B) Developmental timing in *tax-2;bbs-7* mutants was further delayed in comparison to *bbs-7* mutant populations. ANOVA, *** $p<0.001$, $n\geq50$, $N\geq10$ replicates. Data represent mean (hours) ± SD. (C) Roaming defects of *tax-2;bbs-7* and *tax-4 bbs-7* animals were no different compared to *bbs-7* single animals. Kruskal-Wallis with Dunn's, ns – $p\geq0.05$, $n\geq25$, $N\geq2$ replicates. Data represent mean squares roamed ± SEM.

3.4.6 BBS Proteins are Required in Multiple Sensory Neurons to Regulate Body Size

To investigate whether BBS proteins regulate body size strictly through body cavity neurons like GCY-35/GCY-36, I expressed a functional BBS-7 (transgenic) or GFP::BBS-2 (integrated) in the AQR, PQR and URX neurons of *bbs-7* or *bbs-2* mutants, respectively. The small body size of respective *bbs* mutants was not rescued (**Figure 14A**). I did, however, observe a complete rescue of the body size with a pan-neuronally expressed *GFP::BBS-2* in *bbs-2* mutants (**Figure 14A**). Moreover, I observed a full or partial rescue of the body size defects when a functional BBS-7 was expressed in at least two non-overlapping groups of sensory neurons AWB, AWC, AWA, ADF and ASH, or, ADL, ADF, ASH, PHA and PHB (**Figure 14A**). All these neurons have sensory cilia exposed to outside of the body cavity. Therefore, while the GCY-35/GCY-36 sGC functions through body cavity neurons to regulate body size, restoring ciliary function in these neurons alone does not sufficiently alter cGMP signalling to restore body size. Alternatively, other BBS-expressing sensory neurons that input onto the body cavity neurons, may serve to regulate body size. Regardless, the observation that BBS proteins can influence body size through different groups of sensory neurons is reminiscent of the previously reported observation that the body size of *egl-4(lf)* mutants could be rescued by restoring EGL-4 expression in non-overlapping sets of sensory neurons (Fujiwara *et al.* 2002).

3.4.7 GCY-35/GCY-36 Acts as a Dominant Effector in BBS-Mediated Body Size Regulation

That multiple, non-overlapping and non-body cavity ciliated sensory neurons (CSNs) regulate body size suggests a cumulative effect on cGMP signalling-mediated body size regulation by BBS proteins in multiple sensory neurons, or, a predominating effect by body cavity neurons in BBS-mediated body size regulation through GCY-35/GCY-36. The first model predicts that additional GCs in other sensory neurons would epistatically suppress body size. The *C. elegans* genome encodes 7 sGCs and 27 receptor-like GCs (rGCs) (Ortiz *et al.* 2006). Single loss-of-function mutations in other sGCs, GCY-31, GCY-32, GCY-33, GCY-34 and GCY-37 all failed to alter *bbs-7* body size defects (**Figure 15 and data not shown**). Of 16 rGC mutants tested, four exhibited modifying effects, two very mildly suppressing and two significantly exacerbating the smaller body size of *bbs-7* animals, but none suppressed *bbs-7* mutant phenotypes comparably to *gcy-35/gcy-36* (**Figure 14B and 15A**). I examined the effect of several double and triple rGC

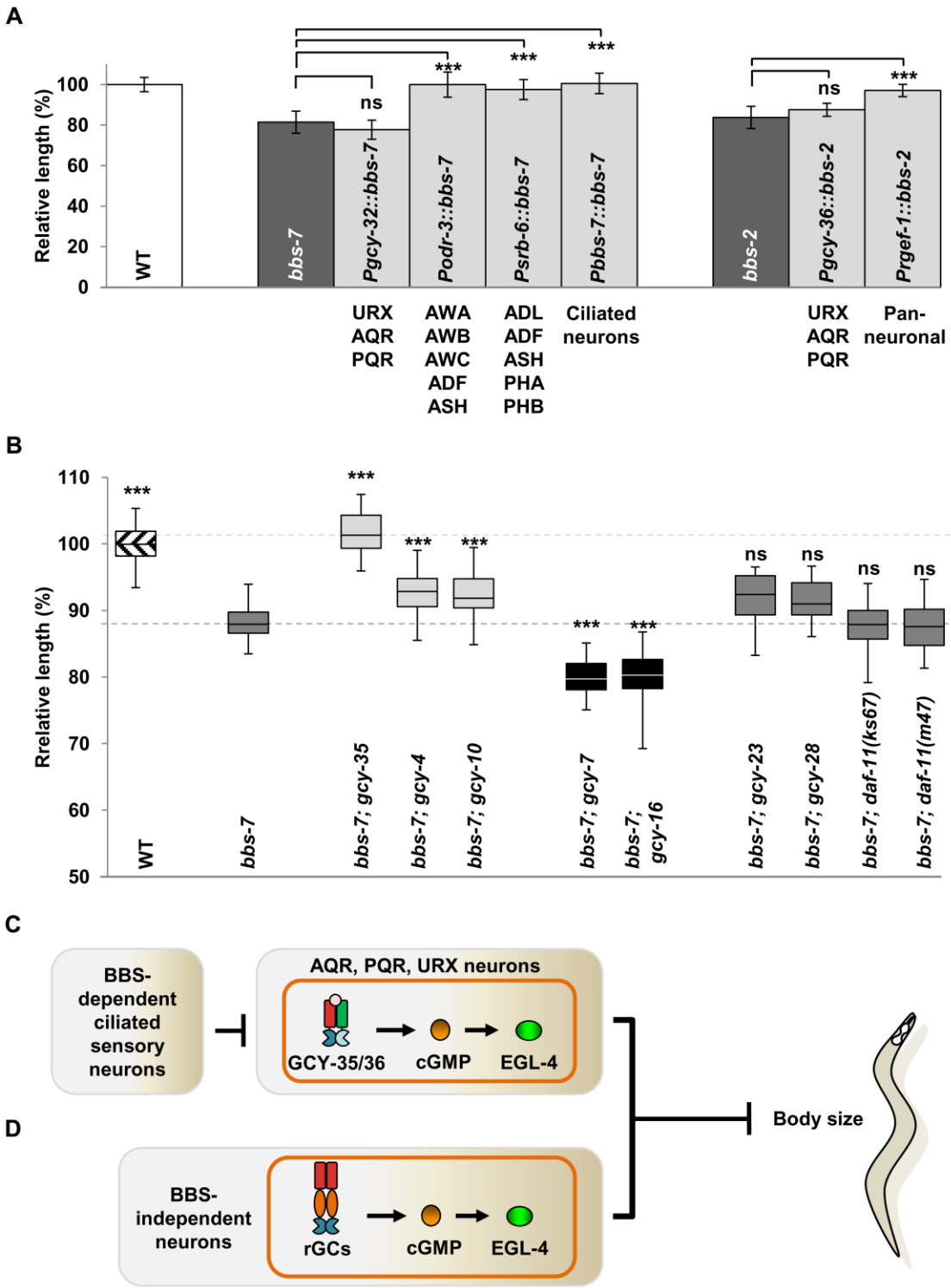

Figure 14. Multiple sensory neurons influence the body size of *bbs* mutants (A) The expression of wild-type BBS protein in body cavity neurons was insufficient to rescue body length defects of *bbs-7* and *bbs-2* mutants, while expression in other ciliated sensory neurons (light bars) restored body length. ANOVA with Tukey, *** $p<0.001$; ns – $p\geq0.05$, $n\geq11$. Data represent mean ± SD normalized against wild-type body length. (B) GCY-35, but not other GCY mutants, exhibited a strong suppression effect on *bbs-7* mutant body length. Box and whisker plot of additional *gcy* mutants showing partially improved body length (light bars), decreased body length (black bars), and no change (dark bars) in comparison to *bbs-7*

mutants. Boxes represent 25th-75th percentile of populations with maximum and minimum values as whiskers. Dashed lines represent wild-type and *bbs-7* mean body length. ANOVA with Tukey, *** p<0.001; ns – p≥0.05 compared to *bbs-7* mutants. Data represent mean ± SD normalized against wild-type body length. (C-D) A model for ciliary and cGMP-mediated body size regulation. (C) GCY-35/GCY-36 activity produces cGMP in the body cavity neurons and activates EGL-4 to inhibit body size. This process is influenced by BBS proteins present in other ciliated sensory neurons. (D) Some ciliated sensory neurons producing other GCs undergo a BBS-independent EGL-4 activation to influence body size and developmental timing.

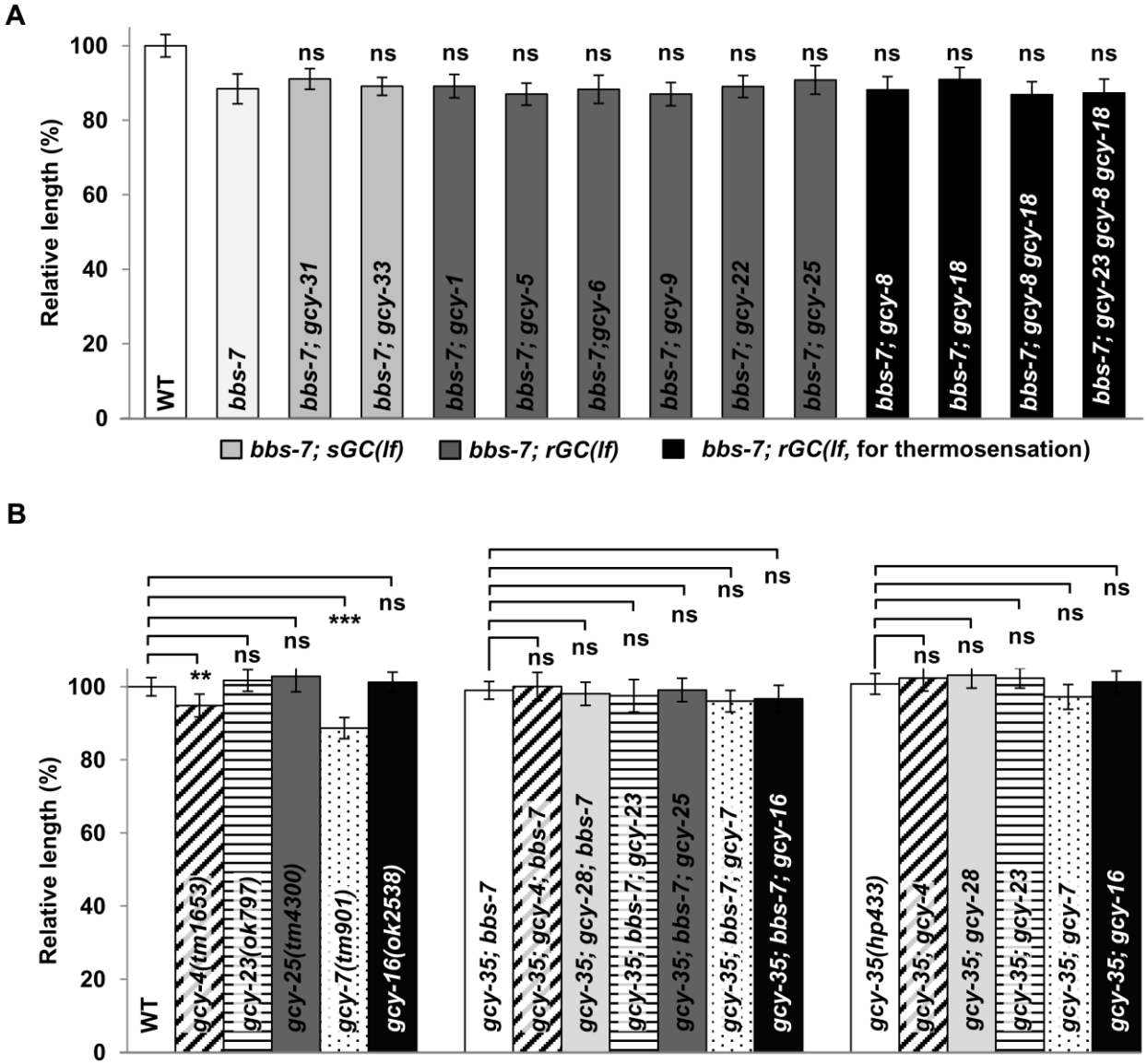

Figure 15. Mutations in other guanylate cyclases do not suppress *bbs-7* body size defects (A) Mutant alleles of multiple sGC genes (gray bars) and rGC genes (dark bars) did not exhibit a significant modifying effect on *bbs-7* mutants. The loss of functionally redundant rGCs (*gcy-8, -18, -23*) (Inada *et al.* 2006) does not significantly modify *bbs-7* body size defects either (black bars). ANOVA with Tukey, ns – p<0.05, n≥30. (B) Suppression of *bbs-7* body size by the loss of *gcy-35* was not significantly influenced by the loss of additional rGCs. ANOVA with Tukey, *** p<0.001; ** p<0.01; ns – p≥0.05, n≥20. All data represent mean ± SD normalized against wild-type body length.

mutants on *bbs-7* body size to explore the possibility that multiple rGCs function redundantly (Inada *et al.* 2006) but did not observe obvious suppression effect in these additional mutants (**Figure 15A**).

I further examined the combinational effect of *gcy-35* and other rGC mutants on *bbs-7*, including a mildly suppressing allele (*gcy-4(tm1653*)), two exacerbating alleles (*gcy-7(tm901)* and *gcy-16(ok2538)*) and three alleles that previously had no visible effect in *bbs-7* mutants (*gcy-23(ok797)*, *gcy-28(tm2411)* and *gcy-25(tm4300)*). I did not observe a significant body size improvement between *gcy-35;bbs-7* and these triple mutants (**Figure 15B**). Therefore with the caveat that I have not exhausted the examination of all single or combinational GC mutants, GCY-35/GCY-36, through the body cavity neurons, act uniquely as a predominating effector for BBS-mediated body size regulation.

3.5 Discussion

In the present study, I show that *C. elegans bbs* mutants exhibit reduced body length, delayed development and altered roaming pattern, in addition to known sensory defects. These phenotypes depend, fully or in part, on the GCY-35/GCY-36 sGC complex, through its effector EGL-4 PKG, in the AQR, PQR and URX body cavity neurons. On the other hand, body size can also be regulated via multiple, non-overlapping sets of BBS-expressing non-body cavity sensory neurons. I propose that the loss of *C. elegans* BBS function in ciliated sensory neurons leads to non-cell autonomous, aberrant cGMP-PKG signalling in body cavity neurons, which contributes to abnormal body size and delayed development.

3.5.1 *C. elegans bbs* Mutants Exhibit Non-Cell Autonomous Phenotypes

Ciliated sensory neurons transduce environmental cues into behavioural responses. In *C. elegans bbs* mutants, defective IFT and ciliary functions are reflected by chemosensory and thermosensory deficits (Blacque *et al.* 2004; Tan *et al.* 2007). Given the restricted expression of *C. elegans* BBS proteins in sensory neurons, the additional *bbs* phenotypes such as developmental timing, body and inferred cell size, and roaming indicate that in addition to sensory perception, sensory neurons also participate in developmental regulation in a non-cell autonomous manner. These *bbs* phenoptypes are not recapitulated by several *dyf*/IFT motor

mutants, implying that BBS proteins affect sensory neuron function beyond their observed role in IFT.

While all *bbs* mutants share these phenotypes, they exhibit small differences in the severity of phenotypic expression that could be attributed to specific allelic effects. Alternatively, BBS proteins could possess certain degrees of unknown functional specificity. This may not be so surprising given the difference in phenotypic expression among BBS patient populations (Carmi *et al.* 1995; Beales *et al.* 1997; Billingsley *et al.* 2010), as well as the observation that tissue-specific BBS isoforms are responsible for some syndromic features (Pretorius *et al.* 2010; Pretorius *et al.* 2011).

The involvement of primary cilia in signalling during development (Badano *et al.* 2006) also positions them to affect development in a non-autonomous fashion. For example, mouse BBS proteins are required in the hypothalamus to regulate leptin receptor trafficking and to prevent the onset of obesity (Seo *et al.* 2009). BBS dysfunction therefore contributes to increased adiposity partly in a non-cell autonomous manner. The additional phenotypes of *C. elegans bbs* mutants, highlights the global and non-cell autonomous consequence of BBS dysfunction, which may also account for some phenotypic features in other ciliopathy models.

3.5.2 The GCY-35/GCY-36 sGC Regulates Body Size Through a Mechanism Divergent from Oxygen Sensing

Previous studies established that the GCY-35/GCY-36 sGC can regulate oxygen sensation through either the body cavity neurons, or another group of neurons (Cheung *et al.* 2004; Gray *et al.* 2004; Chang *et al.* 2006). Activated by oxygen, this complex catalyzes the conversion of GTP to cGMP, which subsequently activates the cGMP-gated cation channel TAX-2/TAX-4 to initiate hyperoxic avoidance responses (Zimmer *et al.* 2009). Additional sGCs can act in body cavity neurons or other neurons under specific hypoxic conditions (Cheung *et al.* 2005; Zimmer *et al.* 2009).

GCY-35/GCY-36 modifies body size through a mechanism partly divergent from that of hyperoxic avoidance. GCY-35 is only necessary and sufficient in body cavity neurons that either have ciliated dendrites (Coates *et al.* 2002) or express some ciliated neuron-specific genes (Kunitomo *et al.* 2005). Furthermore, the loss of EGL-4, but not TAX-2 or TAX-4, suppresses

the body size defects of *bbs* and *dyf* mutants. The loss of TAX-2 and TAX-4, in fact, slightly exacerbated *bbs* phenotypes (**Figure 13**), which may reflect an increased cGMP pool for EGL-4 activation or the loss of a potential EGL-4 phosphorylation target (L'Etoile *et al.* 2002). As well, despite some sGCs having overlapping expression profiles with GCY-35/GCY-36, other oxygen-responsive sGC mutants failed to suppress *bbs-7* body size defects under standard culture conditions - possibly due to low activity under normoxia. Therefore, body cavity neurons, through GCY-35/GCY-36 activity, participate in developmental regulation through an alternate cGMP effector.

EGL-4 is present fairly ubiquitously, but the activation of EGL-4 in sensory neurons exerts a dominant influence on body size (Fujiwara *et al.* 2002). The genetic epistasis of both *egl-4(lf)* and *egl-4(gf)* alleles over that of *bbs* and *bbs;gcy-35* argues in favour of BBS proteins and EGL-4 functioning through a shared cellular pathway to regulate body size and developmental timing. The partially additive body size defects observed in *bbs-7;egl-4(ad450)* animals may further support elevated cGMP expression levels as the biochemical consequences of the *ad450* allele remain unclear. This mutation of the cGMP-binding domain of EGL-4 may result in augmented binding kinetics or a loss of autoinhibitory interactions, thus facilitating increased kinase activity. Speculatively, in the former case, the upregulated kinase activity of *egl-4(ad450)* mutants could be further augmented by increased concentrations of cGMP present in *bbs* mutants. Expression of EGL-4(*gf*) in the body cavity neurons of *gcy-35;bbs-7* mutants specifically alleviated the rescuing effect on body size, which also suggests that increased EGL-4 activity, driven by increased availability of cGMP in body cavity neurons, may contribute to the body size defects of some *bbs* mutants (**Figure 14C**).

3.5.3 BBS Proteins Affect Body Size Indirectly Through Body Cavity Neurons

The body size defects of ciliary mutants are rescued by non-overlapping sets of sensory neurons. However, restoring BBS function in body cavity neurons is insufficient to rescue the observed body size defects, giving rise to a possibility that the effect of cGMP signalling by body cavity neurons is indirectly moderated by a non-cell autonomous, IFT-independent function of BBS proteins in ciliated sensory neurons. Furthermore, that URX, a pair of non-ciliated neurons, play a necessary role in this suppression indicates that BBS proteins are not directly influencing body size in these neurons. My genetic analyses of the modifying effect of other GC mutants also

support this scenario, as I have not found additional GC mutants that potently restore the body size of *bbs* mutants.

Furthermore, unlike other GCs which may require certain IFT elements for ciliary localization (Jensen *et al.* 2010), the localization of GCY-35/GCY-36 appears independent of BBS function. URX localization is not perturbed by the loss of a putative isoprenylation signal in GCY-36 (Cheung *et al.* 2004) nor are there apparent localization defects to GCY-35/GCY-36 in the AQR or PQR from my own observations. In additiona, the AQR and PQR, unlike amphid channel neurons, are also exposed to the pseudocoelomic space and the sGC complex may be activated through passive diffusion of oxygen through ciliary or plasma membranes, independent of BBS function.

These results do not exclude the possibility that other GCs function redundantly in non-body cavity sensory neurons to influence body size through EGL-4/PKG (**Figure 14D**). The overexpression of *egl-4(gf)* in body cavity neurons was incapable of further reducing the body size of *gcy-35;bbs-7* animals beyond that of *bbs-7* mutants. This is in concordance with the ablation of body cavity neurons, which did not phenocopy the large body size of EGL-4 loss of function mutants, suggesting additional neuronal groups influence body size through EGL-4/PKG signalling. This study, however, establishes body cavity neurons as a predominating cGMP-PKG effector in body size regulation, and the ciliated sensory neurons as playing a key role in moderating cGMP signalling of these effector neurons.

Mechanisms on how dysfunctional ciliary sensory neurons lead to elevated cGMP-PKG signalling in these neurons are unknown. The body cavity neurons, AQR, PQR and URX do not receive extensive or direct synaptic inputs from sensory neurons where BBS proteins are sufficient to rescue body size. The non-cell autonomous effect of BBS proteins in ciliated sensory neurons therefore suggests a potential involvement of indirect synaptic inputs, or other forms of neuronal communications, such as peptidergic and/or hormonal signalling between these neuronal groups. For example, body cavity neurons express the *C. elegans* homologue of the neuropeptide NPY receptor (de Bono *et al.* 1998), making their activity susceptible to modulation by neuropeptides, some of which could be secreted by sensory neurons (Rogers *et al.* 2003). Sensory neurons also secrete insulin/IGF-like ligands, some of which may systematically affect neuronal states (Pierce *et al.* 2001; Cornils *et al.* 2011). Indeed, insulin and leptin have

been shown to regulate the activity of specific hypothalamic neurons (Belgardt *et al.* 2008; Klockener *et al.* 2011). Speculatively, *C. elegans* BBS proteins could affect the secretion of multiple signals by ciliated sensory neurons to regulate cGMP/EGL-4 signalling in the body cavity neurons.

3.5.4 A Potential Involvement of Aberrant cGMP Signalling in Ciliopathies

While aberrant PCP, Shh and Wnt signalling underlie a number of ciliopathy features, the biology behind other ciliopathy features such as photoreceptor degeneration, and reduced body size in neonatal *Bbs* mice (Nishimura *et al.* 2004) remains unexplained. cGMP signalling plays key roles in biological processes such as phototransduction, axonal guidance, and synaptic plasticity (reviewed in (Schlossmann *et al.* 2005; Hofmann *et al.* 2006)). PKGs have also been implicated in photoreceptor degeneration and dwarfism (Pfeifer *et al.* 1996; Paquet-Durand *et al.* 2009). It is worth exploring the involvement of cGMP signalling in the underlying pathophysiology of BBS and other ciliopathy features.

3.6 References

Ansley, S. J., J. L. Badano, *et al.* (2003). "Basal body dysfunction is a likely cause of pleiotropic Bardet-Biedl syndrome." Nature **425**(6958): 628-633.

Badano, J. L., C. C. Leitch, *et al.* (2006). "Dissection of epistasis in oligogenic Bardet-Biedl syndrome." Nature **439**(7074): 326-330.

Baker, K. and P. L. Beales (2009). "Making sense of cilia in disease: the human ciliopathies." Am J Med Genet C Semin Med Genet **151C**(4): 281-295.

Beales, P. L., A. M. Warner, *et al.* (1997). "Bardet-Biedl syndrome: a molecular and phenotypic study of 18 families." J Med Genet **34**(2): 92-98.

Belgardt, B. F., A. Husch, *et al.* (2008). "PDK1 deficiency in POMC-expressing cells reveals FOXO1-dependent and -independent pathways in control of energy homeostasis and stress response." Cell Metab **7**(4): 291-301.

Berbari, N. F., A. D. Johnson, *et al.* (2008a). "Identification of ciliary localization sequences within the third intracellular loop of G protein-coupled receptors." Mol Biol Cell **19**(4): 1540-1547.

Berbari, N. F., A. K. O'Connor, *et al.* (2009). "The primary cilium as a complex signaling center." Curr Biol **19**(13): R526-535.

Billingsley, G., J. Bin, *et al.* (2010). "Mutations in chaperonin-like BBS genes are a major contributor to disease development in a multiethnic Bardet-Biedl syndrome patient population." J Med Genet **47**(7): 453-463.

Blacque, O. E., M. J. Reardon, *et al.* (2004). "Loss of C. elegans BBS-7 and BBS-8 protein function results in cilia defects and compromised intraflagellar transport." Genes Dev **18**(13): 1630-1642.

Brenner, S. (1973). "The genetics of behaviour." Br Med Bull **29**(3): 269-271.

Carmi, R., K. Elbedour, *et al.* (1995). "Phenotypic differences among patients with Bardet-Biedl syndrome linked to three different chromosome loci." Am J Med Genet **59**(2): 199-203.

Chang, A. J., N. Chronis, *et al.* (2006). "A distributed chemosensory circuit for oxygen preference in C. elegans." PLoS Biol **4**(9): e274.

Cheung, B. H., F. Arellano-Carbajal, *et al.* (2004). "Soluble guanylate cyclases act in neurons exposed to the body fluid to promote C. elegans aggregation behavior." Curr Biol **14**(12): 1105-1111.

Cheung, B. H., M. Cohen, *et al.* (2005). "Experience-dependent modulation of C. elegans behavior by ambient oxygen." Curr Biol **15**(10): 905-917.

Coates, J. C. and M. de Bono (2002). "Antagonistic pathways in neurons exposed to body fluid regulate social feeding in Caenorhabditis elegans." Nature **419**(6910): 925-929.

Corbit, K. C., P. Aanstad, *et al.* (2005). "Vertebrate Smoothened functions at the primary cilium." Nature **437**(7061): 1018-1021.

Corbit, K. C., A. E. Shyer, *et al.* (2008). "Kif3a constrains beta-catenin-dependent Wnt signalling through dual ciliary and non-ciliary mechanisms." Nat Cell Biol **10**(1): 70-76.

Cornils, A., M. Gloeck, *et al.* (2011). "Specific insulin-like peptides encode sensory information to regulate distinct developmental processes." Development **138**(6): 1183-1193.

de Bono, M. and C. I. Bargmann (1998). "Natural variation in a neuropeptide Y receptor homolog modifies social behavior and food response in C. elegans." Cell **94**(5): 679-689.

Eichers, E. R., M. M. Abd-El-Barr, *et al.* (2006). "Phenotypic characterization of Bbs4 null mice reveals age-dependent penetrance and variable expressivity." Hum Genet **120**(2): 211-226.

Fujiwara, M., P. Sengupta, *et al.* (2002). "Regulation of body size and behavioral state of C. elegans by sensory perception and the EGL-4 cGMP-dependent protein kinase." Neuron **36**(6): 1091-1102.

Gray, J. M., D. S. Karow, *et al.* (2004). "Oxygen sensation and social feeding mediated by a C. elegans guanylate cyclase homologue." Nature **430**(6997): 317-322.

Gumienny, T. L., L. T. MacNeil, *et al.* (2007). "Glypican LON-2 is a conserved negative regulator of BMP-like signaling in Caenorhabditis elegans." Curr Biol **17**(2): 159-164.

Hirose, T., Y. Nakano, *et al.* (2003). "Cyclic GMP-dependent protein kinase EGL-4 controls body size and lifespan in C elegans." Development **130**(6): 1089-1099.

Hofmann, F., R. Feil, *et al.* (2006). "Function of cGMP-dependent protein kinases as revealed by gene deletion." Physiol Rev **86**(1): 1-23.

Huangfu, D., A. Liu, *et al.* (2003). "Hedgehog signalling in the mouse requires intraflagellar transport proteins." Nature **426**(6962): 83-87.

Inada, H., H. Ito, *et al.* (2006). "Identification of guanylyl cyclases that function in thermosensory neurons of Caenorhabditis elegans." Genetics **172**(4): 2239-2252.

Inglis, P. N., G. Ou, *et al.* (2007). "The sensory cilia of Caenorhabditis elegans." WormBook: 1-22.

Jensen, V. L., N. J. Bialas, *et al.* (2010). "Localization of a guanylyl cyclase to chemosensory cilia requires the novel ciliary MYND domain protein DAF-25." PLoS Genet **6**(11): e1001199.

Jin, H., S. R. White, *et al.* (2010). "The conserved Bardet-Biedl syndrome proteins assemble a coat that traffics membrane proteins to cilia." Cell **141**(7): 1208-1219.

Jones, C., V. C. Roper, *et al.* (2008). "Ciliary proteins link basal body polarization to planar cell polarity regulation." Nat Genet **40**(1): 69-77.

Kim, S. K., A. Shindo, *et al.* (2010). "Planar cell polarity acts through septins to control collective cell movement and ciliogenesis." Science **329**(5997): 1337-1340.

Klockener, T., S. Hess, *et al.* (2011). "High-fat feeding promotes obesity via insulin receptor/PI3K-dependent inhibition of SF-1 VMH neurons." Nat Neurosci **14**(7): 911-918.

Koesling, D. and A. Friebe (1999). "Soluble guanylyl cyclase: structure and regulation." Rev Physiol Biochem Pharmacol **135**: 41-65.

Kulaga, H. M., C. C. Leitch, *et al.* (2004). "Loss of BBS proteins causes anosmia in humans and defects in olfactory cilia structure and function in the mouse." Nat Genet **36**(9): 994-998.

Kunitomo, H., H. Uesugi, *et al.* (2005). "Identification of ciliated sensory neuron-expressed genes in Caenorhabditis elegans using targeted pull-down of poly(A) tails." Genome Biol **6**(2): R17.

L'Etoile, N. D., C. M. Coburn, *et al.* (2002). "The cyclic GMP-dependent protein kinase EGL-4 regulates olfactory adaptation in C. elegans." Neuron **36**(6): 1079-1089.

Lin, F., T. Hiesberger, *et al.* (2003). "Kidney-specific inactivation of the KIF3A subunit of kinesin-II inhibits renal ciliogenesis and produces polycystic kidney disease." Proc Natl Acad Sci U S A **100**(9): 5286-5291.

Lucas, K. A., G. M. Pitari, *et al.* (2000). "Guanylyl cyclases and signaling by cyclic GMP." Pharmacol Rev **52**(3): 375-414.

Marion, V., C. Stoetzel, *et al.* (2009). "Transient ciliogenesis involving Bardet-Biedl syndrome proteins is a fundamental characteristic of adipogenic differentiation." Proc Natl Acad Sci U S A **106**(6): 1820-1825.

Morita, K., A. J. Flemming, *et al.* (2002). "A Caenorhabditis elegans TGF-beta, DBL-1, controls the expression of LON-1, a PR-related protein, that regulates polyploidization and body length." EMBO J **21**(5): 1063-1073.

Nachury, M. V., A. V. Loktev, *et al.* (2007). "A core complex of BBS proteins cooperates with the GTPase Rab8 to promote ciliary membrane biogenesis." Cell **129**(6): 1201-1213.

Nagamatsu, Y. and Y. Ohshima (2004). "Mechanisms for the control of body size by a G-kinase and a downstream TGFbeta signal pathway in Caenorhabditis elegans." Genes Cells **9**(1): 39-47.

Nishimura, D. Y., M. Fath, *et al.* (2004). "Bbs2-null mice have neurosensory deficits, a defect in social dominance, and retinopathy associated with mislocalization of rhodopsin." Proc Natl Acad Sci U S A **101**(47): 16588-16593.

Ortiz, C. O., J. F. Etchberger, *et al.* (2006). "Searching for neuronal left/right asymmetry: genomewide analysis of nematode receptor-type guanylyl cyclases." Genetics **173**(1): 131-149.

Otto, E. A., T. W. Hurd, *et al.* (2010). "Candidate exome capture identifies mutation of SDCCAG8 as the cause of a retinal-renal ciliopathy." Nat Genet **42**(10): 840-850.

Ou, G., O. E. Blacque, *et al.* (2005). "Functional coordination of intraflagellar transport motors." Nature **436**(7050): 583-587.

Ou, G., M. Koga, *et al.* (2007). "Sensory ciliogenesis in Caenorhabditis elegans: assignment of IFT components into distinct modules based on transport and phenotypic profiles." Mol Biol Cell **18**(5): 1554-1569.

Pan, X., G. Ou, *et al.* (2006). "Mechanism of transport of IFT particles in C. elegans cilia by the concerted action of kinesin-II and OSM-3 motors." J Cell Biol **174**(7): 1035-1045.

Paquet-Durand, F., S. M. Hauck, *et al.* (2009). "PKG activity causes photoreceptor cell death in two retinitis pigmentosa models." J Neurochem **108**(3): 796-810.

Patterson, G. I. and R. W. Padgett (2000). "TGF beta-related pathways. Roles in Caenorhabditis elegans development." Trends Genet **16**(1): 27-33.

Pfeifer, A., A. Aszodi, *et al.* (1996). "Intestinal secretory defects and dwarfism in mice lacking cGMP-dependent protein kinase II." Science **274**(5295): 2082-2086.

Pierce, S. B., M. Costa, *et al.* (2001). "Regulation of DAF-2 receptor signaling by human insulin and ins-1, a member of the unusually large and diverse C. elegans insulin gene family." Genes Dev **15**(6): 672-686.

Pretorius, P. R., M. A. Aldahmesh, *et al.* (2011). "Functional analysis of BBS3 A89V that results in non-syndromic retinal degeneration." Hum Mol Genet.

Pretorius, P. R., L. M. Baye, *et al.* (2010). "Identification and functional analysis of the vision-specific BBS3 (ARL6) long isoform." PLoS Genet **6**(3): e1000884.

Raizen, D. M., K. M. Cullison, *et al.* (2006). "A novel gain-of-function mutant of the cyclic GMP-dependent protein kinase egl-4 affects multiple physiological processes in Caenorhabditis elegans." Genetics **173**(1): 177-187.

Rogers, C., V. Reale, *et al.* (2003). "Inhibition of Caenorhabditis elegans social feeding by FMRFamide-related peptide activation of NPR-1." Nat Neurosci **6**(11): 1178-1185.

Rohatgi, R., L. Milenkovic, *et al.* (2007). "Patched1 regulates hedgehog signaling at the primary cilium." Science **317**(5836): 372-376.

Ross, A. J., H. May-Simera, *et al.* (2005). "Disruption of Bardet-Biedl syndrome ciliary proteins perturbs planar cell polarity in vertebrates." Nat Genet **37**(10): 1135-1140.

Schlossmann, J., R. Feil, *et al.* (2005). "Insights into cGMP signalling derived from cGMP kinase knockout mice." Front Biosci **10**: 1279-1289.

Schneider, L., C. A. Clement, *et al.* (2005). "PDGFRalphaalpha signaling is regulated through the primary cilium in fibroblasts." Curr Biol **15**(20): 1861-1866.

Seo, S., D. F. Guo, *et al.* (2009). "Requirement of Bardet-Biedl syndrome proteins for leptin receptor signaling." Hum Mol Genet **18**(7): 1323-1331.

Swoboda, P., H. T. Adler, *et al.* (2000). "The RFX-type transcription factor DAF-19 regulates sensory neuron cilium formation in C. elegans." Mol Cell **5**(3): 411-421.

Tan, P. L., T. Barr, *et al.* (2007). "Loss of Bardet Biedl syndrome proteins causes defects in peripheral sensory innervation and function." Proc Natl Acad Sci U S A **104**(44): 17524-17529.

Tayeh, M. K., H. J. Yen, *et al.* (2008). "Genetic interaction between Bardet-Biedl syndrome genes and implications for limb patterning." Hum Mol Genet **17**(13): 1956-1967.

Tobin, J. L. and P. L. Beales (2009). "The nonmotile ciliopathies." Genet Med **11**(6): 386-402.

Yen, H. J., M. K. Tayeh, *et al.* (2006). "Bardet-Biedl syndrome genes are important in retrograde intracellular trafficking and Kupffer's vesicle cilia function." Hum Mol Genet **15**(5): 667-677.

You, Y. J., J. Kim, *et al.* (2008). "Insulin, cGMP, and TGF-beta signals regulate food intake and quiescence in C. elegans: a model for satiety." Cell Metab **7**(3): 249-257.

Zaghloul, N. A. and N. Katsanis (2009). "Mechanistic insights into Bardet-Biedl syndrome, a model ciliopathy." J Clin Invest **119**(3): 428-437.

Zimmer, M., J. M. Gray, *et al.* (2009). "Neurons detect increases and decreases in oxygen levels using distinct guanylate cyclases." Neuron **61**(6): 865-879.

Chapter 4
Analysis of Signalling Pathways that Affect the Body size of *Caenorhabditis elegans*

4

4.1 Introduction

I previously identified that cGMP signalling defects in *C. elegans bbs* mutants cause a decreased body size phenotype (Mok *et al.* 2011). I did not observe defects to the subcellular localization of GCY-35 or GCY-36 in *bbs* mutants and cell-specific rescues demonstrated a non-cell autonomous role for these proteins. My experiments indicated that EGL-4 is a downstream interactor to the GCY-35/36 complex, specifically in body cavity neurons but did not elucidate the mechanistic relationships between BBS, GCY-35/GCY-36 and EGL-4 activation in body cavity neurons.

Although I have demonstrated a clear genetic relationship between these three groups, expanding my findings to more complex animal models or proceeding with human cohort analysis requires that I elucidate this relationship through an examination of the pathophysiology of body size defects and their relationship with cGMP signalling.

As an example, the human photoreceptor uses an intricate cGMP signalling pathway to effect vision. The human photoreceptor is normally depolarized at -40 mV. This is accomplished using a combination of cGMP-gated (CNG) sodium channels and selective potassium channels (reviewed in (Fu 1995)). Guanylate cyclases are constitutively active, helping to maintain an open state on the CNG channels that activate voltage-gated calcium channels. The inward current of Ca+ ions induces release of the excitatory neurotransmitter glutamate. When light photons reach the outer segment, isomerization of 11-*cis* retinal to all-*trans* retinal leads to a conformational change in rhodopsin and the eventual binding of GTP-bound transducin subunits to the inhibitory γ subunits of phosphodiesterases (PDEs) to activate the α and β subunits that will catalyse cGMP to GMP. The closing of CNGs leads to the hyperpolarization of the photoreceptor cell, and prevents the further release of glutamate. This on/off switching of glutamate release – the basis of phototransduction – requires a delicate balance of cGMP production by guanylate cyclases and turnover by the phosphodiesterases.

Although *C. elegans* does not possess a photosensory system like that of the human eye, it does rely upon cGMP signalling for primitive phototransduction (Liu *et al.* 2010). Furthermore, the *C. elegans* genome encodes for homologous cGMP signalling components of the human phototransduction pathway: guanylate cyclases, phosphodiesterases, and cyclic nucleotide-gated channels. cGMP-dependent protein kinases have also been implicated in photoreceptor degeneration, which is a cardinal feature of BBS (Paquet-Durand *et al.* 2009).

cGMP-signalling, however, has roles in other cell types and mammalian systems, where primary cilia may influence this conserved system. Notably, the encoding of cGMP-signalling components in various eukaryotic genomes appears strongly linked to the presence of primary cilia as well (Johnson *et al.* 2010). Thus a thorough analysis of *C. elegans* cGMP-signalling components is required to clarify the body size phenomenon I have previously reported.

I therefore proceeded with a survey to determine whether the subcellular localization of EGL-4 within *bbs* mutants was perturbed. I also initiated a candidate gene screen of other genes related to cGMP signalling to determine if any may be associated with the cGMP-signalling defects in *bbs* mutants. The identification of additional modifiers in the cGMP pathway will elucidate the specific mechanisms through which BBS proteins influence *C. elegans* body size, while the discovery of novel modifiers may introduce new molecular and signalling pathways reliant upon ciliary or BBS function.

4.2 Putative cGMP Signalling Components

The *C. elegans* genome is known to encode five soluble guanylate cyclases (sGCs), twenty-seven receptor guanylate cyclases (rGCs) (Yu *et al.* 1997), six phosphodiesterases and one phosphodiesterase delta-like protein which may be involved in cGMP turnover (PDEs), six cyclic nucleotide gated ion channels (CNGs) (Coburn *et al.* 1996; Cho *et al.* 2004; Cho *et al.* 2005), and two cGMP-dependent protein kinases (PKGs) (Stansberry *et al.* 2001) (**Figure 16**).

In addition, a number of genes have been identified as putative upstream components of cGMP signalling. The HSP90 orthologue, DAF-21, may regulate the function of multiple rGCs (Birnby *et al.* 2000). Likewise, the eight-transmembrane protein LITE-1 activates cGMP signalling upstream of the rGCs DAF-11 and ODR-10 in phototransduction. In cGMP turnover, the G-

protein coupled receptor (GPCRs) GPA-3 has been shown to upregulate PDE expression (Hahm *et al.* 2009) and may therefore influence cGMP accumulation within neurons.

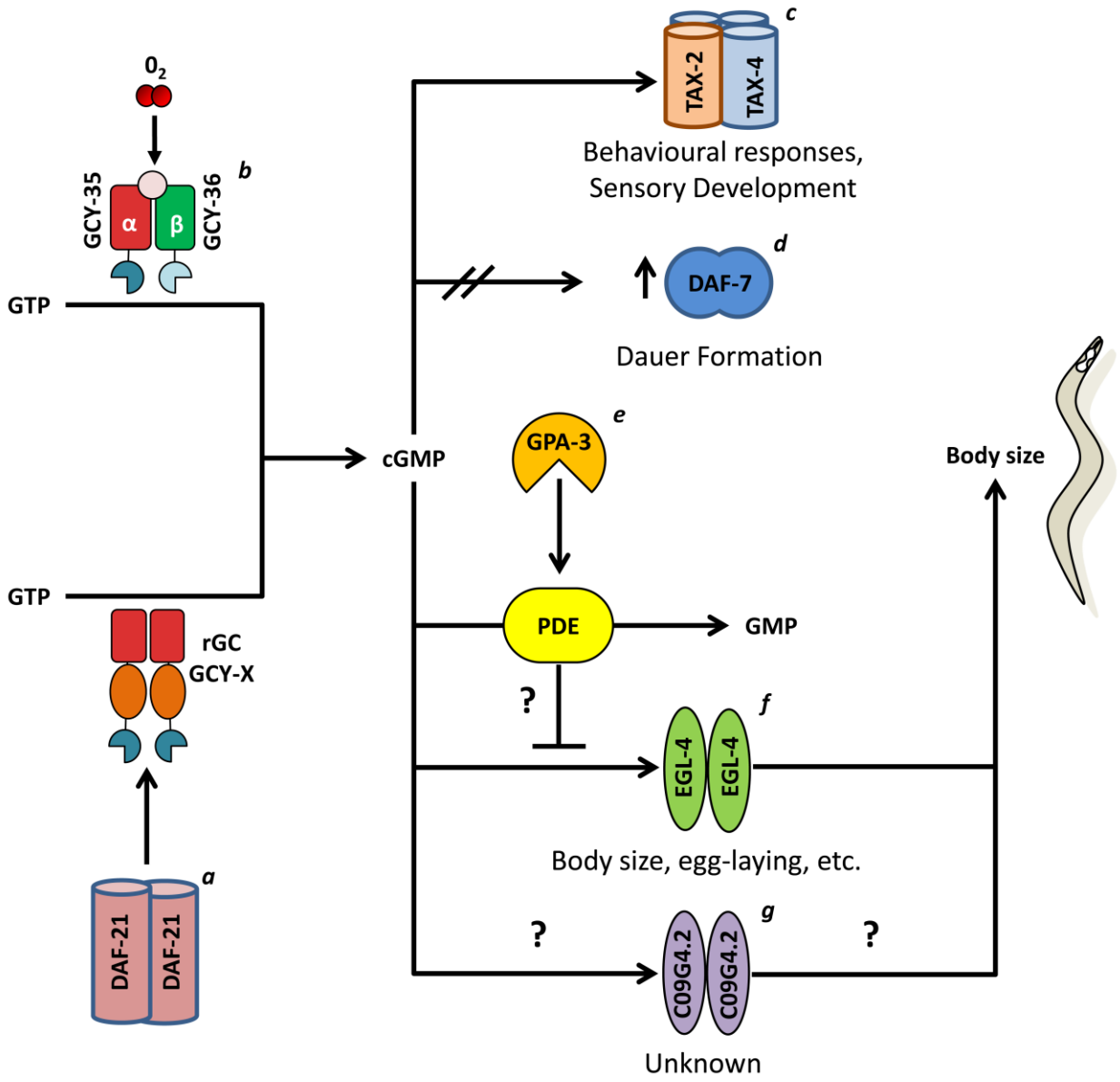

Figure 16. Candidate components of the *C. elegans* cGMP signalling pathway. The guanylate cyclases catalyze the formation of cGMP which can be used as a secondary messenger to directly or indirectly influence downstream components including the cGMP-gated ion channel TAX-2/4, cGMP-responsive TGF-β ligand DAF-7, the phosphodiesterases (PDE), or cGMP-dependent protein kinases (EGL-4, C09G4.2). Modified from (Birnby *et al.* 2000)(a), (Mok *et al.* 2011)(b), (Coburn *et al.* 1996)(c), (Murakami *et al.* 2001)(d), (Hahm *et al.* 2009)(e) (Fujiwara *et al.* 2002)(f), (Stansberry *et al.* 2001)(g).

4.2.1 cGMP-Dependent Protein Kinases

cGMP-dependent protein kinases (PKGs) play an important role in a number of biological processes (reviewed in (Hofmann *et al.* 2006; Paquet-Durand *et al.* 2009)). The human genome encodes two major classes of PKGs, cGKI (cGKIα, cGKIβ) and cGKII, which perform differing roles (Hofmann *et al.* 2006). The *C. elegans* genome encodes two putative orthologues of the mammalian PKGs (Stansberry *et al.* 2001).

4.2.1.1 PKG EGL-4, Signals in the Nucleus

EGL-4 has reported roles in olfactory adaptation, lethargus, lifespan, and body size. The multiple isoforms of EGL-4 are differentially expressed (Stansberry *et al.* 2001; Fujiwara *et al.* 2002; L'Etoile *et al.* 2002; Hirose *et al.* 2003; Raizen *et al.* 2006). The largest transcript in particular, isoform *a*, is expressed predominantly in the *C. elegans* nervous system, including the sensory neurons.

Under the context of olfactory adaptation, in well-fed wild-type populations, an exposure to odorants (benzaldehyde, butanone, or isoamyl) detected by the AWC neurons results in the initial attraction of animals to the odor source. Within 30 minutes (short term exposure), however, attraction decreases. Beyond 60 minutes (long-term exposure), animals begin to ignore the odorant. In a starved state wild-type populations will develop a persistent repulsive response after long-term exposure to “attractive” odorants. Recent studies have demonstrated a critical role for localization of EGL-4 to the nucleus during the long-term adaptation of odorant response behaviours in AWC neurons (L'Etoile *et al.* 2002; Lee *et al.* 2010).

L’Etoile *et al*. identified a putative nuclear localization signal (NLS) at the N-terminus of the serine/threonine kinase domain of EGL-4 that contributes to long-term adaptation (L'Etoile *et al.* 2002). In AWC neurons, long-term exposure to benzaldehyde or butanone causes an NLS-dependent translocation of GFP::EGL-4 to the nucleus without altering the GFP::EGL-4 localization in other sensory neurons (Lee *et al.* 2010). Constructs of GFP::EGL-4(ΔNLS) retain moderate long-term adaptation behaviours implying that factors such as cytoplasmic EGL-4 signalling may contribute to short and long-term behaviour adaptation. Lee *et al*. demonstrated that nuclear GFP::EGL-4 localization can dissipate over time while animals still exhibit avoidance behaviours, thus implying a persistent effect initiated by temporary nuclear

localization of GFP::EGL-4 (Lee *et al.* 2010). The nuclear localization of EGL-4 may initiate persistent behavioural changes by binding to histone deacetylase complexes (Hao *et al.* 2011).

4.2.1.2 C09G4.2 is a Secondary PKG of Unknown Function

In addition to EGL-4, the *C. elegans* genome encodes an uncharacterized PKG, C09G4.2, which shares 58% similarity with EGL-4, mostly in the C-terminus portion of the serine/threonine-protein kinase domain. C09G4.2, like EGL-4, is an orthologue of the human PRKG1 (OMIM #176894). *C09G4.2* has multiple alternatively spliced isoforms, which may be differentially expressed. The function of this putative PKG remains to be explored in many regards, such as body length regulation, odor perception and potential functional redundancy with EGL-4.

4.2.2 Phosphodiesterases

Cyclic nucleotide phosphodiesterases degrade the secondary messengers cAMP and cGMP through activation by an array of substrates thereby regulating the subcellular localization and duration of this signalling pathway (reviewed in (Lugnier 2006)). The mammalian PDEs are classified into 11 subfamilies based on their sequence divergence and substrate specificity (cAMP and/or cGMP). PDE superfamily members all share a common catalytic domain capable of binding either cAMP and/or cGMP proximal to the C-terminus of the protein. The N-terminus of the protein contains a regulatory region that can dictate the expression or function of each PDE family member, including calmodulin (CaM) or cGMP-binding domains, upstream conserved regions of regulation (UCR1, UCR2), a signal-detecting PAS (Period, Arnt, Sim) domain, or specific targeting domains (reviewed in (Conti 2000)).

The *C. elegans* genome encodes for six putative PDEs and one PDE delta-like orthologue although additional unidentified PDEs may remain. Their expression patterns vary; a number of them are likely expressed in the nervous system (**Table 11**). Among the PDE orthologues, *pde-1*, *pde-2*, and *pde-5* are the likely to hydrolyze cGMP based on their homology to mammalian PDEs (Lugnier 2006). Therefore these *C. elegans* PDEs are promising candidates in regulating cGMP turnover events relevant to body size regulation (**Figure 16**). Of particular interest, *pde-1* and *pde-5* expression is specifically upregulated by GPA-3, the alpha subunit of a heterotrimeric G-protein (Hahm *et al.* 2009). Using an integrated array (*syIs25)* of the gain-of function mutational allele *gpa-3*(Q205L), Hahm *et al*. identified that excess GPA-3(Q205L) expressed in

the nervous system significantly increased *pde-1* and *pde-5* expression, while only slightly increasing *pde-2* expression.

Table 11. List of *C. elegans* phosphodiesterases

Human PDE	*C. elegans* PDE	Alleles	Expression Pattern	Putative Function
FLJ34415, highly similar to PDE1C-001	*T04D3.3, pde-1*	*ok2924, gk906, gk891, tm3765*	Nervous system: head neurons, neurons along body, tail neurons, unidentified cells in head	Calcium/calmodulin (CaM)-dependent PDE. Preferentially hydrolyzes cGMP
FLJ16750, PDE2A-003	*R08D7.6, pde-2*	*tm3098*	Pharynx, pharyngeal-intestinal valve, intestine, reproductive system, body wall muscle, nervous system	Stimulated by both cGMP/cAMP to hydrolyze cGMP/cAMP. cGMP is preferred as substrate and effector
cGMP-inhibited PDE3B-001	*E01F3.1, pde-3*	*n4438, tm2274, tm1998, gk2878*	Hypodermis, nervous system, intestine	Hydrolyzes cAMP at a higher rate than cGMP but has greater affinity for cGMP
PDE4D-001	*R153.1, pde-4*	*ce268, tm2525, ok1290, tm2536*	Nervous system (non-active zone of synapses)	cAMP PDE, required for negative regulation of cAMP pools in synaptic signalling network for locomotion and sleep-like behaviour
PDE10A-201	*C32E12.2, pde-5*	*ok3102, tm3617*	Unknown	cAMP and cAMP-inhibited cGMP PDE
PDE8A-001	*Y95B8A.10, pde-6*	*ok3410*	Unknown	High-affinity cAMP-specific, IBMX-insensitive
PDE6D-001	*C27H5.1, pdl-1*	*gk157, tm970*	Nervous system, head neurons, tail neurons, pharynx	GPCR-regulated cGMP PDE that regulates gustatory plasticity

Concomitantly, an increased *pde-1* and *pde-5* expression resulted in a decreased expression of red fluorescent protein (RFP) within cells expressing a cGMP responsive *Pdaf-7::RFP* transgenic reporter. Hahm *et al*. further identified through the use of the cGMP analog 8-Bromo-

cGMP, that both *pde-1* and *pde-5* transcription was upregulated by increasing cGMP concentrations thus implying the involvement of a negative feedback mechanism in cGMP regulation.

4.2.3 DAF-21 Regulates Receptor Guanylate Cyclase Functions

The *C. elegans* genome encodes seven soluble guanylate cyclases (sGCs) and an additional twenty-seven receptor guanylate cyclases (rGCs). These rGCs are usually homo- or heterodimeric proteins with a similar topology: an N-terminal extracellular domain followed by a transmembrane region. There is an intracellular kinase homology domain that appears to be inactive, as well as a conserved cyclase domain (Birnby *et al.* 2000).

While the *C. elegans* sGCs are expressed in two primary groups of neurons (BAG/FLP and AQR/PQR/URX), rGCs are expressed diversely in the sensory neurons of *C. elegans* (**Table 12**) (Yu *et al.* 1997; Zimmer *et al.* 2009). Some rGCs may act redundantly as in GCY-8, GCY-18, and GCY-23, which are expressed in the same neurons and act redundantly in thermosensation (Inada *et al.* 2006). On the other hand, rGCs may be expressed asymmetrically in paired sensory neurons to function as separate environmental sensors as observed in the ASER and ASEL neurons (Yu *et al.* 1997; Pierce-Shimomura *et al.* 2001).

Many guanylate cyclases are expected to have specific activation properties. Thermosensory GCYs in the AFD neurons, for example, appear to react to specific temperature changes dependent upon culturing conditions (Inada *et al.* 2006), while others such as ODR-1 and DAF-11 are expressed in AWC neurons to facilitate olfactory reception via chemotaxis responses to specific ligands (Birnby *et al.* 2000; L'Etoile *et al.* 2000). The GCY-35/GCY-36 complex is activated in high oxygen states compared to low oxygen states as seen in GCY-31/GCY-33 (Zimmer *et al.* 2009). A recent study identified that *gcy-12* may participate upstream of *egl-4* in body size regulation although an anlaysis of this relationship is pending (Fujiwara *et al.* 2010). To the best of my knowledge, guanylate cyclases have not been previously reported as regulators of *bbs* body size despite their logical relationship to PKG EGL-4. The physiological functions of many rGCs remain largely uncharacterized.

A regulator of rGC function was discovered through the genetic studies on DAF-21, the *C. elegans* orthologue of the mammalian HSP90. Birnby *et al*. observed that *daf-11* and *hsp90/daf-*

21 mutants shared similar phenotypes in dauer formation and chemosensation (Birnby *et al.* 2000). Birnby *et al*. hypothesized that DAF-21 may have a novel role as a regulator of guanylate cyclases through the rGC kinase homology domain. Therefore, this HSP90 orthologue may also act as a direct upstream component to the production of cGMP in *C. elegans* neurons.

Overall, given the diverse range of guanylate cyclases and my findings with GCY-35/36, there remains the possibility that other GCs, alone or in combination, or upstream regulators of cGMP production, may act to influence *C. elegans* body size.

Table 12. Guanylate cyclases and their expression patterns in *C. elegans*

Guanylate cyclase	Type	Putative or Predicted Function	Reported Expression Pattern	Available Alleles
gcy-1	rGC	Potassium chemotaxis	ASER, ASI, PVT, URX, AIY, intestine	*tm2669*
gcy-2	rGC	Predicted chemosensory receptor	AWA, ASI, RIA, PVT	None
gcy-3	rGC		ASER, ASI, PVT	*gk1544*
gcy-4	rGC	Chemosensory receptor	ASER, ASI, PVT	*tm1653*
gcy-5	rGC	Homologous to rat NPY receptor A	ASER, nervous system, head neurons, amphids	*ok920, ok930, tm897*
gcy-6	rGC		ASEL	*ok1293, tm1449*
gcy-7	rGC		ASEL	*tm901*
gcy-8	rGC	AFD Thermotaxis	AFD	*tm949, oy44*
gcy-9	rGC	Membrane GC	Weak occasional and variable expression in non-neuronal cells	*n4470, tm2816*
gcy-10 *odr-1*	rGC	AWC Chemosensation	AWC, AWB, ASI, ASK, ASJ, interneuron L1	*ky29, n1933, n1930, n1936*
gcy-11	rGC		Pharyngeal muscles	*pkP5302*
gcy-12	rGC	Temperature-dependent GC activity	PHA, AWC, ASE, AFD	*nj10*
gcy-13	rGC		RIM	None
gcy-14	rGC	Sodium and lithium chemotaxis	ASEL, AWC (faint), PVT	*ok2236, tm4105, tm4210, pe1102*

gcy-15	rGC	Membrane GC	ASG (faint)	*None*
gcy-16 *gcy-20*	rGC		ASEL, AWC (faint), excretory gland and canal cells	*ok2538, gk1227, gk1184*
gcy-17 *gcy-24*	rGC		PHA	*gk1155, tm4516, gk2739*
gcy-18 *gcy-26*	rGC	AFD Thermotaxis	AFD, AIM. Larval: intestine, nervous system, head neurons	*nj38, ok3047*
gcy-19	rGC	Predicted chemosensory receptor	IL2, ASE (faint), additional faint sensory neurons	*ok2472, pe1103*
gcy-21	rGC		ASG, ADL (faint)	*None*
gcy-22	rGC		ASER	*tm2364*
gcy-23	rGC	AFD Thermotaxis	AFD	*nj37, ok797*
gcy-25	rGC		AQR, PQR, URX	*tm4300*
gcy-27	rGC		ASK, ASI, ASJ	*gk1523, gk1267*
gcy-28	rGC		Head neurons, ventral cord, tail neurons, body-wall, muscle, hypodermis, somatic gonad, intestine	*ky713, tm2411, ky887, tm3028*
gcy-29	rGC		ASE, AQC, AVK, AFD	*ok2475*
daf-11	rGC	Dauer formation	AWB, AWC, ASI, ASJ, ASK	*ks67, m47, mg295, p169, sa203*
gcy-31	sGC	Hypoxic response	BAG	*ok296*
gcy-32	sGC	Predicted fluid homeostasis	AQR, PQR, URX	*ok995*
gcy-33	sGC	Hypoxic response	BAG	*ok232*
gcy-34	sGC	Predicted fluid homeostasis	AQR, PQR, URX	*ok1012, ok2953*
gcy-35	sGC	Hyperoxic response	AQR, PQR, URX	*hp433, ok769*
gcy-36	sGC	Hyperoxic response	AQR, PQR, URX	*db66*
gcy-37	sGC	Predicted fluid homeostasis	AQR, PQR, URX	*ok384*

Shaded boxes represent untested rGC genes

4.3 Results

4.3.1 EGL-4 Overexpression Does Not Phenocopy *bbs* Body Size Defects

In order to better elucidate my model, I examined the body length phenotypes in *egl-4(lf)* and *bbs-7;egl-4(lf)* mutants using the overexpression of pan-neuronal EGL-4 protein. I hypothesized that if body size defects of *bbs* mutants were caused by an increase in *egl-4* expression, then excess EGL-4 protein would be sufficient to cause a decrease in body size similar to *bbs* or *egl-4(gf)* mutants. In both *egl-4* and *bbs-7;egl-4* mutants, body size was rescued to wild-type levels (**Figure 17A**), although *bbs-7;egl-4* animals appeared to have a slightly better rescue than in *egl-4* animals. Overall these results suggest that *bbs* body size defects are not related to overexpression of EGL-4 protein. Moreover, this suggests that *bbs* defects are related to cGMP production or turnover since excess EGL-4 protein in a wild-type background is not activated at high enough concentrations to mimic *bbs* body size defects. Alternatively, this could also indicate that downstream EGL-4 signalling effects are normally limited. In a *bbs* mutant background, however, EGL-4 signalling could be occurring in an uninhibited or upregulated manner. Furthermore, the overexpression of a *Pgcy-36*-driven EGL-4 protein in body cavity neurons was insufficient to restore *egl-4* body size defects nor was there any synergistic effect when using both pan-neuronal and body-cavity expression of EGL-4 in either mutant backgrounds, implying that EGL-4 activity is required beyond body cavity neurons, even in a *bbs* mutant background.

4.3.2 EGL-4 May Regulate Body Size Through Multiple Modalities

The identification of EGL-4 as a downstream signalling effector in the body cavity neurons led me to postulate that the nuclear localization of EGL-4 (L'Etoile *et al.* 2002; Lee *et al.* 2010) might be important to body size regulation. If nuclear expression is important for body size regulation, then *bbs* mutants may have increased, prolonged, or altered EGL-4 nuclear localization. Using a GFP::EGL-4 construct expressed in either body cavity neurons by the *gcy-36* promoter, or in sensory neurons under the endogenous *egl-4a* promoter, I compared synchronized wild-type, *bbs-7* and *gcy-35* animals at 0-5, 28, and 48 hours post hatching for changes in the expression or localization of EGL-4::GFP.

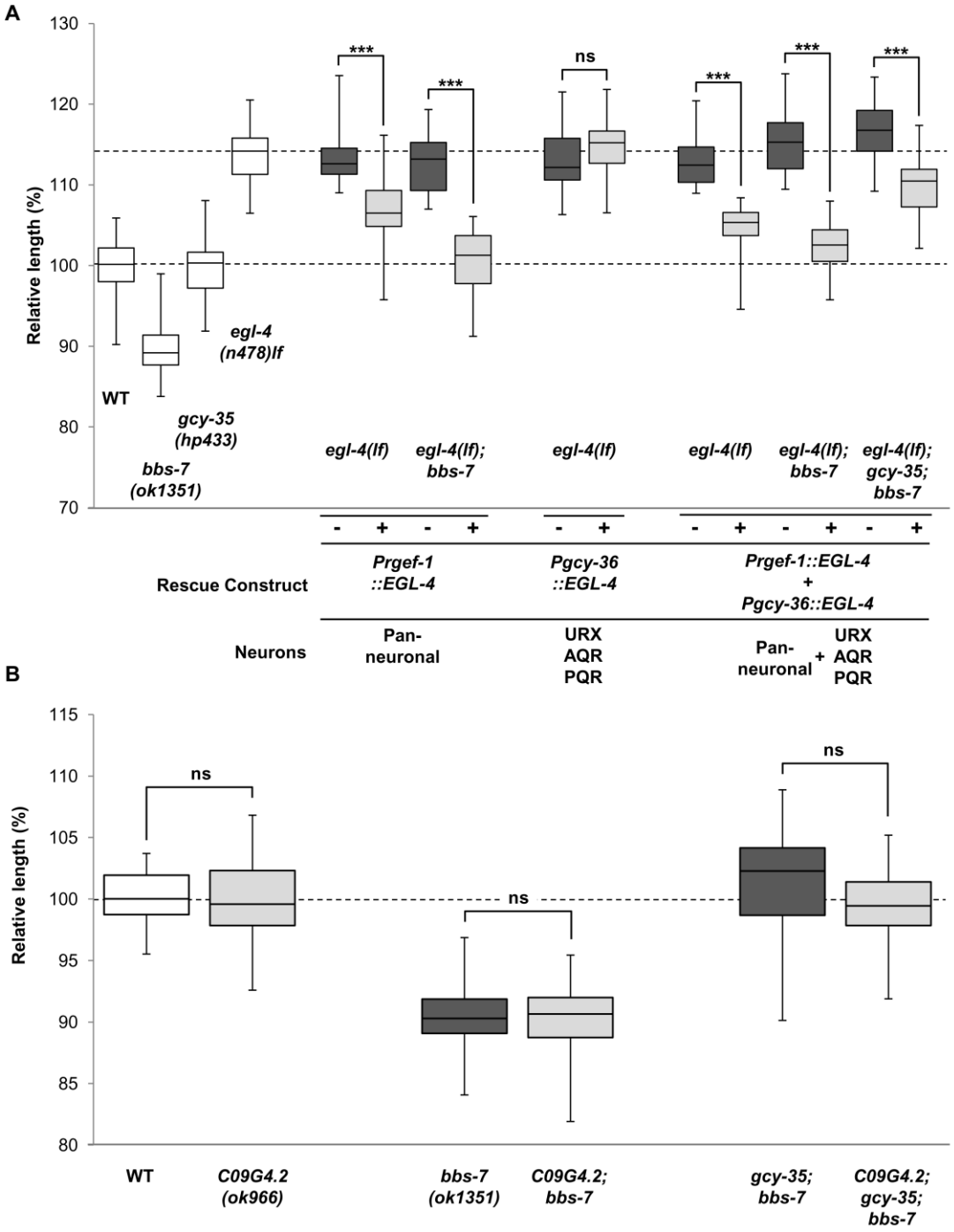

Figure 17. EGL-4 does not regulate body size through body cavity neurons alone (A) The pan-neuronal production of wild-type EGL-4 was sufficient to reduce *egl-4(lf)* mutant body size. Likewise the same rescue was insufficient to return *egl-4(lf);bbs-7* animals to a *bbs*-like size although they did show a better rescue than in *egl-4(lf)* single animals. The production of wild-type EGL-4 in body cavity neurons alone, was insufficient to effect any rescue in *egl-4(lf)* animals nor did the co-expression of both rescuing vectors show any synergistic action. (B) The putative PKG C09G4.2 does not rescue the body size of *bbs-7* mutants. *C09G4.2(ok966)IV* animals do not have apparent body size defects, not does the allele have any visible effect in *bbs-7(ok1351)III* or *gcy-35(hp433)I;bbs-7(ok1351)III* mutant backgrounds. Boxes represent 25th-75th percentile of populations with maximum and minimum values as whiskers. ANOVA with Tukey, *** $p<0.001$; ns – $p\geq0.05$. Data represent mean ± SD normalized against wild-type body length.

In body cavity neurons, I did detect rare instances of nuclear localization of GFP::EGL-4 but GFP signals were mainly cytoplasmic. Overall, there were no obvious differences between wild-type, *bbs-7* and *gcy-35* genotypes (**Figure 18**). Likewise, using the endogenous *egl-4a* promoter, I was unable to identify excessive nuclear localization in any of the genotypes used at any of the time points observed (**Figure 19**). I did, however, detect a consistent nuclear signal in an unidentified cell type within all three genotypes. These results thus indicate that unlike odor perception mediated by the AWC neurons, EGL-4 may regulate body size through either transient or low levels of nuclear signalling to initiate long-term developmental changes. Optionally, similar to short-term behavioural modification, EGL-4 may also initiate body size regulation via non-nuclear mechanisms in body cavity neurons (Lee *et al.* 2010).

4.3.3 C09G4.2 is not a Modifier of *bbs* Body Length

A second, candidate PKG, C09G4.2, may also help regulate body size. To test this possibility, I first used a deletion allele (*ok966*), which spans the first exon of isoform *a* and second exon of isoforms *a* and *c*, to examine the effects of a potential loss of function mutation on *bbs* body size. *C09G4.2(ok966)* animals did not display aberrant body size when compared to wild-type populations, and *bbs-7;C09G4.2(ok966)* shared the characteristics of *bbs* body size phenotype (**Figure 17B**). There was also no apparent synergistic effect when comparing the body size of *gcy-35;bbs-7* and *gcy-35;bbs-7;C09G4.2(ok966)* animals. *bbs-7;C09G4.2(ok966)* animals did not have obvious changes to developmental timing or altered roaming/dwelling behaviours in comparison to *bbs* mutants. These observations indicate that this additional PKG may not have a significant role downstream of *bbs* genes in developmental regulation. These results should be further verified with an additional deletion allele, *tm3878*, which encompasses the third last exon of all annotated isoforms.

Figure 18. *bbs* mutants show no visible defects to EGL-4 localisation in body cavity neurons. GFP signals by *Pgcy-36::GFP::EGL-4* expressed in wild type (A-B, G-I, P-R), *gcy-35(hp433)* (C-D, J-L, S-U) or *bbs-7(ok1351)* (E-F, M-O, V-X) mutants synchronized to L1 (4 hours post-hatch, A-F), L2 (28 hours post-hatch, G-O), and L4 (48 hours post-hatch, P-X). The strongest signals were observed at the cellular membrane and along or at the tips of dendrites (white arrowheads) in body cavity neurons. *gcy-35;bbs-7* or *bbs-7* animals did not exhibit obvious changes to expression or localization in comparison to wild-type animals. Analysis was completed on strains made from the same original extrachromosomal line. Shown here are representative images of animals at various stages.

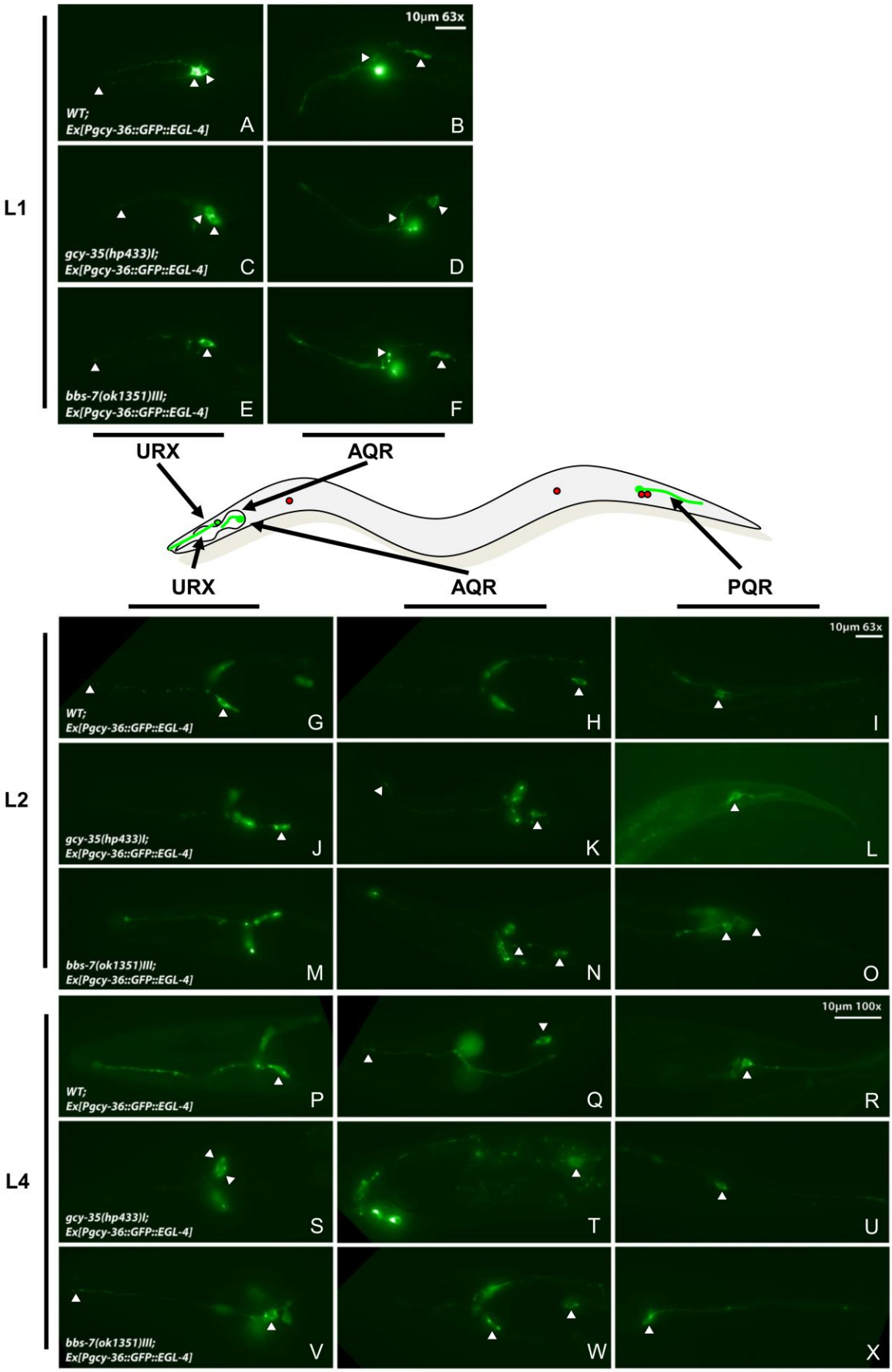
L1
10µm 63x
WT;
Ex[Pgcy-36::GFP::EGL-4]
A
B
gcy-35(hp433)I;
Ex[Pgcy-36::GFP::EGL-4]
C
D
bbs-7(ok1351)III;
Ex[Pgcy-36::GFP::EGL-4]
E
F
URX
AQR
URX
AQR
PQR
L2
10µm 63x
WT;
Ex[Pgcy-36::GFP::EGL-4]
G
H
I
gcy-35(hp433)I;
Ex[Pgcy-36::GFP::EGL-4]
J
K
L
bbs-7(ok1351)III;
Ex[Pgcy-36::GFP::EGL-4]
M
N
O
L4
10µm 100x
WT;
Ex[Pgcy-36::GFP::EGL-4]
P
Q
R
gcy-35(hp433)I;
Ex[Pgcy-36::GFP::EGL-4]
S
T
U
bbs-7(ok1351)III;
Ex[Pgcy-36::GFP::EGL-4]
V
W
X

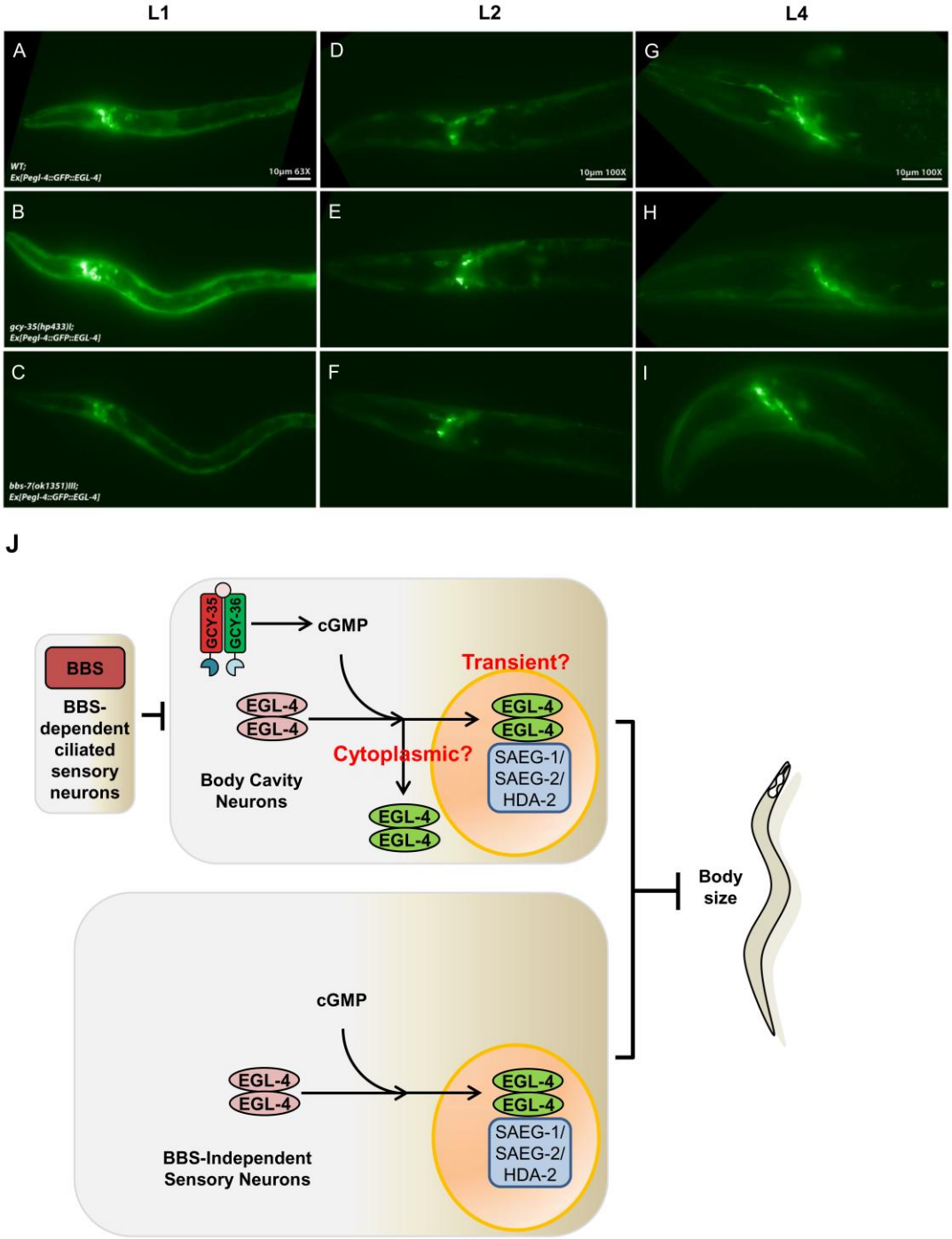

Figure 19. *bbs* mutants show no visible defects to EGL-4 localisation in endogenously expressing neurons. GFP signals by *Pegl-4::GFP::EGL-4* expressed in wild type (A, D, G), *gcy-35(hp433)* (B, E, H) or *bbs-7(ok1351)* (C, F, I) mutants synchronized to L1 (4 hours post-hatch, A-C), L2 (28 hours post-hatch, D-F), and L4 (48 hours post-hatch, G-I). GFP::EGL-4 expression was observed most strongly in the nervous system and hypodermis, with cells most prominently in the head and tail neurons. *gcy-35;bbs-7* or *bbs-7* animals did not exhibit obvious changes to expression or localization in comparison to wild-type animals. Analysis was completed on strains made from the same original extrachromosomal line. Shown here are representative images of animals at various stages. (J) Model of EGL-4 signalling in body size regulation of *bbs* mutants suggests that EGL-4 signalling in body size neurons may be transiently nuclear or cytoplasmic.

4.3.4 PDE-5 Regulates Body Size in Parallel to BBS Proteins

My model postulates that BBS proteins regulate body size via the sensory neurons to influence the effect of cGMP signalling in body cavity neurons (**Figure 14**). In addition, the lack of body size defects in EGL-4 overexpressing transgenic lines supports a perturbation of cGMP regulation or downstream EGL-4 signalling. Given the variety of *C. elegans* phosphodiesterases and their predicted roles in the regulation of cAMP and/or cGMP turnover (**Table 11**), I investigated whether, in the context of the body cavity neurons, PDEs regulate body size by limiting EGL-4 activation.

If a specific PDE acts directly downstream of GCY-35 to regulate cGMP, I hypothesized that such a PDE mutant would have a decreased body size similar to those of *bbs* mutants, and that the loss of *gcy-35/gcy-36* would restore its body size defect (**Figure 20A**). If, however, PDEs function in both sensory and body cavity neurons then it may not be feasible to discern this relationship through genetic interaction alone (**Figure 20B**). I constructed combinational mutants between *pde-1*, *pde-2*, *pde-3*, *pde-4*, *pde-5*, *pde-6*, and *pdl-1* (**Table 11**) with *bbs-7*, and *gcy-35* or *gcy-36* mutants to assess the possible effects of these cGMP regulators on body size.

I assessed the body length of *pde-1*, *pde-4*, *pde-5*, and *pdl-1* mutant combinations (**Figure 21**). The body size of single *pde-1*, *pde-4*, and *pdl-1* mutants was not distinguishable from wild-type populations. The body size of *pde-1(ok2924);bbs-7* animals had mild, but statistically significant improvement in body size when compared to *bbs-7* controls. *pde-1(ok2924)* did not alter the body size in a *gcy-36(db66)* or *bbs-7;gcy-36* mutant background, suggesting that it may mildly rescue *bbs* size defects in the same pathways as *gcy-35*/*gcy-36* (**Figure 21A**).

The *pde-4(ok1290)* allele, on the other hand, further reduced the body size of both *bbs-7* and *gcy-35;bbs-7* mutant backgrounds suggesting that *pde-4*, a cAMP responsive PDE, may influence body size more profoundly in a sensitized background such as *bbs-7*.(**Figure 21B**). The *pdl-1(gk157)* allele had no discernable effect in combination with a *bbs-7* mutation (**Figure 21C**), suggesting that *pdl-1* does not play a significant role in *bbs*-mediated body size regulation

In contrast to other *pde* mutants examined, *pde-5(ok3102)* mutants shared a decreased body size, to a similar degree as the *bbs-7* mutants. *pde-5;bbs-7* animals showed an exacerbated body size

defect, indicating that *pde-5* may serve to regulate body size in non-body cavity neurons, in a pathway that acts parallel to or additively with *bbs* body size regulation (**Fig 22A**). Consistent with this notion, *pde-5 gcy-35;bbs-7* mutants exhibited a similar body size to that of single *pde-5* mutants. Despite this, the effect of *pde*-5 should be further examined. Another *pde-5* allele, *nj49,* did not exhibit an obvious body size defect, and failed to modify the body size defects of *gcy-36* or *bbs-7;gcy-36* mutants (**data not shown**). This indicates that the effect I observed with *ok3102* is either allele-specific, or, caused by closely associated background mutations in the *ok3102* strain.

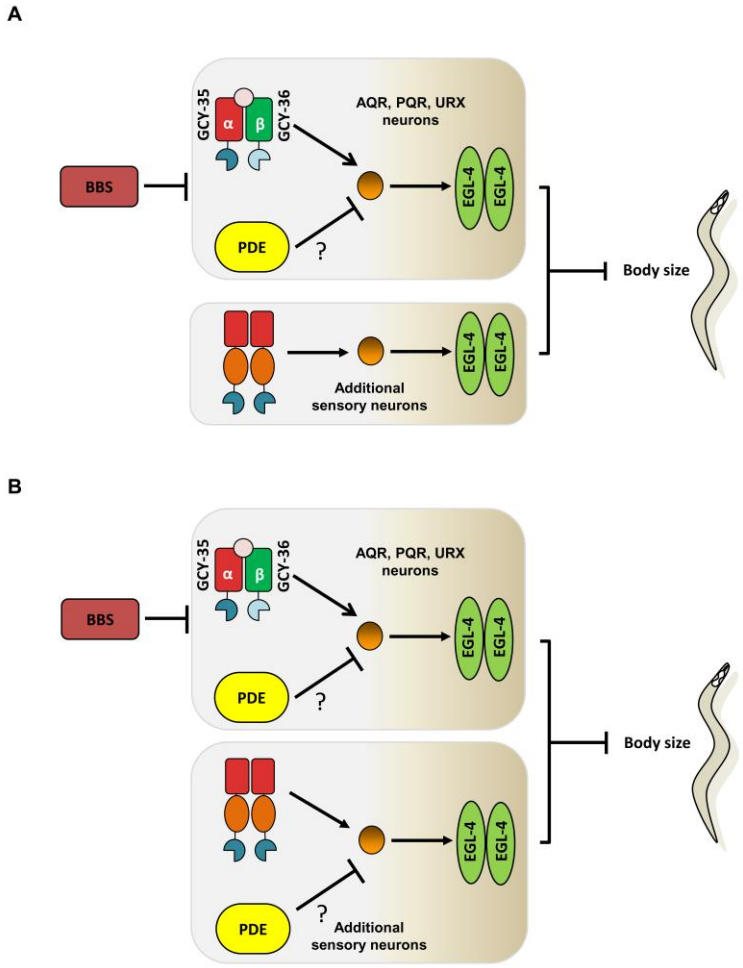

Figure 20. Hypothesized model of PDE interaction in *bbs* mutant animals. Phosphodiesterase expression varies between orthologues, although a number of *pde* genes are expressed within the neurons and/or nervous system. The regulation of body size through the cGMP-PKG signalling pathway in body cavity neurons may also involve PDE activity as a negative regulator. If this were the case (A) then the loss of a particular *pde* may mimic *bbs* mutant body size defects. Furthermore these defects would be abrogated by the loss of *gcy-35*. It may be the case (B), however, that PDE activity in additional sensory neurons could phenocopy *bbs* mutant body size while remaining unrescued by the loss of GCY-35 activity in body cavity neurons.

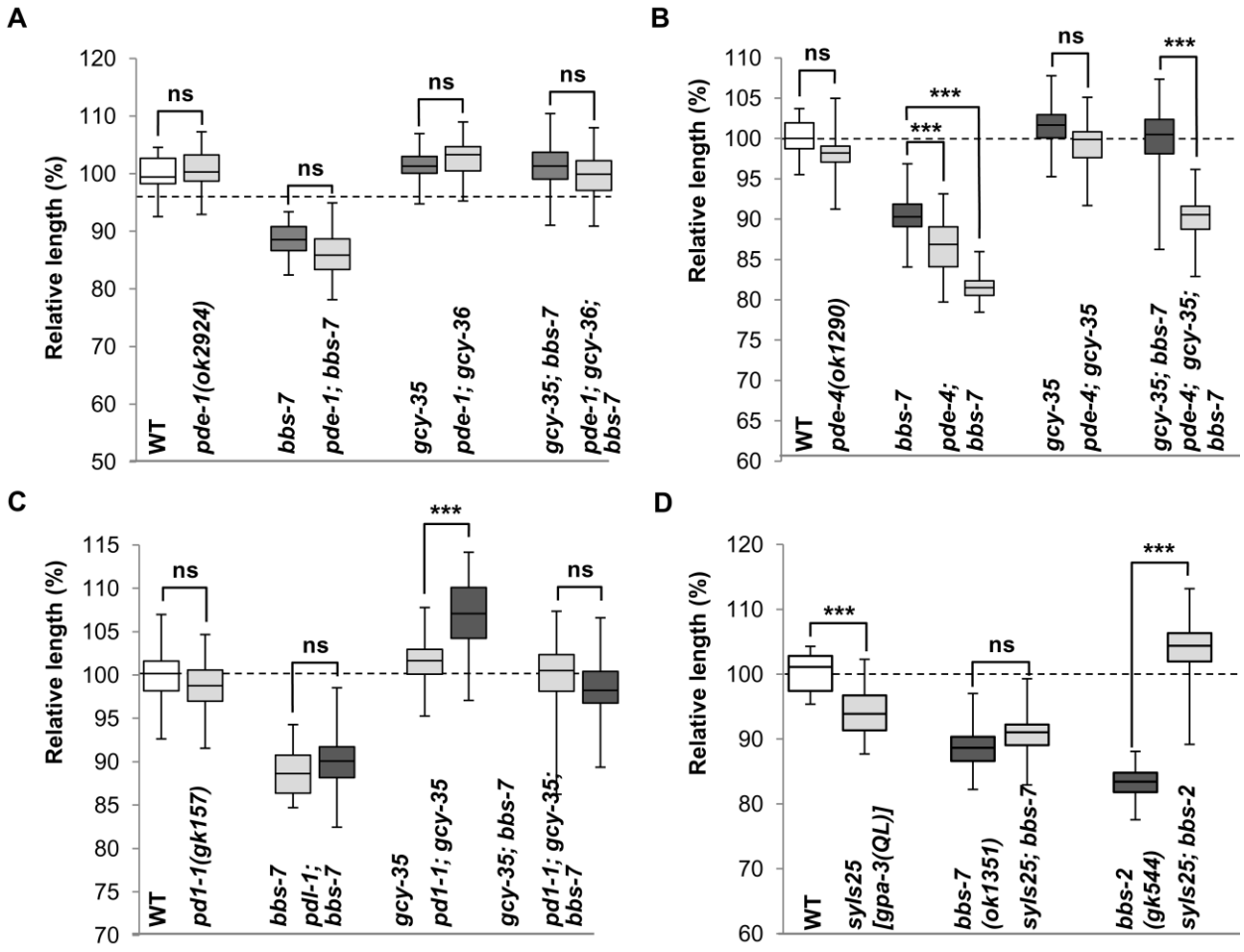

Figure 21. Phosphodiesterases do not play a direct role in body cavity neurons to regulate *bbs* body size. (A) *pde-1(ok2924)* mutants appeared to partially suppress *bbs-7* defects while the effects of the *gcy-35*(*hp433*) allele are epistatic to *pde-1(ok2924)*. (B) *pde-4(ok1290)* may synergistically influence body size in a *bbs* mutant background. *pde-4(ok1290)* decreased body size in both *bbs-7* and *gcy-35;bbs-7* mutant background while having little to no effect in wild-type and *gcy-35* backgrounds. (C) *pdl-1(gk157)* had a minor effect on improving the body size of *gcy-35* mutants while having no effect on improving *bbs-7* defects. (D) The over expression the gain of function allele of *gpa-3* by the transgene *sylS25[gpa-3(Q205L); dp-20(+)]* did not rescue *bbs-7* defects but suppressed *bbs-2* body size defects. Boxes represent 25th-75th percentile of populations with maximum and minimum values as whiskers. ANOVA with Tukey, *** $p<0.001$; ns – $p\geq0.05$. Data represent mean ± SD normalized against wild-type body length.

4.3.5 GPA-3 Overexpression Does Not Suppress BBS Body Size Defects

I initiated an additional investigation into the roles of PDE-1 and PDE-5 in cGMP signalling for body size regulation using a gain of function allele of GPA-3 (Zwaal *et al.* 1997; Hahm *et al.* 2009). Overexpression of the *gpa-3(Q205L)* gain of function allele is capable of reducing the

overall cGMP concentration in ciliated neurons by upregulating *pde-1* and *pde-5* transcription. Thus, if these PDEs are downstream of *bbs* genes, their overexpression should suppress the body size defect of *bbs* mutants. I tested this hypothesis by crossing an integrated overexpression transgene *syIs25*(*Pgpa-3::gpa-3(Q205L) dpy-20(wt)*) in *bbs-7* mutants (**Figure 21D**). *bbs-7;syIs25* animals did not exhibit body size suppression in comparison to *bbs-7* controls. I did, however, observe a suppression of *bbs-2(gk544)* body size defects by *syIs25*.

Given that *pde-1* mutant animals showed little interaction with *bbs-7* and *gcy-36,* it is likely that its overexpression would have little effect. The lack of suppression in *bbs-7;syIs25* animals affirms that *pde-5* and *bbs-7* are likely influencing body size in separate neurons or parallel pathways (**Figure 22B**). Alternatively, the positive regulation of *pde-1* and *pde-5* expression by increased cGMP concentrations may be facilitated in a GPA-3-dependent manner. Thus, if GPA-3 function or localization is BBS-dependent, as other mammalian GPCRs appear to be (Berbari *et al.* 2008a; Berbari *et al.* 2008b), then increased GPA-3 activity would fail to upregulate PDEs sufficiently to suppress the *bbs* body size defect.

Lastly, given that *dpy-20* and *bbs-2* are both located on LGIV, the true genotypes observed may have been *bbs-7;dpy-20(e2182);syIs25[gpa-3(Q205L);dpy-20(wt)]* and *bbs-2;syIs25[gpa-3(Q205L);dpy-20(wt)]*. Therefore the disparity in phenotypes observed may be due to *dpy-20(wt)* overexpression rather than a specific effect of *gpa-3(Q205L).* It may also be that the effect seen is specific between *bbs* genes implying possible diverse functions or roles. Transgenic expression of *gpa-3(Q205L)* in a *bbs* background without the overexpression of *dpy-20* or other body size-related markers is required to verify these observations.

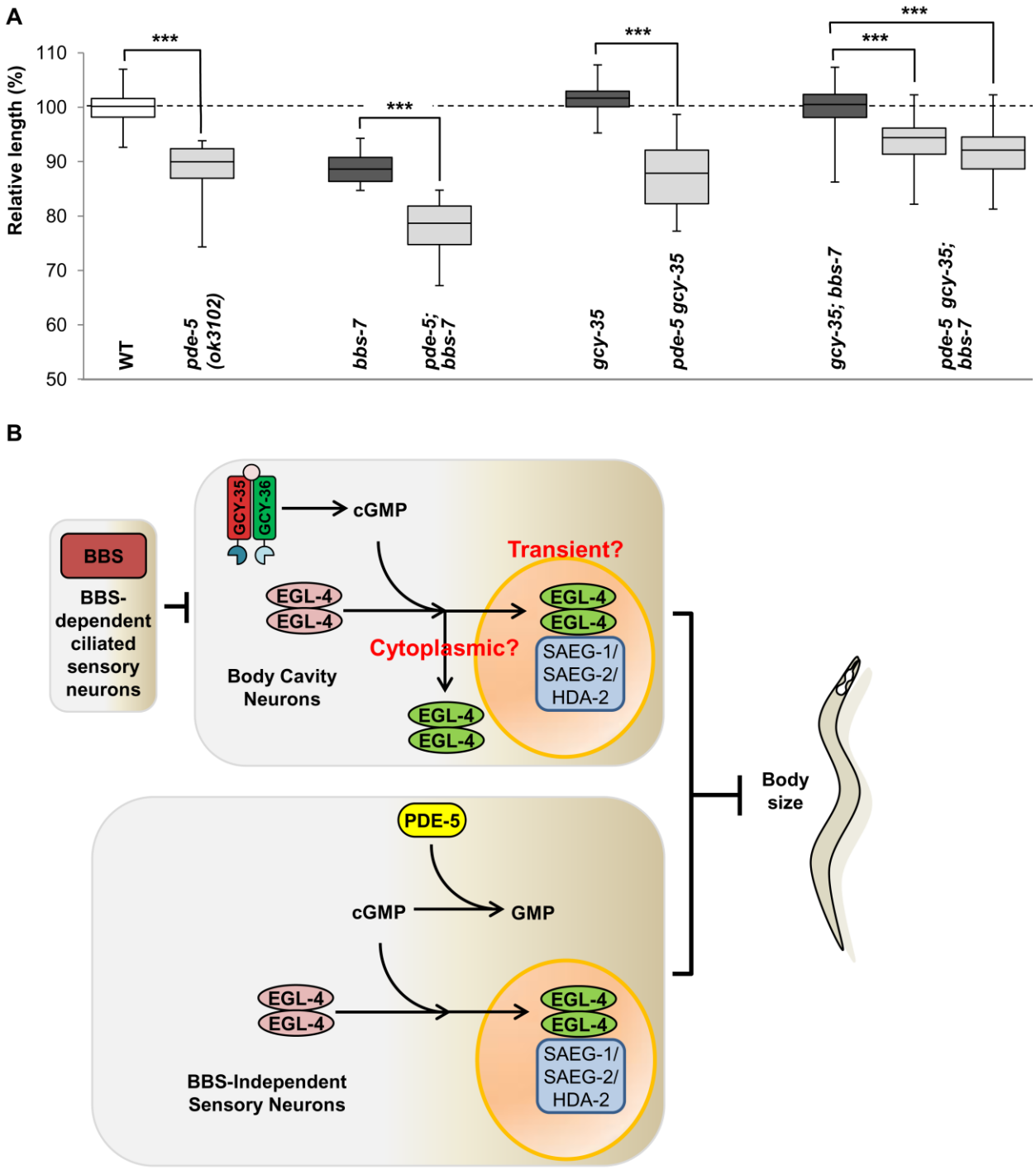

Figure 22. *pde-5* regulates body size in parallel to bbs defects (A) pde-5(ok3102) had an overall epistatic effect on body size. The loss of *pde-5* results in a decreased body size, synergistic with that of *bbs-7* mutation and epistatic to the effects of *gcy-35*. Boxes represent 25th-75th percentile of populations with maximum and minimum values as whiskers. ANOVA with Tukey, *** $p<0.001$; ns – $p\geq0.05$. Data represent mean ± SD normalized against wild-type body length. (B) Model of PDE-5 signalling roles in *bbs* body size regulation. Body size data suggests that PDE-5 regulates body size in non-body cavity neurons in parallel to the body size defects exhibited by *bbs* mutants.

4.3.6 The Loss of Non-Redundant rGCs Does Not Rescue Body Size Defects of *bbs* Mutants

Having demonstrated that EGL-4 plays a key role in *bbs* body size regulation within body cavity neurons, I was unable to identify additional guanylate cyclases in other neurons that shared roles similar to GCY-35/36 (**Figure 15**). Despite this, EGL-4 has been shown to regulate body size through multiple neurons. I therefore assessed the efficacy of reducing overall cGMP production in non-body cavity neurons through the concomitant disruption of multiple rGCs. Double rGC mutations, *gcy-4(tm1653); gcy-23(ok797)*, *gcy-28(tm2411);gcy-23(ok797)*, or *gcy-7(tm901) gcy-16(ok2538)*) exhibited no modification effects on *bbs-7* mutants. The same rGC mutant combinations in a *gcy-35;bbs-7* background did not yield additional suppression effects beyond *gcy-35;bbs-7* mutants controls (**Figure 23A**). Therefore, additional rGC suppression alleles for *bbs* small body size remain to be identified and may only manifest in untested genes or uncharacterized combinations thereof.

4.3.7 DAF-21, the Mammalian HSP90 Orthologue, Rescues *bbs* Body Size Defects

In order to investigate whether any rGCs played a role in *bbs* body size regulation, I proceeded with an analysis using *daf-21(p673)* mutants. DAF-21, the mammalian HSP90 orthologue in *C. elegans* was previously reported to play an important role in dauer formation, likely through an rGC DAF-11 (Birnby *et al.* 2000). It was hypothesized that DAF-21 may regulate the property of multiple rGC proteins through their shared kinase homology domain (KHD) in other biological processes. While I was unable to identify a specific rGC - including *daf-11* (**Figure 23B**) - that acts as a regulator of *bbs* body size defects, I found that the *daf-21(p673)* recessive gain of function allele suppressed the body size defects of *bbs* mutants, (**Figure 23C**) supporting the notion that DAF-21 may regulate rGCs. *daf-21(p673)* hypomorphic mutants had no apparent body length defects at young adult stages. *bbs-2;daf-21* and *bbs-7;daf-21* mutants exhibited a wild-type body length, indicating that *daf-21* does act as a suppressor of *bbs* body size defects (**Figure 23C**). Notably *gcy-35;daf-21* animals were slightly larger than *gcy-35* controls suggesting that the effects of mutations in *daf-21* and *gcy-35* are cumulative or acting in parallel. In support of this, *gcy-35;bbs-2;daf-21* and *gcy-35;bbs-7;daf-21* animals had no additional body size suppression beyond *gcy-35;bbs-7* control animals. These results thus indicate that *daf-21*

may be a potential modifier in regulating *bbs* mutant body size through affecting multiple, functionally redundant rGCs in non body cavity neurons (**Figure 24**).

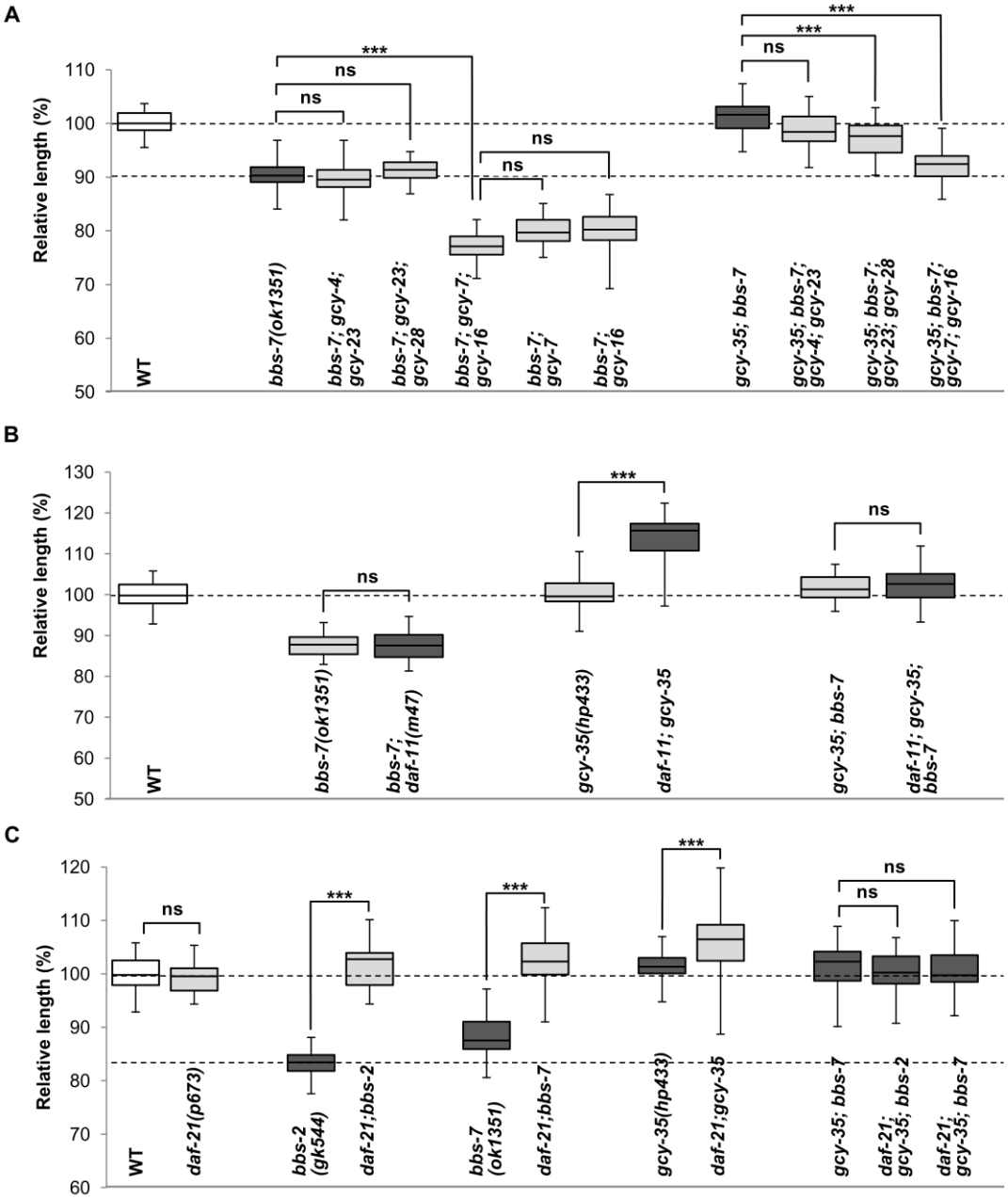

Figure 23. Additional receptor-type guanylate cyclases and related components can play a synergistic role to body size. (A) While the receptor-type guanylate cyclase (rGC) *daf-11(m47)* mutants appear to have an increased body size, this effect is suppressed by the *bbs-7(ok1351)* mutant allele. (B) The loss of multiple independent rGCs does not rescue body size. *gcy-35;bbs-7;gcy-23;gcy-28* and *gcy-35;bbs-7;gcy-7;gcy-16* mutants had a decreased body size in comparison to *gcy-35;bbs-7* controls. (C) The hypomorphic *daf-21(p673)* allele rescues *bbs-2* body size defects and increases *gcy-35* body size but does not affect *gcy-35;bbs-2* or *gcy-35;bbs-7* mutants. Boxes represent 25th-75th percentile of populations with maximum and minimum values as whiskers. ANOVA with Tukey, *** $p<0.001$; ns – $p\geq0.05$. Data represent mean ± SD normalized against wild-type body length.

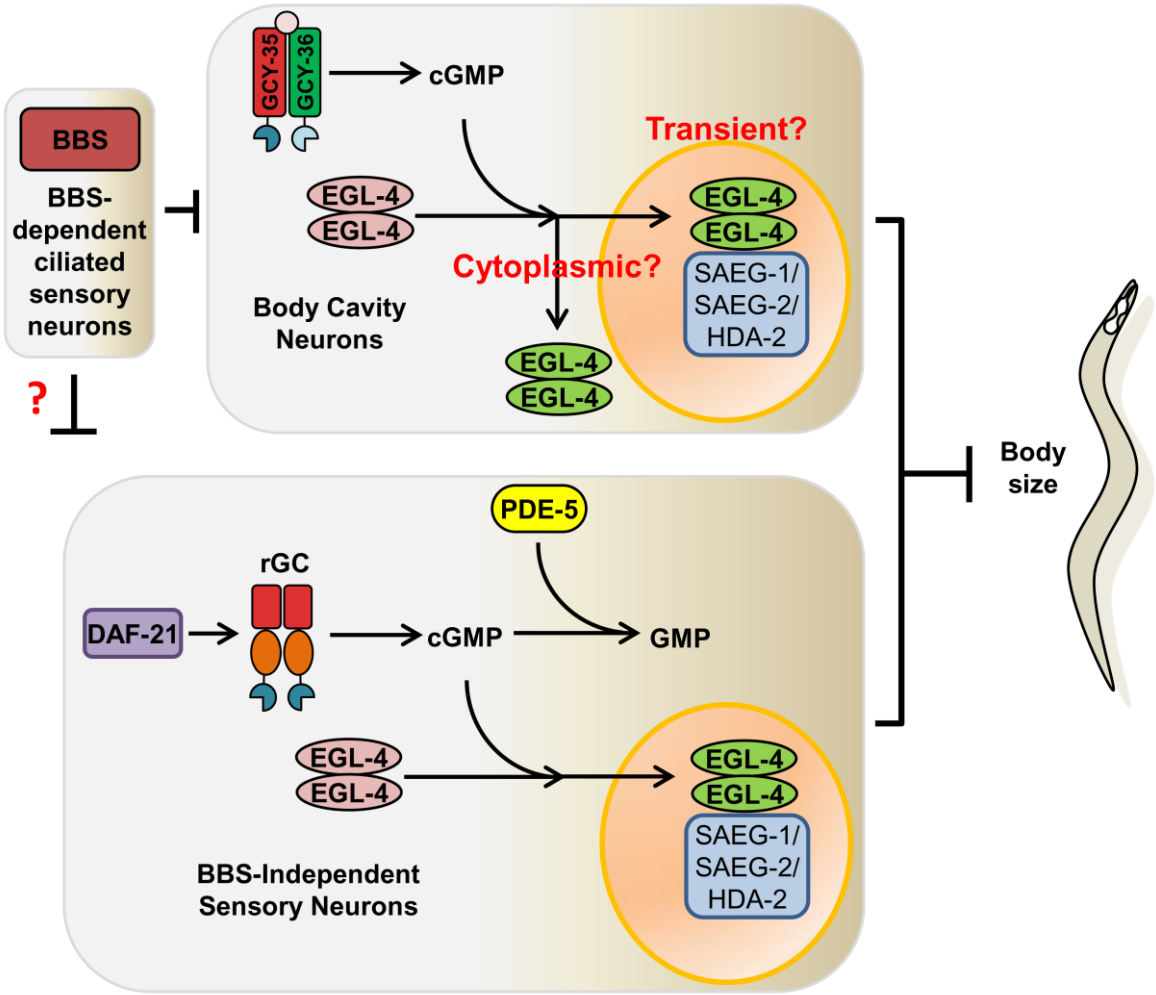

Figure 24. Model of receptor-type guanylate cyclase function in *bbs* body size regulation. Although additional rGC mutant alleles have not successfully suppressed *bbs* body size defects, the use of a *daf-21(p673)* hypomorphic allele suggests that some combination of rGCs act in parallel to body cavity neuron regulation of *bbs* body size.

4.3.8 *mobs-2*: an Additional Suppressor of *bbs-7* Body Size Defects through a Forward Genetics Approach

Through the course of this study, I have focused on candidates of the cGMP signalling pathway beginning with the GCY-35/36 locus that suppresses *bbs* body size. While working with the *daf-11(m47)* allele, however, I identified an additional background mutation that was capable of suppressing *bbs-7* body size defects (**Figure 25**). Non-complementation tests have shown that this locus (*mobs-2*) is complementary to *gcy-35* and *gcy-36*. Similar to *gcy-35* or *gcy-36*, *mobs-2* is capable of significantly improving *bbs-7* body size defects without harbouring any visible size or constitutive dauer defects itself.

The further analysis of *mobs-2*, could lead to the identification of additional cGMP signalling pathway components or separate signalling pathways that are also involved in *bbs* body size regulation. The elucidation of this gene would be part of a future project.

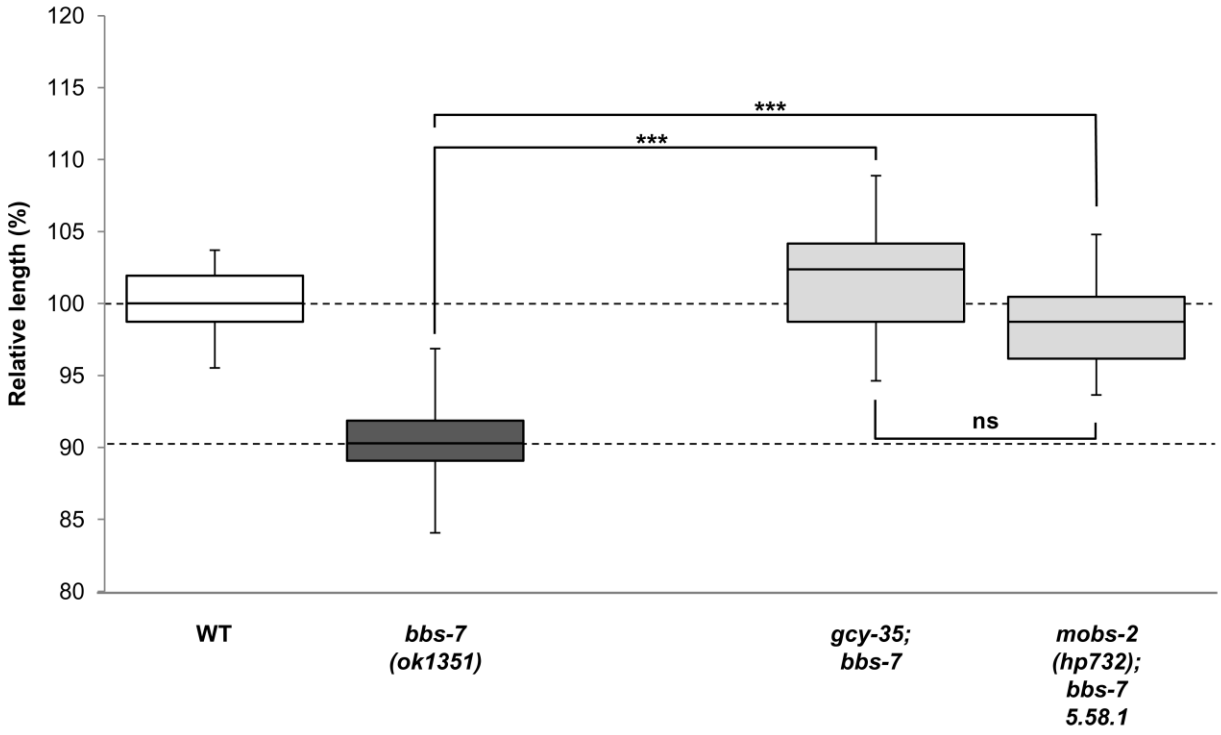

Figure 25. *mobs-2* is a suppressing locus similar to *gcy-35*. The unmapped locus *mobs-2(hp732)* suppresses *bbs-7* body size defects in a manner similar to *gcy-35(hp433)*. Boxes represent 25th-75th percentile of populations with maximum and minimum values as whiskers. ANOVA with Tukey, *** $p<0.001$; ns – $p\geq0.05$. Data represent mean ± SD normalized against wild-type body length.

4.4 Discussion

4.4.1 A change in cGMP/EGL-4 Signalling in *bbs* Mutants May be Transient or Does not involve Nuclear Translocation

The response of *C. elegans* to odorants follows two stages: an initial short-term response that requires EGL-4 activity in the cytoplasm, and a long-term response in which EGL-4 activity appears initially restricted to the nucleus (L'Etoile *et al.* 2002; Lee *et al.* 2010). Only long-term odorant exposure resulted in an observable nuclear accumulation of EGL-4 in the *odr-1*-expressing AWC neurons (Lee *et al.* 2010). My observation that within the body cavity and sensory neurons, GFP::EGL-4 localization does not show obvious difference between wild-type and *bbs* mutant populations suggests two important features of body size regulation in *bbs*

mutants. First, that GFP::EGL-4 is not retained or accumulated at visible levels in the nucleus of body cavity neurons as my results showed no specific nuclear localization within the body cavity neurons during multiple larval stages in wild-type, *bbs-7*, and *gcy-35* animals. Likewise, strong nuclear localization was not observed for GFP::EGL-4 in other sensory neurons under the endogenous *egl-4a* promoter. These results indicate that EGL-4 nuclear signalling may be transient or non-nuclear, as observed in some forms of odorant adaptation (Lee *et al.* 2010). Second, the overall expression levels of GFP::EGL-4 in *bbs-7* animals appears unperturbed, indicating that the loss of BBS proteins does not necessarily promote increased expression of EGL-4, although small changes may be obscured by the overexpression of the GFP::EGL-4 marker. This data is in concordance with my *egl-4* rescue data, that the overexpression of wild-type EGL-4 in multiple neurons is insufficient to cause a *bbs*-like body size. Therefore EGL-4-mediated regulation of *C. elegans* body size may operate through an increase in cytoplasmic or transient nuclear signalling events without an increase in protein expression.

4.4.2 Phophodiesterases Do Not Directly Influence *bbs* Body Size in Body Cavity Neurons

Several phosphodiesterases antagonize specific rGCs during dauer formation (Hahm *et al.* 2009). *pde-1* and *pde-5* transcript levels were increased in response to increased cGMP levels, or in response to increased signalling by GPCRs such as GPA-3 (G-protein alpha subunit). Although PDEs are cGMP regulatory proteins, my genetic analysis did not identify those that are specific to *bbs* body size regulation in the context of the body cavity neuron cGMP-PKG pathway. I cannot rule out, however, the possibility that multiple PDEs may function redundantly to influence cGMP-PKG signalling in body cavity neurons.

Some *pde* mutants did alter the body length of *C. elegans*; *pde-5* in particular may play a role in body size regulation. The loss of *bbs-7* function, however, can further decrease the size of *pde-5* mutants. The body size of *pde-5;bbs-7;gcy-35* was reverted to that of *pde-5* single mutants. Therefore, *pde-5* mutants may affect cGMP-PKG activity in a similar but more severe manner than *bbs* mutants. More specifically, these observations argue against *pde-5* being an active component of cGMP regulation in body cavity neurons alone although it may be active in other neurons. These results also require confirmation that the effect of *pde-5* mutants was not caused by uncharacterized background mutations linked to the *ok3102* allele.. More detailed

experiments examining *pde* mutant combinations and cell-specific rescues are required to clarify these results.

4.4.3 Receptor Guanylate Cyclases May Regulate *bbs* Body Size

C. elegans expresses seven soluble guanylate cyclases and twenty-seven receptor guanylate cyclases throughout the sensory and body cavity neurons (Yu *et al.* 1997). My search for additional sGC and rGC mutants that mediate a suppression effect on *bbs* mutants was not successful. However, there may be untested rGCs that act like *gcy-35*/*gcy-36* in body size regulation. For example, recent publications hinted that *gcy-12* may play a significant role in body size regulation in coordination with *egl-4* (cited as *in preparation* in (Fujiwara *et al.* 2010; Jensen *et al.* 2010)). My observations on the HSP90 orthologue, DAF-21, supports this notion. Previous studies postulated that DAF-21 stabilizes the function of rGCs such as DAF-11 (Birnby *et al.* 2000). *daf-21(p673)* suppresses the body size defects of *bbs* mutants, indicating that DAF-21 plays a role in BBS-mediated body size regulation. If overall cGMP regulation of production activates EGL-4 then a drastic decrease or complete loss of cGMP production will mimic *egl-4(lf)* mutants. *gcy-35;daf-21* mutants exhibit a synergistic increase in body size greater than that of wild-type controls that could be progressing towards that of *egl-4(lf)* mutants, suggesting that sGCs and DAF-21 function in parallel in EGL-4 activation. If DAF-21 indeed acts as an rGC regulator, these observations indicate that multiple rGCs function redundantly in *bbs* body size regulation. These results, however, require further investigation in order to confirm that decreased DAF-21 activity suppresses *bbs* body size defects specifically through the deactivation or inhibition of rGC activity. The observed effects caused by *daf-21(p673)* may be largely coincidental due to the large role DAF-21 plays in multiple developmental pathways (reviewed in (Haslbeck *et al.* 2011)). This is partially substantiated by the inability of multiple *daf-11* alleles to rescue *bbs* body size defects, despite the shared dauer phenotypes and relationship between DAF-21 and DAF-11 (Birnby *et al.* 2000). It is also possible that these effects are due to a closely associated mutation in a nearby locus.

4.5 References

Berbari, N. F., A. D. Johnson, *et al.* (2008a). "Identification of ciliary localization sequences within the third intracellular loop of G protein-coupled receptors." Mol Biol Cell **19**(4): 1540-1547.

Berbari, N. F., J. S. Lewis, *et al.* (2008b). "Bardet-Biedl syndrome proteins are required for the localization of G protein-coupled receptors to primary cilia." Proc Natl Acad Sci U S A **105**(11): 4242-4246.

Birnby, D. A., E. M. Link, *et al.* (2000). "A transmembrane guanylyl cyclase (DAF-11) and Hsp90 (DAF-21) regulate a common set of chemosensory behaviors in caenorhabditis elegans." Genetics **155**(1): 85-104.

Cho, S. W., J. H. Cho, *et al.* (2005). "Identification and characterization of a putative cyclic nucleotide-gated channel, CNG-1, in C. elegans." Mol Cells **19**(1): 149-154.

Cho, S. W., K. Y. Choi, *et al.* (2004). "A new putative cyclic nucleotide-gated channel gene, cng-3, is critical for thermotolerance in Caenorhabditis elegans." Biochem Biophys Res Commun **325**(2): 525-531.

Coburn, C. M. and C. I. Bargmann (1996). "A putative cyclic nucleotide-gated channel is required for sensory development and function in C. elegans." Neuron **17**(4): 695-706.

Conti, M. (2000). "Phosphodiesterases and cyclic nucleotide signaling in endocrine cells." Mol Endocrinol **14**(9): 1317-1327.

Fu, Y. (1995). "Phototransduction in Rods and Cones."

Fujiwara, M., P. Sengupta, *et al.* (2002). "Regulation of body size and behavioral state of C. elegans by sensory perception and the EGL-4 cGMP-dependent protein kinase." Neuron **36**(6): 1091-1102.

Fujiwara, M., T. Teramoto, *et al.* (2010). "A novel zf-MYND protein, CHB-3, mediates guanylyl cyclase localization to sensory cilia and controls body size of Caenorhabditis elegans." PLoS Genet **6**(11): e1001211.

Hahm, J. H., S. Kim, *et al.* (2009). "Endogenous cGMP regulates adult longevity via the insulin signaling pathway in Caenorhabditis elegans." Aging Cell **8**(4): 473-483.

Hao, Y., N. Xu, *et al.* (2011). "Nuclear cGMP-Dependent Kinase Regulates Gene Expression via Activity-Dependent Recruitment of a Conserved Histone Deacetylase Complex." PLoS Genet **7**(5): e1002065.

Haslbeck, V., C. J. Kaiser, *et al.* (2011). "Hsp90 in non-mammalian metazoan model systems." Biochim Biophys Acta.

Hirose, T., Y. Nakano, *et al.* (2003). "Cyclic GMP-dependent protein kinase EGL-4 controls body size and lifespan in C elegans." Development **130**(6): 1089-1099.

Hofmann, F., R. Feil, *et al.* (2006). "Function of cGMP-dependent protein kinases as revealed by gene deletion." Physiol Rev **86**(1): 1-23.

Inada, H., H. Ito, *et al.* (2006). "Identification of guanylyl cyclases that function in thermosensory neurons of Caenorhabditis elegans." Genetics **172**(4): 2239-2252.

Jensen, V. L., N. J. Bialas, *et al.* (2010). "Localization of a guanylyl cyclase to chemosensory cilia requires the novel ciliary MYND domain protein DAF-25." PLoS Genet **6**(11): e1001199.

Johnson, J. L. and M. R. Leroux (2010). "cAMP and cGMP signaling: sensory systems with prokaryotic roots adopted by eukaryotic cilia." Trends Cell Biol **20**(8): 435-444.

L'Etoile, N. D. and C. I. Bargmann (2000). "Olfaction and odor discrimination are mediated by the C. elegans guanylyl cyclase ODR-1." Neuron **25**(3): 575-586.

L'Etoile, N. D., C. M. Coburn, *et al.* (2002). "The cyclic GMP-dependent protein kinase EGL-4 regulates olfactory adaptation in C. elegans." Neuron **36**(6): 1079-1089.

Lee, J. I., D. M. O'Halloran, *et al.* (2010). "Nuclear entry of a cGMP-dependent kinase converts transient into long-lasting olfactory adaptation." Proc Natl Acad Sci U S A.

Liu, J., A. Ward, *et al.* (2010). "C. elegans phototransduction requires a G protein-dependent cGMP pathway and a taste receptor homolog." Nat Neurosci **13**(6): 715-722.

Lugnier, C. (2006). "Cyclic nucleotide phosphodiesterase (PDE) superfamily: a new target for the development of specific therapeutic agents." Pharmacol Ther **109**(3): 366-398.

Mok, C. A., M. P. Healey, *et al.* (2011). "Mutations in a Guanylate Cyclase GCY-35/GCY-36 Modify Bardet-Biedl Syndrome-Associated Phenotypes in Caenorhabditis elegans." PLoS Genet **7**(10): e1002335.

Murakami, M., M. Koga, *et al.* (2001). "DAF-7/TGF-beta expression required for the normal larval development in C. elegans is controlled by a presumed guanylyl cyclase DAF-11." Mech Dev **109**(1): 27-35.

Paquet-Durand, F., S. M. Hauck, *et al.* (2009). "PKG activity causes photoreceptor cell death in two retinitis pigmentosa models." J Neurochem **108**(3): 796-810.

Pierce-Shimomura, J. T., S. Faumont, *et al.* (2001). "The homeobox gene lim-6 is required for distinct chemosensory representations in C. elegans." Nature **410**(6829): 694-698.

Raizen, D. M., K. M. Cullison, *et al.* (2006). "A novel gain-of-function mutant of the cyclic GMP-dependent protein kinase egl-4 affects multiple physiological processes in Caenorhabditis elegans." Genetics **173**(1): 177-187.

Stansberry, J., E. J. Baude, *et al.* (2001). "A cGMP-dependent protein kinase is implicated in wild-type motility in C. elegans." J Neurochem **76**(4): 1177-1187.

Yu, S., L. Avery, *et al.* (1997). "Guanylyl cyclase expression in specific sensory neurons: a new family of chemosensory receptors." Proc Natl Acad Sci U S A **94**(7): 3384-3387.

Zimmer, M., J. M. Gray, *et al.* (2009). "Neurons detect increases and decreases in oxygen levels using distinct guanylate cyclases." Neuron **61**(6): 865-879.

Zwaal, R. R., J. E. Mendel, *et al.* (1997). "Two neuronal G proteins are involved in chemosensation of the Caenorhabditis elegans Dauer-inducing pheromone." Genetics **145**(3): 715-727.

Chapter 5
Discussion and Future Directions

5

5.1 Discussion

5.1.1 BBS Proteins Have Novel Roles in *C. elegans* Development

I have confirmed that loss of function *bbs* mutants share a number of ciliary phenotypes including defects of overall cilia integrity (*dyf*), as well as the mislocalization of ciliary proteins (Blacque *et al.* 2004; Mok *et al.* 2011). Here I have identified additional defects to developmental timing, overall body size, and exploration behaviours. As additional *dyf* mutants, including those of cilia-specific motor components, do not all share these defects, these 'additional' *BBS*-related phenotypes are not merely the result of defective ciliary function.

An unexpected observation of my studies in Chapter 3 was that BBS proteins exert a non-cell autonomous role in body size regulation. More specifically, the BBS proteins act non-cell autonomously to influence the sGC-PKG signalling in body cavity neurons (URX, AQR, and PQR). Among them, URX neurons contribute most critically to body size regulation. URX neurons have no apparent ciliary structures meaning that the influence of BBS proteins must be non-cell autonomous. Likewise, the expression of BBS proteins in the body cavity neurons was incapable of rescuing body size defects exhibited by *bbs* mutants, whereas the expression of wild-type BBS in other sensory neurons could. Taken together, these findings imply that BBS proteins influence body size, without directly functioning in body cavity neuron cilia to do so. Such a function is likely to be divergent from its known role in IFT motor coordination.

Although an extra ciliary role for BBS proteins requires further verification, I speculate that it does involve a BBSome-like complex as the reduced body size defect is observed across multiple *bbs* mutants, mutant alleles are non-additive, and BBS-9 proteins (mutants of which have the smallest body size) appear core to body size regulation. Localization studies, however, show the bulk of BBS protein signals to be present at the transition zone and transporting along the ciliary axoneme. Thus it is possible that BBS proteins are specifically influencing unidentified factors in a periciliary function to regulate body size upstream of body cavity neurons.

5.1.2 Body Cavity Neurons Influence Body Size in a Context-Specific Manner

Body cavity neurons regulate body size through cGMP-PKG signalling. This influence is most apparent in the context of a *bbs* mutant background where body cavity neurons appear to strongly influence overall body size. The loss of either of the sGCs GCY-35 or GCY-36 can result in a dramatic restoration or suppression of *bbs* body size defects. Cell-specific rescues of *gcy-35* and *gcy-36* have identified that this sGC's influence is localized to the body cavity neurons and is most strongly influenced by the non-ciliated URX neuron. Furthermore, an overexpression of the *egl-4(gf)* allele in the body cavity neurons, reverts the suppression effects in *gcy-35;bbs-7* animals. Lastly, the genetic ablation of these neurons confirmed that these neurons are capable of rescuing *bbs* body size defects. In a wild-type background, the loss of *gcy-35/gcy-36* or the ablation of their effector neurons only results in a negligible increase in body size (2-3%), in comparison to a minimum 10% increase in *bbs;gcy-35* strains. There is no effect in a wild-type background. Therefore the influence of the body cavity neurons is only apparent in the *bbs* mutant genotype background.

In a wild-type background, *gcy-35/gcy-36* loss-of-function mutations have negligible effect on body size indicating that cGMP-PKG signalling in the body cavity neurons cannot be the sole site of regulation in body size. This notion is confirmed by the lack of body size defects in wild-type animals expressing *egl-4(gf)* in body cavity neurons; the failure to rescue *egl-4(lf)* body size defects by the expression of wild-type *egl-4* in body cavity neurons; and the large, rather than wild-type, body size exhibited by *bbs-7;egl-4(lf)* animals. Thus in wild-type animals, multiple neurons, in addition to the body cavity neurons, must contribute to the regulation of body size through cGMP-PKG signalling.

Analogous systems of neuronal communication have already been identified in *C. elegans*. Dauer formation, for example is the process by which environmental stimuli such as decreasing food sources and overcrowding cause larval animals to enter an immature, quiescent stage capable of surviving for long periods of starvation (Cassada *et al.* 1975; Golden *et al.* 1984a; Golden *et al.* 1984b). This process is influenced by the TGF-β ligand, DAF-7, which is required to prevent entry into the dauer stage (Ren *et al.* 1996). DAF-7 is expressed specifically in ASI neurons located in the head of the animal, but receptors for it are located diversely in the nervous

system (Gunther *et al.* 2000). The loss of this gene, however, is capable of influencing the entire developmental pathway of this animal.

Taken together, these data suggest that BBS proteins can non-cell autonomously influence the regulation of signalling systems in other neurons. The *bbs* mutants are sensitized genetic backgrounds that reveal the subtle and complex neuronal groups that eventually influence body size. In this case, the body cavity neurons were revealed as important factors in *bbs* body size regulation. Given their exposure to the pseudocoelomic space and various body fluids, these neurons are well positioned to receive and transmit molecular signals important to homeostasis, survival (Cheung *et al.* 2004; Gray *et al.* 2004) and thus body size regulation as well.

5.1.3 GCY-35/GCY-36 Play Specific Roles in Body Size Regulation

I have shown that loss of function mutations in *gcy-35* and *gcy-36* restore body size defects of *bbs* mutants. Furthermore I have identified that the GCY-35/GCY-36 complex is an upstream component to activate the PKG EGL-4. To my knowledge, this work led to the first identification of specific guanylate cyclases that activate EGL-4 in regards to body size regulation. While some rGCs are responsible for EGL-4 activation in odorant behaviours (L'Etoile *et al.* 2002; Lee *et al.* 2010), thus far GCY-35/GCY-36 are uniquely confirmed as upstream components for EGL-4 in *bbs* mutant developmental timing and body size regulation.

Besides GCY-35/GCY-36, the only other identified effective upstream cGMP-related component is in the HSP90 orthologue DAF-21. Postulated to have a regulatory role for a subset of rGCs, a hypomorphic allele of *daf-21* robustly suppresses *bbs* defects to a similar degree as *gcy-35*. This effect, however, may be related to factors such as non-BBS-specific activation and regulation of EGL-4 or pleiotropic DAF-21 functions.

Therefore, until all possible GCs can be examined, it appears that GCY-35/GCY-36 share previously unidentified roles in body size regulation. Factors that may qualify the GCY-35/GCY-36 sGC complex for such a unique role include responsiveness to normoxic conditions (Zimmer *et al.* 2009), specific cellular expression or context, or lack of dependence upon BBS function for localization to dendritic endings, ciliated or otherwise.

5.1.4 EGL-4 Signalling Influences Body Size Via Separate Neurons in Multiple Cellular Pathways

In this work I show that the body cavity neurons regulate *bbs* body size using a cGMP-PKG pathway while being insufficient to fully regulate body size in wild-type animals, implicating a role for similar signalling in additional sets of sensory neurons. This notion is confirmed by the lack of phenocopy in body size between *gcy-35(lf)* and *egl-4(lf)* animals; the large, rather than wild-type, body size exhibited by *bbs-7*;*egl-4(lf)* animals; the failure to rescue *egl-4(lf)* body size defects by the expression of wild-type *egl-4* in body cavity neurons; and the lack of a decreased body size in wild-type animals (unlike *gcy-35;bbs-7* mutants) expressing *egl-4(gf)* in body cavity neurons. Furthermore, previous studies have shown that the expression of wild-type *egl-4* in some groups of non body cavity neurons was also sufficient to abrogate *egl-4(lf)* body size phenotypes (Fujiwara *et al.* 2002).

From my study of *pde-5*, which has been shown to regulate cGMP turnover, I have also noted that these mutants share body size defects that are additive to that of *bbs-7* mutants. It is possible that a loss of PDE-5 activity may result in increased EGL-4 signalling, in neurons independent of body cavity neurons, which contributes to the body size defects observed in *pde-5;bbs-7* animals. Taken together, it is clear that while body cavity neurons do play a role in influencing the body size of *bbs* mutants, the activation of EGL-4 signalling in other neurons also contributes to body size. Likewise, in wild-type animals, multiple neurons, in addition to the body cavity neurons, must contribute to the regulation of body size through cGMP-PKG signalling.

My exploration of GFP::EGL-4 nuclear localization did not identify an obvious increase of GFP::EGL-4 expression in *bbs* mutants nor did I observe a stable accumulation of nuclear GFP::EGL-4 in *bbs* mutants. Despite these findings, a recent study showed that nuclear EGL-4 interacts with multiple histone deacetylases (*saeg-1*, *saeg-2*, *hda-2*) and that the loss of these interactors was sufficient to revert *egl-4(gf)* body size to that of wild-type animals (Hao *et al.* 2011). It is worth noting that the loss of these downstream components was insufficient to convert the body size of *egl-4(gf)* to that of *egl-4(lf)* (Hao *et al.* 2011). In addition, short term behaviour modification in the AWC neurons of *egl-4(lf)* mutants can be restored with an EGL-4(ΔNLS) construct, indicating that cytoplasmic signalling events are within the repertoire of this PKG (Lee *et al.* 2010). Coupled with my GFP::EGL-4 data, this suggests that in a *bbs* mutant

background, EGL-4 may transiently signal within the nucleus or it may signal in pathways that do not necessarily require its accumulation in the nucleus.

In conclusion, I hypothesize that body cavity neurons and other unidentified neurons must regulate EGL-4 activity redundantly, through different cellular mechanisms.

5.2 Future Directions

5.2.1 Further Dissecting the Role of BBSome Proteins in IFT

In *C. elegans* the BBS proteins are thought to function mainly in the association between the anterograde motors heterotrimeric Kinesin-II and homodimeric OSM-3, which individually transport at disparate velocities. It is likely that *C. elegans* BBS proteins function as a BBSome-like complex, since single BBS mutants have been observed to accumulate additional GFP proteins at the ciliary body, lacking visible IFT movement of remaining BBS proteins (Ou *et al.* 2007). There remains a question of how the BBS proteins and other ciliary components are transported along the dendrites from the cell body to the ciliated ending.

In mammalian cells, it is reported that BBS proteins are required to target cilia-specific motifs to the primary cilium (Berbari *et al.* 2008a). Similar mechanisms may be involved in the transport of BBS and other ciliary proteins in the nematode. Moreover, could individual proteins serve specialized functions within the complex, allowing the BBSome to maintain partial function despite missing some components? My body length analyses demonstrate that mutations in some BBS proteins exert slightly more severe phenotypes than others. Mutations in *bbs-2* and *bbs-7*, for example appear to be least severe although previous studies have shown these to be important interactors between BBS-chaperonin complexes (Seo *et al.* 2010). Meanwhile, *bbs-9* mutants had the most severe body size defects among all *bbs* single mutants, and were most similar to double and triple *bbs* mutants. This observation is in concordance with findings that mammalian BBS9 acts as a hub protein within the BBSome (Nachury *et al.* 2007).

A careful examination of all potential genetic combinations may not only confirm previous observations about interactions within the BBSome complex but also elucidate key domains of formation. Using currently available mutants, the expression of *bbs* “rescue” constructs containing specific domain deletions or mutations may reveal the conditions under which the BBSome is assembled, transported, and operates. Additionally, these “rescue” constructs may

reveal domains in various BBS proteins that are specific to only a subset of BBS-associated features. By determining how specific BBS domains influence the course of feature manifestation, these types of experiments could be expanded to investigate the effect or importance of known *BBS* patient alleles on determining the severity of human BBS features.

5.2.2 The Role of cGMP Production in *C. elegans* Body Cavity Neurons

The role of cGMP in the body cavity neurons appears two-fold; being required for proper hyperoxic avoidance behaviours and in the regulation of body size. GCY-35/GCY-36 was first identified as an important factor in the aggregation behaviours of *npr-1* mutant animals and in the hyperoxic avoidance behaviours of wild-type animals (Cheung *et al.* 2004; Gray *et al.* 2004).

In *bbs* mutants, it remains unclear as to whether cGMP concentration is perturbed in these neurons or if the downstream cGMP signalling in the body cavity neurons is somehow altered. A number of experiments could indirectly examine this possibility.

If cGMP signalling is perturbed such that the concentration of cGMP signalling molecules is high, I expect in addition to body size regulation defects, behavioural defects in relation to hyperoxic avoidance. An analysis of hyperoxic avoidance behaviours will indirectly measure cGMP activity through the assessment of calcium concentration fluctuations (Zimmer *et al.* 2009). If cGMP levels are increased in *bbs* mutants, I expect that sudden changes to oxygen concentration may elicit weakened calcium influx responses. A comparison between wild-type, *bbs*, and *gcy-35* mutant combinations would help confirm if *bbs* mutant hyperoxic responses are intact.

Common measurements of calcium concentrations within cells involve the use of dynamic fluorescent reporters. Two such reporters use calmodulin-based fluorescent resonance electron transfer (FRET) (Truong *et al.* 2001) or the fusion of GFP, calmodulin and the M13 domain of a myosin light chain kinase (GCaMP) (Nakai *et al.* 2001). The former transfers energy from one fluorophore to another upon calcium-binding while the latter increases in intensity when bound to calcium. Using these concepts, a number of cGMP sensors have been designed by utilizing the cGMP-binding motifs of either PDEs or PKGs (for review see (Nikolaev *et al.* 2009)). The various sensors possess differing kinetics and dynamic ranges but could conceptually be

translated for use in *C. elegans*. These sensors would ultimately be useful in determining whether cGMP concentrations influence body cavity or other groups of neurons to regulate body size.

5.2.3 Determining the Temporal Requirements of cGMP in BBS-Associated Phenotypes

Although I have demonstrated that cGMP-PKG signalling is a key element to determining body size in *bbs* mutant body cavity neurons, it is not clear, at which point this signalling is required to determine body size or delay developmental timing. The study of EGL-4 nuclear localization did not clarify any specific time points at which signalling may be of importance. An alternative method would be to grow animals in the cGMP analog 8-Bromo-cGMP. The growth of wild-type animals in this metabolically stable analog does reduce body size (Hirose *et al.* 2003) although the exact larval stage at which this effect is apparent remains unexplored. 8-Bromo-cGMP could be used as a tool to mimic loss of *bbs* mutations, by transferring developing wild-type animals of varying stages to grow on different concentrations of this analog. This would help clarify the minimal time-point at which cGMP signalling may be perturbed in *bbs* animals. Comparisons could be made between wild-type, *bbs*, and *gcy-35;bbs* animals, with the third background being most important to assessing *bbs*-specific size regulation.

Interestingly, my rescue experiments show that among AQR, PQR, and URX, only URX is necessary for body size reversion as URX alone exhibits a partial reversion of body size using the *Pflp-8::GCY-35* construct. *flp-8* is reported to be expressed in eggs and larvae but not adults. The premature termination of GCY-35 expression in these transgenic animals may account for the partial rescue. These results may indicate that there is both a temporal and persistent reliance upon cGMP-PKG signalling during larval and early adult stages to reduce body size growth.

5.2.4 Determining if Nuclear Localization of PKEG EGL-4 is Required for Body Size Regulation

Increased nuclear localization is a requirement for behavioural changes to long-term benzaldehyde exposure in AWC neurons but not necessarily for AWA and AWB responses to other volatile odorants. Additionally, non-nuclear EGL-4 signalling in AWC neurons causes short-term behavioural changes, suggesting cytoplasmic signalling events (Lee *et al.* 2010). The loss of EGL-4 function results in an abnormally large body size (Daniels *et al.* 2000; Fujiwara *et al.* 2002; Hirose *et al.* 2003) thereby implying a basal level of EGL-4 signalling under wild-type

conditions. It remains unclear, however, if sensory or body cavity neurons require nuclear EGL-4 signalling to normally regulate body size. Recent studies from Hao *et al*., however, show that EGL-4(gf) does interact in the nucleus with specific histone deacetylase proteins thereby supporting that prolonged activation of EGL-4 does appear to cause its localization to the nucleus. The loss of these interacting histone deacetylases, however, only restores *egl-4(gf)* mutant body size to wild-type levels.

If body size regulation does involve the prolonged activation of EGL-4, I expect to have observed clear EGL-4 nuclear localization. My results thus far have not been supportive of this scenario, although this could be due to the sensitivity of my detection methods. I could more directly gauge the physiological function of the potential nuclear localization through the removal of the nuclear localization signal (NLS) in EGL-4. If transient nuclear localization is required for body size regulation, then the expression of an EGL-4(ΔNLS) protein would fail to rescue in an *egl-4(lf)* mutant background. Likewise, the expression of an EGL-4(gf, ΔNLS) in body cavity neurons should also fail to revert body size suppression in *gcy-35;bbs-7* animals.

If body size regulation requires nuclear EGL-4 signalling, it would be important to determine its transcriptional targets that mediate body size regulation. Hao *et al*. used a forward genetics screen of *egl-4(gf)* mutants to identify **S**uppressors of **A**ctivated **EG**L-4 mutants. They identified loss of function mutants for *saeg-1,* which is similar to human transcriptional regulating factor, TRERF1, and zinc-finger protein 541, ZNF541. *saeg-2* is orthologous to the mammalian terminal deoxynucleotidyltransferase interacting protein 1 (*Dnttip1*). They also observed that *saeg-1* and *saeg-2* are capable of suppressing EGL-4(gf) phenotypes including hyperactive egg-laying, dwelling, and decreased body size (Hao *et al.* 2011). TRERF1, interacts with CBP/p300 to regulate the expression of a steroidogenesis factor CYP11A1 (Gizard *et al.* 2001) while also suppressing cell proliferation through interactions with the transcription factor Sp1 (Gizard *et al.* 2005). ZNF541 has been implicated in chromatin remodeling during spermatogenesis. In higher organisms, PKG signalling plays a role in a number of complex organs. Neuronal PKG signalling has been implicated in axon guidance, synaptic plasticity, the control of behaviours such as anxiety, and neurosensory responses to name a few (reviewed in (Hofmann *et al.* 2006)). More recently, PKG activity was shown to play a major role in cGMP-mediated photoreceptor degeneration (Paquet-Durand *et al.* 2009) indicating that EGL-4 nuclear functions do not necessarily encompass general transcriptional machinery. The study of PKG signalling pathways

in *C. elegans bbs* mutants may further elucidate the signalling mechanisms involved in human BBS photoreceptor degeneration.

5.2.5 How do BBS Proteins Regulate Body Size Non-Cell Autonomously From Sensory Neurons to Body Cavity Neurons

My studies identified a potential function of BBS proteins beyond bridging IFT motors. The further exploration of an IFT-independent function may help elucidate both human syndromic features that are applicable to not only *bbs*, but also to other ciliopathies.

I have shown that BBS proteins regulate body size in a non-cell autonomous fashion. How do BBS proteins mediate communication between sensory neurons and the body cavity neurons? What directives can be taken to dissect the mechanisms behind this complex neuronal communication? A pathway that remains unexplored in this work is the network of insulin signalling molecules. These hormones may also be good candidates as a number of insulin (*ins*) mutants are observed to have dauer entry and/or exit defects (Cornils *et al.* 2011) while others may exhibit an influence on overall growth potential (So *et al.* 2011). This is of great interest since a small set of sensory neurons are capable of inducing growth arrest within the entire animal. Speculatively, some sensory neurons may secrete insulins in a BBS-regulated manner, which communicate with body cavity neurons in a hormonal manner. Likewise, a similar form of coordinated synaptic communication could also be responsible for regulating body size in *C. elegans.* However, there are few direct synaptic connections between sensory neurons and body cavity neurons arguing against a simplistic model of neuronal communication to regulate body size. Through the course of this study, Lee *et al.* identified that *bbs* mutants share a hyperactive neuroendocrine secretion phenotype which plays a role in body size regulation, lipid accumulation and feeding behaviours (Lee *et al.* 2011) (see section 5.3.1). Therefore exploring a combination of *bbs* and specific *ins* mutants should be useful in the further elucidation of BBS-related body size regulation mechanisms.

If specific synaptic communication is a key feature in BBS-mediated body size regulation then ablation of BBS-dependent neurons through means such as cell-specific *egl-1* expression, may help to further define which sensory neurons are important for such communication. Tetanus toxin (TeTx) is a neurotoxin that can disrupt synaptic (neurotransmitter) communication through the cleavage of the synaptic vesicle protein synaptobrevin (Schiavo *et al.* 1992). Specific

expression of TeTx in *C. elegans* neurons can be used effectively to disrupt certain synaptic communication as well (Macosko *et al.* 2009). The expression of tetanus toxin (TeTx) under specific neuronal promoters would be an additional method to assess whether synaptic communication from the body cavity neurons or the sensory neurons is critical for body size regulation. Likewise, an analysis of synaptic communication mutants may be helpful in deciphering the additional molecular functions of BBS proteins (reviewed in (Richmond 2005)).

5.2.6 Investigating BBS-Associated Phenotypes in Relation to the mTOR Signalling Pathway

Target of rapamycin (TOR), a serine/threonine kinase important to cellular growth, is conserved throughout a number of species from yeast to humans. TOR forms two major complexes which are characterized by their sensitivity (TORC1) and insensitivity (TORC2) to the drug rapamycin. TORC1 is a well-studied complex involved in signalling and cell growth that is regulated by a number of external and internal growth cues. The TORC2 complex, however, is not well-studied although recent findings with *C. elegans* have defined a genetic relationship between components of TORC2 (*CeRictor, lpo-6*) and the serum and glucocorticoid-induced kinase (*sgk-1*) in regulating developmental phenotypes (Jones *et al.* 2009). Mutants of this pathway share similar phenotypes to that of *bbs* mutants including increased fat accumulation, body size defects, and a slight developmental delay (Jones *et al.* 2009). *lpo-6*, however, regulates size independently of TGF-β/EGL-4, AKT and DAF-16/FOXO signalling and given its phenotypes is a promising interacting candidate for *bbs* body size regulation. The analysis of these *C. elegans Rictor* mutants in conjunction with *bbs* and *gcy-35* mutations may reveal if these body size defects are also parallel (as observed in (Jones *et al.* 2009)). Promising work in zebrafish has shown that treatment with inhibitors of TOR can successfully reduce renal abnormalities – cysts in particular, of *bbs*-MO animals (Tobin *et al.* 2008) which may indicate a genetic relationship with the *bbs* genes.

5.2.7 Does cGMP Signalling Influence or Contribute to Ciliopathy Phenotypes in Other Model Organisms

Can these findings in *C. elegans* translate into other model organisms? A number of options are available for the analysis of cGMP in other organisms. There are both genetic and

pharmaceutical means to test the importance of the GCY-35/GCY-36 mammalian orthologue, GUCY1B2, or other guanylate cyclases.

5.2.7.1 Is cGMP Signalling Altered in Zebrafish?

The vertebrate *Danio rerio* offers a number of unique advantages as a genetic model. Like *C. elegans*, the transparent body during embryogenesis makes it possible to observe obvious developmental defects, spatio-temporal gene expression, and even transient ciliogenesis events such as those observed in the Kupffer's Vesicle.

Moreover, morpholino injection technology has made it possible to temporarily knockdown a variety of genes (many embryonic lethal) during initial developmental stages to observe their influence on viability. Coupled with the ability to rescue gene function by morpholino-insensitive cDNA sequences, this system has become quite amenable and reliable for the study of human allelic influence in disorders such as ciliopathies (Zaghloul *et al.* 2010). In conjunction with simplified pharmaceutical treatment delivery (Zon *et al.* 2005; Bowman *et al.* 2010), the zebrafish is a superb candidate model to investigate the potential involvement of cGMP in relation to BBS protein function.

Relevant questions include whether any *bbs* morpholino phenotypes are shared with wild-type embryos raised in moderate to high doses of the analog 8-Bromo-cGMP. Does the addition of sGC inhibitors in *bbs*-MO fish rescue or perturb any specific phenotypes? Could the reported BBS3L isoform phenotype (Pretorius *et al.* 2010; Pretorius *et al.* 2011) influence cGMP signalling in the eye? Does the same PKG pathway influence developmental phenotypes? Do *bbs*-MO animals produce high levels of cGMP?

5.2.7.2 Is the Role of GCY-35/GCY-36 Conserved in the Murine Model?

Murine models have been key to both confirming and identifying new BBS-specific phenotypes. In this manner, it is likely that this would be the most appropriate model to confirm the presence of aberrant cGMP signalling-mediated phenotypes in *Bbs* mutant animals. For example, during phototransduction, high levels of this secondary messenger are reduced by phosphodiesterase activity, causing the hyperpolarization of the photoreceptor cell and a decrease in glutamate release. A failure in cGMP-turnover prevents the process of phototransduction, which may eventually lead to attrition and photoreceptor death (Davis *et al.* 2008).

Murine tissues could be examined for cGMP concentrations using specific ELISA kits (Marte *et al.* 2008; Oeckl *et al.* 2011) to identify which syndromic features may be cGMP-related. Alternatively, *Bbs* and *Gucy1b2* single or double mutants, if available, could be examined for phenotypes in viability, obesity, or retinopathy amongst other features. Alternatively, *Bbs* mice could also be treated pharmaceutically with sGC inhibitors such as ODQ (Garthwaite *et al.* 1995) to determine if it enhances or ameliorates murine *Bbs* features.

5.2.7.3 Do the Human Orthologues Play a Role in Modulating Aspects of BBS Phenotypes

The pathophysiology of a number of human BBS features and their variability between individuals remains unclear. The study of the role of candidate genes in BBS phenotypes requires an association study assuming the phenotypes are under a complex trait model. This approach requires a large sample size which is a challenge for rare diseases such as BBS. In addition, this requires detailed phenotype information which is a challenge to obtain. In the last several years, through international collaborations, the Héon lab has recruited a cohort of 200 patients with DNA and some detailed phenotype information. Currently the best phenotype information relates to visual function. As guanylate cyclases play an important role in phototransduction, do variations of the GCY-35 human orthologue, GUCY1B2, correlate with visual acuity? Additional phenotype information on this cohort is currently being collected.

The human sGC orthologue GUCY1B2 is most closely related to GCY-35. The function of this sGC, however, remains unclear. One study suggests that this sGC may normally negatively regulate the production of cGMP through competitive binding of the α-component GUCY1A1 versus its normal binding partner GUCY1B1 (Gupta *et al.* 1997). An expression analysis of GUCY1B2 shows very low and variable expression amongst a wide array of tissues including renal and photoreceptor tissues (**Appendix A2**). How this sGC may play a role in regulating cGMP within the photoreceptor or other tissues remains unknown. The identification of even mild influences to the phenotype severity of retinal degeneration, obesity, renal and cognitive impairments could have a great impact on the burdens of this disease.

5.3 Conclusion and Model

5.3.1 *bbs* Mutants Have Hyperactive Neuroendocrine Secretion defects

Recently, Lee *et al*. completed an investigation of *bbs* mutant phenotypes, including body size defects (Lee *et al.* 2011). Lee *et al*. identified that *bbs* mutants had increased secretion of neuropeptides (DAF-7, DAF-28, and FLP-21) from ADL neurons. Interestingly, these secretion defects were cell autonomous and abrogated with ADL expression of wild-type BBS proteins.

Investigating further, Lee *et al*. observed that the increase in neuropeptides was not dependent upon upregulated transcription but was related to conserved exocytosis machinery of the GTPase AEX-6 (Rab27); RBF-1 (rabphilin) an effector of AEX-6; and AEX-3, a RabGEF regulator of AEX-6. Mutant alleles of these genes and *unc-31* were all capable of abrogating the hyperactive neuroendocrine secretion phenotype and the small body size of *bbs* mutants. Thus, BBS proteins were regulating body size through the negative regulation of an RBF-1/AEX-3/UNC-31 endocytosis complex. Furthermore, in concordance with my own findings, Lee *et al*. also observed that IFT mutants had a decrease in neuroendocrine secretion, thus corroborating that BBS proteins are likely functioning in IFT-independent roles (Lee *et al.* 2011).

Lee *et al*. concluded that hyperactive release of neuropeptides via dense core vesicles, from ADL neurons was involved in body size regulation while other neurons such as ASI could be acting in a similar manner.

5.3.2 Hyperactive Neuroendocrine Secretion May Modulate cGMP-PKG Regulation of Body Size in Body Cavity Neurons.

My studies identified a novel *bbs*-associated function that involves the regulation of cGMP-PKG-signalling body cavity neurons, which is critical for body length and developmental timing regulation. The BBS proteins non-cell autonomously regulate body cavity neurons, which require the sGC complex GCY-35/GCY-36 to initiate cGMP signalling through the downstream effector EGL-4. While EGL-4 also regulates body size through other neurons, I have yet to identify specific additional GC mutant loci that alone or in tandem can strongly contribute to body size in *bbs* mutants in a fashion comparable to that of *gcy-35* or *gcy-36*. Together these results indicate that BBS genes eventually regulate *C. elegans* body size through moderating the cGMP-PKG signalling activity level of the body cavity neurons (**Figure 26B**). Additionally,

DAF-21-cGMP-PKG signalling in other sensory neurons, may involve some phosphodiesterases to interact synergistically or in parallel with *bbs* mutations (**Figure 26C**).

Combining these results with the findings of Lee *et al*. it becomes apparent that neuropeptide secretion from ADLs into the pseudocoelomic space could potentially influence or modulate the observed cGMP-PKG signalling in body cavity neurons (**Figure 26A**). Interestingly, from the Lee *et al*. results, both FLP-21 and DAF-28 show increased levels of secretion. FLP-21 is a known ligand for the receptor NPR-1, which is expressed in body cavity neurons and modulates the effects of cGMP signalling in regards to oxygen sensation (Cheung *et al.* 2004; Gray *et al.* 2004). DAF-28 is an insulin-like ligand for the DAF-2 receptor(Li *et al.* 2003). DAF-2 is expressed throughout the larval and adult nervous system and plays an important role in the regulation of downstream transcription via FoxO/DAF-16 (Gottlieb *et al.* 1994; Lin *et al.* 2001). Thus body cavity neuronal regulation of body size could be influenced or modulated via neuropeptides transmitted through the pseudocoelomic space. Likewise, additional neurons participating in cGMP-PKG regulation of body size could also be targets of *bbs*-related hyperactive neuromodulation.

In summary, an intricate balance of multiple neuronal components and multiple signalling pathways regulates body size; *bbs* mutants may perturb such a balance via neuromodulation of cGMP-PKG signalling within the body cavity neurons. These BBS-specific pathways may be conserved in higher organisms and future studies could elucidate their possible relationship to the pleiotropic features of the human syndrome thus having a potential impact on the diagnosis, prognosis and treatment of these patients.

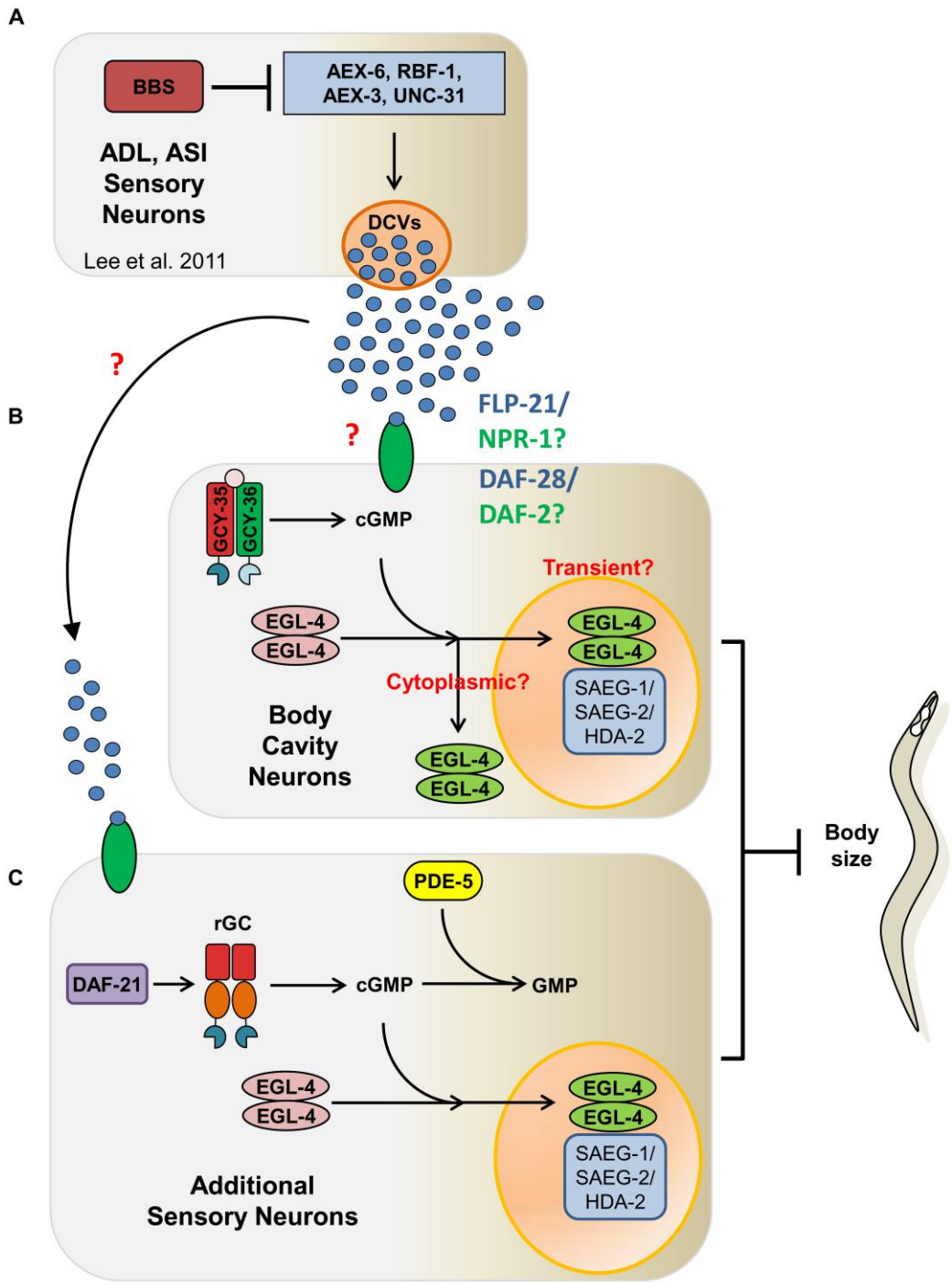

Figure 26. Model of cGMP-PKG body size regulation. (A) BBS proteins in ADL neurons negatively regulate the conserved RBF-1/AEX-3/UNC-31 exocytosis pathway. Loss of BBS proteins results in upregulated neuropeptide release (DAF-7, DAF-21, FLP-21) via dense core vesicles (Lee *et al.* 2011). (B) Neuropeptide receptors such as DAF-2 or NPR-1 may respond to the ligands DAF-28 and FLP-21 respectively. These may neuromodulate the functions of body cavity neurons, thus influencing EGL-4 body size regulation pathway. A similar effect may also influence cGMP-PKG signalling in other sensory neurons (C).

5.4 References

Berbari, N. F., A. D. Johnson, *et al.* (2008a). "Identification of ciliary localization sequences within the third intracellular loop of G protein-coupled receptors." Mol Biol Cell **19**(4): 1540-1547.

Blacque, O. E., M. J. Reardon, *et al.* (2004). "Loss of C. elegans BBS-7 and BBS-8 protein function results in cilia defects and compromised intraflagellar transport." Genes Dev **18**(13): 1630-1642.

Bowman, T. V. and L. I. Zon (2010). "Swimming into the future of drug discovery: in vivo chemical screens in zebrafish." ACS Chem Biol **5**(2): 159-161.

Cassada, R. C. and R. L. Russell (1975). "The dauerlarva, a post-embryonic developmental variant of the nematode Caenorhabditis elegans." Dev Biol **46**(2): 326-342.

Cheung, B. H., F. Arellano-Carbajal, *et al.* (2004). "Soluble guanylate cyclases act in neurons exposed to the body fluid to promote C. elegans aggregation behavior." Curr Biol **14**(12): 1105-1111.

Cornils, A., M. Gloeck, *et al.* (2011). "Specific insulin-like peptides encode sensory information to regulate distinct developmental processes." Development **138**(6): 1183-1193.

Daniels, S. A., M. Ailion, *et al.* (2000). "egl-4 acts through a transforming growth factor-beta/SMAD pathway in Caenorhabditis elegans to regulate multiple neuronal circuits in response to sensory cues." Genetics **156**(1): 123-141.

Davis, R. J., J. Tosi, *et al.* (2008). "Functional rescue of degenerating photoreceptors in mice homozygous for a hypomorphic cGMP phosphodiesterase 6 b allele (Pde6bH620Q)." Invest Ophthalmol Vis Sci **49**(11): 5067-5076.

Fujiwara, M., P. Sengupta, *et al.* (2002). "Regulation of body size and behavioral state of C. elegans by sensory perception and the EGL-4 cGMP-dependent protein kinase." Neuron **36**(6): 1091-1102.

Garthwaite, J., E. Southam, *et al.* (1995). "Potent and selective inhibition of nitric oxide-sensitive guanylyl cyclase by 1H-[1,2,4]oxadiazolo[4,3-a]quinoxalin-1-one." Mol Pharmacol **48**(2): 184-188.

Gizard, F., B. Lavallee, *et al.* (2001). "A novel zinc finger protein TReP-132 interacts with CBP/p300 to regulate human CYP11A1 gene expression." J Biol Chem **276**(36): 33881-33892.

Gizard, F., R. Robillard, *et al.* (2005). "TReP-132 controls cell proliferation by regulating the expression of the cyclin-dependent kinase inhibitors p21WAF1/Cip1 and p27Kip1." Mol Cell Biol **25**(11): 4335-4348.

Golden, J. W. and D. L. Riddle (1984a). "The Caenorhabditis elegans dauer larva: developmental effects of pheromone, food, and temperature." Dev Biol **102**(2): 368-378.

Golden, J. W. and D. L. Riddle (1984b). "A pheromone-induced developmental switch in Caenorhabditis elegans: Temperature-sensitive mutants reveal a wild-type temperature-dependent process." Proc Natl Acad Sci U S A **81**(3): 819-823.

Gottlieb, S. and G. Ruvkun (1994). "daf-2, daf-16 and daf-23: genetically interacting genes controlling Dauer formation in Caenorhabditis elegans." Genetics **137**(1): 107-120.

Gray, J. M., D. S. Karow, *et al.* (2004). "Oxygen sensation and social feeding mediated by a C. elegans guanylate cyclase homologue." Nature **430**(6997): 317-322.

Gunther, C. V., L. L. Georgi, *et al.* (2000). "A Caenorhabditis elegans type I TGF beta receptor can function in the absence of type II kinase to promote larval development." Development **127**(15): 3337-3347.

Gupta, G., M. Azam, *et al.* (1997). "The beta2 subunit inhibits stimulation of the alpha1/beta1 form of soluble guanylyl cyclase by nitric oxide. Potential relevance to regulation of blood pressure." J Clin Invest **100**(6): 1488-1492.

Hao, Y., N. Xu, *et al.* (2011). "Nuclear cGMP-Dependent Kinase Regulates Gene Expression via Activity-Dependent Recruitment of a Conserved Histone Deacetylase Complex." PLoS Genet **7**(5): e1002065.

Hirose, T., Y. Nakano, *et al.* (2003). "Cyclic GMP-dependent protein kinase EGL-4 controls body size and lifespan in C elegans." Development **130**(6): 1089-1099.

Hofmann, F., R. Feil, *et al.* (2006). "Function of cGMP-dependent protein kinases as revealed by gene deletion." Physiol Rev **86**(1): 1-23.

Jones, K. T., E. R. Greer, *et al.* (2009). "Rictor/TORC2 regulates Caenorhabditis elegans fat storage, body size, and development through sgk-1." PLoS Biol **7**(3): e60.

L'Etoile, N. D., C. M. Coburn, *et al.* (2002). "The cyclic GMP-dependent protein kinase EGL-4 regulates olfactory adaptation in C. elegans." Neuron **36**(6): 1079-1089.

Lee, B. H., J. Liu, *et al.* (2011). "Hyperactive Neuroendocrine Secretion Causes Size, Feeding, and Metabolic Defects of C. elegans Bardet-Biedl Syndrome Mutants." PLoS Biol **9**(12): e1001219.

Lee, J. I., D. M. O'Halloran, *et al.* (2010). "Nuclear entry of a cGMP-dependent kinase converts transient into long-lasting olfactory adaptation." Proc Natl Acad Sci U S A.

Li, W., S. G. Kennedy, *et al.* (2003). "daf-28 encodes a C. elegans insulin superfamily member that is regulated by environmental cues and acts in the DAF-2 signaling pathway." Genes Dev **17**(7): 844-858.

Lin, K., H. Hsin, *et al.* (2001). "Regulation of the Caenorhabditis elegans longevity protein DAF-16 by insulin/IGF-1 and germline signaling." Nat Genet **28**(2): 139-145.

Macosko, E. Z., N. Pokala, *et al.* (2009). "A hub-and-spoke circuit drives pheromone attraction and social behaviour in C. elegans." Nature **458**(7242): 1171-1175.

Marte, A., O. Pepicelli, *et al.* (2008). "In vivo effects of phosphodiesterase inhibition on basal cyclic guanosine monophosphate levels in the prefrontal cortex, hippocampus and cerebellum of freely moving rats." J Neurosci Res **86**(15): 3338-3347.

Mok, C. A., M. P. Healey, *et al.* (2011). "Mutations in a Guanylate Cyclase GCY-35/GCY-36 Modify Bardet-Biedl Syndrome-Associated Phenotypes in Caenorhabditis elegans." PLoS Genet **7**(10): e1002335.

Nachury, M. V., A. V. Loktev, *et al.* (2007). "A core complex of BBS proteins cooperates with the GTPase Rab8 to promote ciliary membrane biogenesis." Cell **129**(6): 1201-1213.

Nakai, J., M. Ohkura, *et al.* (2001). "A high signal-to-noise Ca(2+) probe composed of a single green fluorescent protein." Nat Biotechnol **19**(2): 137-141.

Nikolaev, V. O. and M. J. Lohse (2009). "Novel techniques for real-time monitoring of cGMP in living cells." Handb Exp Pharmacol(191): 229-243.

Oeckl, P. and B. Ferger (2011). "Simultaneous LC-MS/MS analysis of the biomarkers cAMP and cGMP in plasma, CSF and brain tissue." J Neurosci Methods.

Ou, G., M. Koga, *et al.* (2007). "Sensory ciliogenesis in Caenorhabditis elegans: assignment of IFT components into distinct modules based on transport and phenotypic profiles." Mol Biol Cell **18**(5): 1554-1569.

Paquet-Durand, F., S. M. Hauck, *et al.* (2009). "PKG activity causes photoreceptor cell death in two retinitis pigmentosa models." J Neurochem **108**(3): 796-810.

Pretorius, P. R., M. A. Aldahmesh, *et al.* (2011). "Functional analysis of BBS3 A89V that results in non-syndromic retinal degeneration." Hum Mol Genet.

Pretorius, P. R., L. M. Baye, *et al.* (2010). "Identification and functional analysis of the vision-specific BBS3 (ARL6) long isoform." PLoS Genet **6**(3): e1000884.

Ren, P., C. S. Lim, *et al.* (1996). "Control of C. elegans larval development by neuronal expression of a TGF-beta homolog." Science **274**(5291): 1389-1391.

Richmond, J. (2005). "Synaptic function." WormBook: 1-14.

Schiavo, G., F. Benfenati, *et al.* (1992). "Tetanus and botulinum-B neurotoxins block neurotransmitter release by proteolytic cleavage of synaptobrevin." Nature **359**(6398): 832-835.

Seo, S., L. M. Baye, *et al.* (2010). "BBS6, BBS10, and BBS12 form a complex with CCT/TRiC family chaperonins and mediate BBSome assembly." Proc Natl Acad Sci U S A **107**(4): 1488-1493.

So, S., K. Miyahara, *et al.* (2011). "Control of body size in C. elegans dependent on food and insulin/IGF-1 signal." Genes Cells **16**(6): 639-651.

Tobin, J. L. and P. L. Beales (2008). "Restoration of renal function in zebrafish models of ciliopathies." Pediatr Nephrol **23**(11): 2095-2099.

Truong, K., A. Sawano, *et al.* (2001). "FRET-based in vivo Ca2+ imaging by a new calmodulin-GFP fusion molecule." Nat Struct Biol **8**(12): 1069-1073.

Zaghloul, N. A., Y. Liu, *et al.* (2010). "Functional analyses of variants reveal a significant role for dominant negative and common alleles in oligogenic Bardet-Biedl syndrome." Proc Natl Acad Sci U S A **107**(23): 10602-10607.

Zimmer, M., J. M. Gray, *et al.* (2009). "Neurons detect increases and decreases in oxygen levels using distinct guanylate cyclases." Neuron **61**(6): 865-879.

Zon, L. I. and R. T. Peterson (2005). "In vivo drug discovery in the zebrafish." Nat Rev Drug Discov **4**(1): 35-44.

Appendices

6 Appendix 1: *mobs-1(hp433)* Mapping

6.1 *mobs-1(hp433)* Rough Maps to LGI

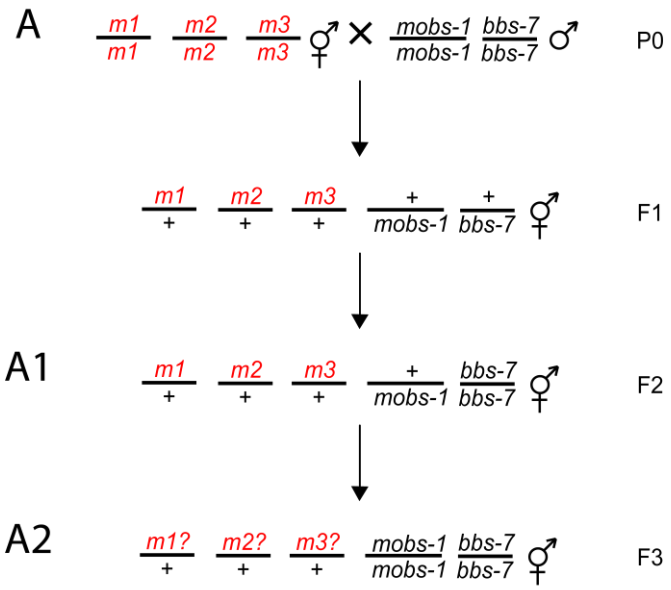

B

LG	Marker	Observed/Total	%
I	dpy-5	6/69 - 3/55	8.7 - 5.5
II	rol-6	30/49 - 26/43	61.2 - 61.5
IV	unc-5	29/55 - 27/43	52.7 - 62.8
V	dpy-11	31/50 - 28/39	62.0 - 71.8
X	lon-2	49/78 - 45/61	62.8 - 73.8

Figure 27. Generic rough mapping scheme for *mobs-1*. A) Rough mapping was performed using two mapping strains carrying chromosomal marker mutations with visible phenotypes along three linkage groups (*dpy-5*(I);*rol-6*(II);*unc-32*(III) and *unc-5*(IV);*dpy-11*(V);*lon-2*(X)) crossed to *mobs-1(hp433);bbs-7(n1606)* males. Phenotypically short worms were selected and genotyped for *bbs-7(n1606)III* (A1). Confirmation in F3 progeny for *m1*, *m2*, and *m3* combinations as well as normal (*mobs-1*) worms was required (A2). Groups of F3 L4s were grown overnight and then phenotypically normal F3s (as many as possible) were then selected for self-fertilization. F4s were then observed for segregation of *m1*, *m2*, and *m3* markers. Unlinked mutations were expected to segregate with *mobs-1* in 2/3 of all cases while linked mutations would segregate at a very low ratio. Note the special case of LGIII since *bbs-7(n1606)III* was used as part of the process. B) Resulting ratios for mapping markers on LGI, LGII, LGIV, LGV, LGX. Observed/Total shows the original and an adjusted score based on secondary observations (ie F3 animals may not have been *mobs-1* homozygous).

Using two mapping strains that carry visible mutations as chromosomal markers, I proceeded to roughly map the *hp433* allele to a linkage group (**Figure 27A**). Independent segregation between *mobs-1* and *bbs-7* was observed on numerous occasions, identifying the two genes as unlinked. Therefore the marker for LGIII (*unc-32*) was not followed as the *bbs-7(n1606)* mutation was also required to map the synthetic suppression of the *bbs-7* body size phenotype.

I followed the segregation of the markers from the mapping strains, and identified that *dpy-5* segregated with *mobs-1* at a rate below the expected 2/3s of animals observed (**Figure 27B**). I therefore concluded that *mobs-1(hp433)* was located on LGI.

6.2 *mobs-1(hp433)* Snip-SNP Mapping Identifies 93kb Interval

Using the *dpy-5 mobs-1(hp433)I;bbs-7(n1606)III* strain from rough mapping, I proceeded to generate a *dpy-5 mobs-1(hp433)I;bbs-7(ok1351)III* and crossed it with the polymorphic Hawaiian *C. elegans* strain (CB4586) (**Figure 28A**). Intial results using the standard snip-SNP (DraI) markers (Davis *et al.* 2005), indicated that *mobs-1(hp433)* was to the right of *dpy-5*. I next generated a *mobs-1(hp433) unc-54(I);bbs-7(ok1351)III* strain and proceeded to perform a similar mapping strategy as previously (**Figure 28A**). With all suppressed recombinant strains, I verified that the *hp433* allele was present and not due to a recessive locus originating from the CB4586 strains (**Figure 28B**). I also verified that the suppression observed in recombinant strains was not due to a dominant polymorphism originating from CB4586 (**Figure 28C**)

Using three recombinant strains, I identified nearby breakpoints surrounding an N2-specific region that would contain *mobs-1(hp433)*. The surrounding breakpoints were pkP1132 (physical position: 13, 282, 540) and uCE1-1426 (physical position: 13, 375, 903). These breakpoints generated a maximum interval of 93, 363 base pairs (**Table 13**)

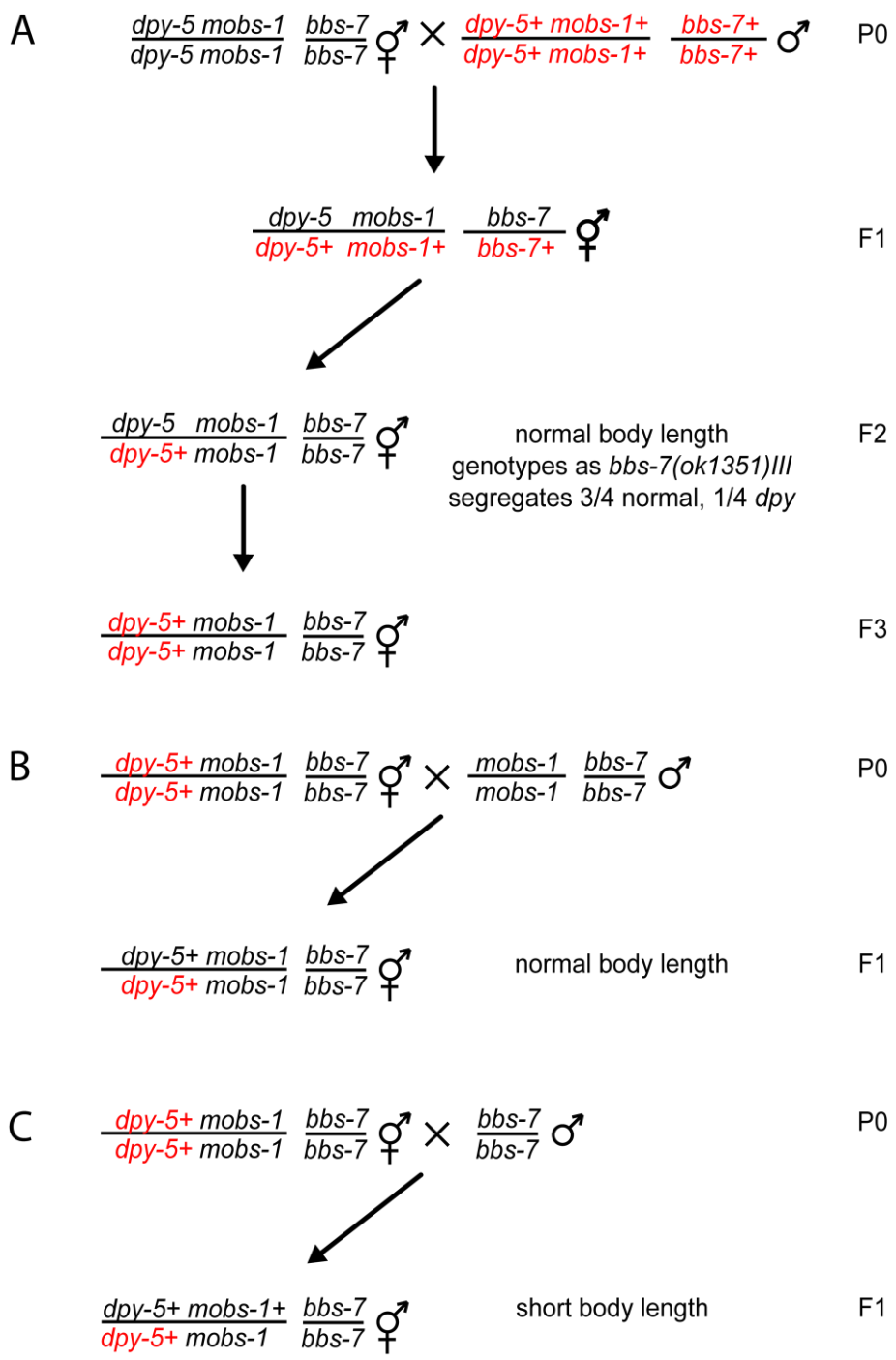

Figure 28. Snip SNP mapping scheme using mutational markers on LGI. A) A schematic of the snip-SNP mapping cross using the Hawaiian strain CB4856 (depicted in red). 200 F2 L4 animals are individually plated and allowed self-cross. F2 animals were then phenotyped by body size and exploration behaviour before being genotyped for *bbs-7(ok1351)*. F2 animals that genotyped as *bbs-7(ok1351)* homozygous but were normal for body length were followed in the F3 progeny and those with 1/4 *dpy-5* animals were kept. From these remaining F2 lines, non *dpy-5* animals were picked, homozygosed and genotyped along snip-SNP markers. (B) Snip-SNP lines were back-crossed against *mobs-1;bbs-7* animals to confirm the presence of *mobs-1(hp433)*. (C) Snip-SNP strains were back-crossed to *bbs-7* animals to check for the presence of dominant suppressors of *bbs-7* body length that may originate in the CB4856 line.

Table 13. Summary of SNP mapping results using *dpy-5* and *unc-54* markers

			dpy-5 mobs-1; bbs-7 strain #			*mobs-1 unc-54; bbs-7* strain #		
SNP	Enzyme	Map	87	159	339	48	218	395
dpy-5	-	0	+/-	+/-	+/-	+/+	+/+	+/+
pkP1132	TaqI	14.35	CB/N2	N2	CB/N2	N2	N2	N2
pkP1073	AatII	17.19	CB/N2	N2	CB/N2	N2	N2	N2
pkP1133*	DraI	17.33	N2		**CB/N2**	-	-	-
pkP1138	DraI	18.46	N2	N2	N2	N2	N2	N2
uCE1-1426**	Sequenced	19.37	-	-	-	**CB/N2**	N2	**CB/N2**
snp_Y48G10[2]	Sequenced	20.97	-	-	-	CB/N2	CB/N2	CB/N2
snp_Y78G2[9]	Sequenced	21.49	-	-	-	CB/N2	CB/N2	CB/N2
unc-54	-	27.97	+/+	+/+	+/+	+/-	+/-	+/-

*physical position at LGI: 13,282,540

**physical position at LGI: 13,375,903

Interval length: 93,363bp

6.3 *mobs-1(hp433)* Fosmids Containing *gcy-35* Rescue *bbs-7* Body Size Suppression

The interval identified by snip-SNP mapping was mostly covered by three fosmids (**Figure 29A**). Individual injection of each of these fosmids was capable of rescuing the suppression effects of *mobs-1(hp433);bbs-7(ok1351)* animals (**Table 14**). The overlap between these three fosmids only contained two genes: *T04D3.5* and *gcy-35*. An MluI-digested version of WRM0641cB09 (cB09-MluI, **Figure 29B**), truncates *gcy-35* along the 3' end while encompassing the entire putative coding region of T04D3.5 including 666 base pairs of upstream sequence. Injection of this truncated fosmid failed to rescue the suppression effect in *mobs-1(hp433);bbs-7* animals (**Table 14**). I therefore concluded that *mobs-1* is *gcy-35*.

Figure 29. Snip-SNP mapping interval encompasses a number of fosmids. (A) Most genes within the snip-SNP mapping interval identified are present in one of three fosmids: *WRM067aC10*, *WRM064cB09*, and *WRM0613cC03*. (B) Fosmids were enzyme digested to produce smaller fragments containing fewer genes. Of note *cB09-MluI* has a partially deleted copy of *gcy-35*.

Table 14. Summarized results of *mobs-1* fosmid rescue injections

Fosmid	Contains *gcy-35*	Contains *T04D3.5*	Rescues *mobs-1* phenotype	Total strains observed
WRM0673aC10	Yes	Yes	Yes	4/4
WRM0641cB09	Yes	Yes	Yes	4/4
WRM0613cC03	Yes	Yes	Yes	6/6
WRM0641cB09/MluI	Partial deletion of 3' end	Yes	No	10/10

6.4 Genomic Sequencing Analysis Identified 2bp Deletion in *gcy-35(hp433)*

I proceeded to sequence the exons of *gcy-35* and identified a two base pair deletion in exon 8 (**Table 15**, **Figure 30A**). This deletion results in a silent change at amino position 322 (**Figure 30B**) while also causing a frameshift in the proceeding sequence leading to a premature termination codon at amino position 328 (Ile322IleFS328X, c.966_67delAT). This mutation results in a truncation of the C-terminal guanylyl cyclase catalytic domain (**Figure 30C**).

Table 15. Summary of *gcy-35* sequencing results

Primer pair	Exons Contained	Forward sequencing results	Reverse sequencing results
3438/3439	1,2	wild type	wild type
3440/3441	3	wild type	wild type
3442/3443	4, 5	wild type	wild type
3444/3445	6, 7	wild type	Not completed
3446/3447	**8, 9, 10**	**2bp deletion in exon 8**	**2bp deletion in exon 8**
3448/3449	11, 12, 13	wild type	Not completed
3448/3476	11, 12, 13	Not completed	wild type
3450/3451	14, 15	wild type	wild type
3452/3453	16, 17	wild type	Not completed

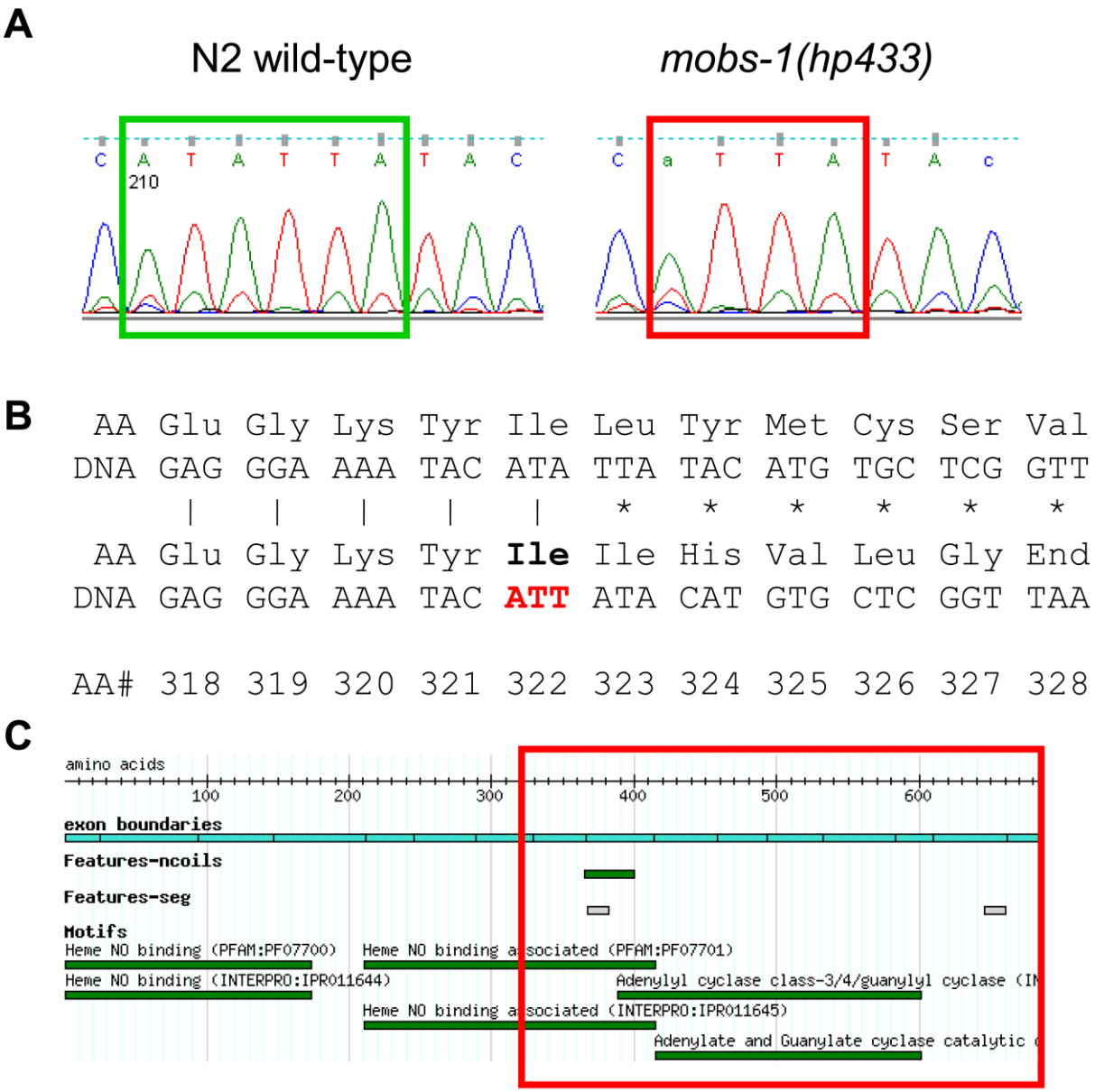

Figure 30. Sequencing results of *gcy-35* in *mobs-1(hp433);bbs-7* mutants. (A) Sequencing of exon 8 identified a two base pair deletion (c.966_67delAT). (B) The *hp433* mutation results in a Ile322IleFS328X mutation, causing a truncation of the C-terminal guanylyl cyclase catalytic domain (C).

6.5 References

Davis, M. W., M. Hammarlund, *et al.* (2005). "Rapid single nucleotide polymorphism mapping in C. elegans." BMC Genomics **6**: 118.

7 Appendix 2: *GUCY1B2* Tissue Expression Pattern

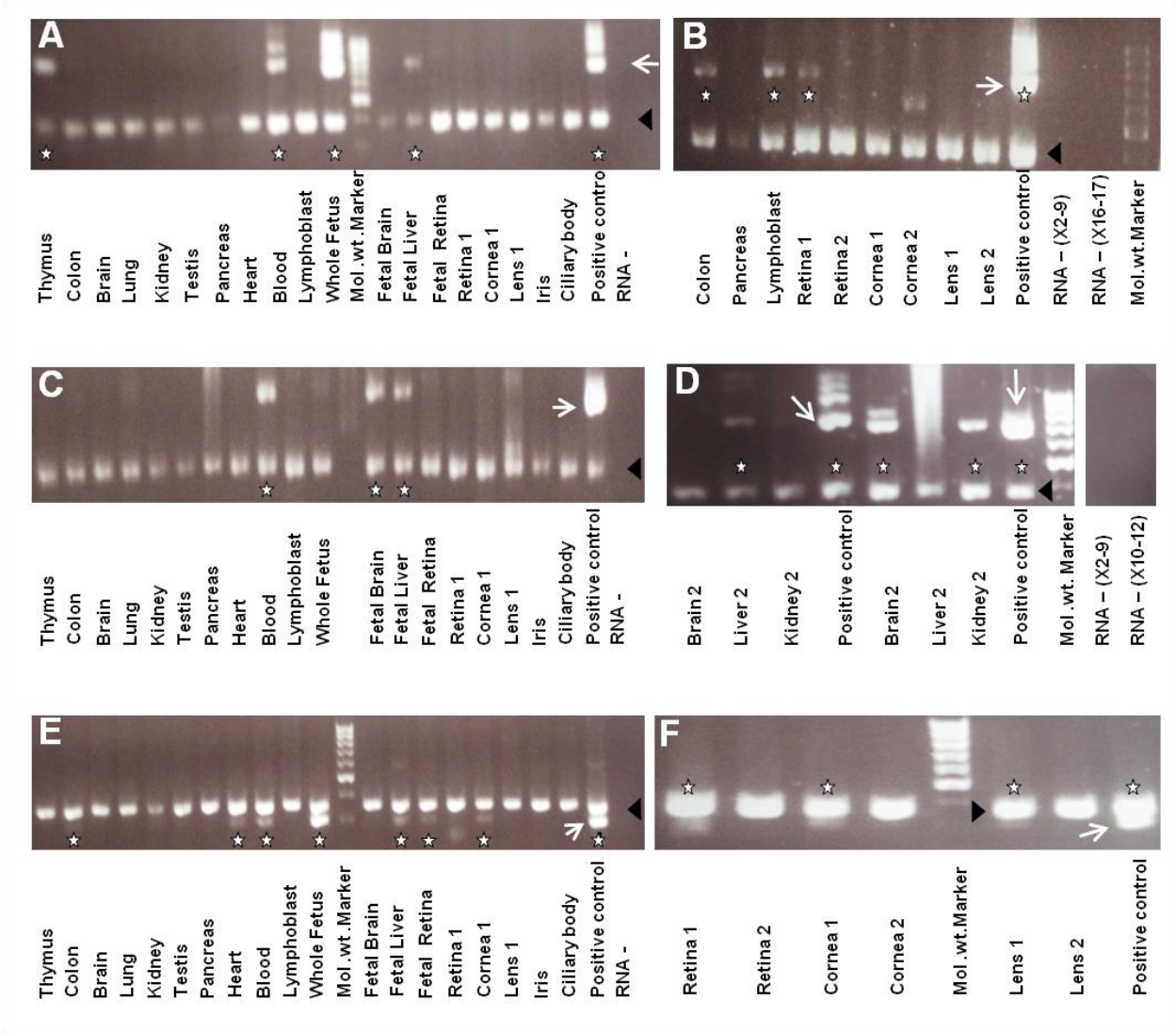

Figure 31. Expression of *GUCY1B2* across multiple tissue panels. The expression of *GUCY1B2* amplified by RT-PCR reactions in different human tissues, compared with the positive control (HEK293 cDNA). In order to cover the different isoforms of *GUCY1B2*, its expression (white stars) was shown by different primer pair amplification (white arrows) for Exons 2-9 (A, B, D-left), Exons 10-12 (C, D-right), Exons 16-17 (E, F) with GAPDH expression (black arrowhead) used as a positive control for amplification. Amplification of at least two exonic fragments was consistently present in blood, whole fetus and fetal liver tissues. Expression in other tissues was more variable with inconsistencies between different sample sources, and identical aliquots from the same tissue. I did, however, see consistent expression in retinal (B, F) and corneal tissues (B, E, F). RT-PCR analysis by M. Jagadeesan

8 Appendix 3: Strains Used in this Study

8.1 *bbs* Strains

VC837 *bbs-1(ok1111)I*, RB1268 *bbs-7(ok1351)III*, MT3645 *bbs-7(n1606)III*, VC1168 *bbs-2(gk544)IV*, VC1062 *bbs-9(gk471)*, MX52 *bbs-8(nx77)V*, ZM2090 *bbs-1(ok1111)I;bbs-7(ok1351)III*, ZM2091 *bbs-1(ok1111)I;bbs-8(nx77)V*, ZM2092 *bbs-7(ok1351)III;bbs-8(nx77)V*, ZM2093 *bbs-1(ok1111)I;bbs-7(ok1351)III;bbs-8(nx77)V*

8.2 *dyf* Strains

CB1033 *che-2(e1033)X*, ZM5814 *che-3(e1124)I*, ZM5816 *che-3(ok1574)I*, ZM5825 *che-11(e1810)V*, ZM5821 *osm-3(p802)IV*, ZM5823 *osm-5(p813)X*, ZM5812 *osm-6(p811)V*, ZM6333 *klp-11(tm324)IV*

8.3 sGC Strains

ZM2085 *gcy-35(hp433)I*, RB906 *gcy-35(ok769)I*, RB1048 *gcy-32(ok995)V*, RB1062 *gcy-34(ok1012)V*, RB626 *gcy-37(ok384)IV*, RB564 *gcy-31(ok296)X*, CZ3715 *gcy-33(ok232)V*, AX1297 *gcy-36(db66)X*

8.4 rGC Strains

FX02669 *gcy-1(tm2669)II*, FX01653 *gcy-4(tm1653)II*, RB1010 *gcy-5(ok930)II*, FX01449 *gcy-6(tm1449)V*, FX00901 *gcy-7(tm901)V*, IK800 *gcy-8(oy44)IV*, FX02816 *gcy-9(tm2816)X*, CX2065 *gcy-10(n1936)X*, RB1935 *gcy-16(ok2538)V*, IK429 *gcy-18(nj38)IV*, FX02364 *gcy-22(tm2364)II*, RB924 *gcy-23(ok797)IV*, FX04300 *gcy-25(tm4300)IV*, FX02411 *gcy-28(tm2411)II*, FK183 *daf-11(ks67)V*, DR47 *daf-11(m47)V*

8.5 cGMP-related Strains

PR671 *tax-2(p671)I*, FK103 *tax-4(ks28)III*, CX7102 *qaIs2241[Pgcy-36::egl-1]X*, MT1073 *egl-4(n478)IV*, DA521 *egl-4(ad450)IV*, RB1038 *C09G4.2(ok966)IV*, JT6130 *daf-21(p673)V*

8.6 *pde* Strains

RB2164/ZM6168 *pde-1(ok2924)I*, ZM6188 *pde-3(nj59)II*, RB1575 *pde-4(ok1290)II*, RB2279/ZM6170 *pde-5(ok3102)*, ZM6446 *pde-5(nj49)I*, RB2470 *pde-6(ok3410)I*,

VC282/ZM6174 *pdl-1(gk157)II*, *TQ1828 pde-5(nj49) pde-1(nj57)I;pde-3(nj59)II;pde-2(tm3098)III*, ZM5833 *syIs25[Pgpa-3::gpa-3(Q205L)]X*

8.7 TGF-β Strains

ZM643 *dbl-1(ev580)V*, CB678 *lon-2(e678)X*

8.8 sGC Combination Strains

ZM2087 *gcy-35(hp433)I;bbs-7(ok1351)III*, ZM2086 *gcy-35(hp433)I;bbs-7(n1606)III*, ZM3703 *gcy-35(ok769)I;bbs-7(ok1351)III*, ZM4059 *bbs-7(ok1351)III;gcy-36(db66)X*, ZM3861 *bbs-7(ok1351)III;gcy-32((ok995)V*, ZM3862 *bbs-7(ok1351)III;gcy-34(ok1012)V*, ZM3863 *bbs-7(ok1351)III;gcy-37(ok384)IV*, ZM5309 *bbs-7(ok1351)III;gcy-31(ok296)X*, ZM5269 *bbs-7(ok1351)III;gcy-33(ok232)V*, ZM4174 *gcy-35(hp433)I;bbs-7(ok1351)III;gcy-36(db66)X*, ZM3704 *gcy-35(hp433)I;bbs-8(nx77)V*, ZM3859 *gcy-35(hp433)bbs-1(ok1111)I*, ZM3705 *gcy-35(ok769)I;bbs-2(gk544)IV*, ZM3856 *gcy-35(ok769)I;bbs-8(nx77)V*, ZM3857 *gcy-35(ok769)bbs-1(ok1111)I*, ZM5464 *gcy-33(ok232)I;bbs-7(ok1351)III;gcy-31(ok296)X*

8.9 rGC Combination Strains

ZM5725 *gcy-1(tm2669)II;bbs-7(ok1351)III*, ZM5726 *gcy-4(tm1653)II;bbs-7(ok1351)III*, ZM5613 *gcy-5(ok930)II;bbs-7(ok1351)III*, ZM5727 *bbs-7(ok1351)III;gcy-6(tm1449)V*, ZM5728 *bbs-7(ok1351)III;gcy-7(tm901)V*, ZM5465 *bbs-7(ok1351)III;gcy-8(oy44)IV*, ZM5729 *bbs-7(ok1351)III;gcy-9(tm2816)X*, ZM5614 *bbs-7(ok1351)III;gcy-16(ok2538)V*, ZM5466 *bbs-7(ok1351)III;gcy-18(nj38)IV*, ZM5730 *bbs-7(ok1351)III;gcy-22(tm2364)V*, ZM5612 *bbs-7(ok1351)III;gcy-23(ok797)IV*, ZM5731 *bbs-7(ok1351)III;gcy-5(tm4300)V*, ZM5732 *bbs-7(ok1351)III;gcy-28(tm2411)I*, ZM5615 *bbs-7(ok1351)III; gcy-8(oy44) gcy-18(nj38)*, ZM5733 *bbs-7(ok1351)III; gcy-23(ok797) gcy-8(oy44) gcy-18(nj38)*, ZM5467 *bbs-7(ok1351)III;odr-10(n1936)X*, ZM4928 *bbs-7(ok1351)III;daf-11(m47)V*, ZM5616 *bbs-7(ok1351)III;daf-11(ks67)V*, ZM5991 *gcy-35(hp433)I;gcy-23(ok797)IV*, ZM5992 *gcy-35(hp433)I;gcy-23(ok797)IV;bbs-7(ok1351)III*, ZM5993 *gcy-35(hp433)I;gcy-4(tm1653)II*, ZM5994 *gcy-35(hp433)I;gcy-4(tm1653)II;bbs-7(ok1351)III*, ZM5996 *gcy-35(hp433)I;bbs-7(ok1351)III;gcy-25(tm4300)IV*, ZM5997 *gcy-28(tm2411) gcy-35(hp433)I; bbs-7(ok1351)III*, ZM5998 *gcy-35(hp433)I;gcy-16(ok2538)V*, ZM5999 *gcy-35(hp433)I;bbs-7(ok1351)III;gcy-16(ok2538)V*, ZM6000 *gcy-35(hp433)I;gcy-7(tm901)V*, ZM6001 *gcy-35(hp433)I;bbs-7(ok1351)III;gcy-*

7(tm901)V, ZM6357 *gcy-28(tm2411) gcy-35(hp433)I*, ZM6358 *gcy-28(tm2411)I;bbs-7(ok1351)III;gcy-23(ok797)IV*, ZM6359 *gcy-28(tm2411) gcy-35(hp433)I;bbs-7(ok1351)III;gcy-23(ok797)IV*, ZM6360 *gcy-4(tm1653)II;bbs-7(ok1351)III;gcy-23(ok797)IV*, ZM6361 *gcy-35(hp433)I;gcy-4(tm1653)II;bbs-7(ok1351)III;gcy-23(ok797)IV*, ZM6362 *bbs-7(ok1351)III;gcy-7(tm901) gcy-16(ok2538)V*, ZM6363 *gcy-35(hp433)I;bbs-7(ok1351)III;gcy-7(tm901) gcy-16(ok2538)V*

8.10 *dyf* Combination Strains

ZM5817 *gcy-35(hp433)I;che-2(e1033)X*, ZM5815 *gcy-35(hp433) che-3(e1124)I*, ZM5818 *gcy-35(hp433) che-3(ok1574)I*, ZM5826 *gcy-35(hp433)I;che-11(e1810)V*, ZM5822 *gcy-35(hp433)I;osm-3(p802)IV*, ZM5824 *gcy-35(hp433)I;osm-5(p813)X*, ZM5813 *gcy-35(hp433)I;osm-6(p811)V*, ZM6334 *gcy-35(hp433)I;klp-11(tm324)IV*

8.11 *pde* Combination Strains

ZM6436 *pde-1(ok2924)I;gcy-36(db66)I*, ZM6435 *pde-1(ok2924)I;bbs-7(ok1351)III*, ZM6364 *pde-1(ok2924)I;bbs-7(ok1351)III;gcy-36(db66)X*, ZM6447 *pde-1(nj57)I;gcy-36(db66)I*, ZM6450 *pde-1(nj57)I;bbs-7(ok1351)III*, ZM6449 *pde-1(nj57)I;bbs-7(ok1351)III;gcy-36(db66)X*, ZM6186 *gcy-35(hp433)I;pde-2(tm3098)III*, ZM6185 *pde-2(tm3098) bbs-7(ok1351)III*, ZM6187 *gcy-35(hp433)I;pde-2(tm3098) bbs-7(ok1351)III*, ZM6189 *gcy-35(hp433)I;pde-3(nj59)II*, ZM6190 *pde-3(nj59)II;bbs-7(ok1351)III*, ZM6191 *gcy-35(hp433)I;pde-3(nj59)II;bbs-7(ok1351)III*, ZM6180 *gcy-35(hp433)I;pde-4(ok1290)II*, ZM6179 *pde-4(ok1290)II;bbs-7(ok1351)III*, ZM6181 *gcy-35(hp433)I;pde-4(ok1290)II;bbs-7(ok1351)III*, ZM6438 *pde-5(ok3102) gcy-35(hp433)I*, ZM6437 *pde-5(ok3102);bbs-7(ok1351)III*, ZM6439 *pde-5(ok3102) gcy-35(hp433)I;bbs-7(ok1351)III*, ZM6452 *pde-5(nj49)I;gcy-36(db66)X*, ZM6453 *pde-5(nj49)I;bbs-7(ok1351)III; gcy-36(db66)X* ZM6183 *pde-6(ok3410) gcy-35(hp433)I*, ZM6182 *pde-6(ok3410)I;bbs-7(ok1351)III*, ZM6184 *pde-6(ok3410) gcy-35(hp433)I;bbs-7(ok1351)III*, ZM6441 *gcy-35(hp433)I;pd1-1(gk157)II*, ZM6440 *pd1-1(gk157)II;bbs-7(ok1351)III*, ZM6442 *gcy-35(hp433)I; pd1-1(gk157)II;bbs-7(ok1351)III*, ZM5827 *bbs-7(ok1351)III;syIs25[Pgpa-3::gpa-3(Q205L)]X*, ZM5829 *bbs-2(gk544)IV;syIs25[Pgpa-3::gpa-3(Q205L)]X*

8.12 TGF-β Combination Strains

ZM4178 *gcy-35(hp433)I;dbl-1(ev580)V*, ZM4171 *bbs-7(ok1351)III;dbl-1(ev580)V*, ZM2087 *gcy-35(hp433)I;bbs-7(ok1351)III*, ZM4058 *gcy-35(hp433)I;lon-2(e678)X*, ZM3735 *bbs-7(ok1351)III;lon-2(e678)X*, ZM4170 *gcy-35(hp433)I;bbs-7(ok1351)III;lon-2(e678)X*

8.13 Additional Candidate *bbs* Suppressor Strains

ZM5274 *tax-2(p671)I; bbs-7(ok1351)III*, ZM5270 *tax-4(ks28) bbs-7(ok1351)III*, ZM4729 *gcy-35(hp433)I; egl-4(n478)IV*, ZM4727 *bbs-7(ok1351)III; egl-4(n478)IV*, ZM4730 *gcy-35(hp433)I; bbs-7(ok1351)III; egl-4(n478)IV*, ZM5272 *gcy-35(hp433)I; egl-4(ad450)IV*, ZM5273 *bbs-7(ok1351)III; egl-4(ad450)IV*, ZM5271 *gcy-35(hp433)I; bbs-7(ok1351)III; egl-4(ad450)IV*, ZM6233-35 *bbs-7(ok1351)III;mobs-2(hp732)*, ZM6354 *C09G4.2(ok966)IV*, ZM6355 *bbs-7(ok1351)III;C09G4.2(ok966)IV*, ZM6356 *gcy-35(hp433)I;bbs-7(ok1351)III;C09G4.2(ok966)IV*, ZM6006 *gcy-35(hp433)I;daf-21(p673)V*, ZM6007 *gcy-35(hp433)I;bbs-7(ok1351)III;daf-21(p673)V*, ZM6008 *gcy-35(hp433)I;bbs-2(gk544)IV;daf-21(p673)V*

8.14 Strains used for mapping *gcy-35(hp433)*

8.15 Transgenic strains used in this study

Extrachromosomal arrays (*hpEx* lines) were generated by co-injecting various DNA constructs at ~10-20ng/ul with co-injection markers at 10ng/ul. The following are the strains and genotypes of the *hpEx* lines used in this study.

8.15.1 Rescuing Lines for *bbs* Animals

ZM(1990, 1992) *bbs-7(n1606)III; hpEx(463,465)[bbs-7(wt)+Podr-1::GFP])*, ZM2001 *bbs-7(ok1351)III; hpEx472[bbs-7(wt)+Podr-1::GFP]*, ZM(2460-2463) *bbs-8(nx77)V; hpEx(636-639)[bbs-8(wt)+Podr-1::GFP]*, ZM(2464-2470) *bbs-1(ok1111)I; hpEx(640-646)[bbs-1(wt)+Podr-1::GFP]*, ZM(4007-4008) *bbs-2(gk544)IV; hpEx(1551-1552)[Prgef-1::BBS-2+Podr-1::GFP]*, ZM2459 *gcy-35(hp433)I; bbs-7(n1606)III; hpEx635[bbs-7+Podr-1::GFP]*

8.15.2 Rescuing Lines for *gcy-35(hp433)I; bbs-7(ok1351)III* Animals

ZM3390 *gcy-35(hp433)I; bbs-7(ok1351)III; hpEx1251[WRM0641cB09+Podr-1]*, ZM3391 *gcy-35(hp433)I; bbs-7(ok1351)III; hpEx1252[WRM063aC10+Podr-1])*, ZM(3393-3394) *gcy-35(hp433)I;bbs-7(ok1351)III; hpEx(1256-1257)[WRM0613cC03+Podr-1]*, ZM3395 *gcy-35(hp433)I; bbs-7(ok1351)III; hpEx1262[WRM0641cB09/MluI+Podr-1]).*

8.15.3 Cell-specific Rescue Lines for *gcy-35(hp433)I;bbs-7(ok1351)III* Animals

ZM(3629-3632) *gcy-35(hp433)I;bbs-7(ok1351)III; hpEx(1360-1363)[Pgcy-36::GCY-35(non-isoprenylated)+Podr-1]*, ZM(3633-3635) *gcy-35(hp433)I;bbs-7(ok1351)III; hpEx1364-1366[Plad-2::GCY-35(isoprenylated)+Podr-1]*, ZM(3747-3748) *gcy-35(hp433)I; bbs-7(ok1351)III; hpEx(1367-1368)[pJH1374+Podr-1]*, ZM(4062-4063) *gcy-35(hp433)I; bbs-7(ok1351)III; hpEx(1568-1569)[pJH1493+Podr-1]*

8.15.4 Transgenic Lines to Examine the Subcellular Localisation of GCY-35 and GCY-36

ZM4064 *gcy-36(db66)X; hpEx1570[Pgcy-36::GFP::GCY-36+Podr-1::GFP]*, ZM4065 *bbs-7(ok1351)III; gcy-36(db66)X; hpEx1571[Pgcy-36::GFP::GCY-36+ Podr-1::GFP]*, ZM5540 *gcy-35(hp433)I; hpEx2312[pJH1867+Podr-1::GFP]*, ZM(5538-5539) *gcy-35(hp433)I; bbs-7(ok1351)III; hpEx(2310-2311)[pJH1867+Podr-1::GFP]*, ZM5529 *hpIs215[Pgcy-36::GFP::GCY-36](X)*, ZM5530 *bbs-7(ok1351)III; hpIs215(X)*, ZM6068 *gcy-35(hp433)I; hpEx2537[Pgcy-36::GFP::GCY-35+Pmyo-3::RFP]*, ZM6067 *bbs-7(ok1351)III; hpEx2537[Pgcy-36::GFP::GCY-35+Pmyo-3::RFP]*, ZM6078 *hpEx2537[Pgcy-36::GFP::GCY-35+Pmyo-3::RFP]*

8.15.5 EGL-4 Gain of Function Expression Lines

ZM(5534-5536) *gcy-35(hp433)I; bbs-7(ok1351)III; hpEx(2306-2308)[Pgcy-36::egl-4(ad450)+Podr-1::GFP]*, ZM5537 *N2; hpEx2309[Pgcy-36::egl-4(ad450)+Podr-1::GFP]*

8.15.6 EGL-4 Rescue and Expression Lines

ZM6081 *gcy-35(hp433)I; hpEx2535[Pgcy-36::GFP::EGL-4a+Pmyo-3::RFP]*, ZM6079 *bbs-7(ok1351)III; hpEx2535[Pgcy-36::GFP::EGL-4a+Pmyo-3::RFP]*, ZM6080 *hpEx2535[Pgcy-*

36::GFP::EGL-4a+Pmyo-3::RFP], ZM6084 *gcy-35(hp433)I; hpEx2536[Pegl-4a::GFP::EGL-4a+Pmyo-3::RFP]*, ZM6082 *bbs-7(ok1351)III; hpEx2536[Pegl-4a::GFP::EGL-4a+Pmyo-3::RFP]*, ZM6083 *hpEx2536[Pegl-4a::GFP::EGL-4a+Pmyo-3::RFP]*

9 Appendix 4: Additional *Pegl-4a*::GFP::EGL-4 localization images

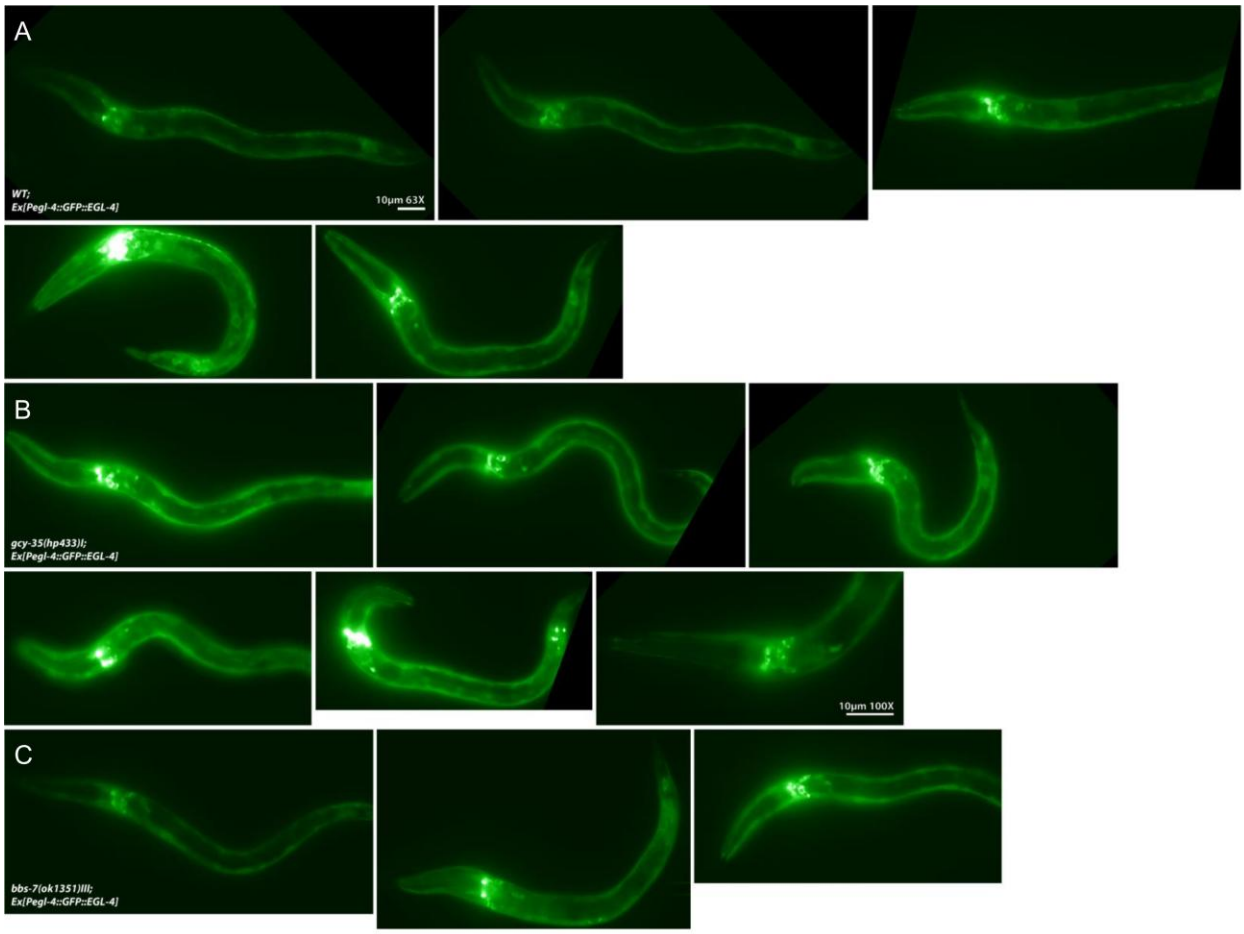

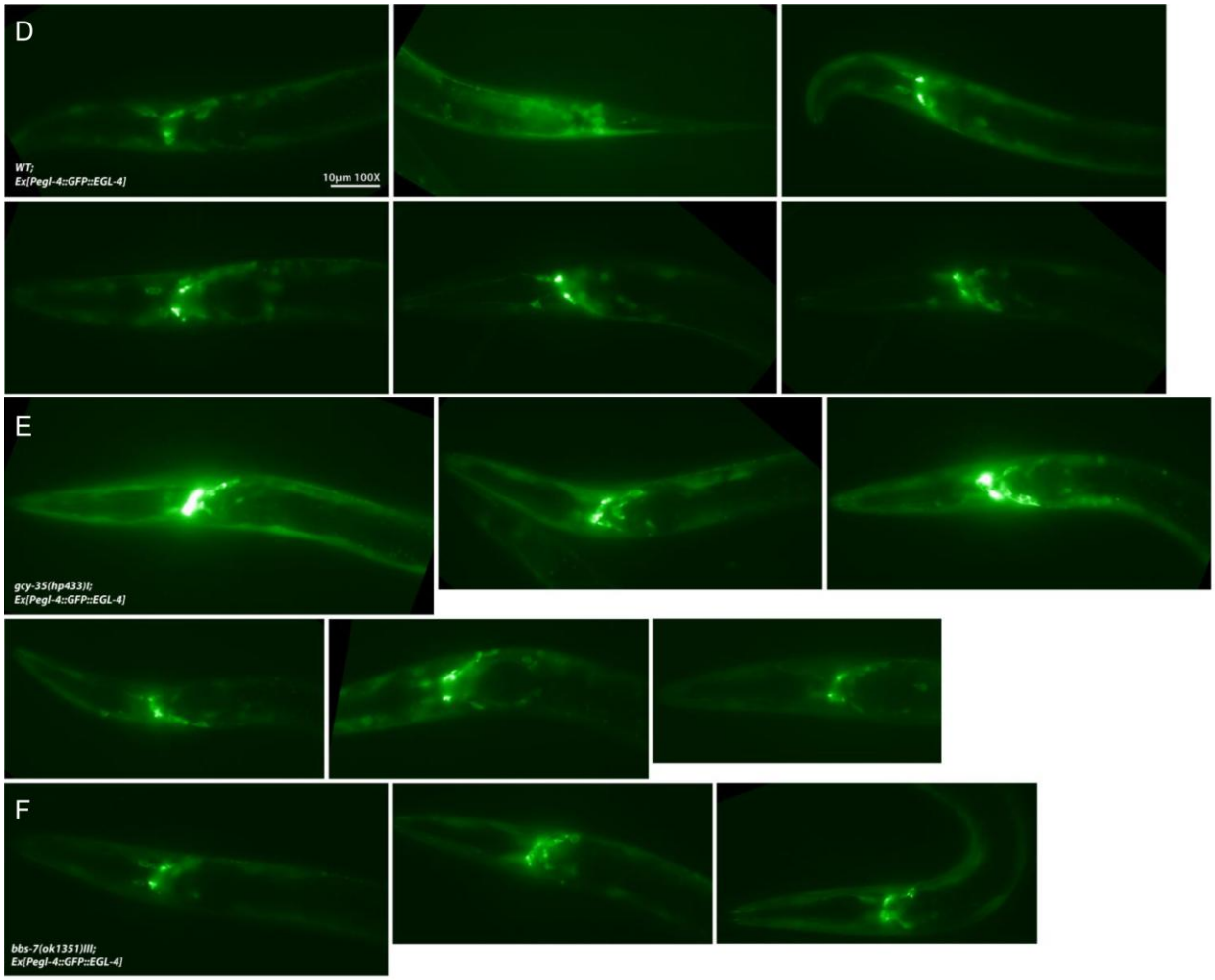
D
WT;
Ex[Pegl-4::GFP::EGL-4]
10µm 100X
E
gcy-35(hp433)I;
Ex[Pegl-4::GFP::EGL-4]
F
bbs-7(ok1351)III;
Ex[Pegl-4::GFP::EGL-4]

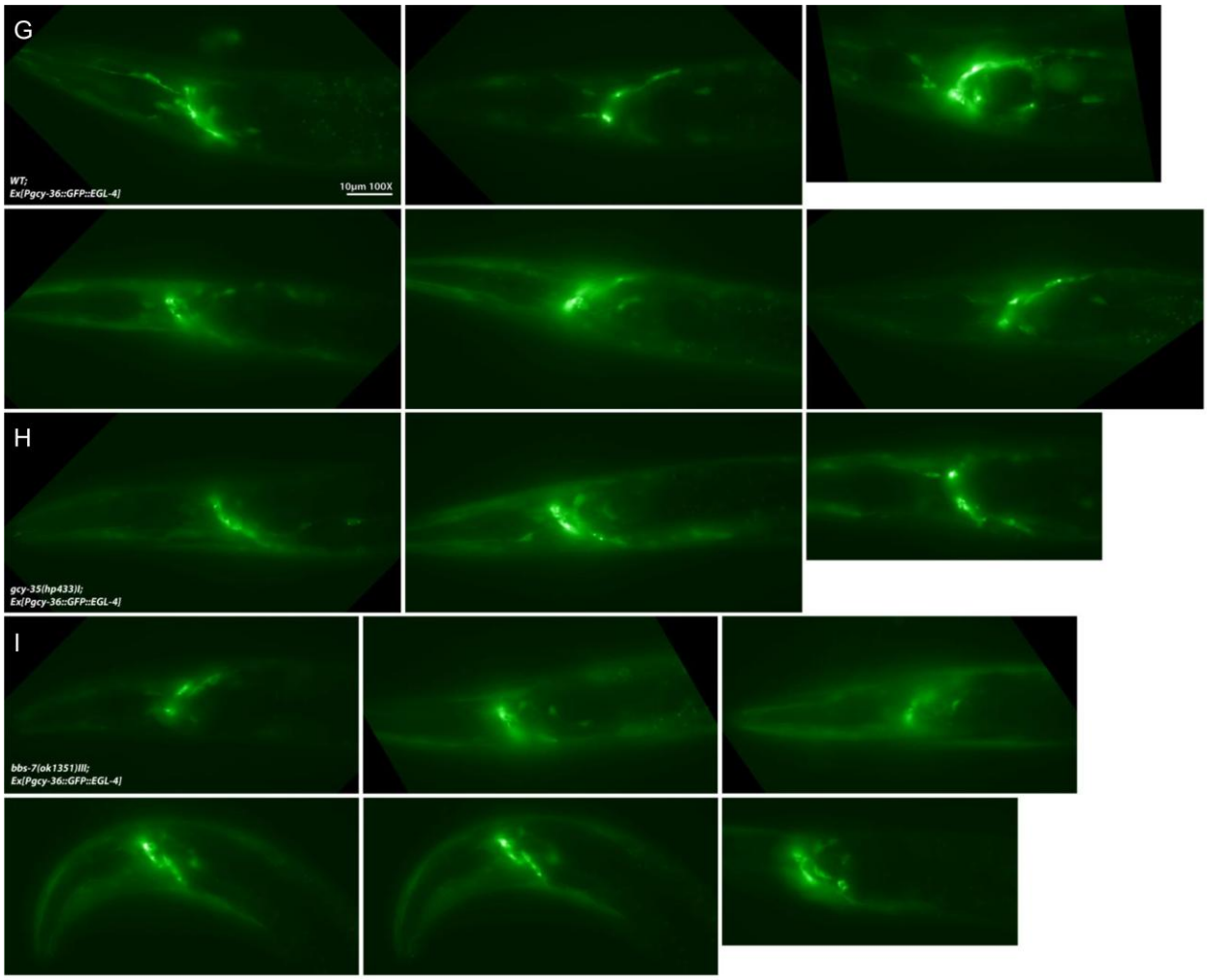

Figure 32. Additional representative images of EGL-4 localisation in endogenously expressing neurons. GFP signals by *Pegl-4a::GFP::EGL-4* expressed in wild type (A, D, G), *gcy-35(hp433)* (B, E, H) or *bbs-7(ok1351)* (C, F, I) mutants synchronized to L1 (4 hours post-hatch, A-C), L2 (28 hours post-hatch, D-F), and L4 (48 hours post-hatch, G-I). GFP::EGL-4 expression was observed most strongly in the nervous system and hypodermis, with cells most prominently in the head and tail neurons. *gcy-35;bbs-7* or *bbs-7* animals did not exhibit obvious changes to expression or localization in comparison to wild-type animals. Analysis was completed on strains made from the same original extrachromosomal line. Shown here are representative images of animals at various stages.